

# **University of Alberta**

Lipase-catalyzed interesterification between canola oil and fully-hydrogenated canola oil in contact with supercritical carbon dioxide

by

Ehsan Jenab

A thesis submitted to the Faculty of Graduate Studies and Research  
in partial fulfillment of the requirements for the degree of

Doctor of Philosophy  
in  
Bioresource and Food Engineering

Department of Agricultural, Food and Nutritional Science

©Ehsan Jenab  
Spring 2013  
Edmonton, Alberta

Permission is hereby granted to the University of Alberta Libraries to reproduce single copies of this thesis and to lend or sell such copies for private, scholarly or scientific research purposes only. Where the thesis is converted to, or otherwise made available in digital form, the University of Alberta will advise potential users of the thesis of these terms.

The author reserves all other publication and other rights in association with the copyright in the thesis and, except as herein before provided, neither the thesis nor any substantial portion thereof may be printed or otherwise reproduced in any material form whatsoever without the author's prior written permission.

*This dissertation is dedicated to my parents Zahra Souveizi  
and Valiollah Jenab and my brothers and sister*

## Abstract

Despite the policies targeting reduction of partially hydrogenated fats because of concerns over *trans* fatty acids (TFA), which have been shown to be a major risk factor for cardiovascular diseases, partial hydrogenation is still employed in the margarine industry. Lipase-catalyzed interesterification is an alternative method to eliminate TFA formation in hardened fats. However, conventional techniques suffer from long reaction times or use of organic solvents. The objective of this thesis was to develop lipase-catalyzed interesterification between canola oil and fully-hydrogenated canola oil (FHCO) using supercritical carbon dioxide (SCCO<sub>2</sub>).

Fundamental physical properties such as viscosity, density and volumetric expansion of canola oil and its blend with FHCO were determined at different temperatures and pressures. When equilibrated with SCCO<sub>2</sub> at pressures of up to 10 MPa, the viscosity of canola oil and its blend decreased by 80-90% of that at atmospheric pressure. As well, the density at elevated pressures increased by 3.5-5%, while volumetric expansion increased by 40-46%.

The performance and reusability of Lipozyme TL IM and RM IM for interesterification between canola oil and FHCO under SCCO<sub>2</sub> were investigated. Both enzymes showed similar performance. Exposure time of up to 12 h and pressurization/depressurization steps of up to 12 times under SCCO<sub>2</sub> did not affect the activity or the structure of the enzymes significantly. Both enzymes showed good reusability for several times for interesterification without any significant change in degree of interesterification. Pressurization/depressurization reduced

the moisture content of the enzymes and consequently the formation of reaction intermediates during the reaction.

Optimal reaction conditions to obtain the maximum conversion rate were 65 °C/10 MPa/2 h/6% (w/v) Lipozyme TL IM of substrates. The triglyceride (TG) composition, thermal behaviour, solid fat content, polymorphism and microstructural and rheological properties of initial blends were modified considerably due to the formation of new mixed TG during interesterification.

The fundamental data and optimized reaction conditions obtained in this research are essential for process and equipment design. As well, the physicochemical characterization of final products will aid in the formulation of more healthy products and address a critical industrial demand in terms of formulation options for margarines and similar products.

## Acknowledgement

My special thanks to Dr. Feral Temelli as her second generation, whose great and unbelievable mentorship and supervision enabled me to finish this project besides gaining lots of experience from her in various aspects. Thanks Dr. Temelli for being such a great supervisor. I would also like to thank my M.Sc. supervisor, Dr. Karamatollah Rezaei, who brought me to the field of supercritical fluids and taught me lots of elements of doing research from scratch.

I would like to thank Dr. Jonathan Curtis and Dr. Randall Weselake for being in my supervisory committee and their valuable feedback during my PhD program. Many thanks to Dr. Jonathan Curtis for providing his lab equipment. Special thanks to Dr. Larry Unsworth from the Department of Chemical and Materials Engineering for being on my examining committee. Special thanks to Dr. Paul Charpentier from Department of Chemical and Biochemical Engineering of the University of Western Ontario for accepting to be my external examiner.

I would also like to thank my great lab mates and friends, Dr. Ozan Nazim Ciftci, Dr. Bernhard Seifried, Dr. Lauren Comin, Jaime Calderon, Dr. Oguz Akin, Mei Sun, Deniz Ciftci, Mehdi Omidghane and Mohammadsadegh Amiri for their helpful support during my PhD program. Special thanks to Yuan Yuan Zhao for helping me with LC/MS analysis and Ereddad Kharraz for helping me with DSC and PLM. Special thanks also to Jody Forsland who is doing a great job on administrative work in the department. Thanks to Dr. Kelvin Lien and Gary Sedgwick who provided assistance with the analytical aspects of my project and the fabulous technicians in SEM and XRD labs of Earth and Atmospheric Sciences Department.

I am also grateful to AVAC Ltd. and Bioactive Oil Program for funding my project and their financial support.

Ultimately, I would like to thank my parents, my brothers and sister and all of my friends who gave me enthusiasm, motivation and positive feelings.

## Table of contents

1. INTRODUCTION AND THESIS OBJECTIVES.....	1
1.1. Hypothesis.....	4
1.2. Thesis objectives.....	4
1.3. References .....	5
2. LITERATURE REVIEW .....	8
2.1. Supercritical fluids.....	8
2.1.1. Physical properties of supercritical fluids .....	10
2.1.1.1. Viscosity .....	11
2.1.1.2. Density .....	13
2.1.2. Motivation for the use of SCCO <sub>2</sub> in reactions .....	15
2.2. Modification of lipids .....	15
2.2.1. Blending .....	16
2.2.2. Fractionation .....	16
2.2.3. Lipid reactions .....	17
2.2.3.1. Hydrogenation reaction.....	17
2.2.3.2. Hydrolysis reaction .....	18
2.2.3.3. Esterification reaction .....	20
2.2.3.4. Interesterification reaction .....	21
2.2.3.4.1. Chemical interesterification .....	23
2.2.3.4.2. Enzymatic interesterification .....	24
2.2.3.4.2.1. Mechanism of lipase-mediated interesterification .....	25
2.2.3.4.2.2. Kinetics of lipase-catalyzed reactions .....	27
2.3. Biocatalysis reactions using SCCO <sub>2</sub> .....	30
2.3.1. Fundamental behaviour of reaction systems in contact with SCCO <sub>2</sub> ....	32
2.3.1.1. Phase behaviour and solubility of reactants and products .....	33
2.3.1.2. Diffusivity of solutes.....	34
2.3.1.3. Physical properties of the liquid phase in equilibrium with high pressure CO <sub>2</sub> .....	35
2.3.2. Reaction kinetics .....	37
2.3.2.1. Reaction rate and activation volume.....	37
2.3.3. Enzyme efficiency under SCCO <sub>2</sub> .....	40
2.3.3.1. Enzyme stability.....	40
2.3.3.2. Effect of water.....	44
2.3.3.2.1. The role of enzyme support .....	44

2.3.3.2.2. The role of reaction media .....	46
<b>2.4. Concluding remarks .....</b>	<b>47</b>
<b>2.5. References .....</b>	<b>48</b>
3. VISCOSITY MEASUREMENT AND MODELING OF CANOLA OIL AND ITS BLEND WITH FULLY-HYDROGENATED CANOLA OIL IN EQUILIBRIUM WITH SUPERCRITICAL CARBON DIOXIDE .....	59
<b>3.1. Introduction.....</b>	<b>59</b>
<b>3.2. Material and methods.....</b>	<b>62</b>
3.2.1. Materials .....	62
3.2.2. Viscosity determination .....	63
3.2.2.1. Apparatus to measure viscosity .....	63
3.2.2.2. Experimental design and protocols .....	64
3.2.3. Determination of CO <sub>2</sub> solubility in the liquid phase.....	66
3.2.3.1. Apparatus to measure CO <sub>2</sub> solubility.....	66
3.2.3.2. Experimental design and protocols .....	67
<b>3.3. Results and discussion .....</b>	<b>68</b>
3.3.1. Viscosity as a function of pressure and temperature.....	68
3.3.2. Rheological behaviour .....	74
3.3.3. Viscosity as a function of mass fraction of CO <sub>2</sub> in the liquid phase.....	78
<b>3.4. Conclusions.....</b>	<b>83</b>
<b>3.5. References .....</b>	<b>84</b>
4. DENSITY AND VOLUMETRIC EXPANSION OF CANOLA OIL AND ITS BLEND WITH FULLY-HYDROGENATED CANOLA OIL IN EQUILIBRIUM WITH SUPERCRITICAL CARBON DIOXIDE .....	87
<b>4.1. Introduction.....</b>	<b>87</b>
<b>4.2. Materials and methods .....</b>	<b>89</b>
4.2.1. Materials .....	89
4.2.2. Solubility measurements of CO <sub>2</sub> in the liquid phase .....	91
4.2.3. Volumetric expansion measurements .....	91
4.2.4. Density measurements .....	94
<b>4.3. Results and discussion .....</b>	<b>97</b>
4.3.1. Modeling CO <sub>2</sub> solubility in the liquid lipid phase at elevated pressures using cubic equations of state .....	97
4.3.2. Volumetric expansion .....	103

4.3.3. Density .....	108
<b>4.4. Conclusions.....</b>	<b>115</b>
<b>4.5. References .....</b>	<b>116</b>
5. PERFORMANCE OF TWO IMMOBILIZED LIPASES FOR INTERESTERIFICATION BETWEEN CANOLA OIL AND FULLY- HYDROGENATED CANOLA OIL UNDER SUPERCRITICAL CARBON DIOXIDE..... 119	
<b>5.1. Introduction.....</b>	<b>119</b>
<b>5.2. Materials and methods .....</b>	<b>122</b>
5.2.1. Materials .....	122
5.2.2. Lipase-catalyzed interesterification .....	123
5.2.3. Activity of immobilized lipases exposed to SCCO <sub>2</sub> and pressurization/depressurization cycles.....	124
5.2.4. Analysis of reaction intermediates .....	125
5.2.5. Determination of degree of interesterification .....	126
5.2.6. Structural and morphological analysis of enzymes.....	128
5.2.6.1. Fourier transform infrared spectroscopy (FTIR) .....	128
5.2.6.2. Field emission scanning electron microscopy (FE-SEM) .....	128
5.2.6.3. X-ray photoelectron spectroscopy (XPS) .....	129
5.2.7. Statistical analysis .....	129
<b>5.3. Results and discussion .....</b>	<b>130</b>
5.3.1. Performance and reusability of Lipozyme TL IM and RM IM .....	130
5.3.2. Immobilized lipases under SCCO <sub>2</sub> conditions.....	137
5.3.2.1. Effect of exposure time and pressurization/depressurization on enzyme activity .....	137
5.3.2.2. Effect of exposure time and pressurization/depressurization on enzyme structure .....	144
<b>5.4. Conclusions.....</b>	<b>148</b>
<b>5.5. References .....</b>	<b>149</b>
6. LIPASE-CATALYZED INTERESTERIFICATION BETWEEN CANOLA OIL AND FULLY-HYDROGENATED CANOLA OIL IN CONTACT WITH SUPERCRITICAL CARBON DIOXIDE: OPTIMIZATION AND PHYSICOCHEMICAL PROPERTIES OF PRODUCTS .....	
<b>6.1. Introduction.....</b>	<b>151</b>
<b>6.2. Materials and methods .....</b>	<b>153</b>

6.2.1. Materials .....	153
6.2.2. Process optimization .....	154
6.2.2.1. Experimental set up and reaction protocols .....	154
6.2.2.2. Determination of degree of interesterification .....	156
6.2.3. Characterization of the products .....	157
6.2.3.1. Reaction protocol .....	157
6.2.3.2. Purification of the reaction products .....	158
6.2.3.3. Determination of the reaction intermediates .....	159
6.2.3.4. Determination of the triglyceride composition .....	159
6.2.3.5. Melting characteristics .....	160
6.2.3.6. Solid fat content .....	160
<b>6.3. Results and discussion .....</b>	<b>161</b>
6.3.1. Effect of reaction parameters on degree of interesterification .....	161
6.3.2. Physicochemical properties of the products .....	165
6.3.2.1. Chemical composition of the products.....	165
6.3.2.2. Melting and crystallization behaviour .....	170
6.3.2.3. Solid fat content .....	173
<b>6.4. Conclusions.....</b>	<b>175</b>
<b>6.5. References .....</b>	<b>175</b>
<b>7. POLYMORPHISM, MICROSTRUCTURE AND RHEOLOGICAL PROPERTIES OF ENZYMATICALLY INTERESTERIFIED CANOLA OIL AND FULLY-HYDROGENATED CANOLA OIL UNDER SUPERCRITICAL CARBON DIOXIDE .....</b>	<b>179</b>
<b>7.1. Introduction.....</b>	<b>179</b>
<b>7.2. Materials and methods .....</b>	<b>181</b>
7.2.1. Materials .....	181
7.2.2. Enzymatic interesterification under SCCO <sub>2</sub> .....	181
7.2.3. Purification of the reaction products.....	182
7.2.4. X-ray diffraction analysis .....	182
7.2.5. Polarized light microscopy .....	183
7.2.6. Rheological properties .....	184
<b>7.3. Results and discussion .....</b>	<b>184</b>
7.3.1. Polymorphism of the initial blends and the interesterified products ....	185
7.3.2. Microstructure of initial blends and interesterified products .....	190
7.3.3. Rheological properties of initial blends and interesterified products ...	193
<b>7.4. Conclusions .....</b>	<b>196</b>

<b>7.5. References .....</b>	<b>196</b>
<b>8. CONCLUDING REMARKS .....</b>	<b>199</b>
<b>    8.1. Summary and conclusions.....</b>	<b>199</b>
<b>    8.2. Recommendations for future work .....</b>	<b>205</b>
<b>    8.3. Potential significance .....</b>	<b>207</b>
<b>    8.4. References .....</b>	<b>209</b>

## List of tables

<b>Table 2-1.</b> Critical properties of fluids of interest in supercritical process .....	10
<b>Table 2-2.</b> Physical properties of supercritical fluids (SCF) compared to those of liquid and gas .....	11
<b>Table 3-1.</b> Fatty acid composition of fully-hydrogenated canola oil (FHCO) and canola oil considering fatty acids of more than 1% .....	62
<b>Table 3-2.</b> Viscosity (mPa.s) of canola oil and its blend with canola stearin saturated with CO <sub>2</sub> at various pressures and temperatures at a shear rate of 300 s <sup>-1</sup> .....	69
<b>Table 3-3.</b> Model parameters for the correlation of viscosity of CO <sub>2</sub> -expanded canola oil using Equation (3.2) .....	74
<b>Table 3-4.</b> Power law parameters (flow behaviour index ‘n’ and logarithm of consistency index ‘K’) for canola oil and its blend with fully-hydrogenated canola oil (FHCO) (30 wt.%), both saturated with CO <sub>2</sub> at different temperatures .....	75
<b>Table 3-5.</b> Fitting results of Grunberg and Nissan model (Model 1, Eq. (3.7)) and modified Grunberg and Nissan model (Model 2, Eq. (3.10)) to experimental viscosity data of canola oil and its blend with fully-hydrogenated canola oil (FHCO) in equilibrium with CO <sub>2</sub> .....	83
<b>Table 4-1.</b> Fatty acid composition of fully-hydrogenated canola oil (FHCO) and canola oil .....	90
<b>Table 4-2.</b> Critical properties of carbon dioxide, canola oil and its blend with fully-hydrogenated canola oil (FHCO) (30 wt.%). ....	99
<b>Table 4-3.</b> Optimal binary interaction parameters correlated with Peng-Robinson equation of state (PR-EoS) using Quadratic (Q) and Panagiotopoulos-Reid (PR) mixing rules for CO <sub>2</sub> -saturated liquid lipid phase .....	102
<b>Table 4-4.</b> Optimal binary interaction parameters correlated with Soave-Redlich-Kwong equation of state (SRK-EoS) using Quadratic (Q) and Panagiotopoulos-Reid (PR) mixing rules for CO <sub>2</sub> -saturated liquid lipid phase .....	103
<b>Table 4-5.</b> Density of CO <sub>2</sub> -expanded canola oil at various temperatures and pressures.....	109
<b>Table 4-6.</b> Density of CO <sub>2</sub> -expanded canola oil and fully-hydrogenated canola oil blend (FHCO) (30 wt.%) at 70 °C at different pressures.....	110
<b>Table 4-7.</b> Modified Tait equation parameters (C=0.0446) .....	115
<b>Table 5-1.</b> The effect of reusing Lipozyme TL IM and RM IM for interesterification between canola oil and fully-hydrogenated canola oil up to 4 times of 7 h each under SCCO <sub>2</sub> at 65 °C and 17.5 MPa on triglycerides composition (mol.%) and conversion rate (%) .....	133

<b>Table 5-2.</b> The effect of reusing Lipozyme TL IM and RM IM for transesterification of canola oil and fully-hydrogenated canola oil up to 4 times of 7 h each under SCCO <sub>2</sub> at 65 °C and 17.5 MPa on reaction intermediates (or hydrolysis products) (wt.%).....	134
<b>Table 5-3.</b> The effect of exposure time of Lipozyme TL IM and RM IM to SCCO <sub>2</sub> at 65 °C and 17.5 MPa on triglyceride composition (mol%) and conversion rate of interesterified canola oil and fully-hydrogenated canola oil (70:30 w/w) under SCCO <sub>2</sub> at the same conditions for 2 h. Interesterification with untreated enzymes at the same conditions is considered as control .....	138
<b>Table 5-4.</b> The effect of exposure time of Lipozyme TL IM and RM IM to SCCO <sub>2</sub> at 65 °C and 17.5 MPa on produced reaction intermediates (wt. %) of interesterified canola oil and fully-hydrogenated canola oil (70:30 w/w) under SCCO <sub>2</sub> at the same conditions for 2 h. Interesterification with untreated enzymes at the same conditions is considered as control .....	139
<b>Table 5-5.</b> The effect of pressurization/depressurization cycles of Lipozyme TL IM and RM IM under SCCO <sub>2</sub> at 65 °C and 17.5 MPa on triglyceride composition (mol %) of interesterified canola oil and fully-hydrogenated canola oil (70:30 w:w) and conversion rate under SCCO <sub>2</sub> at the same conditions for 2 h. Interesterification with untreated enzymes at the same conditions is considered as control .....	140
<b>Table 5-6.</b> The effect of pressurization/depressurization cycles of Lipozyme TL IM and RM IM under SCCO <sub>2</sub> at 65 °C and 17.5 MPa on reaction intermediates (wt. %) of interesterified canola oil and fully-hydrogenated canola oil (70:30 w/w) using SCCO <sub>2</sub> at the same conditions for 2 h. Interesterification with untreated enzymes at the same conditions is considered as control .....	142
<b>Table 6-1.</b> Triglyceride composition (% peak area) of canola oil and fully-hydrogenated canola oil (FHCO).....	166
<b>Table 6-2.</b> Amounts of reaction intermediates (wt.%) of non-interesterified initial blends (NIB) of canola oil and fully-hydrogenated canola oil (FHCO) and enzymatically interesterified productss (EIP) and purified enzymatically interesterified products (PEIP) in contact with SCCO <sub>2</sub> at 65 °C and 10 MPa after 2 h using SCCO <sub>2</sub> -dried enzymes.....	168
<b>Table 6-3.</b> Triglyceride composition (% peak area) of non-interesterified initial blends (NIB) of canola oil and fully-hydrogenated canola oil (FHCO) and purified enzymatically interesterified products (PEIP) obtained at 65 °C and 10 MPa after 2 h using SCCO <sub>2</sub> -dried enzyme .....	169
<b>Table 7-1.</b> Polymorphic forms of non-interesterified blends (NIB) and purified enzymatically interesterified products (PEIP) of canola oil and fully-hydrogenated canola oil (FHCO) crystallized at 24 °C and 5 °C for 12 h .....	188

## List of figures

<b>Figure 2-1.</b> Schematic phase diagram of pure CO <sub>2</sub> .....	9
<b>Figure 2-2.</b> Viscosity of CO <sub>2</sub> at sub and supercritical conditions at different temperatures and pressures .....	12
<b>Figure 2-3.</b> Density of CO <sub>2</sub> at sub and supercritical conditions at different temperatures and pressures .....	14
<b>Figure 2-4.</b> Catalytic mechanism for lipase-mediated interesterification .....	26
<b>Figure 3-1.</b> High pressure rheometer: 1, CO <sub>2</sub> cylinder; 2, CO <sub>2</sub> filter; 3, and 12, pressure gauges; 4, 10, 14, and 15, needle valves; 5, 7, and 11 check valves; 6, piston pump; 8, high pressure cell; 9, pressure regulator; 13, rheometer equipped with high pressure cell .....	64
<b>Figure 3-2.</b> Phase equilibria unit: 1, CO <sub>2</sub> cylinder; 2, CO <sub>2</sub> filter; 3 and 8, pressure gauges; 4, 6, 7, 14, and 16, needle valves; 5, manual pump; 9, light source; 10, temperature indicator; 11, heated water bath; 12, high pressure view vessel; 13, magnetic stirrer; 15, video camera.....	67
<b>Figure 3-3.</b> Viscosity of canola oil in equilibrium with CO <sub>2</sub> as a function of pressure at different temperatures at a shear rate of 300 s <sup>-1</sup> . Curves fitted based on Equation (3.2). Error bars represent standard deviation based on three replications .....	70
<b>Figure 3-4.</b> Viscosity of canola oil in equilibrium with CO <sub>2</sub> as a function of pressure at 40 °C determined in this study at a shear rate of 300 s <sup>-1</sup> compared to the literature data for fish oil (Seifried and Temelli, 2011) and cocoa butter (Calvignac et al., 2010) both at 40 °C.....	72
<b>Figure 3-5.</b> Viscosity of canola oil and the blend containing 30 wt.% FHCO in equilibrium with CO <sub>2</sub> as a function of pressure at 65 °C at a shear rate of 300 s <sup>-1</sup> . Error bars represent standard deviation based on three replications.....	73
<b>Figure 3-6.</b> Flow behaviour index of canola oil as a function of pressure at different temperatures. Error bars represent standard deviation based on three replications .....	77
<b>Figure 3-7.</b> Consistency index of canola oil saturated with CO <sub>2</sub> at different temperatures as a function of pressure. Error bars represent standard deviation based on three replications .....	77
<b>Figure 3-8.</b> Solubility of CO <sub>2</sub> in canola oil and its blend with fully-hydrogenated canola oil (FHCO) (30 wt.%) at different pressures and temperatures.....	79
<b>Figure 3-9.</b> Viscosity of CO <sub>2</sub> -saturated canola oil and its blend with fully-hydrogenated canola oil (FHCO) (30 wt.%) at different temperatures as a function of mass fraction of CO <sub>2</sub> .....	80

<b>Figure 4-1.</b> Volumetric expansion in the high pressure view cell: a) The glass micro-scale and its stainless steel holder designed for measuring volumetric expansion; b) Images of canola oil in equilibrium with CO <sub>2</sub> at different pressures at 40 °C .....	92
<b>Figure 4-2.</b> Apparatus for measuring density of liquids in equilibrium with CO <sub>2</sub> . A) view cell, B) temperature controlled air bath, C) electric heaters, D) glass sinker, E) syringe pump, F) CMOS camera with microscope lens, G) light source, H) circulation pump, I) thermistor, J) computer, K) CO <sub>2</sub> tank. Insert: 3D model of spring balance with sinker and microscopic scale to measure density .....	95
<b>Figure 4-3.</b> P-x diagrams of CO <sub>2</sub> -saturated liquid lipid phases at different temperatures and pressures correlated by Peng-Robinson equation of state (PR-EoS) and Soave-Redlich-Kwong equation of state (SRK-EoS) using quadratic (Q) and Panagiotopoulos-Reid (PR) mixing rules (lines) and experimental data (markers) found in this and previous (Section 3.3.3) studies: a) CO <sub>2</sub> -expanded canola oil at 40 °C; b) CO <sub>2</sub> -expanded canola oil at 70 °C; c) CO <sub>2</sub> -expanded canola oil and fully-hydrogenated canola oil blend (FHCO) (30 wt.%) at 70 °C. Error bars represent standard deviation based on three replications .....	101
<b>Figure 4-4.</b> Relative volumetric expansion of canola oil and its blend with fully-hydrogenated canola oil (FHCO) (30 wt.%) in equilibrium with CO <sub>2</sub> at various pressures and temperatures. Error bars represent standard deviation based on triplicate measurements.....	104
<b>Figure 4-5.</b> a) Relative volumetric expansion of canola oil and its blend with fully-hydrogenated canola oil (FHCO) (30 wt.%) versus mass fraction of CO <sub>2</sub> in the lipid liquid phase, and b) pressure versus mass fraction of CO <sub>2</sub> at various temperatures .....	107
<b>Figure 4-6.</b> Density of canola oil at 40, 55, and 70 °C and its blend with fully-hydrogenated canola oil (FHCO) (30 wt.%) at 70 °C in equilibrium with CO <sub>2</sub> as a function of pressure. Curves represent correlation based on the modified Tait equation (Eq. (4.21)) .....	110
<b>Figure 4-7.</b> Density of pure canola oil at various temperatures and pressures..	112
<b>Figure 4-8.</b> Density of canola oil and its blend with fully-hydrogenated canola oil (FHCO) (30 wt.%) in equilibrium with high pressure CO <sub>2</sub> as a function of pressure determined in this study compared to literature data for CO <sub>2</sub> -saturated fish oil at 70 °C (Seifried and Temelli, 2009).....	112
<b>Figure 4-9.</b> The density of canola oil at 40 and 70 °C and its blend with fully-hydrogenated canola oil (30 wt. %) at 70 °C in equilibrium with high pressure CO <sub>2</sub> versus the mass fraction of CO <sub>2</sub> in the liquid lipid phase in this study and the literature data for CO <sub>2</sub> -saturated fish oil at 40 °C (Seifried and Temelli, 2009) .....	113
<b>Figure 5-1.</b> Performance of Lipozyme TL IM and RM IM for interesterification between canola oil and fully-hydrogenated canola oil (70:30 w/w) under SCCO <sub>2</sub> at 65 °C and 17.5 MPa over 7.5 h: (a) Conversion rate and (b) total amount of produced intermediates during the reaction .....	131

- Figure 5-2.** Triglyceride (TG) components of interesterified canola oil and fully-hydrogenated canola oil (70:30 w/w) under  $\text{SCCO}_2$  at 65 °C and 17.5 MPa over 7.5 h of reaction: (a) Lipozyme TL IM and (b) Lipozyme RM IM ..... 132
- Figure 5-3.** The effect of reusing of immobilized lipases for interesterification between canola oil and fully-hydrogenated canola oil (70:30 w/w) under  $\text{SCCO}_2$  at 65 °C and 17.5 MPa with each cycle of 7 h on the total amount of intermediates produced during the reaction. Bars with the same superscripts for each enzyme type have no significant difference ( $p > 0.05$ ) ..... 135
- Figure 5-4.** FE-SEM micrographs of immobilized lipases before and after reuse (4×7 h) for interesterification between canola oil and fully-hydrogenated canola oil under  $\text{SCCO}_2$  at 65°C and 17.5 MPa ..... 136
- Figure 5-5.** The effect of pressurization/depressurization cycles of Lipozyme TL IM and RM IM under  $\text{SCCO}_2$  at 65°C and 17.5 MPa on total amount of produced intermediates during interesterification of canola oil and fully-hydrogenated canola oil (70:30 w/w) under  $\text{SCCO}_2$  at the same conditions for 2 h. The interesterification with untreated enzymes is considered as control treatment. Bars with the same letter in each enzyme type have no significant difference ( $p > 0.05$ ) ..... 143
- Figure 5-6.** Infrared spectra of untreated and  $\text{SCCO}_2$ -treated Lipozyme RM IM and TL IM with 12 pressurization/depressurization cycles (12 p/d) at 17.5 MPa and 65°C in (a) and (c) and baseline corrected and normalized spectra in the region of amide I in (b) and (d): (a) and (b) represent Lipozyme TL IM; (c) and (d) represent Lipozyme RM IM ..... 146
- Figure 5-7.** FE-SEM micrographs of immobilized lipases before and after 12 pressurization/depressurization cycles under  $\text{SCCO}_2$  at 65°C and 17.5 MPa .... 147
- Figure 6-1.** High pressure batch stirred reactor: 1,  $\text{CO}_2$  cylinder; 2, Syringe pump; 3, 7, 11, 12, and 13, Shut-off valve; 4, Pressure gauge; 5, Temperature controller; 6, Rupture disk; 8, High pressure vessel; 9, Heating Jacket; 10, Stirrer; 14, Collector..... 154
- Figure 6-2.** Effect of Lipozyme TL IM load (w/v of initial substrates) on the conversion rate of interesterification between canola oil and fully-hydrogenated canola oil (FHCO) (70:30, w/w) in contact with  $\text{SCCO}_2$  at 65 °C and 17.5 MPa over 7.5 h ..... 162
- Figure 6-3.** Effect of pressure on the conversion of lipase-catalyzed interesterification between canola oil and fully-hydrogenated canola oil (FHCO) (70:30, w/w) with Lipozyme TL IM at 6% (w/v) of initial substrates in contact with  $\text{SCCO}_2$  at 65 °C over 7.5 h ..... 163
- Figure 6-4.** Effect of the ratio (%, w/w) of canola oil and fully-hydrogenated canola oil (FHCO) (wt.% FHCO) on lipase-catalyzed interesterification in contact with  $\text{SCCO}_2$  at 65 °C and 10 MPa over 7.5 h ..... 165
- Figure 6-5.** DSC of canola oil, fully hydrogenated canola oil (FHCO), their non-interesterified initial blends (NIB) and purified enzymatically interesterified

products (PEIP) in contact with $\text{SCCO}_2$ at 65 °C and 10 MPa after 2 h using $\text{SCCO}_2$ -dried enzyme: (a) melting profile and (b) crystallization profile.....	171
<b>Figure 6-6.</b> SFC evolution of non-interesterified initial blends (NIB) of canola oil and fully-hydrogenated canola oil (FHCO) and purified enzymatically interesterified products (PEIP) of canola oil and FHCO in contact with $\text{SCCO}_2$ at 65 °C and 10 MPa after 2 h using $\text{SCCO}_2$ -dried enzyme .....	174
<b>Figure 7-1.</b> X-ray diffraction patterns for non-interesterified initial blends (NIB) and purified enzymatically interesterified products (PEIP) of canola oil and fully-hydrogenated canola oil (FHCO) crystallized for 12 h at (a) 24 °C and (b) 5 °C .....	186
<b>Figure 7-2.</b> Crystal morphology of non-interesterified initial blends (NIB) and purified enzymatically interesterified products (PEIP) of canola oil and fully-hydrogenated canola oil (FHCO) crystallized at 24 °C for 12 h: (a) FHCO; (b) 10% FHCO (NIB); (c) 30% FHCO (NIB); (d) 30% FHCO (PEIP); (e) 50% FHCO (NIB); and (f) 50% FHCO (PEIP). ....	191
<b>Figure 7-3.</b> Storage ( $G'$ ) and loss ( $G''$ ) moduli as a function of strain for non-interesterified initial blends (NIB) and purified enzymatically interesterified products (PEIP) of canola oil and fully-hydrogenated canola oil (FHCO) crystallized at 25 °C for 2 h. Solid and empty markers represent $G'$ and $G''$ , respectively .....	194
<b>Figure 7-4.</b> Storage ( $G'$ ) and loss ( $G''$ ) moduli determined in the linear viscoelastic (LVE) range of non-interesterified initial blends (NIB) and purified enzymatically interesterified products (PEIP) of canola oil and fully-hydrogenated canola oil (FHCO) crystallized at 24 °C for 2 h .....	194

## List of abbreviations

A <sub>12</sub>	binary parameter
AARD	average absolute relative deviation
AMF	anhydrous milk fat
APPI-MS	atmospheric pressure photo ionization detector
BSTFA	N,O-bis-(trimethylsilyl) trifluoracetamide
CX	CO <sub>2</sub> -expanded
D	binary diffusion coefficient
DG	diglycerides
DSC	differential scanning calorimetry
ELSD	evapourative light scattering
EoS	equation of state
FAEE	fatty acid ethyl ester
FDA	food and drug administration
FE-SEM	field emission scanning electron microscopy
FFA	free fatty acid
FHCO	fully-hydrogenated canola oil
FTIR	fourier transform infrared spectroscopy
G'	storage modulus
G''	loss modulus
GC	gas chromatography
G <sub>ij</sub>	interaction parameter
HPLC	high performance liquid chromatography
K	consistency index
k <sub>m</sub>	michaelis-menten
LVE	linear viscoelastic
MG	monoglyceride
MW	molecular weight (g mol <sup>-1</sup> )
n	flow behaviour index
N <sub>A</sub>	avogadro number
NIB	non-interesterified initial blend
P <sub>C</sub>	critical pressure (MPa)
PEIP	purified enzymatically interesterified product
PLM	polarized light microscopy
PR	Peng-Robinson
RD	relative deviation
SCCO <sub>2</sub>	supercritical carbon dioxide
SCF	supercritical fluid
SFC	solid fat content

SRK	soave-redlich-kwong
T <sub>ambient</sub>	ambient temperature
T <sub>C</sub>	critical temperature (K)
TFA	<i>trans</i> fatty acid
TG	triglyceride
TMCS	trimethylchlorosilane
v	molar volume (cm <sup>3</sup> mol <sup>-1</sup> )
V <sub>0</sub>	volume at atmospheric pressure
V <sub>C</sub>	critical molar volume (cm <sup>3</sup> mol <sup>-1</sup> )
V <sub>P</sub>	volume at elevated pressure
w	mass fraction
x	mole fraction
XPS	x-ray photoelectron spectroscopy
XRD	x-ray diffraction
ΔV <sup>±</sup>	activation volume
ΔV <sub>rel</sub>	relative volume change

### Greek symbols

γ	shear rate (s <sup>-1</sup> )
η	viscosity (mPa.s)
ρ	density (kg m <sup>-3</sup> )
σ	shear stress (Pa)
υ	reaction rate
ω	acentric factor

## **1. Introduction and thesis objectives**

Canola is the major oilseed crop of Canada with triolein as the main triglyceride (TG) component in its oil. Triolein is composed of a glycerol backbone, esterified with three oleic acids, which is a mono-unsaturated fatty acid. The functional, physicochemical and nutritional properties of TG are determined by the nature and type of fatty acids present in their structures (Ratnayake and Daun, 2004). Canola oil, like other edible oils, is not always ideal for final use in some food applications; therefore, modification of fats and oils is carried out because of nutritional, physical, functional, and economic reasons.

Partial hydrogenation is one of the main processes employed for the modification of fats and oils, but hardened fats produced by partial hydrogenation contain *trans* fatty acids (TFA) (Puri, 1978; Martin et al., 2007). TFA are undesirable from a nutritional stand point since they have been shown to be a major risk factor for cardiovascular diseases (Judd et al., 2002; Baer et al., 2004; Ascherio, 2006). Despite recent government policies to reduce the use of partially hydrogenated fats in many countries, the worldwide production of partial hydrogenated vegetable oils is estimated to be at 6 million tons/y (Beers et al., 2008).

The U.S. Food and Drug Administration (FDA) has ruled that the amount of *trans* fats in a food item must be stated on the label; a food item can be labeled as 0% *trans* if it contains less than 0.5 g *trans* fats per serving (Tang et al., 2012). Therefore, there is an urgent need to find alternative methods that reduce TFA content in plastic fats.

Interesterification can be an approach for eliminating the formation of *trans*-isomers (Ribeiro et al., 2009). The most common type of interesterification used for the production of margarines and confectionary fats is chemical interesterification in which metal alkylate catalysts are used (Petrauskaitė et al., 1998a, b; Karabulut et al., 2004; Dian et al., 2007). This type of modification of fats leads to a fully random structure of TG because there is no selectivity for fatty acid positioning on the glycerol backbone. Also, the catalysts used in this procedure are toxic and lead to darkening of the final products; therefore, downstream processes are necessary to remove color and catalysts. On the other hand, lipase-catalyzed reactions can take place under milder conditions with fewer side reactions, leading to cleaner final products. Another very important advantage of the lipase-catalyzed reactions is the selectivity for fatty acid positioning on the glycerol backbone by using stereo-specific lipases. Thus, lipase-catalyzed reactions using *sn*-1,3 stereo-specific lipases offer better control over reactions (Marangoni and Rousseau, 1995; Xu, 2003).

Stricter environmental regulations related to the use of organic solvents in many areas of the fats and oils industry and increasing demand for “natural” products have stimulated the search for sustainable technologies for lipid processing (Seifried and Temelli, 2010).

Supercritical fluid technology is a rapidly growing alternative to some of the conventional methods of extraction, reaction, fractionation and analysis (Schutz, 2007). This is due to several factors: (1) Supercritical fluids (SCF) allow high rates of mass transfer due to their high diffusivity and low viscosity; (2) the

solvation power of a SCF, as well as its performance as reaction media, are easily influenced by temperature and pressure; and (3) the supercritical solvent is readily removed after extraction or reaction by reducing pressure (Subramaniam and McHugh, 1986; Ramsey et al., 2009).

Supercritical carbon dioxide (SCCO<sub>2</sub>), at pressure and temperature conditions above its critical point of 7.4 MPa and 31 °C, has solvent properties in between those of a liquid and a gas. SCCO<sub>2</sub> can be used as reaction media since its low viscosity and high diffusivity enhance transport of substrates and products through the pores of enzyme support, resulting in the hypothesis that it can lead to higher reaction rates (Hammond et al., 1985; Randolph et al., 1985; Wimmer and Zarevucka, 2010). Conducting lipid reactions in one single supercritical phase is not feasible because of the low solubility of lipids in SCCO<sub>2</sub> at moderate pressures. However, enzymatic reactions can be conducted in the liquid phase of lipids saturated with CO<sub>2</sub> under moderate pressures and benefit from the advantages offered by CO<sub>2</sub>-expanded (CX) lipids (Seifried and Temelli, 2010).

In spite of the many advantages of conducting reactions in SCCO<sub>2</sub>, there are only a few studies about lipase-catalyzed modification of fats and oils using SCCO<sub>2</sub>. Therefore, fundamental studies are necessary to demonstrate the effects of various processing parameters involved in conducting the lipase-catalyzed interesterification between CX-canola oil and fully-hydrogenated canola oil (FHCO) on the physical properties (viscosity, density, CO<sub>2</sub> solubility, and volumetric expansion) of the initial substrates, reaction conversion rates, and product composition as well as the physicochemical properties of the final

product. Better understanding of the physical properties of vegetable oils in contact with  $\text{SCCO}_2$  will be helpful for designing high pressure processes and potential scale up. As well, determining the physicochemical properties the final reaction products is essential for optimal formulation of base-stocks of margarine and confectionary fats to meet industrial demands.

### **1.1. Hypothesis**

Herein, it was hypothesized that  $\text{SCCO}_2$  can be used as a reaction medium for lipase-catalyzed interesterification of vegetable oils to produce a base-stock for zero-*trans* margarine.

### **1.2. Thesis objectives**

The overall objective of this thesis research was to accomplish lipase-catalyzed interesterification between canola oil and FHCO in contact with  $\text{SCCO}_2$  using a high pressure batch stirred reactor. The specific objectives were:

- To determine the viscosity and rheological behaviour of canola oil and its blend with FHCO in equilibrium with  $\text{SCCO}_2$ , as well as the solubility of  $\text{CO}_2$  in canola oil, and its blend at different temperatures and pressures, and to correlate the viscosity data with mass fraction of  $\text{CO}_2$  in the liquid phase using correlative methods (Chapter 3),
- To determine the density and volumetric expansion of canola oil and its blend with FHCO in equilibrium with  $\text{SCCO}_2$  at different temperatures and pressures, and to apply engineering models for the solubility of  $\text{CO}_2$  in

the liquid phase and for the density of the liquid phase using cubic equations of state and correlative methods (Chapter 4),

- To determine the performance and reusability of two immobilized lipases, Lipozyme TL IM and RM IM, under  $\text{SCCO}_2$  for interesterification between canola oil and FHCO, and to investigate the effects of incubation of immobilized lipases under  $\text{SCCO}_2$  and pressurization/depressurization cycles at 65 °C and 17.5 MPa on enzyme activity and potential structural changes (Chapter 5),
- To conduct interesterification between canola oil and FHCO in contact with  $\text{SCCO}_2$  using Lipozyme TL IM in order to determine the effects of enzyme load, pressure, and the ratio of initial reactants on conversion rate, and to determine the composition and physical properties (melting behaviour and solid fat content) of the initial blend and final products obtained at optimal conditions (Chapter 6), and
- To study polymorphism, microstructure and rheological properties of canola oil and FHCO blends before and after interesterification in contact with  $\text{SCCO}_2$  (Chapter 7).

### 1.3. References

Ascherio, A. (2006). Trans fatty acids and blood lipids. *Atherosclerosis Supplements*, **7** (2): 25-27.

Baer, D.J., Judd, J.T., Clevidence, B.A. and Tracy, R.P. (2004). Dietary fatty acids affect plasma markers of inflammation in healthy men fed controlled diets: A randomized crossover study. *American Journal of Clinical Nutrition*, **79** (6): 969-973.

Beers, A., Ariaansz, R. and Okonek, D. (2008). *Trans* fatty acids. In *Trans isomer control in hydrogenation of edible oils*, A.J. Dijkstra, R.J. Hamilton and W. Hamm, Eds. Blackwell Publishing Ltd: Oxford, pp 147-180.

Dian, N., Sundram, K. and Idris, N.A. (2007). Effect of chemical interesterification on triacylglycerol and solid fat contents of palm stearin, sunflower oil and palm kernel olein blends. *European Journal of Lipid Science and Technology*, **109** (2): 147-156.

Hammond, D.A., Karel, M., Klibanov, A.M. and Krukonis, V.J. (1985). Enzymatic-reactions in supercritical gases. *Applied Biochemistry and Biotechnology*, **11** (5): 393-400.

Judd, J.T., Baer, D.J., Clevidence, B.A., Kris-Etherton, P., Muesing, R.A. and Iwane, M. (2002). Dietary *cis* and *trans* monounsaturated and saturated fat and plasma lipids and lipoproteins in men. *Lipids*, **37** (2): 123-131.

Karabulut, I., Turan, S. and Ergin, G. (2004). Effects of chemical interesterification on solid fat content and slip melting point of fat/oil blends. *European Food Research and Technology*, **218** (3): 224-229.

Marangoni, A.G. and Rousseau, D. (1995). Engineering triacylglycerols: The role of interesterification. *Trends in Food Science & Technology*, **6**: 329-335.

Martin, C.A., Milinsk, M.C., Visentainer, J.V., Matsushita, M. and De-Souza, N.E. (2007). Trans fatty acid-forming processes in foods: A review. *Anais Da Academia Brasileira De Ciencias*, **79** (2): 343-350.

Petrauskaite, V., De Greyt, W., Kellens, M. and Huyghebaert, A. (1998a). Physical and chemical properties of *trans*-free fats produced by chemical interesterification of vegetable oil blends. *Journal of the American Oil Chemists' Society*, **75** (4): 489-493.

Petrauskaite, V., De Greyt, W.F., Kellens, M.J. and Huyghebaert, A.D. (1998b). Chemical interesterification of vegetable oil blends: Optimization of process parameters. *Ocl-Oleagineux Corps Gras Lipides*, **5** (1): 65-69.

Puri, P.S. (1978). Correlations for *trans*-isomer formation during partial hydrogenation of oils and fats. *Journal of the American Oil Chemists' Society*, **55** (3): A263-A263.

Ramsey, E., Sun, Q.B., Zhang, Z.Q., Zhang, C.M. and Gou, W. (2009). Mini-review: Green sustainable processes using supercritical fluid carbon dioxide. *Journal of Environmental Sciences-China*, **21** (6): 720-726.

Randolph, T.W., Blanch, H.W., Prausnitz, J.M. and Wilke, C.R. (1985). Enzymatic catalysis in a supercritical fluid. *Biotechnology Letters*, **7** (5): 325-328.

Ratnayake, W.M.N. and Daun, J.K. (2004). Chemical composition of canola and rapeseed oils. In *Rapeseed and canola oil: Production, processing, properties and uses*, F.D. Gunstone, Ed. CRC Press: Boca Raton, FL, USA, pp 37-79.

Ribeiro, A.P.B., Basso, R.C., Grimaldi, R., Gioielli, L.A. and Goncalves, L.A.G. (2009). Effect of chemical interesterification on physicochemical properties and industrial applications of canola oil and fully hydrogenated cottonseed oil blends. *Journal of Food Lipids*, **16** (3): 362-381.

Schutz, E. (2007). Supercritical fluids and applications- a patent review. *Chemical Engineering & Technology*, **30** (6): 685-688.

Seifried, B. and Temelli, F. (2010). Unique properties of carbon dioxide-expanded lipids. *INFORM-International News on Fats, Oils and Related Materials*, **21** (1): 10-12.

Subramaniam, B. and McHugh, M.A. (1986). Reactions in supercritical fluids-a review. *Industrial & Engineering Chemistry Process Design and Development*, **25** (1): 1-12.

Tang, L., Hu, J.N., Zhu, X.M., Luo, L.P., Lei, L., Deng, Z.Y. and Lee, K.T. (2012). Enzymatic interesterification of palm stearin with cinnamomum camphora seed oil to produce zero-trans medium-chain triacylglycerols-enriched plastic fat. *Journal of Food Science*, **77** (4): C454-C460.

Wimmer, Z. and Zarevucka, M. (2010). A review on the effects of supercritical carbon dioxide on enzyme activity. *International Journal of Molecular Sciences*, **11** (1): 233-253.

Xu, X. (2003). Engineering of enzymatic reactions and reactors for lipid modification and synthesis. *European Journal of Lipid Science and Technology*, **105**: 289-304.

## **2. Literature review<sup>1</sup>**

### **2.1. Supercritical fluids**

Although organic solvents have been used extensively in the processing of biomaterials, concerns over their use in the food industry and environmental issues related to their use in industrial and analytical applications are growing (Johnson and Lusas, 1983; Ikeda, 1992). Therefore, the use of compressed gases, and in particular supercritical or near-critical fluids, has received growing attention over the last two decades. Their adjustable solvent power and the possibility to eliminate solvent residues in the final products make supercritical fluids (SCF) more advantageous than organic solvents for extraction and biocatalysis (Almeida et al., 1998).

The density of SCF can be easily adjusted to the process needs, only by changing temperature and pressure. Other important properties of SCF are their very low surface tension, low viscosity, and moderately high diffusion coefficient, resulting in improvement of mass transfer properties in reactions compared to organic solvents (Cernia et al., 1998; Srivastava et al., 2003; Romero et al., 2005). When a pure component is heated over its critical temperature at pressures above its critical pressure, it is neither a gas nor a liquid, but in a state referred to as the

---

<sup>1</sup> A version of Section 2.3 was published.

Rezaei K., Temelli F. and Jenab E. (2007). Effects of pressure and temperature on enzymatic reactions in supercritical fluids, *Biotechnol. Adv.*, 25 (3): 272-280. (Reprinted with permission from Elsevier.)

Rezaei K., Jenab E. and Temelli F. (2007). Effects of water on enzyme performance with an emphasis on the reactions in supercritical fluids, *Crit. Rev. Biotechnol.*, 27(4): 183-195. (Reprinted with permission from Informa Health.)

supercritical state. There is no phase boundary between vapour and liquid in the supercritical state because the densities of vapour and liquid phases are equal and they are not distinguishable from each other (Fig. 2-1).

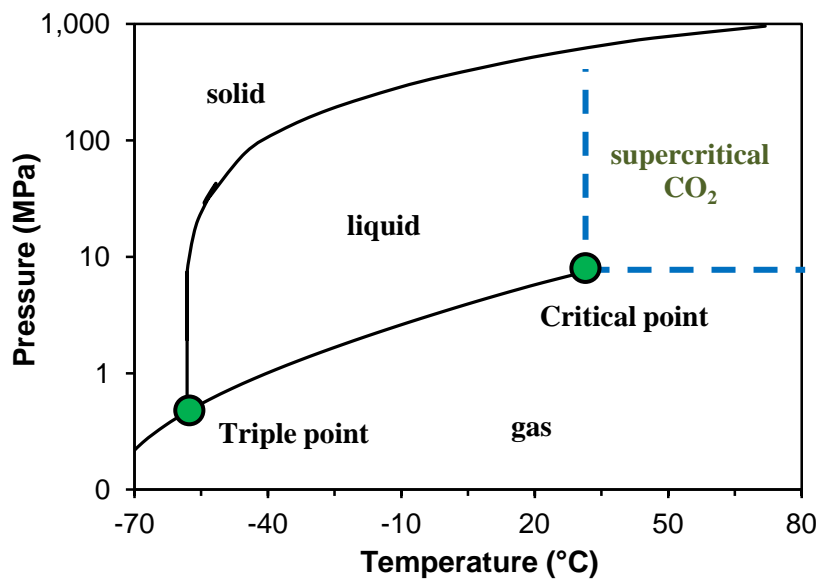


**Figure 2-1.** Schematic phase diagram of pure CO<sub>2</sub>.

Among the various SCF listed in Table 2-1, supercritical carbon dioxide (SCCO<sub>2</sub>) is the solvent of choice for food and pharmaceutical applications. SCCO<sub>2</sub> has moderate critical pressure and temperature of 7.4 MPa and 31 °C, respectively. Furthermore, SCCO<sub>2</sub> is inexpensive, readily available and safe. It provides a non-oxidizing environment that suppresses the formation of undesirable oxidation products during extraction and/or reaction. SCCO<sub>2</sub> does suffer from having a low solvent power when working with hydrophilic substrates; however, solubility of such products can be enhanced by adding a

polar co-solvent such as ethanol into  $\text{SCCO}_2$  (Friedrich et al., 1982; Fattori et al., 1988; Gómez and de la Ossa, 2000).

**Table 2-1.** Critical properties of fluids of interest in supercritical process (Pereda et al., 2007).

Fluid	Critical temperature $T_c$ (°C)	Critical pressure $P_c$ (MPa)
$\text{CO}_2$	30.97	7.37
Ethane	32.15	4.87
Propane	96.65	4.25
Water	373.95	22.06
Ammonia	132.25	11.35
n-Hexane	234.35	3.02
Methanol	239.45	8.09

### 2.1.1. Physical properties of supercritical fluids

SCF display properties that are mostly intermediate to those of liquid and gaseous states. Table 2-2 compares the orders of magnitude of some common physical properties of SCF with those corresponding to the liquid and vapour states (Pereda et al., 2007). The liquid-like density of SCF provides its high solvent power, whereas the gas-like viscosity and diffusivity, together with zero surface tension, impart excellent transport properties to the SCF compared to liquid organic solvents. Therefore, special transport properties of supercritical fluids make them feasible for processes involving mass transfer such as extraction, reaction, and fractionation (Subramaniam and McHugh, 1986; Lopes et al., 2012; Rawson et al., 2012). Although measuring physical properties of SCF, especially when solutes are dissolved in them, is challenging, these

properties are essential for better understanding of real processing situations (Yener et al., 1998).

**Table 2-2.** Physical properties of supercritical fluids (SCF) compared to those of liquid and gas (Pereda et al., 2007).

Physical property	Gas (T <sub>ambient</sub> )	SCF (T <sub>C</sub> , P <sub>C</sub> )	Liquid (T <sub>ambient</sub> )
Density (kg m <sup>-3</sup> )	0.6-2	200-500	600-1600
Viscosity (mPa.s)	0.01-0.3	0.01-0.03	0.2-3
Thermal conductivity (W m <sup>-1</sup> K <sup>-1</sup> ) *	0.01-0.025	maximum	0.1-0.2
Diffusion coefficient (10 <sup>6</sup> m <sup>2</sup> s <sup>-1</sup> )	10-40	0.07	0.0002-0.002
Surface tension (N m <sup>-1</sup> )	-	-	20-40

\*Thermal conductivity has maximum values in the near critical region, highly dependent on temperature.

### 2.1.1.1. Viscosity

Viscosity is a measure of the resistance of a fluid to flow when deformed by shear stress. The viscosity of a fluid depends on thermodynamic state variables such as temperature, pressure and density. Generally, the viscosity of fluids in the supercritical state at isothermal conditions increases with pressure and at isobaric conditions it decreases with temperature (Mukhopadhyay, 2000; Kemmere, 2005). Figure 2-2 shows the variation of CO<sub>2</sub> viscosity with at different temperatures and pressures (Lemmon et al., 2010).

There are different methods for measuring the viscosity of pure CO<sub>2</sub> or binary and multi-component mixtures of SCCO<sub>2</sub> containing a solute. High pressure capillary instrument, oscillating disc viscometer, falling ball viscometer, and rolling ball viscometer are the most commonly used methods to measure

viscosity at high pressures. Determining the viscosity of CO<sub>2</sub> near the critical point is quite challenging due to the high compressibility of the fluid phase. Therefore, there are discrepancies in the reported data for the viscosity of CO<sub>2</sub> at the critical point (Michels et al., 1957).

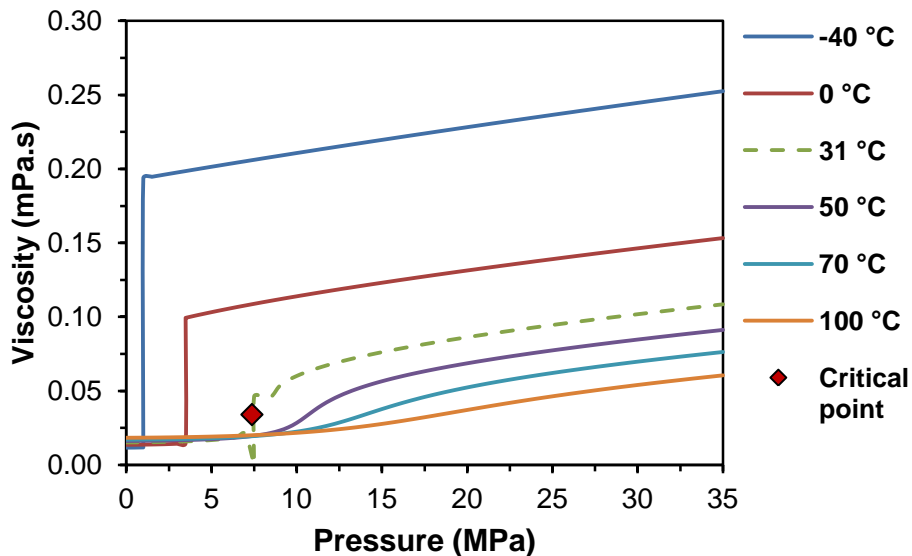


**Figure 2-2.** Viscosity of CO<sub>2</sub> at sub and supercritical conditions at different temperatures and pressures (data from Lemmon et al., 2010).

For designing separation processes using SCCO<sub>2</sub>, knowing the change in viscosity when solutes are dissolved in SCCO<sub>2</sub> is essential but such data are scarce in the literature (Yener et al., 1998; Tuan et al., 1999). For instance, Tuan et al. (1999) measured the viscosity of SCCO<sub>2</sub>/methyl oleate and SCCO<sub>2</sub>/anhydrous milk fat (AMF) at 40 °C from 10.6 to 25 MPa using a high pressure capillary viscometer. They found that solubility of 4% (wt.%) of methyl oleate caused a 14-17% increase in mixture viscosity compared to pure CO<sub>2</sub>. The

viscosities of  $\text{SCCO}_2$ +oleic acid and  $\text{SCCO}_2$ +AMF mixtures were measured at much smaller concentrations than methyl oleate because of their lower solubility in  $\text{SCCO}_2$ . Oleic acid at only 1.5% (wt.%) level contributed a 5-6% increase in viscosity, while the contribution of AMF was larger, at about 8%. Therefore, the dissolution of a small amount of such lipid-based solutes  $\text{SCCO}_2$  results in a dramatic change in the viscosity of the mixture, which, in turn, will affect the mass transfer rates during separation processes.

### **2.1.1.2. Density**

Figure 2-3 shows the variation of  $\text{CO}_2$  density with pressure at different temperatures. The solvent strength of supercritical fluids, which is an important factor in solubility-based separation processes, depends on their density. Therefore, the density of SCF and subsequently solvent strength can be adjusted by changing pressure and temperature. The density increases with pressure at different temperatures, but the slope of the isotherms in the region close to the critical point is steeper than that at higher pressures and temperatures (Lemmon et al., 2010).

Similar to viscosity of  $\text{SCCO}_2$ +solute mixtures (Section 2.1.1.1), the change in density when solutes are dissolved in  $\text{SCCO}_2$  is important to know for the design of separation processes. The densities of different  $\text{SCCO}_2$ +solutes mixtures were mainly measured by a vibrating tube densimeter, for example for capsaicin (Elizalde-Solis and Galicia-Luna, 2006) and  $\alpha$ -tocopherol (Pečar and Doleček, 2008). Pečar and Doleček (2008) measured the densities of  $\alpha$ -tocopherol in

SCCO<sub>2</sub> from 35 to 60 °C and within the pressure range of 10 to 40 MPa using a vibrating tube densimeter. They showed that the density of a SCCO<sub>2</sub>+α-tocopherol mixture containing  $5.0 \times 10^{-4}$  mole fraction of α-tocopherol changed from 720.3 to 972.0 kg.m<sup>-3</sup> at 35 °C and from 297.1 to 890.1 kg.m<sup>-3</sup> at 60 °C with a pressure increase from 10 to 40 MPa. Major change in the density with pressure was observed at higher temperatures. They also reported density enhancement with increasing concentration of α-tocopherol in SCCO<sub>2</sub> although the mixtures were infinitely dilute.

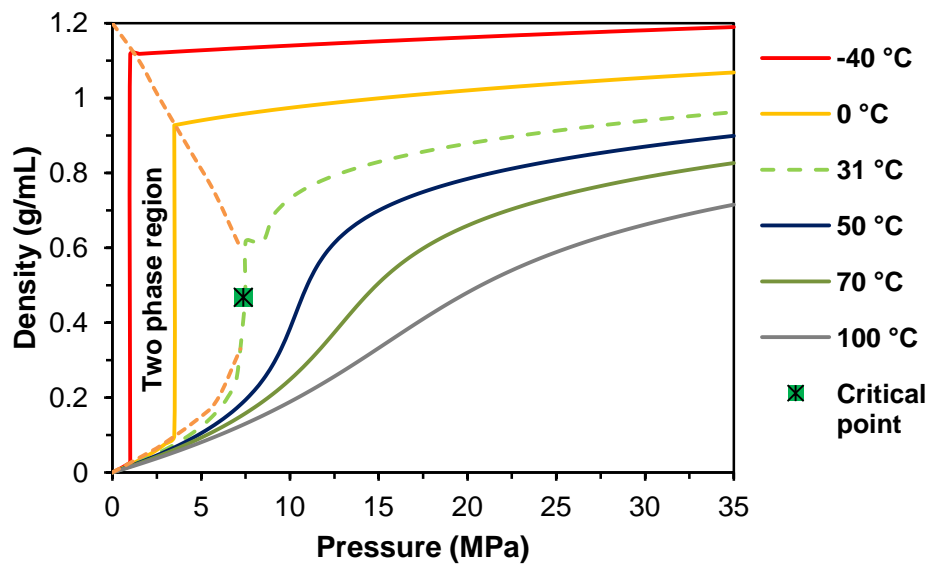


**Figure 2-3.** Density of CO<sub>2</sub> at sub and supercritical conditions at different temperatures and pressures (data from Lemmon et al. 2010).

### **2.1.2. Motivation for the use of SCCO<sub>2</sub> in reactions**

As SCCO<sub>2</sub> is a non-polar solvent, it is a potential media to conduct lipid reactions. Compressed gases, in particular SCCO<sub>2</sub>, possesse certain advantages over organic solvents for chemical catalysis and biocatalysis including the ability to adjust solvent power and eliminate solvent residues (Almeida et al., 1998). Compared to organic solvents, SCCO<sub>2</sub> is easily removed upon depressurization and does not require energy consuming downstream processes like evapouration or distillation. As discussed above, the lower viscosity and the higher diffusivity of SCCO<sub>2</sub> cause easier transport of substrates to the active sites of catalysts and in the case of enzymes within the pores of an enzyme support and, as a result, easier access to the enzyme sites leading to higher levels of reaction rates in SCCO<sub>2</sub> than in organic solvents (Cernia et al., 1998; Srivastava et al., 2003; Romero et al., 2005). In addition, SCCO<sub>2</sub> media is inert, non-flammable, non-carcinogenic, and non-mutagenic offering health and safety benefits. Based on all these advantages, performing lipid reactions in SCCO<sub>2</sub> media has received growing attention over the past decade.

### **2.2. Modification of lipids**

Vegetable oils and fats should have optimal physical, chemical and nutritional properties for their end use in food products. The most important physical properties of fats and oils are their thermal properties, including melting and crystallization behaviour. The most important chemical property is oxidative stability and those from nutritional point of view are the amount of *trans* isomers

and having an appropriate balance between saturated, monounsaturated and polyunsaturated fatty acids. In order to achieve the targeted properties and make vegetable oils and fats suitable for final use, modification of their physical, chemical and nutritional properties are performed using different techniques (Gunstone, 2006) as discussed in the following sections.

### **2.2.1. Blending**

Blending is a physical method in which two or more fats and/or oils are mixed in order to produce a product with a specified fatty acid composition to meet consistency and stability requirements. Blending can be used for producing shortenings, margarines, frying oils, and even salad oils. The base-stocks may be hydrogenated fats or oils, interesterified oils, or oil fractions, depending on the specification of the final product. The process can be monitored by measuring fatty acid composition, solid fat content and melting point until they reach the desired level (Senanayake and Shahidi, 2005).

### **2.2.2. Fractionation**

Fractionation is a process in which fats and oils are separated into fractions with different melting points. Fractionation may be used in the vegetable oil industry for removing undesirable components as in dewaxing and winterization or producing two or more functional fractions from the same original product (Krishnamurthy and Kellens, 1996). There are two main commercial processes for the fractionation of oils, which are dry fractionation and solvent fractionation. In

dry fractionation, the process has three main steps, including cooling of the oil to form nuclei for crystallization, progressive growth of crystalline and separation of crystals and liquid phases (Calliauw et al., 2010). The solvent fractionation process is based on the solubility of triglycerides (TG) in the solvent, which is dictated by fatty acid composition and distribution of fatty acids on the glycerol backbone and the nature of the solvent (Bernardini, 1976). Cocoa butter substitutes or replacers, stearin, and olein are the main products of fractionation (Illingworth, 2002).

### **2.2.3. Lipid reactions**

#### **2.2.3.1. Hydrogenation reaction**

Hydrogenation is a process employed in the vegetable oil industry to produce hardened fat from oil in order to improve physical properties for specific applications like base-stock for margarine and shortening. This process involves saturation of carbon-carbon double bonds of fatty acids by adding hydrogen in the presence of a catalyst. Vegetable oils are hydrogenated in order to form semisolid or plastic fats with functional characteristics such as sharp melting point, oxidative stability and plasticity (Senanayake and Shahidi, 2005). During hydrogenation, simultaneous reactions occur including saturation of double bonds, migration of double bonds to new positions within the fatty acid chain, and *cis-trans*-isomerization. Therefore, the double bonds in the carbon chain of fatty acids might switch to *trans* configuration and result in the formation of *trans* fatty acids (TFA) (Dijkstra, 2006).

Most unsaturated bonds in vegetable oils naturally occur in the *cis*-form. During partial hydrogenation, part of the *cis*-isomers is changed to *trans*-isomers. *Trans* isomers have dramatically higher melting points as compared to those of *cis* isomers. Therefore, the formation of *trans*-isomers is desirable in margarine such that a higher melting point can be achieved without developing a higher level of nutritionally undesirable saturated compounds. Altering hydrogenation conditions to produce higher (or lower) *trans*-isomers is referred to as “*trans*-isomer selectivity”. *Cis-trans*-isomerization is enhanced by temperature, catalyst contamination, H<sub>2</sub> pressure, catalyst dosage and lower degree of agitation during the hydrogenation process (Farr, 2005).

TFA are undesirable from the nutritional stand point since they have been shown to be a major risk factor for cardiovascular diseases (Combe et al., 2007). Therefore, health concerns about TFA have led to growing interest in interesterification, fractionation, and blending of saturated and polyunsaturated oils as alternate methods to hydrogenation.

#### **2.2.3.2. Hydrolysis reaction**

Hydrolysis reaction is mainly used to produce free fatty acids (FFA) which are used as feed stock for other industrial processes like soap production, emulsifiers, polymers, candles, and printing ink (Sonntag, 1979). The hydrolysis of carboxylic acid esters has been studied widely and a detailed mechanism has been established for both conventional (Jencks and Carriuolo, 1960; Maskill, 1999) and enzymatic reactions (Murty et al., 2002). Equation (2.1) shows the

overall reaction of esters with water through the nucleophilic attack of hydroxide at the carbonyl oxygen with the subsequent loss of alcohol moiety (Wolfe and Jeffers, 2000).



Hydrolysis of TG as major components of lipids can be typically carried out at 100–260 °C and 100–7000 kPa using 0.4–1.5 (w/w) initial water to oil ratio with or without catalysts such as acid-base catalyst (Moquin and Temelli, 2008). Lipase-catalyzed hydrolysis is an alternative method to hydrolyze lipids at lower temperatures with fewer side reactions, thus resulting in a cleaner final product. It is especially useful for hydrolysis of thermally unstable oils. It is also possible to hydrolyze TG in supercritical and subcritical media with or without the presence of enzymes. Moquin and Temelli (2008) benefitted from the properties of SCCO<sub>2</sub> in order to produce FFA from canola oil in the absence of any enzymes. They conducted reactions in SCCO<sub>2</sub> media at 250 °C and 10-30 MPa using different molar ratios of canola oil to water. They found that the maximum rate of FFA production was not affected by supercritical media (CO<sub>2</sub> vs. N<sub>2</sub>) or pressure but reaching the maximum rate was delayed at 30 MPa. Rezaei and Temelli (2000a) reported the continuous enzymatic hydrolysis of canola oil using SCCO<sub>2</sub>. They found that by pumping canola oil, water and SCCO<sub>2</sub> through a pack bed reactor containing immobilized Lipozyme RM IM, 63-67% conversion of TG could be achieved at 24-38 MPa, 35-55 °C and 3.7 L/min CO<sub>2</sub> flow rate after 4 h of reaction.

### 2.2.3.3. Esterification reaction

Esters are conventionally produced when carboxylic acids are heated with alcohols in the presence of an acid catalyst. The catalyst used is usually concentrated sulphuric acid and p-toluene sulphonic acid (Chongkhong et al., 2007; Marchetti and Errazu, 2008). The use of such catalysts has several practical and environmental problems, such as the side reactions, corrosion of the equipment, high volatility and the need for tedious isolation of products and removal of salt waste (Joseph et al., 2005). Equation (2.2) shows the reaction between an acid and an alcohol in which R and R' can be the same or different.



Lipase-catalyzed esterification is an alternative method to perform the reaction under milder conditions, which can be conducted in organic solvents or using  $\text{SCCO}_2$  as reaction media to enhance mass transfer properties. Tai and Brunner (2011) conducted enzymatic esterification of glycerol and palmitic acid in acetone expanded by high pressure  $\text{CO}_2$  using different enzymes at 40-60 °C and 6.5-8.5 MPa. They reported the optimal reaction condition to be 8.5 MPa, 50 °C, and 25% of Novozyme 435 based on the amount of dissolved fatty acid. Other researchers also investigated the esterification of oleic acid with an alcohol in  $\text{SCCO}_2$  media (Marty et al., 1990, 1992; Knez et al., 1995; Goddard et al., 2000; Laudani et al., 2007a,b).

#### 2.2.3.4. Interesterification reaction

Interestesterification, which is an acyl-exchange reaction, includes acidolysis, alcoholysis, and transesterification (Feuge, 1962; Going, 1967). Acidolysis reaction is the exchange of acyl groups between free fatty acids or their ethyl esters and TG (Eq. (2.3)).

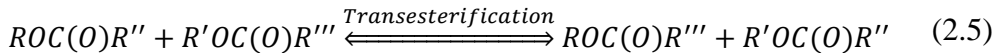


This reaction is employed to incorporate specific fatty acids with specific nutritional benefits to the TG in plant oils to improve nutritional properties (Chnadhapuram and Sunkireddy, 2012; Palla et al., 2012).

Alcoholysis is the esterification between an ester and an alcohol (Eq. (2.4)). The main use of this reaction is in glycerolysis of oils to produce monoglycerides (MG) and diglycerides (DG) (Sonntag, 1982; Willis and Marangoni, 2002).



Transesterification is the exchange of acyl groups between two esters regardless of whether they are in individual or in different fats or oils (Eq. (2.5)).



This reaction is predominantly used to improve the physicochemical properties of final products such as melting behaviour, textural properties, crystal

structure, solid fat content and oxidative stability compared to the initial material by changing the position of fatty acids in TG of individual fats and oils and their blends. Therefore, as a replacement of partial hydrogenation, transesterification is important in producing margarine and shortening products with zero-*trans* fatty acid content and improved physicochemical properties as well as in synthesizing cocoa butter substitutes and structured lipids having specific nutritional properties (Marangoni and Rousseau, 1995; Willis and Marangoni, 2002). In general, in order to produce base-stocks for margarines and shortenings, transesterification is conducted with a blend of a vegetable oil with high oleic acid content and a vegetable oil with high saturated fat, like stearin fraction or fully-hydrogenated fat. However, the type of fatty acids present and their distribution on the glycerol backbone is important in terms of nutritional aspects.

The type of fatty acid in the *sn*-2 position of TG is important because the main carriers of fatty acids through the intestinal wall are 2-monoglycerides, which are produced by pancreatic lipases during digestion. Therefore, enzymatic interesterification of fats and oils can be a good way to control the type of fatty acids present in the *sn*-2 positions of TG. Stearic acid is a long chain fatty acid with a melting point higher than the body temperature. Therefore, TG with a high amount of stearic acid has poor absorption in the human body due to their high melting point and thus poor emulsion formation and micellar solubilization in the intestinal tract (Hashim and Babayan, 1978). In addition, stearic acid has been claimed not to raise the cholesterol level in the plasma, unlike fatty acids with 4-10 carbons (Bonanome and Grundy, 1988). Thus, fully-hydrogenated oils like

fully-hydrogenated canola oil (FHCO), containing a high amount of tristearin are excellent substrates for making structured or modified lipids and fats with reduced calories (Finley et al., 1994).

All of the interesterification reactions discussed above can be conducted using either chemical catalysts or enzymes like lipases. These two types of interesterification are discussed in more detail in the following sections.

#### **2.2.3.4.1. Chemical interesterification**

In chemical interesterification using metal alkylate catalysts, acyl groups are incorporated randomly onto the glycerol backbone and this reaction produces a complete positional randomization of acyl groups in TG. The most common catalyst used for this purpose is sodium methoxide ( $\text{NaOCH}_3$ ), which has the following properties (Laning, 1985; Marangoni and Rousseau, 1995):

- 1- It is active at low temperatures ( $< 50^\circ\text{C}$ ).
- 2- It is a very strong alkaline catalyst, stronger than sodium hydroxide.
- 3- It is very reactive and in the presence of moisture it decomposes exothermically into sodium hydroxide and methanol.
- 4- It is a hazardous compound and requires careful handling and controlled storage.

Therefore, the oil to be used for interesterification should be refined to have a moisture content of less than 0.01%, free fatty acids of less than 0.05%, phosphorus content of less than 2 ppm, and peroxide value of less than 0.5 meq/kg.

Chemical interesterification can be conducted in two ways: random or directed. In random chemical interesterification (Ribeiro et al., 2009), the reaction is conducted at temperatures higher than the melting point of the highest melting TG, leading to complete shuffling of fatty acids among the available TG. In directed chemical interesterification (Kowalski et al., 2004), the temperature of the reaction is kept lower than the melting point of the highest melting TG. In this case, the trisaturated TG produced during the reaction would crystallize out and cannot participate in the reaction anymore, thus at equilibrium the reaction would proceed to produce more trisaturated TG. Carbonyl addition and Claisen condensation are two main mechanisms that have been proposed for chemical interesterification (Marangoni and Rousseau, 1995).

#### **2.2.3.4.2. Enzymatic interesterification**

In enzymatic interesterification, using random or regiospecific (1,3- or 2-specific) and fatty acid specific lipases as catalysts, the incorporation of acyl groups are under control and a desired acyl group can be guided to a specific position of TG because of the region-specificity of the enzyme used. This results in products with a predictable composition in contrast to the random nature of chemically catalyzed interesterification. Therefore, enzymatic interesterification with lipases having different properties is becoming more attractive because of the control of acyl exchange in the TG structure and thus the ability to convert some cheap oils such as soybean oil, rapeseed oil, lard, tallow, etc. to analog, high value-added products and modified fats (Macrae, 1983; Miller et al., 1991; Liua et

al., 1997; Xu, 2003; An et al., 2007; Pomier et al., 2007). Furthermore, enzymatic interesterification has milder reaction conditions, produces less waste, and the recovery and reuse of immobilized enzymes is easier compared to chemical interesterification (Marangoni and Rousseau, 1995; Akoh et al., 1998; Willis et al., 1998; Willis and Marangoni, 2002).

#### **2.2.3.4.2.1. Mechanism of lipase-mediated interesterification**

Commercial lipases can be obtained from plant, animal, and microbial sources. Although lipases have been produced for hydrolysis of lipids and similar materials, they can also catalyze acyl-exchange reactions like alcoholysis, acidolysis, and transesterification (Willis and Marangoni, 2002; Hayes, 2004).

The molecular basis for lipase activity and specificity is poorly understood, but the interesterification activity of several lipases have been reported to be due to the presence of a catalytic triad portion in the active site of the enzyme consisting of aspartic acid/glutamine, histidine, and serine (Xu, 2000; Willis and Marangoni, 2002). Serine is the nucleophilic part of this triad and the other two amino acids are the charge transferring part of the system to improve catalysis. These active sites are buried under a “lid” of a surface loop, which undergoes a conformational change to open a channel for the active site to be accessible to the substrate. This repositioning of the “lid” is thought to be caused by interfacial activation (Xu, 2000; Willis and Marangoni, 2002). As shown in Figure 2-4, the lipase-catalyzed interesterification is thought to have four main steps (Marangoni and Rousseau, 1995):

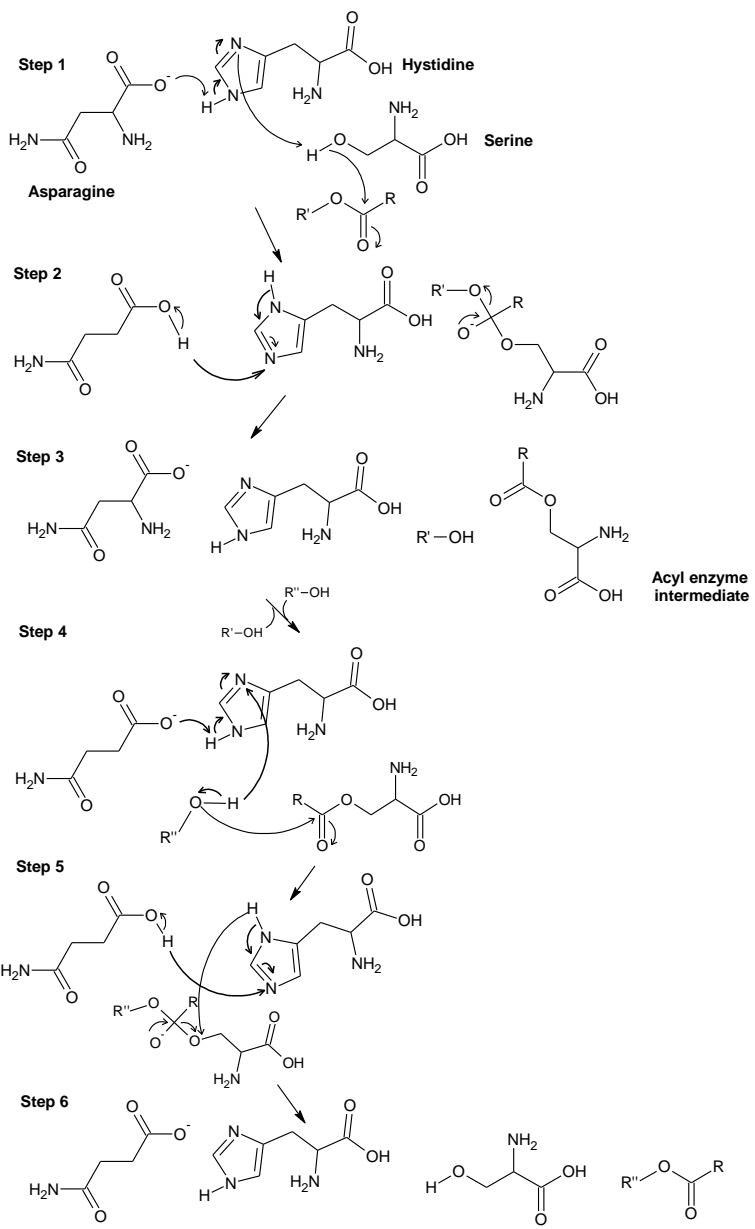


**Figure 2-4.** Catalytic mechanism for lipase-mediated interesterification.<sup>2</sup>

<sup>2</sup> Marangoni A.G. and Rousseau D. (1995). Engineering triacylglycerols: The role of interesterification, *Trends Food Sci. Tech.*, 6 (10): 329-335. (Regraphed with permission from Elsevier.)

In the first step, the nucleophile part of the active site of the enzyme, serine, attacks the carbon of a carbonyl group of a TG, undissociated fatty acid, or a fatty acid alkyl ester. A tetrahedral intermediate is formed in the second step and the other two amino acids enhance the nucleophilic specificity of the hydroxyl group of serine. In the third step, an acyl-enzyme intermediate is formed by breaking the carbon-oxygen bond of ester and resulting in the formation of water or alcohol depending on whether the substrate is TG, fatty acid alkyl ester, or free fatty acid. The alcohol reacts with the acyl-enzyme intermediate and a tetrahedral intermediate is formed again in step four followed by rearranging of this complex to release a new TG and the serine in the active site is activated again. Three types of acyl donors can be used in lipase-catalyzed interesterification: TG, fatty acid ethyl esters, and free fatty acids (Brady et al., 1990; Hayes, 2004).

#### **2.2.3.4.2.2. Kinetics of lipase-catalyzed reactions**

Using simple one substrate kinetic mechanisms does not provide an accurate description of what happens during a reaction as most of the enzymatic reactions are intrinsically multisubstrate-multiproduct reactions (Paiva et al., 2000). According to Cha's method of derivation of rate equation for enzyme-catalyzed reactions under the rapid equilibrium assumption or combined assumptions of equilibrium and steady state, one of the steps of lipase-catalyzed reactions is a rate-limiting step, which is dominant in controlling the rate of the whole reaction, and this rate limiting step can be a chemical transformation involving either enzyme or its intermediate complex (Cha, 1968). Cha's method presumes that all

other steps of the reaction except the rate-limiting step are in a rapid equilibrium state because they are intrinsically much faster (Segel, 1993). The simplest example of rapid equilibrium mechanism is the classic Michaelis-Menten equation (Eq. (2.6)), by relating reaction rate ‘v’ to [S], the concentration of a substrate.

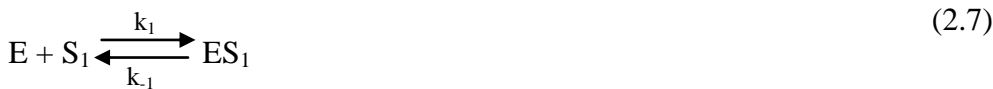
$$v = \frac{d[P]}{dt} = \frac{V_{max}[S]}{K_m + [S]} \quad (2.6)$$

Here, [P] is product concentration;  $V_{max}$  represents the maximum rate achieved by the system and the Michaelis constant,  $K_m$ , is the substrate concentration at which the reaction rate is half of  $V_{max}$ . However, there may be some enzyme species having two or more rapid equilibrium segments isolated by one or more slow steps, which is called partial equilibrium mechanism (Cha, 1968).

To fully achieve the kinetic modeling of enzymatic reactions in precise mathematical terms, the first step is to postulate the elementary steps of the reaction that occur at the molecular level. Then, the postulated mechanism should be translated to mathematical terms according to statistical assumptions that the elementary reaction is the result of either uni-molecular rearrangements or bimolecular collisions of molecules/enzymes. Such processes occur only if the free energy of the (intermediate) activated state is more than the activation energy of the reaction. Therefore, graphical and numerical analysis of the experimental data from enzymatic reactions can predict the mechanism and the kinetic parameters of the system. The graphic method is the most popular tool for

numerical analyses and enzyme classification (Rudolph and Fromm, 1979; Paiva et al., 2000).

According to the mechanism of a lipase-catalyzed reaction, described in Section 2.2.3.4.2.1, the reaction steps in lipase-catalyzed esterification as an example can be expressed as in Equations (2.7) to (2.11) (Gandhi et al., 2000; Willis and Marangoni, 2002):



where, E is the lipase,  $S_1$  is the acid,  $P_1$  is water,  $S_2$  is the alcohol,  $P_2$  is the ester,  $ES_1$  is the first tetrahedral complex between the lipase and acid, EA is the acyl-lipase complex, and  $EP_2$  is the second tetrahedral complex. The first four steps are known as the reversible Ping-Pong Bi-Bi mechanism (Paiva et al., 2000; Chowdary and Prapulla, 2005). The last step (Eq. (2.11)) is included to account for the competitive inhibition of lipase, which generally occurs due to one of the substrates, namely alcohol ( $S_2$ ) (Gandhi et al., 2000). If the initial product concentrations are zero, the expression for the initial reaction rate will be as in Equation (2.12) (Gandhi et al., 2000):

$$v_0 = V_m \left[ 1 + \frac{K_{m1}}{S_1} \left( 1 + \frac{S_2}{K_1} \right) + \frac{K_{m2}}{S_2} \right]^{-1} \quad (2.12)$$

where,

$$V_m = \frac{k_2 k_4}{k_2 + k_4} E_0, K_{m1} = \frac{k_4}{k_1} \left( \frac{k_{-1} + k_2}{k_2 + k_4} \right), K_{m2} = \frac{k_2}{k_3} \left( \frac{k_{-3} + k_4}{k_2 + k_4} \right), K_1 = \frac{k_{-5}}{k_5} \quad (2.13)$$

The parameters  $V_m$ ,  $K_{m1}$ ,  $K_{m2}$ , and  $K_1$  can be calculated by measuring the initial reaction rates; first, at constant fatty acid concentration and different alcohol concentrations, and, then, at constant alcohol concentration and different fatty acid concentrations (Gandhi et al., 2000).

There are different methods to linearize the behaviour of an enzyme such as Lineweaver-Burk (Double-Reciprocal), Logarithmic, Hanes, Eadie-Hofstee, and Eisenthal-Cornish-Bowdern (Lineweaver and Burk, 1934; Dowd and Riggs, 1965; Atkins and Nimmo, 1975). There are differences between these methods according to their statistical validity. To solve this problem in a linear method, data weighting methods or computer methods can be used (Markus et al., 1976). The best way to show the behaviour of enzymes is by using non-linear regression methods because the relationship between the experimental data and the enzymatic behaviour is non-linear (Bravo et al., 2001).

### 2.3. Biocatalysis reactions using $\text{SCCO}_2$

Along with the previously mentioned advantages of  $\text{SCCO}_2$ , the finding that enzymes can retain their biocatalytic activity at high pressures has encouraged the

use of enzymes under supercritical conditions. In the presence of a controlled amount of water, necessary for enzymatic activity, SCCO<sub>2</sub> can be used as the reaction media in which the enzyme kinetics can also be correlated with solvent properties such as dielectric constant and hydrophobicity (Kamat et al., 1992). Therefore, in enzymatic reactions using SCCO<sub>2</sub>, the effects of many parameters, including temperature, pressure, the amount of water, the type of solvent, and the type of enzyme support on the reaction rate and enzyme activity should be considered.

In lipid reactions using high melting fats like fully-hydrogenated vegetable oils or stearin fractions, conducting the reaction at mild temperatures becomes an issue. Performing the reaction under high pressure CO<sub>2</sub> environment helps resolve this issue because the melting point of solid fats in the presence of SCCO<sub>2</sub> decreases with pressure because of the increase in the solubility of SCCO<sub>2</sub> in the lipid phase (Hammam and Sivik, 1993; Guclu-Ustundag and Temelli, 2000). For example, Hammam and Sivik (1993) observed that the melting point of tripalmitin and tristearin reduced from 66 to 50 °C and from 73 to 60 °C, respectively, upon increasing the pressure from 0.1 MPa to 9 MPa in the presence of CO<sub>2</sub>.

Another important factor in biocatalysis reactions, especially in lipid reactions, using SCCO<sub>2</sub> is whether the reaction occurs in a single supercritical phase or in the gas expanded liquid (GXL) phase in contact with the supercritical phase. GXL are alternative media for performing reaction processes. A GXL is a mixed solvent composed of a compressible gas such as CO<sub>2</sub> dissolved in an

organic solvent. CO<sub>2</sub>-expanded liquids (CXL) are the most commonly used class of GXL. By tuning pressure and temperature, which dictates the amount of CO<sub>2</sub> in the CXL, the solvent properties, such as polarity, can span from that of pure CO<sub>2</sub> to that of an organic solvent (Jessop and Subramaniam, 2007).

In solvent-free lipid reactions, the lipid substrate as a liquid phase can be saturated by CO<sub>2</sub> to produce CO<sub>2</sub>-expanded (CX) lipids. CX lipids have different physical properties compared to those of the original liquid lipid phase, which are dependent on the pressure and temperature of the system. Hence, the reaction rate is not only dependent on enzyme activity but also dependent on the effects of pressure and temperature on the physical properties of the expanded liquid lipid phase like volumetric expansion, density, viscosity, and interfacial tension. Any change in these physical properties of the reactants in equilibrium with CO<sub>2</sub> as a result of changes in pressure and temperature can influence the mass transfer properties of the liquid phase and consequently the reaction rate.

### **2.3.1. Fundamental behaviour of reaction systems in contact with SCCO<sub>2</sub>**

Pressure and temperature have a significant influence on the density and transport properties (viscosity, thermal conductivity, and diffusivity) of SCCO<sub>2</sub>. This in turn affects the solubility and transport of reactants and products to/from the enzyme (Knez et al., 2006). A change in the pressure of SCCO<sub>2</sub> influences the density-dependent physical properties, such as partition coefficient, dielectric constant and Hildebrand solubility parameters that indirectly regulates the activity, specificity and stability of enzymes (Nagesha et al., 2004; Habulin et al.,

2005). Pressure and temperature can also directly affect enzyme activity (Ishikawa et al., 1996) and reaction parameters including the rate constant. Pressure can affect the reaction rate due to a change in the concentrations of reactants and products in solution because the partitioning of reaction components between the two phases depends on pressure (Erickson et al., 1990). Changes in pressure can progressively alter the enantioselectivity of enzymatic reactions (Matsuda et al., 2005). For instance, during lipase-catalyzed esterification of primary terpene alcohols such as citronellol with oleic acid in  $\text{SCCO}_2$  (Ikushima et al., 1995a), an optical purity of almost 100% was obtained from a racemic mixture of citronellol simply by manipulating the pressure and temperature in the vicinity of the critical point of  $\text{CO}_2$ . Therefore, it is necessary to understand the effect of having high pressure  $\text{CO}_2$  in the reaction system on parameters influencing the reaction efficiency.

#### **2.3.1.1. Phase behaviour and solubility of reactants and products**

The phase behaviour of the supercritical reaction system should be known in order to understand whether a single supercritical phase or two or more phases are present at the selected conditions. Modifying the pressure, temperature and/or composition of the feed mixture in  $\text{SCCO}_2$  can lead to a homogeneous phase and therefore an efficient reaction. Solubility of reactants and products in the  $\text{SCCO}_2$  and the possibility of phase separation, which may cause mass transfer limitations, dictate if a reaction can be carried out efficiently. Thermodynamic equilibrium of the reaction and how the components of the reaction medium, particularly water

in hydrolytic reactions, partition between the phases can influence the reaction. Reaction rates can be high under mixture critical conditions (McHugh and Krukonis, 1994). Phase equilibria for enzyme-catalyzed reactions in  $\text{SCCO}_2$  were studied by Chrisochou et al. (1995) using lipase-catalyzed transesterification of ethyl acetate and isoamyl alcohol to produce ethanol and isoamyl acetate, as a model reaction. Soave-Redlich-Kwong equation of state and mixing rules of Huron and Vidal were used to predict vapour-liquid equilibrium behaviour of the system (Chrisochou et al., 1995).

### 2.3.1.2. Diffusivity of solutes

Similar to other reaction media, binary diffusion coefficient is an important parameter in  $\text{SCCO}_2$  as well to establish how quickly the substrate moves to the active site of the enzyme and how rapidly the product leaves the active site. In general, the rate determining step for fast reactions is the rate at which the substrates diffuse in the solvent (Clifford, 1994). In such cases, controlling the diffusion coefficient can improve the reaction rate. Equation (2.14) has been used to relate the second order rate constant ( $k_2$ ) to the diffusivity of the solutes, assuming that only two substrates are involved in the reaction (Clifford, 1994):

$$k_2 = 4\pi N_A \rho_{12} \phi (D_X + D_Y) \quad (2.14)$$

Where,  $D_X$  and  $D_Y$  are the binary diffusion coefficients of the substrates in the SCF,  $\rho_{12}$  is the approach distance necessary for the reaction,  $N_A$  is the Avogadro's number and  $\phi$  is a steric or statistical parameter that is less than unity.

Rezaei and Temelli (2000b) reported the binary diffusion coefficients of several fatty acids, fatty acid esters and glycerides in  $\text{SCCO}_2$  at various pressures and temperatures. For these compounds, the diffusion coefficient increased with temperature and decreased with pressure. Such changes in diffusion coefficients influence enzymatic reaction rates. Lozano et al. (2004) observed that a drop in diffusion rate resulted in lower synthetic activity of the enzyme Novozym 435. Possible interactions of the enzyme with  $\text{SCCO}_2$  itself have also been claimed to influence the reaction rate and behaviour in certain reactions (Zagrobelny, 1992; Ikushima et al., 1995b; Matsuda et al., 2005). Furthermore, enzyme stability may be directly influenced by the operational pressure and temperature, regardless of the changes in diffusion coefficients.

### **2.3.1.3. Physical properties of the liquid phase in equilibrium with high pressure $\text{CO}_2$**

As mentioned previously, whether the reaction occurs in a single supercritical phase or in the gas-expanded liquid phase is an important consideration. Therefore, the reaction rate is not only dependent on enzyme activity but also on the effects of pressure and temperature on the physical properties of the  $\text{CO}_2$ -expanded (CX) liquid phase like density, viscosity, and interfacial tension because lipids saturated with  $\text{CO}_2$  under moderate pressure expand in volume, and their physical properties change substantially. Therefore, changes in the physical properties of the reactants due to different conditions of

pressure and temperature can influence the mass transfer properties of the liquid phase and consequently the reaction rate.

Seifried and Temelli (2009) studied the density of fish oil TG and their fatty acid ethyl esters (FAEE) in equilibrium with high pressure CO<sub>2</sub> at 40, 50, and 70 °C from 0.1 to 25 MPa. They found that the density of both fish oil TG and their FAEE increased with pressure and decreased with temperature. The trend for viscosity with increasing pressure is the most striking for TG at 40 °C, where the viscosity of CX-TG decreased by about an order of magnitude from initially around 25 mPa·s to 3 mPa·s with an increase in pressure to about 12 MPa (Seifried and Temelli, 2011).

The density and volumetric expansion of corn oil were studied by Tegetmeier et al. (2000) at temperature ranging from room temperature to 80 °C and pressures of up to 30 MPa. They showed that the density of corn oil increased with an increase in pressure and a decrease in temperature and the maximum change in density was about 5% within the range of their study.

Calvignac et al. (2010) investigated the density of cocoa butter saturated with CO<sub>2</sub> at temperatures of 40, 50, and 80 °C and pressures of up to 25 MPa. They also observed that the density increased linearly with an increase in pressure and a decrease in temperature. They declared that the density was influenced by the dissolution of CO<sub>2</sub> as the density increased linearly up to 25% CO<sub>2</sub> solubilization but above that value the density increase was sharper due to the compression effect. They also studied the volumetric expansion of cocoa butter in equilibrium with CO<sub>2</sub> at 40 and 80 °C.

## **2.3.2. Reaction kinetics**

### **2.3.2.1. Reaction rate and activation volume**

In a supercritical reaction system, it is impossible to separate the absolute effect of a variable such as pressure or temperature on the reaction behaviour from the effects of other variables. This is because changes in one variable can influence several other variables. For example, a change in pressure or temperature may not only influence the enzyme behaviour, but also the kinetics of the reaction and properties of the SCCO<sub>2</sub> as well as the physical properties of the liquid phase in equilibrium with high pressure CO<sub>2</sub>.

Dumont et al. (1992) examined the behaviour of Lipozyme in SCCO<sub>2</sub> and in *n*-hexane to catalyze the reaction between myristic acid and ethanol. Dumont et al. (1992) concurred with Marty et al. (1992) that the mechanism of the reaction was the same in both media. They concluded that substrate inhibition in SCCO<sub>2</sub> was less than that in *n*-hexane because ethanol acted as a co-solvent and enhanced the solubility of myristic acid in SCCO<sub>2</sub> by enhancing the polarity of the medium. Both ethanol and water are more soluble in SCCO<sub>2</sub> than in *n*-hexane. Dumont et al. (1992) further concluded that the co-solvent effect of ethanol caused drying of the enzyme support. This was contrary to the findings of Marty et al. (1992), who showed that the negative effect of ethanol existed even after the addition of a large amount of water to the medium. If drying of the enzyme was the problem, it should have been resolved by the addition of excess water to the batch reactor, but this was not the case.

Partial molar volume of the components is an important property that can have a large influence on the reaction rate in supercritical media (Combes et al., 1992). Transition state analysis can be used to describe the rate increase observed at high pressures. The variation of the reaction rate constant  $k$  with pressure for a bimolecular reaction represented by the equilibrium “ $A + B \rightleftharpoons M^\pm \rightleftharpoons \text{Products}$ ” is given in Equatio (2.15):

$$\left( \frac{\partial \ln k}{\partial P} \right) = \frac{\Delta V^\pm}{RT} \quad (2.15)$$

where, “ $\Delta V^\pm = \bar{V}_M - \bar{V}_A - \bar{V}_B$ ” is the activation volume, which is the difference in the partial molar volumes of the activated complex  $M^\pm$  and the substrates A and B. This equation considers the reaction rate in terms of mole fractions (Clifford, 1994; Srinivas and Mukhopadhyay, 1994; Kamat et al., 1995b). If the activation volume in a reaction is positive, that is, if the activated complex has a higher partial molar volume than the reactants, then increasing pressure will not favor the reaction. For example, an activation volume of +233 mL/mol was reported for the transesterification of *N*-acetyl-L-phenylalanine ethyl ester with 1-propanol catalyzed by subtilisin Carlsberg where an increase in pressure of only 20 MPa caused a six-fold decrease in the catalytic efficiency of subtilisin (Fontes et al., 1998). On the other hand, if activation volume is negative, indicating that the reactants are more voluminous than the activated complex, then the reaction rate will increase with pressure. An example of such a case is transesterification of 1-phenylethanolamine and vinyl acetate in  $\text{SCCO}_2$  catalyzed by *Pseudomonas cepacea* lipase in which with increasing pressure of the reaction

medium the catalytic efficiency of the enzyme improved resulting in negative activation volume (-1340 cm<sup>3</sup>/mol) approaching critical pressure of 7.4 MPa (Celia et al., 2005).

Partial molar volumes are very sensitive to changes in pressure, temperature and mole fractions in the vicinity of the critical point of the reaction mixture or the critical conditions of the solvent, when the solute concentration is low. This was demonstrated by Srinivas and Mukhopadhyay (1994) for the oxidation of cyclohexane to cyclohexanol and cyclohexanone in SCCO<sub>2</sub>. An increase in temperature favored the production of cyclohexanone compared to cyclohexanol. Increasing pressure and temperature reduced the induction period for the production of both products. Activation volumes calculated for the oxidation of cyclohexane at 17 MPa and 137 °C changed from 36 to -775 cm<sup>3</sup>/mol at 20.5 MPa and 160 °C, suggesting that the reaction in SCCO<sub>2</sub> can be greatly improved. However, the reaction would proceed at a high rate at 160 °C because of negative activation volume at this temperature. Srinivas and Mukhopadhyay (1994) showed that the feed composition had a strong influence on the reaction rate. Feed composition was suggested as the main possible reason for the activation volume to be high at 137 °C.

The activation volume for dilute systems is dictated by: (a) the differences in the van der Waals attractive and repulsive forces between the solvent and reactants and between the solvent and activated complex; and (b) the isothermal compressibility of the pure solvent (Combes et al., 1992; Srinivas and Mukhopadhyay, 1994).

The effect of pressure (6 to 25 MPa) on the initial reaction rate for the transesterification of 1-phenyl ethanol and vinyl acetate in  $\text{SCCO}_2$  was investigated by Celia et al. (2005). The reaction was carried out at 50 °C using *Pseudomonas cepacea* lipase. An increase in pressure in the subcritical region decreased the initial reaction rate. However, once the critical pressure (7.4 MPa) was approached, the reaction rate increased dramatically, but a further increase in pressure within the supercritical region caused a decrease in the reaction rate. They explained that an increase in the supercritical phase density led to an increase in the solvation power and, as a result, the concentrations of substrates were higher in the supercritical phase than in the enzymatic solid phase. This should have led to an increased reaction rate because of enhanced mass transfer of the substrate to the enzyme. The observed behaviour is probably better explained by the changes in diffusion coefficients as discussed by Rezaei and Temelli (2000b) and Lozano et al. (2004).

### **2.3.3. Enzyme efficiency under $\text{SCCO}_2$**

#### **2.3.3.1. Enzyme stability**

Long term stability of enzymes under  $\text{SCCO}_2$  environment is an important parameter for potential scale up of such processes. Enzymes are complex folded polypeptide molecules. The folded structure of the polypeptides, or the tertiary structure, is held together by hydrogen bonding, ionic and hydrophobic interactions, and disulfide (S–S) bridges. Enzymes with disulfide bridges are more stable compared to those without such covalent bonding (Kasche et al., 1988).

Kamat et al. (1992; 1995a) claimed that CO<sub>2</sub> covalently bonded to enzymes causing temporary inactivation of the enzyme. In contrast, based on the results of high-pressure electron paramagnetic resonance spectroscopy of cholesterol oxidase from *Gloecocysticum chrysocreas* in SCCO<sub>2</sub> and SCCO<sub>2</sub>+co-solvent mixtures, Randolph et al. (1991) reported that conformational changes due to the variation in pressure (0.1–11.2 MPa) were minimal. Similar results were also reported for the lipase from *Rhizopus arrhizus* by Miller et al. (1991). Shishikura et al. (1994) reported that the immobilized *Mucor miehei* lipase was stable for more than 180 h in SCCO<sub>2</sub> at 9.8 MPa and 60 °C. In contrast, Rezaei and Temelli (2000a) showed that the conversion rate decreased over 24 h of hydrolysis of canola oil in SCCO<sub>2</sub> at 38 MPa and 55 °C using Lipozyme IM, which was attributed to the long exposure of enzyme to the added water in the hydrolysis system.

Pressures above a certain level may impact enzymes negatively. Irreversible enzyme denaturation has been reported at ultra-high pressures (>400 MPa) (Randolph et al., 1991). Such high pressures are said to directly affect the conformation of enzyme molecules. However, within the typical range of pressures applied in most studies targeting supercritical conditions (10–40 MPa), only certain reversible conformational changes may take place, which, in general, do not interfere with the overall performance of the enzyme. However, high temperature is always destructive to enzymes.

Ikushima et al. (1995b) used Fourier transform infrared (FTIR) spectroscopy to monitor enzyme conformation in SCCO<sub>2</sub> during esterification.

Over a limited pressure range of 7.7 to 8.5 MPa, dramatic changes in *Candida cylindracea* lipase occurred, leading to an increase in the rate of esterification reactions. The pressure range in which the enzyme catalyzed the production of optically active compounds overlapped with the pressure range in which the sudden conformational changes took place (Ikushima et al., 1995b). Different enzymes can show substantial changes in activity as a consequence of pressure/temperature induced changes in the properties of SCCO<sub>2</sub>.

Rezaei and Temelli (2000a) investigated the effect of pressure (10–38 MPa) and temperature (35 and 55 °C) on conversion rate and product composition in continuous enzymatic hydrolysis of canola oil in SCCO<sub>2</sub>. *Mucor miehei* lipase immobilized on a macroporous anionic resin (Lipozyme IM) was used. A conversion rate of 63–67% (based on disappearance of TG) was observed at 24–38 MPa. Production of MG and DG was minimum at 10 MPa and 35 °C, but a higher production of MG was achieved at 24 MPa. A higher amount of product was obtained at 24–38 MPa.

The effect of pressure on alcoholysis of ethyl 4-hydroxy-3-methoxy cinnamate with 1-octanol was investigated by Compton and King (2001) using Novozym 435 as a catalyst. At 80 °C, a maximum yield of ~64% was achieved in the pressure range of 10.3–13.8 MPa. The yield declined with a further increase in pressure. In contrast, the yield of various products was not affected by pressure (14–34 MPa) during alcoholysis at 80 °C. Fontes et al. (1998) reported that increasing pressure decreased the catalytic efficiency of Subtilisin Carlsberg suspended in compressed propane, near-critical ethane and especially near-critical

$\text{CO}_2$ . In the latter solvent, the enzyme was completely inactivated at pressures slightly greater than 30 MPa.

The rapid release of  $\text{CO}_2$ , which is dissolved in the bound water of the enzyme due to pressure release and inactivation during pressurization or depressurization may be the two main reasons for potential structural changes in the enzyme, resulting in its inactivation (Nakamura, 1990; Lin et al., 2006).

Srivastava et al. (2003) studied the esterification of myristic acid with ethanol using crude porcine pancreatic lipase in  $\text{SCCO}_2$ . At a constant density of  $0.2 \text{ kg}\cdot\text{m}^{-3}$ , the conversion rate increased with temperature up to  $45^\circ\text{C}$ . A further increase in temperature reduced conversion. Srivastava et al. (2003) argued that for a given enzyme, the optimum temperature was reaction specific.

In the synthesis of butyl butyrate from vinyl butyrate and 1-butanol using Novozym 435, Lozano et al. (2004) showed that within the range of  $40\text{--}60^\circ\text{C}$ , an increase in temperature promoted enzyme activity irrespective of pressure (8–15 MPa). However, at any fixed temperature in the above specified range, an increase in pressure resulted in a decrease in the synthetic activity of the enzyme. This effect was attributed to pressure-related increase in  $\text{SCCO}_2$  density. Best combination of conditions was  $60^\circ\text{C}$  and 8 MPa. Interestingly, when temperature and pressure combinations corresponding to a constant density of  $\text{SCCO}_2$  were used, the enzyme activity levels were similar for the various conditions tested. Nagesha et al. (2004) reported that the yield of fatty acid butyl esters from the free fatty acids of hydrolyzed soy deodorizer distillate decreased with pressure in the range of 12–18 MPa. *Mucor miehei* lipase was used to catalyze the reaction. With

other variables held at their optimal values, the maximum yield of esterification was obtained at 36 °C (Nagesha et al., 2004). Similar results were reported by Rezaei and Temelli (2000a) for enzymatic hydrolysis of canola oil at 24 MPa with optimal temperature of 35 °C.

### **2.3.3.2. Effect of water**

Enzymes require a certain amount of water in their structures in order to maintain their natural conformation, allowing them to deliver their full functionality. Furthermore, as a co-solvent, water can modify the solvent properties such as polarity as well as the solubility of the reactants and product in  $\text{SCCO}_2$ . In addition, depending on the type of the reaction, water can be a substrate (e.g., in hydrolysis) or a product (e.g., in esterification) of the enzymatic reaction, influencing the enzyme turnover in different ways. However, regardless of the type of reaction, the functionality of the enzyme itself is maximum at an optimum level of water, beyond which the enzyme performance declines due to the loss in enzyme stability (Randolph et al., 1991). Furthermore, mass transfer limitations caused by pathway blockage and/or by reduced solubilities of the reactants and/or products can also affect the enzyme performance at higher water levels.

#### **2.3.3.2.1. The role of enzyme support**

The type of enzyme support used for the immobilization of the enzyme has been shown to influence the optimum water level for the reaction (Yahya et al.,

1998). The matrix, pore size, surface area and the hydrophobicity of the enzyme support are among the factors controlling water partitioning between the enzyme or support and the solvent. As a consequence, these factors can influence all water-dependent properties of the reaction system. A negative temperature effect was reported by Marty et al. (1992) on the adsorption of water to the enzymatic solid support, macroporous anionic resin beads. They justified such a loss of water from the enzyme support to be due to the increased partition coefficient of water between the supercritical phase and the solid support at higher temperatures. At higher temperatures, the vapour pressures of compounds are also higher and therefore it is not unusual to have an increased partition coefficient as observed above. The unusual part of their results, however, was that a higher partition of water between the solvent and the support was also observed at higher pressures, which was not consistent with the effect of pressure on the vapour pressure of the compounds. In fact, they found that the increase in the water level in the supercritical phase at higher pressures due to the increased solvating power of the supercritical medium exceeded the reduction in enzyme activity expected by the influence of pressure on the vapour pressure of water (Marty et al., 1992).

Yu et al. (1992) observed that adding 1 mL water to 1 g immobilized *Candida cylindracea* lipase at 13.6 MPa and 40°C resulted in a maximum conversion of 30% for the esterification of ethanol and oleic acid to produce ethyl oleate. Relying on their previous experiments with methyl oleate, Yu et al. (1992) concluded that the enzyme support adsorbed some water because of its hydrophilic nature, in which case, hydrolysis (of ethyl oleate to ethanol and oleic

acid) was also possible due to the presence of extra water on the immobilized lipase.

### **2.3.3.2.2. The role of reaction media**

Another important factor that dictates the optimal water content is the type of solvent used as the reaction medium. Trace levels of water were found to be necessary for the catalysis by maintaining the active conformation of the enzyme molecules through hydrogen bonding (Marty et al., 1992; Kamat et al., 1995b). Since a higher amount of water remains associated with the enzyme structure in hydrophobic solvents, enzymes exhibit higher activity levels in hydrophobic solvents than in hydrophilic solvents. According to Lozano et al. (2004), the synthetic activity of *Candida antarctica* Lipase B in SCCO<sub>2</sub> is far greater than that in all the organic solvents they studied. Also, according to Randolph et al. (1988) cholesterol oxidase was 10-fold less active in dry CO<sub>2</sub> than in a system where water was also present. However, the reduced activity of enzyme in dry CO<sub>2</sub> was reversible since the enzyme regained full activity when 1% (v/v) water was added (Randolph et al., 1988). The activity of Promod 144 (proteinase) was studied by Habulin et al. (2005) in SCCO<sub>2</sub> at 30 MPa as well as in CO<sub>2</sub> at atmospheric pressure. Although the enzyme activity improved by an increase in temperature from 20 to 60 °C under both conditions, the optimum temperature in SCCO<sub>2</sub> was lower than that at atmospheric pressure because of the co-extraction of water from the enzyme microenvironment by SCCO<sub>2</sub> at higher temperatures (Habulin et al., 2005).

Hydrophilic organic solvents absorb water from the enzyme and often denature the enzyme. Therefore, solvent suitability for a reaction may be predicted by measuring a parameter related to solvent hydrophobicity. One such parameter is  $\log P$ , defined as the logarithm of the partition coefficient of a solvent in an octanol/water mixture, whose volume ratio is adjusted based on the expected value of the partition coefficient (Laane et al., 1985).

Madras et al. (2004) studied the effect of water concentration on the synthesis of octyl palmitate from palmitic acid and octanol conducted in  $\text{SCCO}_2$ , supercritical methane and supercritical ethane at the optimum temperature of 55 °C using 5.0 mg of immobilized enzymes, Lipolase and Novozym 435 and free enzyme, pancreatic lipase as catalysts. When the initial water concentration was more than its optimum level (7.9-39.7 mM), a sudden drop in the conversion was observed because of the hydrolysis reaction suppressing the esterification reaction. The optimum water content to achieve the maximum conversion is dependent on the types of solvent, substrate and the enzyme used (Kumar et al., 2004).

#### **2.4. Concluding remarks**

Taking into account the current states of knowledge as summarized in the literature review for reactions of fats and oils in  $\text{SCCO}_2$  media, it seems to be advantageous to conduct lipase-catalyzed interesterification of canola oil and FHCO in equilibrium with high pressure  $\text{CO}_2$ . Considering the lack of information in the literature about the impact of dissolved  $\text{CO}_2$  on the physical

properties of the liquid lipid phase, it would be valuable to determine the physical properties of canola oil and its blend with FHCO in equilibrium with high pressure CO<sub>2</sub>. Such studies would be valuable for better understanding of interesterification in terms of optimizing the reaction conditions and designing the process. Conducting enzymatic reactions in equilibrium with SCCO<sub>2</sub> may negatively affect the performance of enzymes as discussed in this literature review; therefore, it is compelling to study the effects of exposing immobilized lipases to SCCO<sub>2</sub> on their performance.

Finally, after establishing the optimal conditions for conducting the interesterification reaction in equilibrium with SCCO<sub>2</sub>, the physicochemical properties of the final products should be investigated whether to assess their sustainability for use as base-stock for *trans*-free margarines.

## 2.5. References

- Akoh, C.C., Lee, K.T. and Fomuso, L.B. (1998). Synthesis of positional isomers of structured lipids with lipases as biocatalysts. In *Structural modified food fats: Synthesis, biochemistry, and use*, A.B. Christophe, Ed. The American Oil Chemists' Society: Chicago, IL, USA, pp 46-72.
- Almeida, M.C., Ruivo, R., Maia, C., Freire, L., Correa De Sampaio, T. and Barreiros, S. (1998). Novozym 435 activity in compressed gases. Water activity and temperature effects. *Enzyme and Microbial Technology*, **22** (6): 494-499.
- An, G., Ma, W., Sun, Z., Liu, Z., Han, B., Miao, S., Miao, Z. and Ding, K. (2007). Preparation of titania/carbon nanotube composites using supercritical ethanol and their photocatalytic activity for phenol degradation under visible light irradiation. *Carbon*, **45** (9): 1795-1801.
- Atkins, G.L. and Nimmo, I.A. (1975). Comparison of 7 methods for fitting Michaelis-Menten equation. *Biochemical Journal*, **149** (3): 775-777.
- Bernardini, E. (1976). Continuous solvent fractionation of palm oil and other edible oils. *Journal of the American Oil Chemists' Society*, **53** (7): A459-A459.

Bonanome, A. and Grundy, S.M. (1988). Effect of dietary stearic acid on plasma cholesterol and lipoprotein levels. *New England Journal of Medicine*, **318** (19): 1244-1248.

Brady, L., Brzozowski, A.M., Derewenda, Z.S., Dodson, E., Dodson, G., Tolley, S., Turkenburg, J.P., Christiansen, L., Huge-Jensen, B., Norskov, L., Thim, L. and Menge, U. (1990). A serine protease triad forms the catalytic centre of a triacylglycerol lipase. *Nature*, **343** (6260): 767-770.

Bravo, I.G., Bustos, F., De Arriaga, D., Ferrero, M.A., Rodriguez-Aparicio, L.B., Martinez-Blanco, H. and Reglero, A. (2001). A normalized plot as a novel and time-saving tool in complex enzyme kinetic analysis. *Biochemical Journal*, **358** (3): 573-583.

Calliauw, G., Fredrick, E., Gibon, V., De Greyt, W., Wouters, J., Fouber, I. and Dewettinck, K. (2010). On the fractional crystallization of palm olein: Solid solutions and eutectic solidification. *Food Research International*, **43** (4): 972-981.

Calvignac, B., Rodier, E., Letourneau, J.J., dos Santos, P.M.A. and Fages, J. (2010). Cocoa butter saturated with supercritical carbon dioxide: Measurements and modelling of solubility, volumetric expansion, density and viscosity. *International Journal of Chemical Reactor Engineering*, **8**: A73.

Celia, E., Cernia, E., Palocci, C., Soro, S. and Turchet, T. (2005). Tuning *Pseudomonas cepacea* lipase (PCL) activity in supercritical fluids. *Journal of Supercritical Fluids*, **33** (2): 193-199.

Cernia, E., Palocci, C. and Soro, S. (1998). The role of the reaction medium in lipase-catalyzed esterifications and transesterifications. *Chemistry and Physics of Lipids*, **93** (1-2): 157-168.

Cha, S. (1968). A simple method for derivation of rate equations for enzyme-catalyzed reactions under rapid equilibrium assumption or combined assumptions of equilibrium and steady state. *Journal of Biological Chemistry*, **243** (4): 820-825.

Chnadhapuram, M. and Sunkireddy, Y.R. (2012). Preparation of palm olein enriched with medium chain fatty acids by lipase acidolysis. *Food Chemistry*, **132** (1): 216-221.

Chongkhong, S., Tongurai, C., Chetpattananondh, P. and Bunyakan, C. (2007). Biodiesel production by esterification of palm fatty acid distillate. *Biomass & Bioenergy*, **31** (8): 563-568.

Chowdary, G.V. and Prapulla, S.G. (2005). Kinetic study on lipase-catalyzed esterification in organic solvents. *Indian Journal of Chemistry Section B-Organic Chemistry Including Medicinal Chemistry*, **44** (11): 2322-2327.

Chrisochou, A., Schaber, K. and Bolz, U. (1995). Phase equilibria for enzyme-catalyzed reactions in supercritical carbon dioxide. *Fluid Phase Equilibria*, **108** (1-2): 1-14.

Clifford, A.A. (1994). Reactions in supercritical fluids. In *Supercritical fluids: Fundamentals for application*, E. Kiran and J.M.H. Levelt Sengers, Eds. Kluwer Academic Publishers: Dordrecht, Netherlands, pp 449-479.

Combe, N., Clouet, P., Chardigny, J.M., Lagarde, M. and Leger, C.L. (2007). Trans fatty acids, conjugated linoleic acids, and cardiovascular diseases. *European Journal of Lipid Science and Technology*, **109** (9): 945-953.

Combes, J.R., Johnston, K.P., O'Shea, K.E. and Fox, M.A. (1992). Influence of solvent-solute and solute-solute clustering on chemical reactions in supercritical fluids. In *Supercritical fluid technology: Theoretical and applied approaches in analytical chemistry*, F.V. Frank and M.E.P. McNally, Eds. American Chemical Society: Washington DC, pp 31-47.

Compton, D.L. and King, J.W. (2001). Lipase-catalyzed synthesis of triolein-based sunscreens in supercritical CO<sub>2</sub>. *Journal of the American Oil Chemists' Society*, **78** (1): 43-47.

Dijkstra, A.J. (2006). Revisiting the formation of *trans* isomers during partial hydrogenation of triacylglycerol oils. *European Journal of Lipid Science and Technology*, **108** (3): 249-264.

Dowd, J.E. and Riggs, D.S. (1965). A comparison of estimates of Michaelis-Menten kinetic constants from various linear transformations. *The Journal of Biological Chemistry*, **240** (2): 863-869.

Dumont, T., Barth, D., Corbier, C., Branolant, G. and Perrut, M. (1992). Enzymatic reaction kinetic: Comparison in an organic solvent and in supercritical carbon dioxide. *Biotechnology and Bioengineering*, **40** (2): 329-333.

Elizalde-Solis, O. and Galicia-Luna, L.A. (2006). Solubilities and densities of capsaicin in supercritical carbon dioxide at temperatures from 313 to 333 k. *Industrial & Engineering Chemistry Research*, **45** (15): 5404-5410.

Erickson, J.C., Schyns, P. and Cooney, C.L. (1990). Effect of pressure on an enzymatic reaction in a supercritical fluid. *AIChE Journal*, **36** (2): 299-301.

Farr, W.E. (2005). Hydrogenation: Processing technologies. In *Bailey's industrial oil and fat products*, F. Shahidi, Ed. John Wiley & Sons: Hoboken, NJ, USA, pp 385-396.

Fattori, M., Bulley, N.R. and Meisen, A. (1988). Carbon dioxide extraction of canola seed: Oil solubility and effect of seed treatment. *Journal of the American Oil Chemists' Society*, **65**: 968-974.

Feuge, R.O. (1962). Derivatives of fats for use as foods. *Journal of the American Oil Chemists' Society*, **39** (12): 521-527.

Finley, J.W., Klemann, L.P., Leveille, G.A., Otterburn, M.S. and Walchak, C.G. (1994). Caloric availability of salatrim in rats and humans. *Journal of Agricultural and Food Chemistry*, **42** (2): 495-499.

Fontes, N., Nogueiro, E., Elvas, A.M., Correa de Sampaio, T. and Barreiros, S. (1998). Effect of pressure on the catalytic activity of subtilisin Carlsberg suspended in compressed gases. *Biochimica et Biophysica Acta-Protein Structure and Molecular Enzymology*, **1383** (1): 165-174.

Friedrich, J.P., List, G.R. and Heakin, A.J. (1982). Petroleum-free extraction of oil from soybeans with supercritical CO<sub>2</sub>. *Journal of the American Oil Chemists' Society*, **59**: 288-292.

Gandhi, N.N., Patil, N.S., Sawant, S.B., Joshi, J.B., Wangikar, P.P. and Mukesh, D. (2000). Lipase-catalyzed esterification. *Catalysis Reviews-Science and Engineering*, **42** (4): 439-480.

Goddard, R., Bosley, J. and Al-Duri, B. (2000). Lipase-catalysed esterification of oleic acid and ethanol in a continuous packed bed reactor, using supercritical CO<sub>2</sub> as solvent: Approximation of system kinetics. *Journal of Chemical Technology and Biotechnology*, **75** (8): 715-721.

Going, L.H. (1967). Interesterification products and processes. *Journal of the American Oil Chemists' Society*, **44** (9): 414A-456A.

Gómez, A.M. and de la Ossa, E.M. (2000). Quality of wheat germ oil extracted by liquid and supercritical carbon dioxide. *Journal of the American Oil Chemists Society*, **77**: 969-974.

Guclu-Ustundag, O. and Temelli, F. (2000). Correlating the solubility behaviour of fatty acids, mono-, di-, and triglycerides, and fatty acid esters in supercritical carbon dioxide. *Industrial and Engineering Chemistry Research*, **39**: 4756-4766.

Gunstone, F.D. (2006). Introduction: Modifying lipids – why and how? In *Modifying lipids for use in food*, F.D. Gunstone, Ed. CRC Press LLC: Boca Raton, FL, USA, pp 1-8.

Habulin, M., Primožic, M. and Knez, Z. (2005). Stability of proteinase form carica papaya latex in dense gases. *Journal of Supercritical Fluids*, **33** (1): 27-34.

Hammam, H. and Sivik, B. (1993). Phase behaviour of some pure lipids in supercritical carbon dioxide. *Journal of Supercritical Fluids*, **6** (4): 223-227.

Hashim, S.A. and Babayan, V.K. (1978). Studies in man of partially absorbed dietary fats. *American Journal of Clinical Nutrition*, **31** (10): S273-S276.

Hayes, D.G. (2004). Enzyme-catalyzed modification of oilseed materials to produce eco-friendly products. *Journal of the American Oil Chemists' Society*, **81** (12): 1077-1103.

Ikeda, M. (1992). Public health problems of organic solvents. *Toxicological Letters*, **64-65**: 191-201.

Ikushima, Y., Saito, H., Hatakeyama, K. and Ito, S. (1995a). Method for esterification of (s)-citronellol using lipase in supercritical carbon dioxide. U. S. Patent 5,403,739.

Ikushima, Y., Saito, N., Arai, M. and Blanch, H.W. (1995b). Activation of a lipase triggered by interactions with supercritical carbon dioxide in the near-critical region. *Journal of Physical Chemistry*, **99** (22): 8941-8944.

Illingworth, D. (2002). Fractionation of fats. In *Physical properties of lipids*, A.G. Marangoni and S.S. Narine, Eds. Marcel Dekker: New York, NY, USA, pp 411-477.

Ishikawa, H., Shimoda, M., Yonekura, A. and Osajima, Y. (1996). Inactivation of enzymes and decomposition of  $\alpha$ -helix structure by supercritical carbon dioxide microbubble method. *Journal of Agricultural and Food Chemistry*, **44** (9): 2646-2649.

Jencks, W.P. and Carriuolo, J. (1960). Reactivity of nucleophilic reagents toward esters. *Journal of the American Chemical Society*, **82** (7): 1778-1786.

Jessop, P.G. and Subramaniam, B. (2007). Gas-expanded liquids. *Chemical Reviews*, **170**: 2666-2694.

Johnson, J.C. and Lusas, E.W. (1983). Comparison of alternative solvents for oils extraction. *Journal of the American Oil Chemists' Society*, **60**: 181-193.

Joseph, T., Sahoo, S. and Halligudi, S.B. (2005). Bronsted acidic ionic liquids: A green, efficient and reusable catalyst system and reaction medium for Fischer esterification. *Journal of Molecular Catalysis A-Chemical*, **234** (1-2): 107-110.

Kamat, S., Barrera, J., Beckman, E.J. and Russell, A.J. (1992). Biocatalytic synthesis of acrylates in organic solvents and supercritical fluids: Optimization of enzyme environment. *Biotechnology and Bioengineering*, **40** (1): 158-166.

Kamat, S., Critchley, G., Beckman, E.J. and Russell, A.J. (1995a). Biocatalytic synthesis of acrylates in organic solvents and supercritical fluids: Does carbon dioxide covalently modify enzymes? *Biotechnology and Bioengineering*, **46** (6): 610-620.

Kamat, S.V., Beckman, E.J. and Russell, A.J. (1995b). Enzyme activity in supercritical fluids. *Critical Reviews in Biotechnology*, **15** (1): 41-71.

Kasche, V., Schlothauer, R. and Brunner, G. (1988). Enzyme denaturation in supercritical CO<sub>2</sub>: Stabilizing effect of S-S bonds during the depressurization step. *Biotechnology Letters*, **10** (8): 569-574.

Kemmere, M.F. (2005). Supercritical carbon dioxide for sustainable polymer processes. In *Supercritical carbon dioxide: In polymer reaction engineering*, M.F. Kemmere and T. Meyer, Eds. WILEY-VCH Verlag GmbH & Co. KGaA: Weinheim, Germany, pp 1-14.

Knez, Z., Laudani, C.G., Habulin, M. and Primožic, M. (2006). Biochemical reactions in supercritical fluids. In *Functional food ingredients and nutraceuticals: Processing and technologies*, J. Shi, Ed. CRC Press: Boca Raton, FL, USA, pp 111-132.

Knez, Z., Rizner, V., Habulin, M. and Bauman, D. (1995). Enzymatic synthesis of oleyl oleate in dense fluids. *Journal of the American Oil Chemists' Society*, **72** (11): 1345-1349.

Kowalski, B., Tarnowska, K., Gruczynska, E. and Bekas, W. (2004). Chemical and enzymatic interesterification of a beef tallow and rapeseed oil equal-weight blend. *European Journal of Lipid Science and Technology*, **106** (10): 655-664.

Krishnamurthy, R. and Kellens, M. (1996). Fractionation and winterization. In *Bailey's industrial oil and fat products*, Y.H. Hui, Ed. John Wiley: Champaign, IL, USA, Vol. Volume 4, Edible Oil and Fat Products: Processing Technology, pp 301-337.

Kumar, R., Madras, G. and Modak, J. (2004). Enzymatic synthesis of ethyl palmitate in supercritical carbon dioxide. *Industrial and Engineering Chemistry Research*, **43** (7): 1568-1573.

Laane, C., Boeren, S. and Vos, K. (1985). On optimizing organic solvents in multi-liquid-phase biocatalysis. *Trends in Biotechnology*, **3** (10): 251-252.

Laning, S.J. (1985). Chemical interesterification of palm, palm kernel and coconut oils. *Journal of the American Oil Chemists' Society*, **62** (2): 400-407.

Laudani, C.G., Habulin, M., Knez, Z., Porta, G.D. and Reverchon, E. (2007a). Immobilized lipase-mediated long-chain fatty acid esterification in dense carbon dioxide: Bench-scale packed-bed reactor study. *Journal of Supercritical Fluids*, **41** (1): 74-81.

Laudani, C.G., Habulin, M., Knez, Z., Porta, G.D. and Reverchon, E. (2007b). Lipase-catalyzed long chain fatty ester synthesis in dense carbon dioxide: Kinetics and thermodynamics. *Journal of Supercritical Fluids*, **41** (1): 92-101.

Lemmon, E.W., McLinden, M.O. and Friend, D.G. (2010). Thermophysical properties of fluid systems. In *NIST chemistry webbook, NIST standard reference*

database number 69, P.J. Linstrom and W.G. Mallard, Eds. National Institute of Standards and Technology: Gaithersburg, MD, USA, p. 2089.

Lin, T.J., Chen, S.W. and Chang, A.C. (2006). Enrichment of n-3 PUFA contents on triglycerides of fish oil by lipase-catalyzed transesterification under supercritical conditions. *Biochemical Engineering Journal*, **29** (1-2): 27-34.

Lineweaver, H. and Burk, D. (1934). The determination of enzyme dissociation constants. *Journal of the American Chemical Society*, **56**: 658-666.

Liua, K.J., Chengb, H.M., Changc, R.C. and Shawa, J.F. (1997). Synthesis of cocoa butter equivalent by lipase-catalyzed interesterification in supercritical carbon dioxide. *Journal of the American Oil Chemists' Society*, **74** (11): 1477-1482.

Lopes, B.L.F., Sanchez-Camargo, A.P., Ferreira, A.L.K., Grimaldi, R., Paviani, L.C. and Cabral, F.A. (2012). Selectivity of supercritical carbon dioxide in the fractionation of fish oil with a lower content of EPA plus DHA. *Journal of Supercritical Fluids*, **61**: 78-85.

Lozano, P., Villora, G., Gomez, D., Gayo, A.B., Sanchez-Conesa, J.A., Rubio, M. and Iborra, J.L. (2004). Membrane reactor with immobilized *Candida antarctica* lipase b for ester synthesis in supercritical carbon dioxide. *Journal of Supercritical Fluids*, **29** (1-2): 121-128.

Macrae, A.R. (1983). Lipase-catalyzed interesterification of oils and fats. *Journal of the American Oil Chemists' Society*, **60** (2): 243A-246A.

Madras, G., Kumar, R. and Modak, J. (2004). Synthesis of octyl palmitate in various supercritical fluids. *Industrial and Engineering Chemistry Research*, **43** (24): 7697-7701.

Marangoni, A.G. and Rousseau, D. (1995). Engineering triacylglycerols: The role of interesterification. *Trends in Food Science & Technology*, **6** (10): 329-335.

Marchetti, J.M. and Errazu, A.F. (2008). Esterification of free fatty acids using sulfuric acid as catalyst in the presence of triglycerides. *Biomass & Bioenergy*, **32** (9): 892-895.

Markus, M., Hess, B., Ottaway, J.H. and Cornish-Bowden, A. (1976). The analysis of kinetic data in biochemistry. A critical evaluation of methods. *FEBS Letters*, **63** (2): 225-230.

Marty, A., Chulalaksananukul, W., Condoret, J.S., Willemot, R.M. and Durand, G. (1990). Comparison of lipase-catalysed esterification in supercritical carbon dioxide and in n-hexane. *Biotechnology Letters*, **12** (1): 11-16.

Marty, A., Chulalaksananukul, W., Willemot, R.M. and Condoret, J.S. (1992). Kinetics of lipase-catalyzed esterification in supercritical CO<sub>2</sub>. *Biotechnology and Bioengineering*, **39** (3): 273-280.

Maskill, H. (1999). Reactions of nucleophiles with carbonyl compounds. In *Mechanisms of organic reactions*, Oxford University Press Inc.: New York, NY, USA, pp 58-68.

Matsuda, T., Harada, T., Nakamura, K. and Ikariya, T. (2005). Asymmetric synthesis using hydrolytic enzymes in supercritical carbon dioxide. *Tetrahedron Asymmetry*, **16** (5): 909-915.

McHugh, M.P. and Krukonis, V.J. (1994). Phase diagrams for supercritical fluid-solute mixtures. In *Supercritical fluid extraction: Principles and practice*, 2nd ed.; Butterworth-Heinemann: Boston, MA, USA, pp 27-84.

Michels, A., Botzen, A. and Schuurman, W. (1957). The viscosity of carbon dioxide between 0 °C and 75 °C and at pressures up to 2000 atmospheres. *Physica*, **23** (1-5): 95-102.

Miller, D.A., Blanch, H.W. and Prausnitz, J.M. (1991). Enzyme-catalyzed interesterification of triglycerides in supercritical carbon dioxide. *Industrial and Engineering Chemistry Research*, **30** (5): 939-946.

Moquin, P.H.L. and Temelli, F. (2008). Kinetic modeling of hydrolysis of canola oil in supercritical media. *Journal of Supercritical Fluids*, **45** (1): 94-101.

Mukhopadhyay, M. (2000). Fundamental transport processes in supercritical fluid extraction. In *Natural extracts using supercritical carbon dioxide*, CRC Press LLC.: Boca Raton, FL, USA, pp 83-131.

Murty, V.R., Bhat, J. and Muniswaran, P.K.A. (2002). Hydrolysis of oils by using immobilized lipase enzyme: A review. *Biotechnology and Bioprocess Engineering*, **7** (2): 57-66.

Nagesha, G.K., Manohar, B. and Udaya Sankar, K. (2004). Enzymatic esterification of free fatty acids of hydrolyzed soy deodorizer distillate in supercritical carbon dioxide. *Journal of Supercritical Fluids*, **32** (1-3): 137-145.

Nakamura, K. (1990). Biochemical reactions in supercritical fluids. *Trends in Biotechnology*, **8** (10): 288-292.

Paiva, A.L., Balcao, V.M. and Malcata, F.X. (2000). Kinetics and mechanisms of reactions catalyzed by immobilized lipases. *Enzyme and Microbial Technology*, **27** (3-5): 187-204.

Palla, C.A., Pacheco, C. and Carrin, M.E. (2012). Production of structured lipids by acidolysis with immobilized *Rhizomucor miehei* lipases: Selection of suitable reaction conditions. *Journal of Molecular Catalysis B-Enzymatic*, **76**: 106-115.

Pečar, D. and Doleček, V. (2008). Densities of  $\alpha$ -tocopherol+supercritical carbon dioxide mixtures. *Journal of Chemical & Engineering Data*, **53** (4): 929-932.

Pereda, S., Bottini, S. and Brignole, E. (2007). Fundamentals of supercritical fluid technology. In *Supercritical fluid extraction of nutraceuticals and bioactive compounds*, J.L. Martinez, Ed. CRC Press LLC.: Boca Raton, FL, USA, pp 1-24.

Pomier, E., Delebecque, N., Paolucci-Jeanjean, D., Pina, M., Sarrade, S. and Rios, G.M. (2007). Effect of working conditions on vegetable oil transformation in an enzymatic reactor combining membrane and supercritical CO<sub>2</sub>. *Journal of Supercritical Fluids*, **41** (3): 380-385.

Randolph, T.W., Blanch, H.W. and Clark, D.S. (1991). Biocatalysis in supercritical fluids. In *Biocatalysis for industry*, J.S. Dordick, Ed. Plenum Press: New York, NY, USA, pp 219-237.

Randolph, T.W., Blanch, H.W. and Prausnitz, J.M. (1988). Enzyme-catalyzed oxidation of cholesterol in supercritical carbon dioxide. *AICHE Journal*, **34** (8): 1354-1360.

Rawson, A., Tiwari, B.K., Brunton, N., Brennan, C., Cullen, P.J. and O'Donnell, C.P. (2012). Application of supercritical carbon dioxide to fruit and vegetables: Extraction, processing, and preservation. *Food Reviews International*, **28** (3): 253-276.

Rezaei, K. and Temelli, F. (2000a). Lipase-catalyzed hydrolysis of canola oil in supercritical carbon dioxide. *Journal of the American Oil Chemists Society*, **77** (8): 903-909.

Rezaei, K. and Temelli, F. (2000b). Using supercritical fluid chromatography to determine diffusion coefficients of lipids in supercritical CO<sub>2</sub>. *Journal of Supercritical Fluids*, **17** (1): 35-44.

Ribeiro, A.P.B., Basso, R.C., Grimaldi, R., Gioielli, L.A. and Goncalves, L.A.G. (2009). Effect of chemical interesterification on physicochemical properties and industrial applications of canola oil and fully hydrogenated cottonseed oil blends. *Journal of Food Lipids*, **16** (3): 362-381.

Romero, M.D., Calvo, L., Alba, C., Habulin, M., Primozic, M. and Knez, Z. (2005). Enzymatic synthesis of isoamyl acetate with immobilized *Candida antarctica* lipase in supercritical carbon dioxide. *Journal of Supercritical Fluids*, **33** (1): 77-84.

Rudolph, F.B. and Fromm, H.J. (1979). Plotting methods for analysing enzyme rate data. *Methods in Enzymology*, **63**: 139-159.

Segel, I.H. (1993). Steady-state kinetics of multireactant enzymes. In *Enzyme kinetics: Behaviour and analysis of rapid equilibrium and steady-state enzyme systems*, John Wiley & Sons Inc.: New York, NY, USA, pp 506-846.

Seifried, B. and Temelli, F. (2009). Density of marine lipids in equilibrium with carbon dioxide. *Journal of Supercritical Fluids*, **50** (2): 97-104.

Senanayake, S.P.J. and Shahidi, F. (2005). Modification of fats and oils via chemical and enzymatic methods. In *Bailey's industrial oil and fat products*, F. Shahidi, Ed. John Wiley & Sons: Hoboken, NJ, USA, Vol. 3, pp 555-584.

Shishikura, A., Fujimoto, K., Suzuki, T. and Arai, K. (1994). Improved lipase-catalyzed incorporation of long-chain fatty acids into medium-chain triglycerides assisted by supercritical carbon dioxide extraction. *Journal of the American Oil Chemists' Society*, **71** (9): 961-967.

Sonntag, N.O.V. (1979). Fat splitting, esterification and interesterification. In *Bailey's industrial oil and fat products*, D. Swern, Ed. John Wiley & Sons, New York, NY, USA, pp 97-173.

Sonntag, N.O.V. (1982). Glycerolysis of fats and methyl-esters-status, review and critique. *Journal of the American Oil Chemists' Society*, **59** (10): A795-A802.

Srinivas, P. and Mukhopadhyay, M. (1994). Oxidation of cyclohexane in supercritical carbon dioxide medium. *Industrial and Engineering Chemistry Research*, **33** (12): 3118-3124.

Srivastava, S., Madras, G. and Modak, J. (2003). Esterification of myristic acid in supercritical carbon dioxide. *Journal of Supercritical Fluids*, **27** (1): 55-64.

Subramaniam, B. and McHugh, M.A. (1986). Reactions in supercritical fluids-a review. *Industrial & Engineering Chemistry Process Design and Development*, **25** (1): 1-12.

Tai, H.P. and Brunner, G. (2011). Mono- and di-acylglycerol synthesis in CO<sub>2</sub>-expanded acetone. *Journal of Supercritical Fluids*, **59**: 87-91.

Tegetmeier, A., Dittmar, D., Fredenhagen, A. and Eggers, R. (2000). Density and volume of water and triglyceride mixtures in contact with carbon dioxide. *Chemical Engineering and Processing: Process Intensification*, **39** (5): 399-405.

Tuan, D.Q., Zollweg, J.A., Harriott, P. and Rizvi, S.S.H. (1999). Measurement and modeling of viscosity of supercritical carbon dioxide/biomaterial(s) mixtures. *Industrial & Engineering Chemistry Research*, **38** (5): 2129-2136.

Willis, W.M., Lencki, R.W. and Marangoni, A.G. (1998). Lipid modification strategies in the production of nutritionally functional fats and oils. *Critical Reviews in Food Science and Nutrition*, **38** (8): 639-674.

Willis, W.M. and Marangoni, A.G. (2002). Enzymatic interesterification. In *Food lipids: Chemistry, nutrition, and biotechnology* [Online] 2nd ed.; C.C. Akoh and D.B. Min, Eds. Marcel Dekker, New York, NY, USA: New York, NY, USA.

Wolfe, N.L. and Jeffers, P.M. (2000). Hydrolysis. In *Handbook of property estimation methods for chemicals: Environmental and health sciences*, R.S. Boethling, Ed. CRC Press LLC.: Boca Raton, FL, USA, pp 311-334.

Xu, X. (2000). Production of specific-structured triacylglycerols by lipase-catalyzed reactions: A review. *European Journal of Lipid Science and Technology*, **102** (4): 287-303.

Xu, X. (2003). Engineering of enzymatic reactions and reactors for lipid modification and synthesis. *European Journal of Lipid Science and Technology*, **105**: 289-304.

Yahya, A.R.M., Anderson, W.A. and Moo-Young, M. (1998). Ester synthesis in lipase-catalyzed reactions. *Enzyme and Microbial Technology*, **23** (7-8): 438-450.

Yener, M.E., Kashulines, P., Rizvi, S.S.H. and Harriott, P. (1998). Viscosity measurement and modeling of lipid supercritical carbon dioxide mixtures. *Journal of Supercritical Fluids*, **11** (3): 151-162.

Yu, Z.R., Rizvi, S.S.H. and Zollweg, J.A. (1992). Fluid-liquid equilibria of anhydrous milk fat with supercritical carbon dioxide. *Journal of Supercritical Fluids*, **5** (2): 123-129.

Zagrobelny, J. (1992). In situ studies of protein conformation in supercritical fluids: Trypsin in carbon dioxide. *Biotechnology Progress*, **8** (5): 421-423.

### **3. Viscosity measurement and modeling of canola oil and its blend with fully-hydrogenated canola oil in equilibrium with supercritical carbon dioxide<sup>1</sup>**

#### **3.1. Introduction**

As discussed in Section 2.1 supercritical carbon dioxide (SCCO<sub>2</sub>) technology is a rapidly growing alternative to some of the conventional methods of extraction, reaction and fractionation of lipids due to its numerous advantages.

In biocatalytic reactions using SCCO<sub>2</sub> as reaction media, the liquid reactant mixture can expand due to pressure increase and dissolution of CO<sub>2</sub>, causing viscosity reduction, enhancement of the miscibility among reactants, and improvement of the diffusivity of reactants and products to/from the catalyst active site. Information concerning the viscosity of the liquid phase in equilibrium with CO<sub>2</sub> as one of the important physical properties is essential for optimal design of the supercritical fluid separation, fractionation, reaction, and particle formation processes because of the significant impact that viscosity has on mass, heat, and momentum transfer (Kashulines et al., 1991; Tuan et al., 1999; Seifried and Temelli, 2011).

Interestesterification between canola oil and fully-hydrogenated canola oil (FHCO) using SCCO<sub>2</sub> as reaction media is of great interest in an effort to

---

<sup>1</sup> A version of this chapter has been published. Jenab E. and Temelli F. (2011). Viscosity measurement and modeling of canola oil and its blend with canola stearin in equilibrium with high pressure carbon dioxide, *J. Supercrit. Fluids*, 58 (1): 7-14. (Reprinted with permission from Elsevier.)

eliminate the formation of *trans* fatty acids, which is a major concern for conventional hydrogenation of oils employed for the production of margarines. Similar to any other process, information on the physical properties of canola oil and its blend with FHCO saturated with CO<sub>2</sub> is necessary for better understanding of the interesterification process. Among the different physical properties, viscosity has been selected as the focus of this study. Although several studies have reported the viscosity of lipids saturated with CO<sub>2</sub> (Kashulines et al., 1991; Tuan et al., 1999; Calvignac et al., 2010; Seifried and Temelli, 2011), there is a lack of viscosity and rheological data for canola oil and its blend with FHCO saturated with high pressure CO<sub>2</sub>. For example, the viscosity of fish oil triglycerides (Seifried and Temelli, 2011), cocoa butter (Calvignac et al., 2010), anhydrous milk fat (Tuan et al., 1999), and some fatty acids and their methylated derivatives (Kashulines et al., 1991) in equilibrium with high pressure CO<sub>2</sub> has been studied. However, no data are available for the viscosity of canola oil saturated with CO<sub>2</sub> and especially the effect of increased level of saturation on viscosity due to addition of FHCO. Such information for real fat and oil mixtures is needed for better understanding of different SCCO<sub>2</sub> processes involving fat and oil mixtures.

Different methods have been proposed for measuring viscosity under high pressure, which have associated challenges. Falling ball viscometer (Sih et al., 2008; Sih and Foster, 2008; Calvignac et al., 2010) is a method based on the laminar Navier-Stokes model for a Newtonian fluid and a continuity equation for an incompressible fluid, both under steady-state conditions. In this method, ball

terminal velocity, fluid density, and ball density should be known. Lockemann and Schlunder (1995) determined the viscosities of fatty acids and their methyl esters saturated with CO<sub>2</sub> by measuring the velocity of small bubbles rising within a stagnant fluid by taking photographs over time. They created the small bubbles by reducing the pressure by 0.01 MPa. Using a high-pressure capillary viscometer is another method in which the pressure drop is measured by a differential pressure transducer while pumping the test fluid through the capillary and the viscosity is determined by using the Rabinowitsch-Moony equation (Tuan et al., 1999). Rotational rheometer with cup and bob geometry equipped with a high pressure cell was used by Seifried and Temelli (2011) and in this study to measure the viscosity of liquid lipids in equilibrium with high pressure CO<sub>2</sub>. In this method, where the bob rotates at a constant speed and the cup is stationary, the instrument measures the torque required to maintain a constant angular velocity of the bob.

The objectives of this study were (a) to determine the viscosity and rheological behaviour of canola oil and its blend with FHCO (30 wt.%) in equilibrium with CO<sub>2</sub> at temperatures of 40, 50, 65, and 75 °C and pressures of up to 12.4 MPa, (b) to determine the solubility of CO<sub>2</sub> in canola oil at 40 and 65 °C and its blend with FHCO at 65 °C and pressures of up to 20 MPa, and (c) to correlate the viscosity data with mass fraction of CO<sub>2</sub> in the liquid phase using correlative methods.

### **3.2. Material and methods**

#### **3.2.1. Materials**

Canola oil was obtained from Richardson Oilseed Ltd. (Lethbridge, AB, Canada) and FHCO was kindly provided by Canbra Foods Ltd. (Lethbridge, AB, Canada). The fatty acid composition of canola oil and FHCO (Table 3-1) was determined by gas chromatography using the AOCS official method Ce 1-62 (AOCS, 2009). Certified standard calibration oils of various viscosities were used to check the calibration and performance of the rheometer (oils S3, S6, N10, Cannon Instrument Company, State College, PA, USA). Bone dry CO<sub>2</sub> with a purity of 99.99% (Praxair, Edmonton, AB, Canada) was used for the saturation of liquid lipids.

**Table 3-1.** Fatty acid composition of fully-hydrogenated canola oil (FHCO) and canola oil considering fatty acids of more than 1%.\*

<b>Fatty acid</b>	<b>GC area %</b>	
	<b>FHCO</b>	<b>Canola oil</b>
C16:0	8.55±0.29	4.18±0.06
C18:0	74.60±0.32	1.57±0.02
C18:1, <i>trans</i> -Δ <sup>9</sup>	3.44±0.08	-
C18:1, <i>cis</i> -Δ <sup>9</sup>	12.00±0.02	56.46±0.17
C18:1, <i>cis</i> -Δ <sup>11</sup>	-	4.52±0.28
C18:2, <i>cis, cis</i> -Δ <sup>9, 12</sup>	-	19.80±0.14
C18:3, <i>cis, cis, cis</i> -Δ <sup>9, 12, 15</sup>	-	9.49±0.01
C20:1, <i>cis</i> -Δ <sup>5</sup>	-	1.08±0.03
C20:0	1.42±0.1	-
Unknowns	-	2.88±0.57

\* Mean±standard deviation based on three determinations.

### **3.2.2. Viscosity determination**

#### **3.2.2.1. Apparatus to measure viscosity**

The apparatus used to measure viscosity and rheological behaviour was a computer controlled rotational rheometer (UDS200, Anton Paar, Graz, Austria) equipped with a bob and cup setup (CC 23Pr/Q0, Anton Paar, Graz, Austria) in a thermo-stated pressure cell (TEZ 150P, Anton Paar, Graz, Austria) with Peltier temperature control. The cell was equipped with a magnetic coupling pressure head. This apparatus as previously used by Seifried and Temelli (2011) was modified with the addition of a piston pump (Milton Roy, Ivyland, PA, USA) located between the liquid delivery CO<sub>2</sub> cylinder (Praxair, Edmonton, AB, Canada) and a reservoir cylinder (150 mL) to pressurize CO<sub>2</sub> (Fig. 3-1). First, the reservoir cylinder was pressurized and then the pressure in the rheometer cell was allowed to reach the desired level by adjusting the pressure regulator (Swagelok KPP series, Swagelok, Edmonton, AB, Canada) at the outlet of the reservoir cylinder and opening the valve at the inlet of the high pressure cell of rheometer very slowly in order to avoid splashing of the sample placed previously inside the cell.

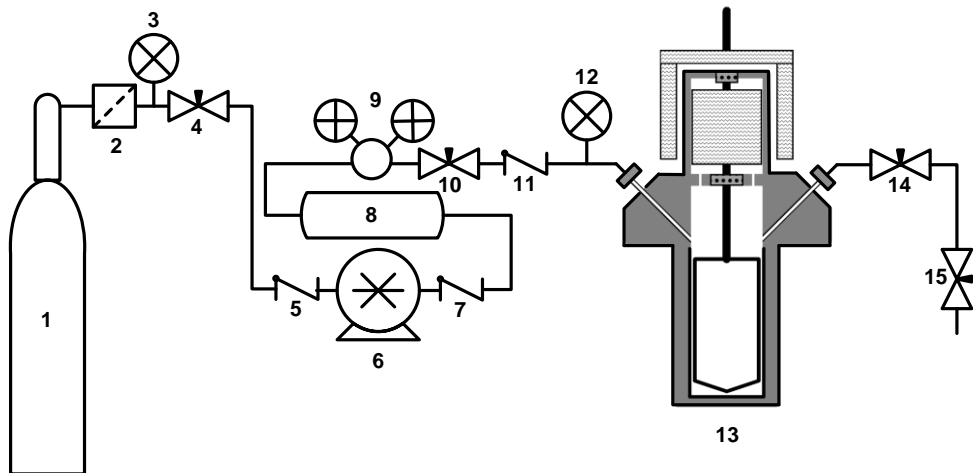


**Figure 3-1.** High pressure rheometer: 1, CO<sub>2</sub> cylinder; 2, CO<sub>2</sub> filter; 3, and 12, pressure gauges; 4, 10, 14, and 15, needle valves; 5, 7, and 11 check valves; 6, piston pump; 8, high pressure cell; 9, pressure regulator; 13, rheometer equipped with high pressure cell.

### 3.2.2.2. Experimental design and protocols

The viscosity of canola oil in equilibrium with CO<sub>2</sub> at temperatures of 40, 50, 65, and 75 °C and the blend of canola oil with FHCO (30 wt.%) at 65 °C and pressures of up to 12.4 MPa was measured according to the protocols used by Sefried and Temelli (2011) with some modification. The level of FHCO in the blend was chosen based on the parallel studies on interesterification between canola oil and FHCO using SCCO<sub>2</sub> as reaction medium (Chapters 5 and 6). The viscosity of the blend was measured only at 65 °C because the melting point of FHCO is between 60-70 °C and it is a solid at lower temperatures. The system and protocols were validated previously by Seifried and Temelli (2011). Because there was no stirrer or mechanical mixer in the system, the equilibration and saturation of the samples required a long time. In this study, saturation method

upon pressurization was used in order to reach equilibrium instead of the faster method of degassing/purging from a higher pressure adopted by Seifried and Temelli (2011) previously. First, the high pressure cell was flushed with CO<sub>2</sub> to expel any air from the cell and then the sample (11.5 mL) was injected into the cell with a syringe followed by flushing with CO<sub>2</sub>, again very slowly, to remove all of the residual air from the sample and inside the cell. After reaching equilibrium at the desired temperature, the viscosity was first measured at atmospheric pressure. The viscosity of samples at different sets of pressure and temperature was measured after 5-7 h, depending on temperature and pressure, when they reached equilibrium and there was no further change in viscosity with time. However, most of the samples were left overnight (approximately 12 h) in the rheometer to ensure that equilibrium was attained. Viscosity determination at each condition was performed in 3-4 replicates.

The viscosity of samples was measured at a constant shear rate of 300 s<sup>-1</sup> at different levels of pressure at each temperature and then the rheological behaviour of the samples was determined by measuring shear stress ( $\sigma$ , Pa) at shear rates ( $\dot{\gamma}$ , s<sup>-1</sup>) ranging from 100-600 s<sup>-1</sup>. To find the flow behaviour index ( $n$ , [ ]) and consistency index ( $K$ , Pa.s<sup>n</sup>) of the samples at different conditions, the Power Law model given in Equation (3.1) was fitted to experimental data using curve expert software.

$$\log\sigma = \log K + n \log \dot{\gamma} \quad (3.1)$$

### **3.2.3. Determination of CO<sub>2</sub> solubility in the liquid phase**

#### **3.2.3.1. Apparatus to measure CO<sub>2</sub> solubility**

CO<sub>2</sub> solubility measurements were carried out using a high pressure view cell, depicted in Figure 3-2 (Phase equilibria unit, Sitec Sieber Engineering, Zurich, Switzerland) with a capacity of 10 mL and equipped with sapphire windows. A microscope (SM-4TZ-FRL-3M, AmScope, Iscope Corp, Chino, CA, USA) with a video camera (MD800E, AmScope, Iscope Corp, Chino, CA, USA) connected to a computer was used to monitor the inside of the cell. The cell was surrounded by a jacket, connected to a circulating water bath with temperature controller. The temperature in the cell was measured by a thermocouple placed on the inner wall of the cell and displayed on a temperature indicator (Eurotherm, Ashbum, VA, USA). The cell was attached to a counter pressure balance piston (i.e. manual pump) for pressurizing the system and to maintain the pressure during sampling. The pressure in the cell was measured by a pressure transducer (Baumer-Haenni, Jegenstorf, Switzerland) with an accuracy of 0.01 MPa connected to a pressure indicator (Eurotherm, Ashbum, VA, USA). A Teflon-coated magnetic bar, driven by an external magnetic stirrer, provided appropriate stirring inside the cell. The sampling valve located at the bottom of the cell was heated to the same temperature as the cell using heating rope, which was connected to a temperature controller.

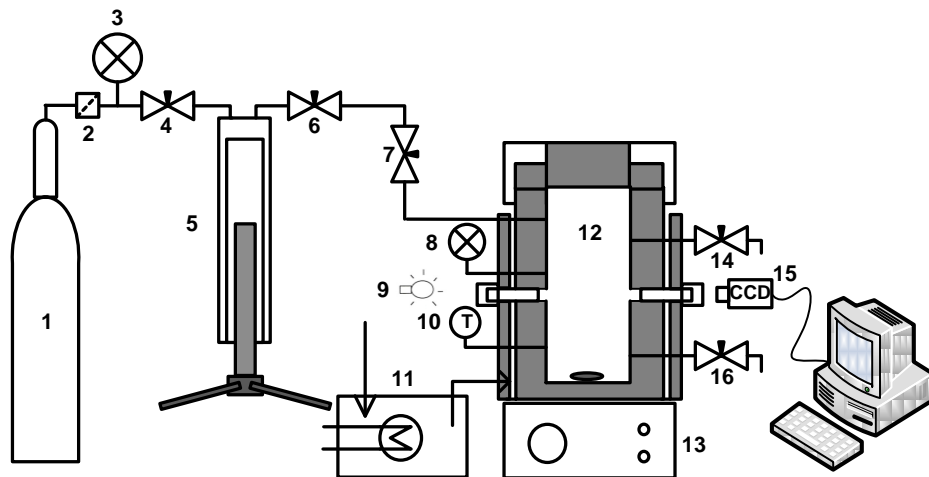


**Figure 3-2.** Phase equilibria unit: 1, CO<sub>2</sub> cylinder; 2, CO<sub>2</sub> filter; 3 and 8, pressure gauges; 4, 6, 7, 14, and 16, needle valves; 5, manual pump; 9, light source; 10, temperature indicator; 11, heated water bath; 12, high pressure view vessel; 13, magnetic stirrer; 15, video camera.

### 3.2.3.2. Experimental design and protocols

The lipid sample (5 mL) was placed inside the high pressure cell and the cell was purged slowly with CO<sub>2</sub> to remove residual air. Once the temperature stabilized, the pressure inside the cell was increased to the desired level by means of the manual pump attached to the cell and the magnetic stirrer was turned on. The samples were stirred for 3-4 h and allowed to settle for another 1-1.5 h under pressure, based on determinations during preliminary studies. Prior to taking a sample from the cell, it was ensured that there were no bubbles in the fluid mixture by monitoring the inside of the cell with the camera. Samples were withdrawn from the bottom of the cell and depressurized to atmospheric pressure while keeping the pressure of the cell constant by adjusting the manual pump and monitoring the inside of the cell for any disturbance of the equilibrium state.

Samples were collected in glass vials sitting in a cold trap and the vials were weighed using an analytical balance before and after sampling. CO<sub>2</sub> released from the sample was collected in a calibrated graduated syringe filled with saturated solution of Na<sub>2</sub>SO<sub>4</sub> to prevent CO<sub>2</sub> dissolution in the water (Hernandez et al., 2008) and its amount was quantified volumetrically based on the displaced liquid volume in the syringe. The mass of CO<sub>2</sub> was determined using the density of CO<sub>2</sub> at the temperature of saturated solution and ambient pressure, available from the NIST Chemistry WebBook based on the Span and Wagner equation of state (Lemmon et al., 2010). CO<sub>2</sub> solubility determinations at each condition were performed in 3-4 replicates. The above protocol was previously verified by Seifried and Temelli (2011) by reproducing literature data (Borch-Jensen and Mollerup, 1997) for CO<sub>2</sub> solubility in fish oil and the data obtained were in agreement with literature data with an average absolute relative deviation (AARD) of about 3.5%.

### **3.3. Results and discussion**

#### **3.3.1. Viscosity as a function of pressure and temperature**

Table 3-2 shows the viscosity of canola oil at 40, 50, 65, and 75 °C and its blend with FHCO (30 wt.%) at 65 °C, both saturated with CO<sub>2</sub> at pressures of up to 12.4 MPa. Both temperature and pressure have a pronounced effect on the viscosity of canola oil and its blend with FHCO saturated with CO<sub>2</sub>.

**Table 3-2.** Viscosity (mPa.s) of canola oil and its blend with canola stearin saturated with CO<sub>2</sub> at various pressures and temperatures at a shear rate of 300 s<sup>-1</sup>.\*

Pressure (MPa)	Temperature (°C)					Canola oil and FHCO blend (30 wt.%)
	40	50	65	75	65	
0.1	32.26±0.14	23.24±0.19	15.44±0.11	12.19±0.20	15.97±0.05	
1.03	24.96±0.51	-	12.55±0.49	10.12±0.43	-	
2.07	17.94±0.68	14.79±0.30	10.92±0.17	8.57±0.63	11.99±0.16	
4.14	10.70±0.06	-	7.56±0.19	6.83±0.51	-	
6.2	6.62±0.11	6.48±0.18	6.04±0.17	5.37±0.14	6.53±0.28	
8.27	4.76±0.30	4.48±0.04	4.67±0.12	4.81±0.12	5.03±0.04	
10.34	4.29±0.24	-	4.03±0.12	4.33±0.16	4.45±0.28	
12.41	4.12±0.30	3.55±0.06	3.89±0.09	4.07±0.22	4.12±0.4	

\* Mean±standard deviation based on three replications.

As shown in Figure 3-3, the viscosity of canola oil in equilibrium with high pressure CO<sub>2</sub> decreased dramatically with temperature at constant pressures up to approximately 10 MPa and above that the variation of viscosity with temperature diminished. At atmospheric pressure, viscosity decreased exponentially with temperature, similar to the viscosity behaviour of other vegetable oils (Noureddini et al., 1992; Calvignac et al., 2010).

The viscosity of the samples investigated decreased exponentially with pressure at each temperature, but the decrease was not pronounced above approximately 10 MPa and reached a fairly constant level. The exponential decrease in viscosity with pressure is mainly due to the dramatic increase in CO<sub>2</sub> solubility in the liquid phase as discussed later and dilution of the liquid oil with a component of very low viscosity.

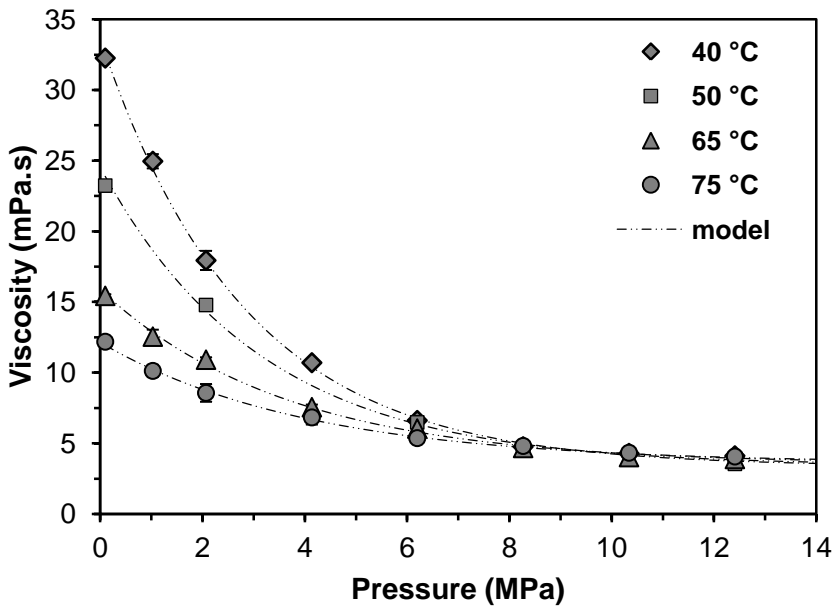


**Figure 3-3.** Viscosity of canola oil in equilibrium with CO<sub>2</sub> as a function of pressure at different temperatures at a shear rate of 300 s<sup>-1</sup>. Curves fitted based on Equation (3.2). Error bars represent standard deviation based on three replications.

At elevated pressures, the mass fraction of CO<sub>2</sub> in the liquid phase increases only slightly and thus the viscosity of the CO<sub>2</sub>-expanded liquid phase remains almost constant. As shown later, the solubility of CO<sub>2</sub> in the liquid phase increases with pressure and decreases with temperature; therefore, at lower temperatures the effect of pressure on viscosity was more pronounced as at 40, 50, 65, and 75 °C the viscosity of canola oil decreased by 87.2, 84.7, 74.8, and 66.6% up to a pressure of 12.4 MPa, respectively, compared to atmospheric pressure.

Findings of this study are consistent with those reported for fish oil (Seifried and Temelli, 2011) and cocoa butter (Venter et al., 2007; Calvignac et al., 2010) saturated with CO<sub>2</sub> where viscosity exponentially decreased as a function of pressure at constant temperature and at elevated pressures the viscosity of liquid

phase reached a fairly constant level. As well, Lockemann and Schlunder (1995) found that the viscosity of oleic acid, methyl myristate, and methyl palmitate in equilibrium with high pressure CO<sub>2</sub> at temperatures of 40, 60, and 80 °C decreased about one order of magnitude up to a pressure of 12.6 MPa to values that were not significantly different.

The viscosity of fatty acids is highly dependent on the chain length and degree of unsaturation (Peter and Jakob, 1991). The viscosity of valeric, oleic, linoleic, and pelargonic acids in equilibrium with C<sub>2</sub>H<sub>6</sub> at 40 °C was studied by Peter and Jakob (1991). They showed that the viscosity increased with fatty acid chain length and decreased with the number of double bonds or the degree of unsaturation. However, such a systematic study is not available for triglycerides with fatty acids of different chain lengths and degrees of saturation. Comparison of the viscosity of canola oil with the literature data for fish oil and cocoa butter saturated with CO<sub>2</sub> at 40 °C (Fig. 3-4) revealed that at constant pressure the viscosity increased with the degree of saturation, similar to the behaviour reported for free fatty acids (Peter and Jakob, 1991). At elevated pressures the viscosities of these three lipids also reached a fairly constant level (Fig. 3-4).

However, at high temperatures (65 °C), as shown in Figure 3-5 the viscosities of canola oil and its blend with FHCO saturated with CO<sub>2</sub> were similar regardless of the degree of saturation because of the dominant effect of high temperature overcoming any viscosity differences due to the degree of saturation.

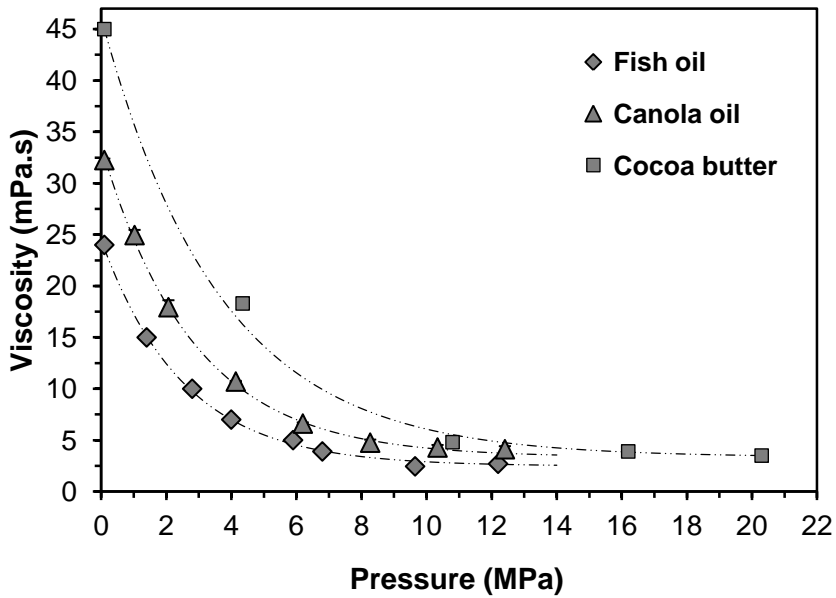


**Figure 3-4.** Viscosity of canola oil in equilibrium with CO<sub>2</sub> as a function of pressure at 40 °C determined in this study at a shear rate of 300 s<sup>-1</sup> compared to the literature data for fish oil (Seifried and Temelli, 2011) and cocoa butter (Calvignac et al., 2010) both at 40 °C.

The empirical model (Eq. (3.2)) proposed by Seifried and Temelli (2011) was fitted to the measured viscosity data as a function of pressure and temperature by minimizing AARD using the solver program of Microsoft Excel.

$$\eta(P, T) = \eta_{\infty}(T) + [\eta_0(T) - \eta_{\infty}(T)] \times e^{[-k(T) \times (P - 0.1)]} \quad (3.2)$$

$$\eta_{\infty}(T) = A_1 + A_2 T \quad (3.3)$$

$$\eta_0(T) = A_3 e^{\left(\frac{A_4}{T}\right)} \quad (3.4)$$

$$k(T) = A_5 e^{A_6 T} \quad (3.5)$$

Where,  $\eta_{\infty}(T)$  is viscosity at elevated pressure,  $\eta_0(T)$  is viscosity at atmospheric pressure, and  $k(T)$  is temperature dependent exponential decline of viscosity by

pressure with pressure in [Pa], temperature in [K], and viscosity in [mPa.s]. The AARD (Eq. (3.6)) can be used to quantify the goodness of the fit:

$$AARD(\%) = \frac{1}{N} \sum \left| \frac{\eta^{cal.} - \eta^{exp.}}{\eta^{exp.}} \right| \times 100 \quad (3.6)$$

where,  $N$  is the number of experimental points,  $\eta^{cal.}$  is the calculated viscosity, and  $\eta^{exp.}$  is experimentally measured viscosity.

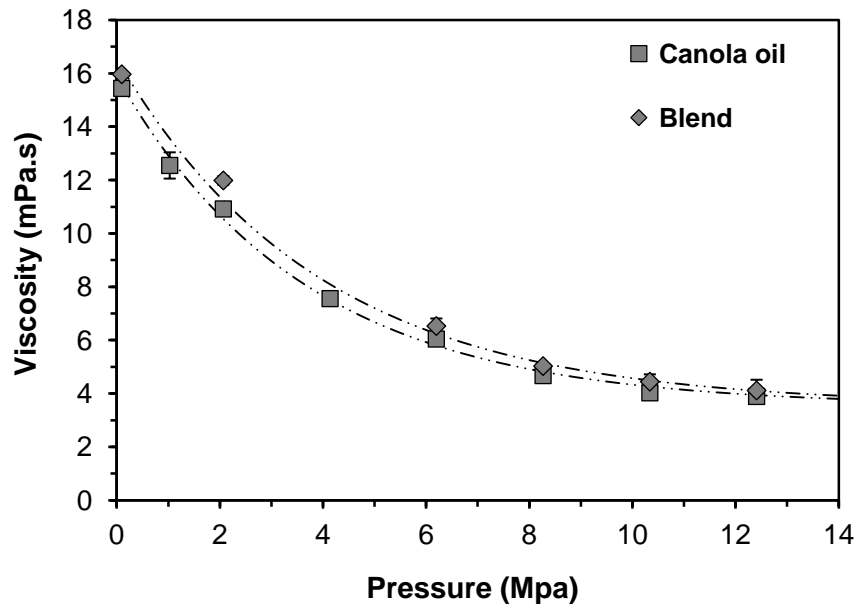


**Figure 3-5.** Viscosity of canola oil and the blend containing 30 wt.% FHCO in equilibrium with CO<sub>2</sub> as a function of pressure at 65 °C at a shear rate of 300 s<sup>-1</sup>. Error bars represent standard deviation based on three replications.

The model given in Equation (3.2) with the calculated parameters presented in Table 3-3 described the experimental data with an AARD of 3.6% within the temperature and pressure ranges considered in this study. Even though having six

parameters may seem excessive, it is believed that having such a correlation would be useful for quick viscosity assessment based only on the operating parameters of temperature and pressure.

**Table 3-3.** Model parameters for the correlation of viscosity of CO<sub>2</sub>-expanded canola oil using Equation (3.2).

<b>Model parameters</b>	
<b>A<sub>1</sub></b>	1.099
<b>A<sub>2</sub></b>	$7.1774 \times 10^{-3}$
<b>A<sub>3</sub></b>	$1.4977 \times 10^{-3}$
<b>A<sub>4</sub></b>	$3.1272 \times 10^3$
<b>A<sub>5</sub></b>	8.3331
<b>A<sub>6</sub></b>	$1.0104 \times 10^{-2}$

### 3.3.2. Rheological behaviour

The rheological behaviour of canola oil at 40, 65, and 75°C and its blend with FHCO (30 wt %) at 65°C saturated with CO<sub>2</sub> up to a pressure of 12.4 MPa was studied at shear rates ranging from 100 to 600 s<sup>-1</sup> (Table 3-4). The flow behaviour was analyzed by linear regression analysis of the logarithm of shear stress versus the logarithm of shear rate, and the flow behaviour index (*n*) and consistency index (*K*) were obtained as the slope and intercept, respectively.

**Table 3-4.** Power law parameters (flow behaviour index ‘n’ and logarithm of consistency index ‘K’) for canola oil and its blend with fully-hydrogenated canola oil (FHCO) (30 wt.%), both saturated with CO<sub>2</sub> at different temperatures.

Pressure (MPa)	Canola oil and FHCO blend (30 wt.%)							
	Temperature (°C)							
	40	65	75	65	n	logK	n	logK
n	logK	n	logK	n	logK	n	logK	n
0.1	1.02±0.01	-1.54±0.02	1.04±0.01	-1.90±0.02	1.04±0.01	-2.00±0.02	1.05±0.03	-1.90±0.07
1.03	1.03±0.02	-1.67±0.04	1.04±0.01	-2.02±0.02	1.06±0.01	-2.12±0.04	-	-
2.07	1.05±0.02	-1.85±0.06	1.05±0.01	-2.09±0.02	1.05±0.03	-2.20±0.09	1.06±0.03	-2.09±0.12
4.14	1.07±0.03	-2.16±0.07	1.08±0.01	-2.30±0.03	1.06±0.02	-2.31±0.04	-	-
6.21	1.13±0.04	-2.51±0.09	1.10±0.02	-2.47±0.06	1.09±0.01	-2.50±0.05	1.14±0.05	-2.47±0.11
8.27	1.12±0.03	-2.62±0.08	1.11±0.03	-2.61±0.09	1.10±0.01	-2.57±0.02	1.14±0.04	-2.61±0.06
10.34	1.16±0.02	-2.74±0.06	1.14±0.04	-2.72±0.09	1.11±0.02	-2.61±0.08	1.16±0.02	-2.72±0.02
12.41	1.19±0.03	-2.85±0.11	1.19±0.02	-2.88±0.07	1.15±0.02	-2.78±0.02	1.21±0.03	-2.88±0.06

The samples exhibited shear-thickening behaviour, which was also reported by Seifried and Temelli (2011) for CO<sub>2</sub>-expanded fish oil and by Hobbie (2006) for CO<sub>2</sub>-expanded corn oil. Peter and Jakob (1991) found that the mixture of pelargonic acid with CO<sub>2</sub> and C<sub>2</sub>H<sub>6</sub> showed shear-thickening behaviour with increasing gas content up to a shear rate of 1000 s<sup>-1</sup> while oleic, linoleic, and valeric acids did not exhibit such behaviour.

The effects of pressure and temperature on the flow behaviour index and consistency index are shown in Figures 3-6 and 3-7, respectively. At all temperatures, the flow behaviour indices were close to 1 at atmospheric pressure and increased almost linearly with pressure up to 1.2 at 12.4 MPa (Fig. 3-6). However, the flow behaviour index of the samples studied here was not as high as that of CO<sub>2</sub>-expanded fish oil ( $n \approx 1.5$ ) at elevated pressures reported by Seifried and Temelli (2011), which might be due to the higher level of unsaturation of fish oil compared to canola oil. On the contrary, the consistency index of CO<sub>2</sub>-expanded canola oil decreased with pressure and reached values close to zero at elevated pressures (Fig. 3-7). The shear-thickening behaviour of the canola oil in equilibrium with high pressure CO<sub>2</sub> could be related to the change in the CO<sub>2</sub>-expanded oil density with pressure, as will be discussed in Chapter 4. CO<sub>2</sub> might fill the void volumes between the triglyceride molecules, resulting in enhanced shear-thickening behaviour at elevated pressures. The molecular basis for shear-thickening behaviour requires further research for better understanding of the interactions between CO<sub>2</sub> and triglyceride components.

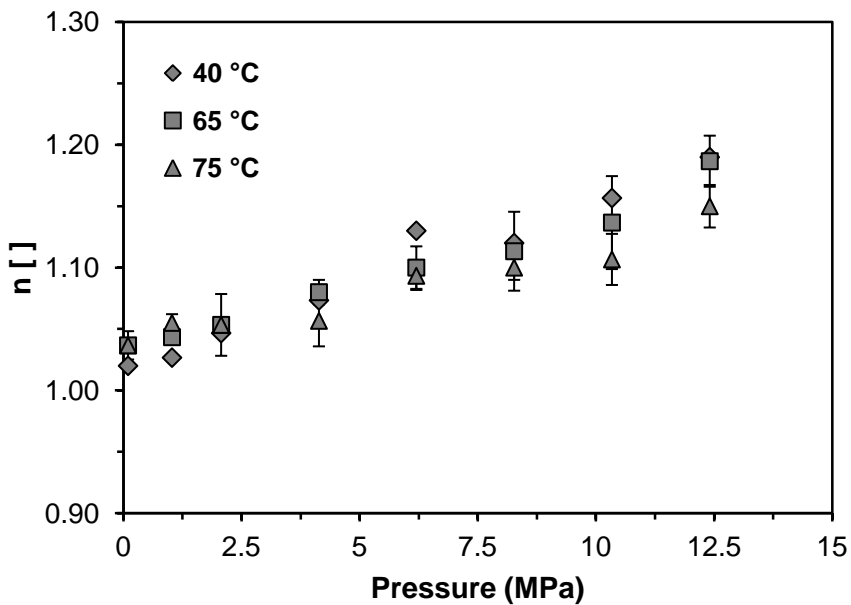


**Figure 3-6.** Flow behaviour index of canola oil as a function of pressure at different temperatures. Error bars represent standard deviation based on three replications.

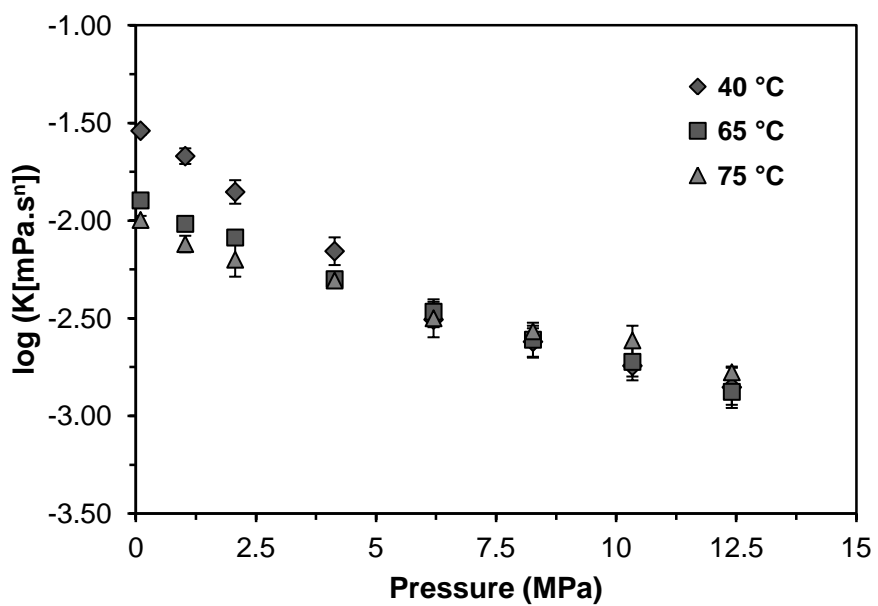


**Figure 3-7.** Consistency index of canola oil saturated with CO<sub>2</sub> at different temperatures as a function of pressure. Error bars represent standard deviation based on three replications.

### **3.3.3. Viscosity as a function of mass fraction of CO<sub>2</sub> in the liquid phase**

Elevated pressures cause a substantial increase in the solubility of CO<sub>2</sub> in the liquid phase of gas-liquid systems. Therefore, the viscosity of the gas-expanded liquid phase in gas-liquid systems is not only a function of pressure and temperature but it can also be a function of mass fraction of CO<sub>2</sub> in the liquid phase.

The solubility of CO<sub>2</sub> in canola oil at 40 and 65 °C and its blend with FHCO (30 wt.%) at 65 °C was measured at pressures of up to 20 MPa. As shown in Figure 3-8, the mass fraction of CO<sub>2</sub> in the liquid phase increased with pressure and decreased with temperature as expected. The solubility of CO<sub>2</sub> increased dramatically up to 10 MPa and above that the rate of increase declined and the solubility reached a plateau at higher pressures, where the solubility of CO<sub>2</sub> reached 24% (w/w) for canola oil at 40°C and 21% (w/w) for its blend with FHCO at 65 °C at 20 MPa. Similar behaviour was reported for triolein and oleic acid (Bharath et al., 1992) and cocoa butter (Venter et al., 2007) saturated with CO<sub>2</sub>. Also, the solubility of CO<sub>2</sub> in canola oil and in its blend with FHCO at 65 °C was similar.

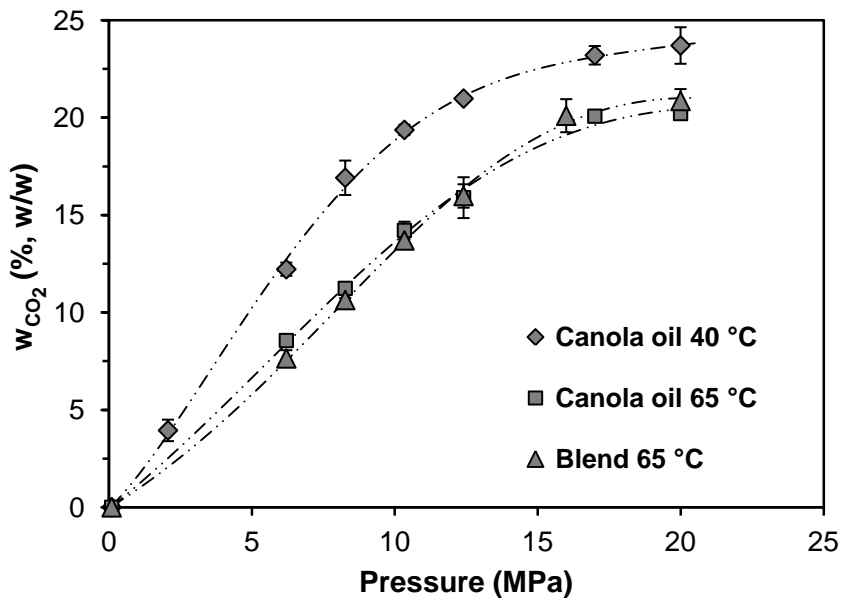


**Figure 3-8.** Solubility of CO<sub>2</sub> in canola oil and its blend with fully-hydrogenated canola oil (FHCO) (30 wt.%) at different pressures and temperatures.

Figure 3-9 displays the viscosity of canola oil at 40 and 65 °C and its blend with FHCO at 65°C at pressures of up to 12.4 MPa as a function of CO<sub>2</sub> mass fraction in the liquid phase. The viscosity decreased with an increase in the mass fraction of CO<sub>2</sub> in the liquid phase, mainly due to the dilution of the liquid oil with a component of very low viscosity, approaching a constant level at CO<sub>2</sub> mass fractions greater than approximately 0.17. At constant CO<sub>2</sub> mass fraction or liquid phase composition, an increase in temperature caused a decrease in liquid viscosity. Also, the degree of viscosity reduction with temperature was less pronounced at higher mass fractions of CO<sub>2</sub>.

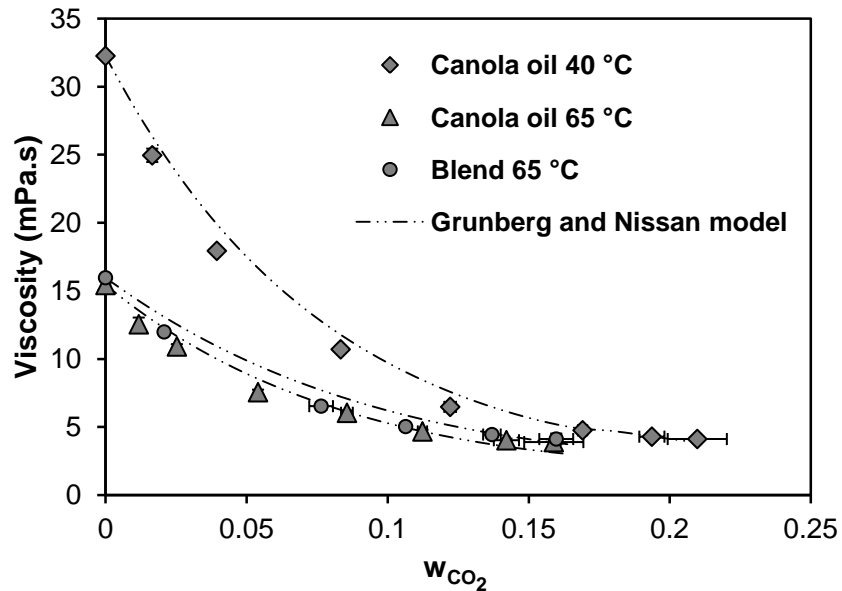


**Figure 3-9.** Viscosity of  $\text{CO}_2$ -saturated canola oil and its blend with fully-hydrogenated canola oil (FHC) (30 wt.%) at different temperatures as a function of mass fraction of  $\text{CO}_2$ .

Correlation and prediction of the viscosity of liquid phases in equilibrium with  $\text{CO}_2$  based on the mole or mass fraction of  $\text{CO}_2$  in liquid phase using modified Ely and Hanley, Grunberg and Nissan, and modified Grunberg and Nissan models have been presented by several authors (Kashulines et al., 1991; Tuan et al., 1999; Calvignac et al., 2010).

Ely and Hanley model, which is based on the corresponding states approach, considering methane as a reference fluid, is a purely predictive model requiring critical properties, density, viscosity, acentric factor, and molecular mass of methane and components of the fluid mixture (Tuan et al., 1999). However, to calculate the viscosity of liquid mixtures with reasonable accuracy, empirical parabolic equations with one adjustable or interaction parameter are the

most effective (Mehrotra et al., 1996). The Grunberg and Nissan model (Eq. (3.7)) is one such empirical parabolic equation that can be used to predict the viscosity of liquid phases saturated with CO<sub>2</sub> (Kashulines et al., 1991):

$$\ln \eta_m = \sum w_i \ln(\eta_i) + \sum \sum w_i w_j G_{ij} \quad (3.7)$$

Where,  $\eta_m$  is mixture viscosity,  $w_i$  is mass fraction of component  $i$ ,  $\eta_i$  is the viscosity of component  $i$  at the system conditions, and  $G_{ij}$  is an interaction parameter that takes into account deviation from ideal behaviour, which is generally system dependent and sometimes temperature dependent (Kashulines et al., 1991). The viscosities of pure vegetable oils (Hobbie, 2006; Schaschke et al., 2006), fatty acids and fatty acid esters (Lockemann and Schlunder, 1995; Duncan et al., 2010) increase with pressure at various temperatures. No data are available on the viscosity of pure canola oil at elevated pressures. However, Hobbie (2006) reported the viscosity of pure corn oil at 37, 56, and 70°C at hydrostatic pressures of up to 25 MPa. A mathematical equation (Eq. (3.8)) showing the effect of pressure and temperature on the viscosity of pure oil was obtained based on the experimental data of Hobbie (2006).

$$\eta_{oil}(T, P) = A(T) \cdot P + \eta_0(T, P_0) \quad (3.8)$$

$$A(T) = 0.0002T^2 - 0.0377T + 1.804 \quad (3.9)$$

Where, P is in [MPa] and T is in [°C].

Considering that the viscosities of corn oil and canola oil at different temperatures and atmospheric pressure are similar, this equation for corn oil was used to calculate the viscosity of pure canola oil and its blend with FHCO at different pressures and temperatures. On the other hand, the equations and models developed for free fatty acids or fatty acid esters would not be directly applicable for the triglycerides of canola oil due to significant differences in their physical properties and composition. Thus, the calculated viscosities of pure canola oil and its blend with FHCO at various temperatures and pressures were used in the Grunberg and Nissan model to predict the viscosity of CO<sub>2</sub>-expanded oil. The pure CO<sub>2</sub> viscosity at different temperatures and pressures was taken from the NIST Chemistry WebBook (Lemmon et al., 2010). Calvignac et al. (2010) simplified the Grunberg and Nissan model to the form given in Equation (3.10) based on three assumptions, including neglecting the mass fraction of CO<sub>2</sub> compared to the oil, considering the variation in oil viscosity with an increase in pressure low enough to be neglected, and neglecting the viscosity of CO<sub>2</sub> compared to that of the oil.

$$\ln \eta_m(T, P) = \ln \eta_{oil}(T, P_0) + w_{CO_2}(T, P) \cdot A_{12}(T) \quad (3.10)$$

Where,  $A_{12}$  is a binary parameter, which is temperature dependent. The values for both  $G_{12}$  and  $A_{12}$  were determined by minimizing AARD using the solver program in Microsoft Excel for the above two models separately and the results were presented in Table 3-5. The Grunberg and Nissan model (Eq. (3.7)) was found to better describe the data because of the lower AARD (7.3%) compared to the one

modified by Calvignac et al. (2010) (Eq. (3.10)). Both binary parameters in the two models were negative, meaning that the interaction of molecules in the mixture was less than what would be expected for individual component viscosities.

**Table 3-5.** Fitting results of Grunberg and Nissan model (Model 1, Eq. (3.7)) and modified Grunberg and Nissan model (Model 2, Eq. (3.10)) to experimental viscosity data of canola oil and its blend with fully-hydrogenated canola oil (FHCO) in equilibrium with CO<sub>2</sub>.

Temperature (°C)	Model 1		Model 2	
	G <sub>12</sub>	AARD (%)	A <sub>12</sub>	AARD (%)
Canola oil	40	-5.84	6.25	-11.32
	65	-5.41	7.45	-10.64
Canola oil and FHCO blend (30 wt. %)	65	-3.99	7.48	-9.34
Average AARD		7.06		11.00

### 3.4. Conclusions

The viscosity of canola oil and its blend with FHCO saturated with CO<sub>2</sub> is highly dependent on temperature and pressure. The viscosity of samples dramatically decreased up to 10 MPa and above that reached a fairly constant level at different temperatures as the viscosity of CO<sub>2</sub>-expanded canola oil at 40 and 75 °C and its blend with FHCO (30 wt. %) at 65 °C decreased by 87.2, 66.6, and 74.2% at 12.4 MPa compared to their viscosities at atmospheric pressure, respectively. The effect of temperature on viscosity diminished at elevated pressures. At high temperatures (65 °C), the viscosities of canola oil and its blend

with FHCO were similar where the effect of temperature dominated the effect of the degree of unsaturation on viscosity. The mass fraction of CO<sub>2</sub> in canola oil and its blend with FHCO, which turns out to have substantial influence on viscosity due to the dilution of the liquid oil with a component of very low viscosity, increased dramatically up to 10 MPa and above that the rate of increase declined until it reached a fairly constant level of 24% for canola oil at 40°C and 21% for canola oil and its blend with FHCO at 65°C at 20 MPa. The Grunberg and Nissan model, which correlates the viscosity data with the mass fraction of CO<sub>2</sub>, described the experimental data reasonably well with AARD of 7.06%. The findings provide insight into the development of interesterification process involving high melting components like FHCO.

### 3.5. References

AOCS Official and Recommended Practices. (2009). (6th ed.) AOCS Press, Champaign, IL, USA.

Bharath, R., Inomata, H., Adschari, T. and Arai, K. (1992). Phase equilibrium study for the separation and fractionation of fatty oil components using supercritical carbon dioxide. *Fluid Phase Equilibria*, **81** (C): 307-320.

Borch-Jensen, C. and Mollerup, J. (1997). Phase equilibria of fish oil in sub- and supercritical carbon dioxide. *Fluid Phase Equilibria*, **138** (1-2): 179-211.

Calvignac, B., Rodier, E., Letourneau, J.J., dos Santos, P.M.A. and Fages, J. (2010). Cocoa butter saturated with supercritical carbon dioxide: Measurements and modelling of solubility, volumetric expansion, density and viscosity. *International Journal of Chemical Reactor Engineering*, **8**: A73.

Duncan, A.M., Ahosseini, A., McHenry, R., Depcik, C.D., Stagg-Williams, S.M. and Scurto, A.M. (2010). High-pressure viscosity of biodiesel from soybean, canola, and coconut oils. *Energy and Fuels*, **24** (10): 5708-5716.

Hernandez, E.J., Mabe, G.D., Senorans, F.J., Reglero, G. and Fornari, T. (2008). High-pressure phase equilibria of the pseudoternary mixture sunflower

oil+ethanol+carbon dioxide. *Journal of Chemical and Engineering Data*, **53** (11): 2632-2636.

Hobbie, M. (2006). Bildung von tropfen in verdichteten gasen und stationäre umströmung fluider partikel bei drücken bis zu 50 MPa. PhD dissertation, Hamburg University of Technology, Hamburg, Germany, p 162.

Kashulines, P., Rizvi, S.S.H., Harriott, P. and Zollweg, J.A. (1991). Viscosities of fatty acids and methylated fatty acids saturated with supercritical carbon dioxide. *Journal of the American Oil Chemists' Society*, **68** (12): 912-921.

Lemmon, E.W., McLinden, M.O. and Friend, D.G. (2010). Thermophysical properties of fluid systems. In *NIST chemistry webbook, NIST standard reference database number 69*, P.J. Linstrom and W.G. Mallard, Eds. National Institute of Standards and Technology: Gaithersburg, MD, USA, p 2089.

Lockemann, C.A. and Schlunder, E.U. (1995). Liquid-phase viscosities of the binary systems carbon dioxide-oleic acid, carbon dioxide-methyl myristate, and carbon dioxide-methyl palmitate at high pressures. *Chemical Engineering and Processing*, **34** (6): 487-493.

Mehrotra, A.K., Monnery, W.D. and Svrcek, W.Y. (1996). A review of practical calculation methods for the viscosity of liquid hydrocarbons and their mixtures. *Fluid Phase Equilibria*, **117** (1-2): 344-355.

Noureddini, H., Teoh, B.C. and Clements, L.D. (1992). Viscosities of vegetable oils and fatty acids. *Journal of the American Oil Chemists' Society*, **69** (12): 1189-1191.

Peter, S. and Jakob, H. (1991). The rheological behaviour of coexisting phases in systems containing fatty acids and dense gases. *Journal of Supercritical Fluids*, **4** (3): 166-172.

Schaschke, C.J., Allio, S. and Holmberg, E. (2006). Viscosity measurement of vegetable oil at high pressure. *Food and Bioproducts Processing*, **84** (3 C): 173-178.

Seifried, B. and Temelli, F. (2011). Viscosity and rheological behaviour of carbon dioxide-expanded fish oil triglycerides: Measurement and modeling. *Journal of Supercritical Fluids*, **59**: 27-35.

Sih, R., Armenti, M., Mammucari, R., Dehghani, F. and Foster, N.R. (2008). Viscosity measurements on saturated gas-expanded liquid systems-ethanol and carbon dioxide. *Journal of Supercritical Fluids*, **43** (3): 460-468.

Sih, R. and Foster, N.R. (2008). Viscosity measurements on saturated gas expanded liquid systems-acetone and carbon dioxide. *Journal of Supercritical Fluids*, **47** (2): 233-239.

Tuan, D.Q., Zollweg, J.A., Harriott, P. and Rizvi, S.S.H. (1999). Measurement and modeling of viscosity of supercritical carbon dioxide/biomaterial(s) mixtures. *Industrial & Engineering Chemistry Research*, **38** (5): 2129-2136.

Venter, M.J., Willems, P., Kareth, S., Weidner, E., Kuipers, N.J.M. and de Haan, A.B. (2007). Phase equilibria and physical properties of CO<sub>2</sub>-saturated cocoa butter mixtures at elevated pressures. *Journal of Supercritical Fluids*, **41** (2): 195-203.

## **4. Density and volumetric expansion of canola oil and its blend with fully-hydrogenated canola oil in equilibrium with supercritical carbon dioxide<sup>1</sup>**

### **4.1. Introduction**

The finding that enzymes can maintain their activities at high pressures in supercritical carbon dioxide (SCCO<sub>2</sub>) media has encouraged their use as catalysts for specific reactions under supercritical conditions, while benefiting from the many advantages of using SCCO<sub>2</sub> (Chapter 1). Due to the limited solubility of lipids in SCCO<sub>2</sub>, conducting lipid reactions in the supercritical phase, in which lipids have been completely dissolved, requires high pressures and temperatures, which is not feasible. Therefore, solvent-free enzymatic reactions can be conducted in the liquid lipid phase in which CO<sub>2</sub> is dissolved, leading to CO<sub>2</sub>-expanded lipids (CX-lipids) with enhanced mass transfer properties (Jessop and Subramaniam, 2007; Seifried and Temelli, 2010; Subramaniam, 2010).

In order to design SCCO<sub>2</sub> processes (extraction, reaction, fractionation, and particle formation) and gas-assisted mechanical expression of oilseeds, as well as to describe quantitatively the mass transfers in such processes, the physical properties of lipids in equilibrium with CO<sub>2</sub> are necessary. These physical properties are including viscosity, interfacial tension, diffusion coefficient, and

---

<sup>1</sup> A version of this chapter has been published. Jenab E. and Temelli F. (2012). Density and volumetric expansion of carbon dioxide-expanded canola oil and its blend with fully-hydrogenated canola oil. *J. Supercrit. Fluids*, 70: 57-65. (Reprinted with permission from Elsevier.)

density of the liquid lipid phase in equilibrium with high pressure CO<sub>2</sub>. All of these properties depend strongly on temperature and pressure, which also dictate the amount of CO<sub>2</sub> solubilized in the liquid phase. However, CO<sub>2</sub> solubilization in the liquid phase and changes in physical properties are often neglected because of the lack of data, leading to errors in predicting mass transport.

Among the different physical properties, density and volumetric expansion have been selected as the focus of this study whereas the viscosity was reported previously (Chapter 3). Although several studies have reported the density of lipids saturated with CO<sub>2</sub> (Tegetmeier et al., 2000; Seifried and Temelli, 2009), there is a lack of density and volumetric expansion data for canola oil and its blend with fully-hydrogenated canola oil (FHCO) saturated with CO<sub>2</sub>.

Different methods have been proposed for measuring the density of a liquid phase in equilibrium with high pressure CO<sub>2</sub>, including high pressure pycnometer (Staby and Mollerup, 1993), vibrating U-tube densitometer based on the dependence of the vibration period of the bent part of the U-tube according to the filling fluid mass and the U-tube mass (Calvignac et al., 2010), and magnetic suspension balance and sinker joined to a high pressure cell based on Archimedes' principle (Tegetmeier et al., 2000).

Considering the different types of lipids, density and volumetric expansion of fish oil triglycerides (Seifried and Temelli, 2009), corn oil (Tegetmeier et al., 2000; Dittmar et al., 2005), and cocoa butter (Venter et al., 2007; Calvignac et al., 2010) in equilibrium with high pressure CO<sub>2</sub> have been studied. However, no data are available on the effect of the level of unsaturation of lipids on density and

volumetric expansion, for example, due to the addition of FHCO. Such information for real fat and oil mixtures is needed for better understanding of different SCCO<sub>2</sub> processes involving fat and oil mixtures. In addition, considerable expenses related to the measurement of CO<sub>2</sub> solubility in the liquid phase can be reduced if reliable thermodynamic models are available for calculation of CO<sub>2</sub> solubility in the liquid phase at elevated pressures. Therefore, the objectives of this study were (a) to determine the density of canola oil at 40, 55, and 70 °C and its blend with FHCO (30 wt. %) at 70 °C in equilibrium with CO<sub>2</sub> at pressures of up to 30 MPa, (b) to determine the volumetric expansion of canola oil at 40 and 70 °C at pressures of up to 25 MPa and its blend with FHCO (30 wt. %) at 70 °C in equilibrium with CO<sub>2</sub> up to 25 MPa, and (c) to apply models for the solubility of CO<sub>2</sub> in the liquid phase and for the density of the liquid phase using cubic equations of state and correlative methods. The CO<sub>2</sub> solubility, volumetric expansion, and density of the blend was measured only at 70 °C because the melting point of FHCO is between 60-70 °C and it is in a solid state at lower temperatures.

## **4.2. Materials and methods**

### **4.2.1. Materials**

FHCO was kindly provided by Richardson Oilseed Ltd. (Lethbridge, AB, Canada) and canola oil purchased from a local store was also manufactured by the same company. The fatty acid profile of canola oil determined by gas chromatography using the AOCS official method Ce 1-62 (AOCS, 2009), was

similar to that reported previously (Section 3.2.1) and the fatty acid profile of FHCO was provided by the supplier (Table 4-1). Canola oil and its blend with FHCO were stored at 4 °C in bottles with their headspaces filled with nitrogen (purity of 99.99%, Praxair, Edmonton, AB, Canada). Bone dry CO<sub>2</sub> (Praxair, Edmonton, AB, Canada) with a purity of 99.9% was used for the saturation of liquid lipids.

**Table 4-1.** Fatty acid composition of fully-hydrogenated canola oil (FHCO) and canola oil.

Fatty acid	GC area %	
	FHCO	Canola oil <sup>a</sup>
C16:0	4.26	4.18±0.06
C18:0	89.87	1.57±0.02
C18:1, <i>trans</i> -Δ <sup>9</sup>	1.44	-
C18:1, <i>cis</i> -Δ <sup>9</sup>	2.66	56.46±0.17
C18:1, <i>cis</i> -Δ <sup>11</sup>	-	4.52±0.28
C18:2, <i>cis, cis</i> -Δ <sup>9, 12</sup>	0.07	19.80±0.14
C18:3, <i>cis, cis, cis</i> -Δ <sup>9, 12, 15</sup>	-	9.49±0.01
C20:1, <i>cis</i> -Δ <sup>5</sup>	-	1.08±0.03
C20:0	1.24	-
Others	0.48	2.88±0.57

<sup>a</sup> Data from Table 3-1.

#### **4.2.2. Solubility measurements of CO<sub>2</sub> in the liquid phase**

The data for the solubility of CO<sub>2</sub> in canola oil at 40 °C and pressures of up to 20 MPa were obtained previously (Section 3.3.3). In this study, the solubility of CO<sub>2</sub> in canola oil and its blend with FHCO (30 wt.%) at 70 °C up to 25 MPa was measured using the same experimental apparatus (Fig. 3-2) and protocols described previously (Section 3.2.3). Briefly, the lipid sample was placed in a high pressure cell with a sapphire window and allowed to reach equilibrium in contact with high pressure CO<sub>2</sub>. Samples were withdrawn from the bottom of the high pressure cell and depressurized to atmospheric pressure while keeping the pressure of the cell constant by adjusting the pressure and monitoring the inside of the cell for any disturbance of the equilibrium state.

The collected samples were weighed and CO<sub>2</sub> released from the sample was collected in a calibrated graduated syringe filled with saturated Na<sub>2</sub>SO<sub>4</sub> solution. The volume of CO<sub>2</sub> was quantified based on the displaced liquid volume in the syringe and converted to mass using the density of CO<sub>2</sub> at the temperature of saturated solution and ambient pressure.

#### **4.2.3. Volumetric expansion measurements**

Volumetric expansion measurements were carried out using a high pressure view cell (Phase equilibria unit, Sitec Sieber Engineering, Zurich, Switzerland) with a capacity of 10 mL and equipped with sapphire windows. Further details of the unit and its schematic (Fig. 3-2) were presented in Section 3.2.3.1. For this study, a device consisting of a stainless steel frame and a microscopic glass scale

(NE41 Graticules, Pyser-SGI LTD., Kent, UK) placed inside the cell was designed to measure the volumetric expansion (Fig. 4-1a). The glass microscopic scale had 200 equally incised divisions over a range of 10 mm. The microscopic scale was calibrated over the range of 5 mm-diameter sapphire window, which could be observed by the camera, by placing the device and the small magnetic bar inside the cell and then pouring different amounts of water into the cell with a calibrated micropipette. The calibration curve was established by plotting the level of water on glass microscopic scale versus the volume of water added.

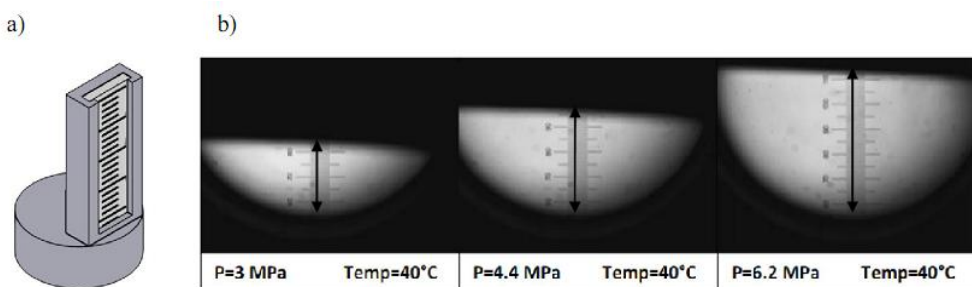


**Figure 4-1.** Volumetric expansion in the high pressure view cell: a) The glass micro-scale and its stainless steel holder designed for measuring volumetric expansion; b) Images of canola oil in equilibrium with  $\text{CO}_2$  at different pressures at  $40^\circ\text{C}$ .

After placing the microscopic scale and magnetic bar inside the cell, the temperature of the cell was allowed to reach the desired level and a certain amount of the lipid sample (approximately 1 mL) was poured into the cell for the level of the sample inside the cell to reach above the bottom edge of the window. Then, the cell was carefully flushed with  $\text{CO}_2$  and equilibrated at the set temperature and atmospheric pressure until the oil level in the cell stabilized on the microscopic scale. At this point, the initial oil level on the scale was recorded

and the calibration curve was used to find the initial volume ( $V_0$ ). The system was then pressurized with  $\text{CO}_2$  using a manual pump. The oil was equilibrated at elevated pressure until a constant oil level on the microscopic scale was observed ( $V_P$ ). At each pressure level, the cell contents were mixed for about 3 h based on preliminary observations to reach equilibrium and the volumetric expansion was followed until there was no change in oil level on the microscopic scale or no change in volume over consecutive measurements taken after 30 min, indicating that the system had reached equilibrium. The final volume of the liquid phase was determined by finding the exact level of oil on the scale and then using the calibration curve. The change in the liquid level with increasing pressure at 40 °C is demonstrated in Figure 4-1b. The exact level of oil on the microscopic scale was determined by taking photos and analyzing them with measurement tools of Foxit Reader software (Foxit Corporation, Fremont, CA, USA). The relative volume change ( $\Delta V_{\text{rel}}$ ) was calculated according to Equation (4.1).

$$\Delta V_{\text{rel}}(\%) = \frac{V_P(T, P) - V_0(T, P_0)}{V_0(T, P_0)} \times 100 \quad (4.1)$$

Where,  $V_0$  and  $V_P$  are the volume of the oil at atmospheric and elevated pressures, respectively. The volumetric expansion of canola oil at 40 °C up to 20 MPa and 70 °C up to 25 MPa and its blend with FHCO (30 wt.%) at 70 °C up to 25 MPa in equilibrium with  $\text{CO}_2$  was measured. The level of FHCO in the blend was chosen based on the parallel studies on interesterification between canola oil and FHCO using  $\text{SCCO}_2$  as reaction medium (Chapter 5 and 6). The measurements were carried out in triplicate for each isotherm condition.

#### **4.2.4. Density measurements**

The method used in this study is based on the Archimedes' principle stating that any object that is completely or partially submerged in a fluid at rest is acted on by an upward or buoyant force. The magnitude of this force is equal to the weight of the fluid displaced by the object, which is related to the volume of the object and density of fluid. A detailed description and schematic of the experimental apparatus used in this study (Fig. 4-2) and the related validation data were reported by Seifried and Temelli (2009). Briefly, the device for density measurement consisted of a stainless steel frame to which a glass sinker was attached using an extension spring by means of a hook equipped with a fine needle pointing at a glass microscopic scale. The whole density measurement set-up was placed inside a 200 mL high pressure view cell (Nova-Swiss, Effretikon, Switzerland) equipped with electrical heaters and placed inside a temperature-controlled insulated air bath. The position of the fine needle pointing at the glass microscopic scale was monitored by means of a camera equipped with a telecentric microscope. The view cell was pressurized with CO<sub>2</sub> using a syringe pump (Model 250D, Teledyne Isco Inc., Lincoln, NE, USA). To speed up the achievement of equilibrium, the previous system (Seifried and Temelli, 2009) was modified and the cell contents were circulated from bottom by using a piston pump (EK1, American Lewa Inc., Holliston, MA, USA) and sprayed back into the cell from the top at a flow rate of approximately 20 mL/min. The piston pump was connected to an AC Motor (P56X3002H-4SID, Reliance Electric, Greenville,

SC, USA) and the flow rate of the pump was controlled by an AC Drive (MD60, Reliance Electric, Greenville, SC, USA).

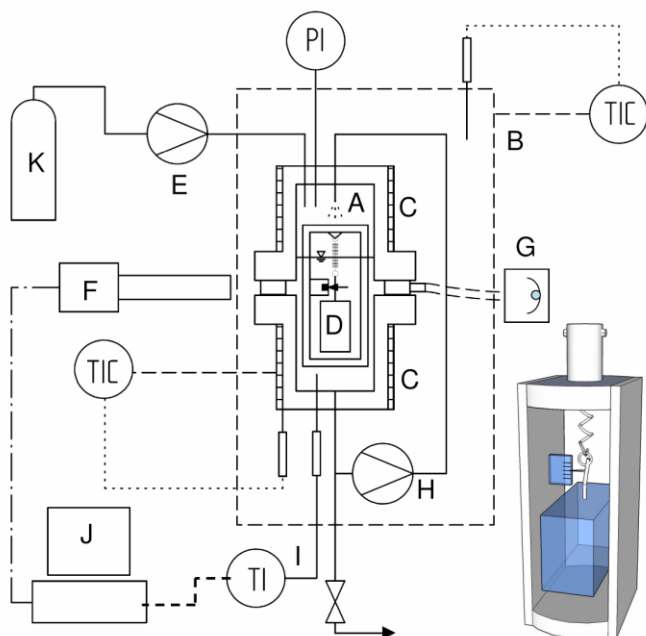


**Figure 4-2.** Apparatus for measuring density of liquids in equilibrium with CO<sub>2</sub>. A) view cell, B) temperature controlled air bath, C) electric heaters, D) glass sinker, E) syringe pump, F) CMOS camera with microscope lens, G) light source, H) circulation pump, I) thermistor, J) computer, K) CO<sub>2</sub> tank. Insert: 3D model of spring balance with sinker and microscopic scale to measure density.<sup>2</sup>

The glass microscopic scale was calibrated at each isotherm condition in triplicate based on the density of pure CO<sub>2</sub> at different pressures before each density measurement. The density of pure CO<sub>2</sub> at different pressures and temperatures was calculated using NIST Chemistry WebBook based on the Span and Wagner equation of state (Lemmon et al., 2010).

---

<sup>2</sup> Seifried B. and Temelli F. (2009). Density of marine lipids in equilibrium with carbon dioxide. *J. Supercrit. Fluids*, 70 (2): 97-104. (Reprinted with permission from Elsevier.)

The densities of canola oil at 40, 55, and 70 °C and its blend with FHCO at 70 °C in equilibrium with CO<sub>2</sub> were determined at pressures ranging from atmospheric pressure to 30 MPa. The measurements were carried out in triplicate for each isotherm. First, the cell was flushed with CO<sub>2</sub> to remove any residual air and then filled with the sample up to a level just above the window of the view cell ensuring complete submersion of the sinker into the liquid phase. At each temperature and pressure condition, the sample was circulated using the piston pump for at least for 3 h to ensure equilibrium was reached based on preliminary studies. After stopping the pump, the images of fine needle pointing at the scale were taken every 30 min. The images were analyzed by measurement tools of Foxit Reader software to find the exact position of the tip of the fine needle on the scale. The density was determined by the position of fine needle on the glass scale using the calibration curve. After observing constant density, the pressure was increased to the next level up to 30 MPa. The temperature of the sample inside the cell was monitored throughout the entire measurement and the variation in temperature was less than ±0.15 °C.

Density of pure canola oil at 40, 55, and 70 °C up to 30 MPa was also measured using Anton Paar DMA 4500 M and DMA HP vibrating tube density meters (Anton Paar, Ashland, VA, USA) for atmospheric pressure and elevated pressures, respectively. The device was calibrated using pure CO<sub>2</sub> and deionized water at each pressure and temperature using their density values available from the NIST Chemistry WebBook (Lemmon et al., 2010).

## 4.3. Results and discussion

### 4.3.1. Modeling CO<sub>2</sub> solubility in the liquid lipid phase at elevated pressures using cubic equations of state

The effects of temperature (40 and 65 °C) and pressure on CO<sub>2</sub> solubility in canola oil and its blend with FHCO in relation to its impact on viscosity were discussed in detail in Chapter 3. In this study, the experimental data for the solubility of CO<sub>2</sub> in canola oil at 40 °C up to 20 MPa and at 70 °C up to 25 MPa, and in its blend with FHCO (30 wt. %) at 70 °C up to 25 MPa were described using cubic equations of state such as Peng-Robinson equation of state (PR-EoS) (Eq. (4.2) to (4.7)) (Klein and Schulz, 1989) and Soave-Redlich-Kwong equation of state (SRK-EoS) (Eq. (4.8) to (4.13)) (Fernández-Ronco et al., 2011).

Peng-Robinson equation of state:

$$P = \frac{RT}{v - b} - \frac{a(T)}{v^2 + 2bv - b^2} \quad (4.2)$$

$$a(T) = a(T_C) \cdot \alpha(T_r, \omega) \quad (4.3)$$

$$a(T_C) = \frac{0.45724 R^2 T_C^2}{P_C} \quad (4.4)$$

$$\alpha(T_r, \omega) = (1 + k(1 - \sqrt{T_r}))^2 \quad (4.5)$$

$$k = 0.37464 + 1.5422\omega - 0.26992\omega^2 \quad (4.6)$$

$$b = \frac{0.0778 R T_C}{P_C} \quad (4.7)$$

Soave-Redlich-Kwong equation of state:

$$P = \frac{RT}{v - b} - \frac{a(T)}{v(v + b)} \quad (4.8)$$

$$a(T) = a_c \cdot \alpha(T) \quad (4.9)$$

$$a_c = \frac{0.42747 R^2 T_c^2}{P_c} \quad (4.10)$$

$$\alpha(T) = (1 + m(1 - \sqrt{T_r}))^2 \quad (4.11)$$

$$m = 0.48 + 1.574\omega - 0.176\omega^2 \quad (4.12)$$

$$b = \frac{0.08664 R T_c}{P_c} \quad (4.13)$$

The critical properties and acentric factor of CO<sub>2</sub> were obtained from the NIST Chemistry WebBook based on the Span and Wagner equation of state (Lemmon et al., 2010). The critical constants of natural products such as fats and oils are difficult to determine experimentally and almost no data can be found in the literature or databanks. However, Yu (1992) estimated all the critical properties and acentric factors based on the Ambrose method for triglycerides with different carbon numbers. Then, Yu (1992) developed different correlative models based on the molecular weight of triglycerides to determine their critical properties and acentric factors. In this study, the average molecular weights of canola oil and its blend with FHCO were determined based on their respective fatty acid composition (Table 4-1). Then, the correlative models proposed by Yu (1992) were employed based on these average molecular weights to calculate their critical properties and acentric factors as reported in Table 4-2.

**Table 4-2.** Critical properties of carbon dioxide, canola oil and its blend with fully-hydrogenated canola oil (FHCO) (30 wt. %).<sup>a</sup>

Component	MW (g/mol)	P <sub>C</sub> (MPa)	T <sub>C</sub> (K)	V <sub>C</sub> (cm <sup>3</sup> /mol)	ω
CO <sub>2</sub>	44.01	7.38	304.13	94.16	0.2239
Canola oil	880.69	0.59	913.47	3213.55	1.6977
Canola oil and FHCO blend (30 wt. %)	881.94	0.59	913.53	3218.63	1.6990

<sup>a</sup> MW: molecular weight; P<sub>C</sub>: critical pressure; T<sub>C</sub>: critical temperature; V<sub>C</sub>: critical molar volume; ω: acentric factor.

Both PR-EoS and SRK-EoS combined with quadratic (Q) (Eq. (4.14) and (4.15)) (Chang et al., 2005) and Panagiotopoulos-Reid (PR) (Eq. (4.16) and (4.17)) (Chang et al., 2005) mixing rules with combining rule in Equations (4.18) and (4.19) were used to describe the experimental data of CO<sub>2</sub> solubility in the liquid lipid phase at elevated pressures and constant temperatures.

Quadratic mixing rule:

$$a_{ij} = \sqrt{a_i a_j} (1 - k_{ij}); k_{ij} = k_{ji} \quad (4.14)$$

$$b_{ij} = \frac{b_i + b_j}{2} (1 - l_{ij}); l_{ij} = l_{ji} \quad (4.15)$$

Panagiotopoulos-Reid mixing rule:

$$a_{ij} = \sqrt{a_i a_j} (1 - k_{ij}^{PR} + \lambda_{ij}^{PR} x_i); \lambda_{ij}^{PR} = k_{ij}^{PR}; -k_{ji}^{PR} = -\lambda_{ji}^{PR} \quad (4.16)$$

$$b_{ij} = \frac{b_i + b_j}{2} (1 - l_{ij}); l_{ij} = l_{ji} \quad (4.17)$$

Combining rule:

$$a = \sum_{i=1}^N \sum_{j=1}^N x_i x_j a_{ij} \quad (4.18)$$

$$b = \sum_{i=1}^N \sum_{j=1}^N x_i x_j b_{ij} \quad (4.19)$$

PE 2000 software (Pfohl et al., 2000) was used to calculate the mole fraction of CO<sub>2</sub> in the liquid lipid phase and optimize the binary interaction parameters by minimizing the average absolute relative deviation (AARD) between experimental ( $x_{CO_2}^{exp}$ ) and calculated ( $x_{CO_2}^{calc}$ ) values as an objective function (Eq. (3.6)).

$$AARD\% = \frac{100}{N} \sum \left| \frac{x_{CO_2}^{exp} - x_{CO_2}^{calc}}{x_{CO_2}^{exp}} \right| \quad (4.20)$$

Figure 4-3 shows the comparison between the experimental and calculated data obtained by PR-EoS and SRK-EoS using the two mixing rules at different conditions. Satisfactory representations of the liquid lipid phase composition in equilibrium with high pressure CO<sub>2</sub> were obtained by both equations of state and applied mixing rules.

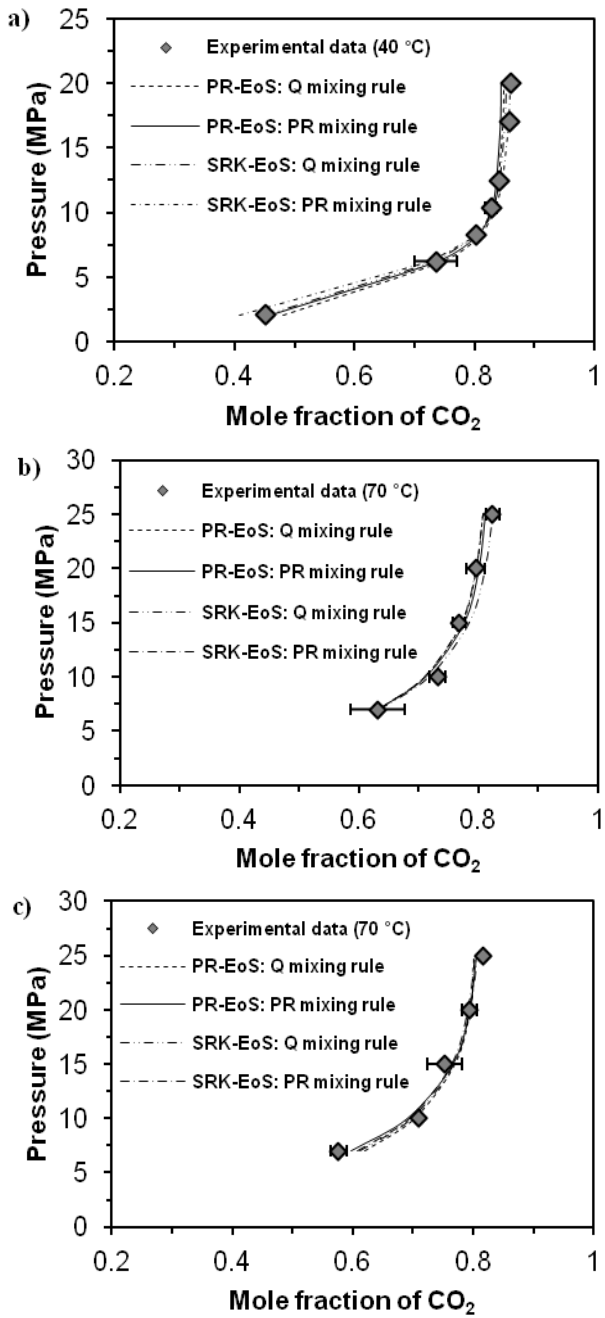


**Figure 4-3.** P-x diagrams of CO<sub>2</sub>-saturated liquid lipid phases at different temperatures and pressures correlated by Peng-Robinson equation of state (PR-EoS) and Soave-Redlich-Kwong equation of state (SRK-EoS) using quadratic (Q) and Panagiotopoulos-Reid (PR) mixing rules (lines) and experimental data (markers) found in this and previous (Section 3.3.3) studies: a) CO<sub>2</sub>-expanded canola oil at 40 °C; b) CO<sub>2</sub>-expanded canola oil at 70 °C; c) CO<sub>2</sub>-expanded canola oil and fully-hydrogenated canola oil blend (FHCO) (30 wt.%) at 70 °C. Error bars represent standard deviation based on three replications.

Chang et al. (2005) also modeled the solubility of CO<sub>2</sub> in unsaturated fatty acid esters using PR-EoS and SRK-EoS. They showed that these equations of state with Q and PR mixing rules successfully correlated the experimental data for binary mixtures of CO<sub>2</sub> and methyl and ethyl esters of fatty acids.

Tables 4-3 and 4-4 show the optimal binary interaction parameters determined by PR-EoS and SRK-EoS using Q and PR mixing rules, respectively. These models were only validated for finding the mole fraction of the components in the CO<sub>2</sub>-saturated liquid lipid phase because the experimental data were obtained only for the liquid phase. In all cases, the AARD was less than 2.3%, demonstrating the goodness of fit of the models. However, the Q mixing rule would be more preferable for modeling the data since it has less fitting parameters compared to the PR mixing rule. The maximum relative deviation (MaxRD) ranged from 2.0 to 7.0% for PR-EoS and from 0.9 to 9.6% for SRK-EoS.

**Table 4-3.** Optimal binary interaction parameters correlated with Peng-Robinson equation of state (PR-EoS) using Quadratic (Q) and Panagiotopoulos-Reid (PR) mixing rules for CO<sub>2</sub>-saturated liquid lipid phase.

Mixing rule	k <sub>ij</sub>	I <sub>ij</sub>	λ <sub>ij</sub>	AARD (%)	MaxRD (%) <sup>a</sup>
Canola oil + CO <sub>2</sub>					
PR-40°C	0.00573	0.03556	-0.05924	0.873	2.008
PR-70°C	0.05508	0.04041	-0.04198	1.197	2.747
Q-40°C	0.07008	0.04935	-	1.656	6.422
Q-70°C	0.10424	0.04745	-	1.152	3.047
Blend <sup>b</sup> + CO <sub>2</sub>					
PR-70°C	0.06117	0.02012	-0.02630	1.846	3.417
Q-70°C	0.09982	0.03926	-	2.317	7.684

$$^a \text{MaxRD} (\%) = \text{Max} \left( \left| 100 \times \left( \frac{x_{\text{CO}_2}^{\text{exp}} - x_{\text{CO}_2}^{\text{calc}}}{x_{\text{CO}_2}^{\text{exp}}} \right) \right| \right).$$

<sup>b</sup> Blend of canola oil and fully-hydrogenated canola oil (FHCO) (30 wt.%).

**Table 4-4.** Optimal binary interaction parameters correlated with Soave-Redlich-Kwong equation of state (SRK-EoS) using Quadratic (Q) and Panagiotopoulos-Reid (PR) mixing rules for CO<sub>2</sub>-saturated liquid lipid phase.

Mixing rule	k <sub>ij</sub>	l <sub>ij</sub>	λ <sub>ij</sub>	AARD (%)	MaxRD (%) <sup>a</sup>
Canola oil + CO <sub>2</sub>					
PR-40°C	0.04452	0.01957	-0.02404	1.999	9.588
PR-70°C	0.05455	0.03876	-0.05913	1.122	3.075
Q-40°C	0.07679	0.03444	-	0.428	0.882
Q-70°C	0.10398	0.03849	-	1.318	2.258
Blend <sup>b</sup> + CO <sub>2</sub>					
PR-70°C	0.04733	0.02345	-0.05845	2.143	5.343
Q-70°C	0.10831	0.03006	-	2.153	5.967

<sup>a</sup> Refer to Table 4-3 for definition.

<sup>b</sup> Blend of canola oil and fully-hydrogenated canola oil (FHCO) (30 wt.%).

### 4.3.2. Volumetric expansion

There is no experimental data available on volumetric expansion of canola oil and its blend with FHCO in equilibrium with high pressure CO<sub>2</sub>. However, there are some studies on the volumetric expansion of other fats and oils like fish oil triglycerides and fatty acid ethyl esters (FAEE) (Seifried and Temelli, 2009), corn oil (Tegetmeier et al., 2000), and cocoa butter (Calvignac et al., 2010). Smith et al. (Smith et al., 1998) also reported the volumetric expansion of some FAEE. The relative volumetric expansion of canola oil in equilibrium with high pressure CO<sub>2</sub> calculated using Equation (4.1) at 40 °C increased almost linearly up to 10 MPa to reach about 40% and remained almost constant with a further increase in pressure (Fig. 4-4). These results are in good agreement with those of Seifried and Temelli (2009) for CO<sub>2</sub>-saturated fish oil triglycerides and FAEE and Calvignac et al. (2010) for CO<sub>2</sub>-saturated cocoa butter in which the relative volumetric

expansion of fish oil and cocoa butter at 40 °C increased up to 10 MPa and reached a nearly constant level above that pressure. On the other hand, as shown in Figure 4-4, the relative volumetric expansion of canola oil and its blend with FHCO at 70 °C increased up to about 15 MPa and above that the rate of volumetric expansion increase started to decline, but did not reach a plateau with pressure even up to 25 MPa. This behaviour was similar to that observed for CO<sub>2</sub>-saturated cocoa butter at 80 °C by Calvignac et al. (2010).

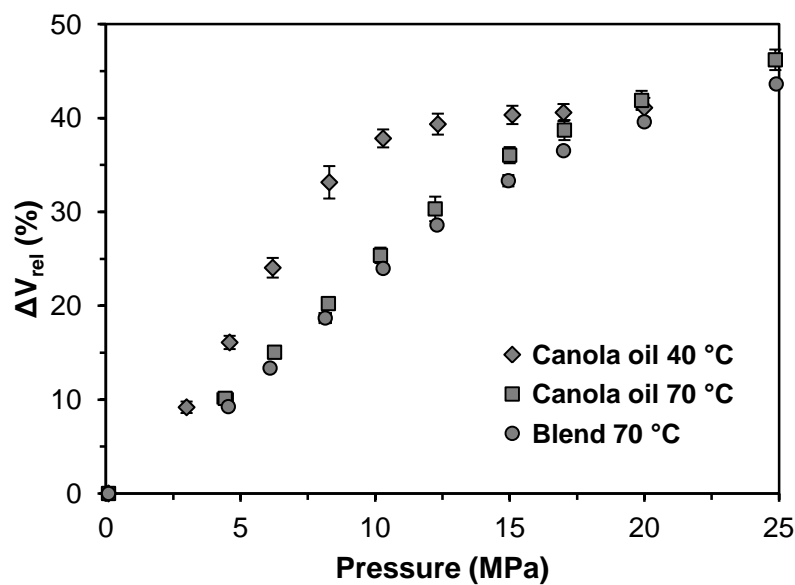


**Figure 4-4.** Relative volumetric expansion of canola oil and its blend with fully-hydrogenated canola oil (FHCO) (30 wt.%) in equilibrium with CO<sub>2</sub> at various pressures and temperatures. Error bars represent standard deviation based on triplicate measurements.

With respect to the effect of the degree of unsaturation, the relative expansions of canola oil and its blend with FHCO at 70 °C were almost similar. This is related to the dominant effect of high temperature, 70 °C, on the

dissolution of CO<sub>2</sub> in the liquid lipid phase over the effect of the degree of unsaturation of the sample. Temperature had a substantial effect on the relative volumetric expansion of canola oil at constant pressure as the volumetric expansion decreased with an increase in temperature from 40 to 70 °C because of a drop in CO<sub>2</sub> solubility; however, this was the case only up to a certain pressure ( $\approx 15$  MPa) at 70 °C, since volumetric expansion had already reached a plateau at 40 °C while it was still increasing at 70 °C. The maximum relative volumetric expansion for canola oil at 40 and 70 °C was about 40 and 46% at the studied range of pressures, respectively. For CO<sub>2</sub>-expanded blend, the relative volumetric expansion reached approximately 43%. The maximum coefficient of variation of volumetric expansion experiment based on triplicate measurements was 6.6% demonstrating the reproducibility of the system.

Determining the solubility of CO<sub>2</sub> in the liquid lipid phase can be helpful to interpret the volumetric expansion behaviour of the oil in equilibrium with high pressure CO<sub>2</sub>. Therefore, experimental data of the CO<sub>2</sub> solubility in the liquid lipid phase at various temperatures and pressures from this and previous (Section 3.3.3) studies were used to describe the relative volumetric expansion as a function of the mass fraction of CO<sub>2</sub> in the liquid lipid phase (Fig. 4-5a). For ease of comparison, the solubility of CO<sub>2</sub> in the liquid phase at different pressures is also presented in terms of mass fraction of CO<sub>2</sub> in Figure 4-5b. The relationship between the relative volumetric expansion and mass fraction of CO<sub>2</sub> for canola oil at 40 °C was almost linear up to about 0.2 (Fig. 4-5a), where the pressure was about 10 MPa (Fig. 4-5b), and above that the relative volumetric expansion

leveled off. This is due to the solubility of CO<sub>2</sub> in the liquid lipid phase which increased with pressure up to 10 MPa and above that it leveled off at higher pressures (Fig. 4-5b). Although the volumetric expansion of canola oil at 40 °C reached a plateau above 10 MPa (Fig. 4-5a), the mass fraction of CO<sub>2</sub> in the liquid phase was still increasing above 10 MPa but at a lower rate and reached a constant value at higher pressures (Fig. 4-5b). This result indicated that the small increase in mass fraction above 10 MPa did not have a substantial effect on volumetric expansion because of the dominant effect of CO<sub>2</sub> compression on top of the liquid phase at pressures above 10 MPa.

This finding was in good agreement with that of Seifried and Temelli (2009) about the relative volumetric expansion of fish oil in equilibrium with high pressure CO<sub>2</sub>. They also showed that the relative volumetric expansion increased with a linear trend up to a CO<sub>2</sub> loading (kg CO<sub>2</sub>/kg oil) of 0.4, where the pressure was about 10 MPa, and after that it leveled off, reaching a fairly constant level. However, for CO<sub>2</sub>-saturated canola oil and its blend with FHCO at 70 °C, the relative volumetric expansion increased with mass fraction of CO<sub>2</sub> in the liquid lipid phase up to 0.15 (Fig. 4-5a), where the pressure was about 15 MPa (Fig. 4-5b), and after that the relative volumetric expansion still increased but at a lower rate, which was also related to the mass fraction of CO<sub>2</sub> in the liquid lipid phase. As shown in Figure 4-5b, the solubility of CO<sub>2</sub> in the liquid lipid phase at 70 °C increased with pressure up to 15 MPa and then with a lower rate above that pressure. In both Figures 4-3 and 4-5, the mole fraction and mass fraction of CO<sub>2</sub>

in the liquid phase versus pressure increased more slowly above about 10 MPa at 40 °C and above 15 MPa at 70 °C.

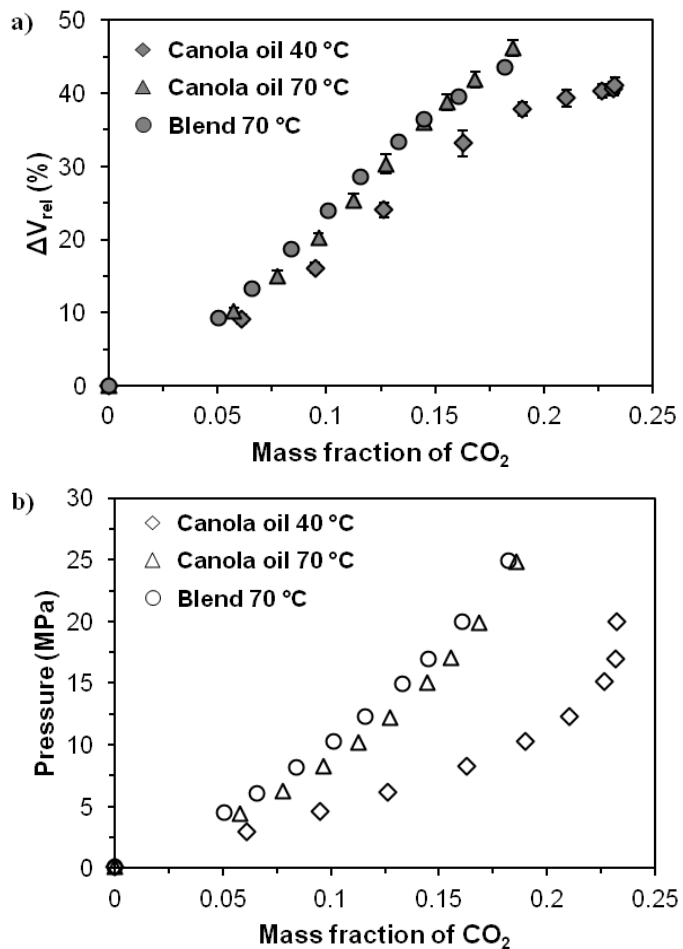


**Figure 4-5.** a) Relative volumetric expansion of canola oil and its blend with fully-hydrogenated canola oil (FHCO) (30 wt.%) versus mass fraction of CO<sub>2</sub> in the lipid liquid phase, and b) pressure versus mass fraction of CO<sub>2</sub> at various temperatures.

However, this increase in Figure 4-3 is not as clear as it is in Figure 4-5. It is important to assess these trends in terms of both mole fraction and mass fraction due to the big difference in the molecular weights of the components under consideration, which are about 880 g/mol for canola oil and 44 g/mol for CO<sub>2</sub>.

### 4.3.3. Density

Densities of canola oil at 40, 55, and 70 °C and its blend with FHCO at 70 °C in equilibrium with high pressure CO<sub>2</sub> were measured at pressures of up to 30 MPa and the results are presented in Tables 4-5 and 4-6, respectively. The density of canola oil at 40, 55, and 70 °C and the blend at 70 °C increased by 4.7, 4.3, 3.5, and 3.6% of its value at atmospheric pressure, respectively. As shown in Figure 4-6, the density of CO<sub>2</sub>-saturated canola oil and the blend increased with pressure and the density of CO<sub>2</sub>-saturated canola oil decreased with temperature at constant pressure. The increase in density with pressure was more pronounced up to about 10 MPa for canola oil at 40 and 55 °C. However, for CO<sub>2</sub>-saturated canola oil and the blend at 70 °C this pressure was about 15 MPa.

Tegetmeier et al. (2000) studied the density of corn oil in equilibrium with high pressure CO<sub>2</sub> from room temperature to 80 °C and pressures of up to 30 MPa using a magnetic suspension balance coupled with a high pressure view cell. They also showed that the density of corn oil increased with an increase in pressure and a decrease in temperature and the maximum change in density was about 5% within the range of their study. Seifried and Temelli (2009) also found that the density of both fish oil triglycerides and their FAEE saturated with CO<sub>2</sub> increased with pressure and decreased with temperature. The solubilization of CO<sub>2</sub> in the liquid lipid phase with pressure increases the density of the liquid lipid phase profoundly although the density of pure CO<sub>2</sub> at each pressure and temperature is less than the density of pure canola oil at the same conditions.

**Table 4-5.** Density of CO<sub>2</sub>-expanded canola oil at various temperatures and pressures.

T (°C)	P (MPa)	Density (kg m <sup>-3</sup> )	T (°C)	P (MPa)	Density (kg m <sup>-3</sup> )	T (°C)	p (MPa)	Density (kg m <sup>-3</sup> )
<b>39.93±0.15</b>	0.1±0.00	903.08±0.65	54.89±0.07	0.1±0.00	893.29±1.33	70.04±0.08	0.1±0.00	885.72±0.71
	2.18±0.02	906.36±0.44		2.08±0.04	896.70±0.33		2.11±0.15	888.40±1.52
	4.23±0.06	912.11±1.70		4.17±0.26	902.37±0.74		4.15±0.10	891.89±1.31
	6.34±0.03	915.51±0.68		6.35±0.09	904.75±1.06		6.41±0.00	893.61±0.40
	8.32±0.06	919.93±1.62		8.24±0.01	908.42±0.75		8.31±0.08	896.34±1.23
	10.20±0.12	923.45±0.60		10.12±0.07	909.69±1.27		10.21±0.00	897.76±0.97
	12.41±0.00	926.31±0.65		12.41±0.01	913.02±0.60		12.49±0.01	900.18±1.74
	14.77±0.04	929.02±0.48		14.79±0.05	914.73±1.19		14.88±0.01	901.18±0.25
	16.91±0.02	931.26±0.73		16.88±0.01	917.39±0.25		19.86±0.04	906.76±0.99
	19.84±0.08	934.30±0.23		19.82±0.05	920.19±0.89		24.92±0.01	911.10±0.82
	24.84±0.01	940.51±0.49		24.84±0.00	926.45±0.97		30.00±0.01	916.94±1.17
	29.98±0.02	945.62±0.42		29.97±0.02	931.66±1.43			

**Table 4-6.** Density of CO<sub>2</sub>-expanded canola oil and fully-hydrogenated canola oil blend (FHCO) (30 wt.%) at 70 °C at different pressures.

T (°C)	P (MPa)	Density (kg m <sup>-3</sup> )
69.99±0.13	0.1±0.00	881.05±0.77
	2.64±0.05	884.82±0.99
	5.86±0.01	888.68±0.75
	10.04±0.00	892.88±1.03
	15.05±0.03	897.80±0.50
	20.2±0.02	902.86±0.40
	25.05±0.01	908.07±0.20
	30.02±0.01	912.52±0.45

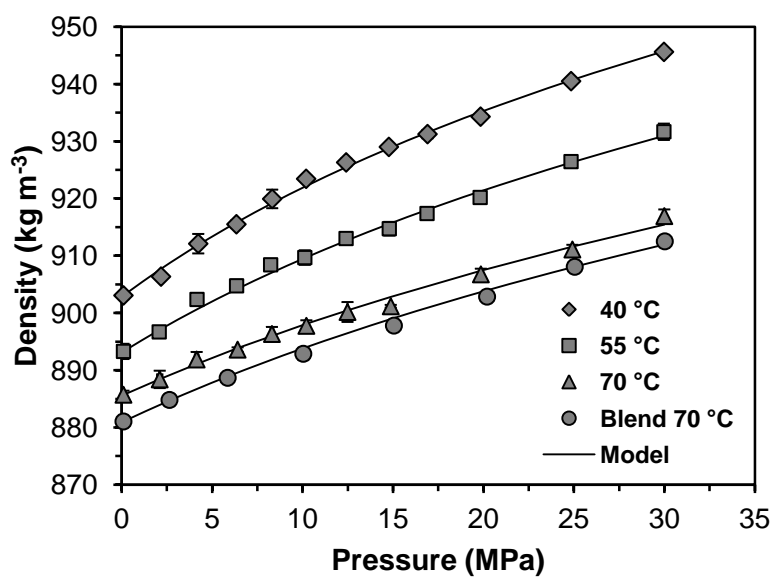


**Figure 4-6.** Density of canola oil at 40, 55, and 70 °C and its blend with fully-hydrogenated canola oil (FHCO) (30 wt.%) at 70 °C in equilibrium with CO<sub>2</sub> as a function of pressure. Curves represent correlation based on the modified Tait equation (Eq. (4.21)).

As shown in Figure 4-7, the density of pure canola oil at 40, 55, and 70 °C up to 30 MPa increased by 1.5, 1.7, and 1.9% of its value at atmospheric pressure, respectively. However, the density of pure canola oil even at 30 MPa at all studied temperatures was lower than the density of CO<sub>2</sub>-saturated canola oil at the same condition. Other researchers (Tegetmeier et al., 2000; Seifried and Temelli, 2009; Calvignac et al., 2010) hypothesized that the CO<sub>2</sub> molecules would fill the void volumes between triglyceride molecules of the liquid lipid phase and that they would act as a lubricant, which could enhance the compressibility of the liquid lipid phase. Therefore, the density of the liquid lipid phase in equilibrium with high pressure CO<sub>2</sub> is not only dependent on the solubility of CO<sub>2</sub> in the liquid phase but also dependent on the compressibility of the liquid phase under high pressure. At high temperature, the slope of density vs. pressure curve below and above 15 MPa decreased compared to those at lower temperatures. This is due to the lower solubility of CO<sub>2</sub> and higher kinetic energy of triglyceride molecules inhibiting compression.

Regarding the effect of degree of unsaturation of the samples, comparison of the densities of canola oil, the blend, and the literature data for fish oil saturated with CO<sub>2</sub> at 70 °C revealed that at constant pressure and temperature the density increased with the degree of unsaturation (Fig. 4-8).

In order to better understand the effect of CO<sub>2</sub> solubility in the liquid lipid phase on density, it is more interesting to assess the density of CO<sub>2</sub>-saturated liquid phase as a function of the mass fraction of CO<sub>2</sub> in the liquid lipid phase.

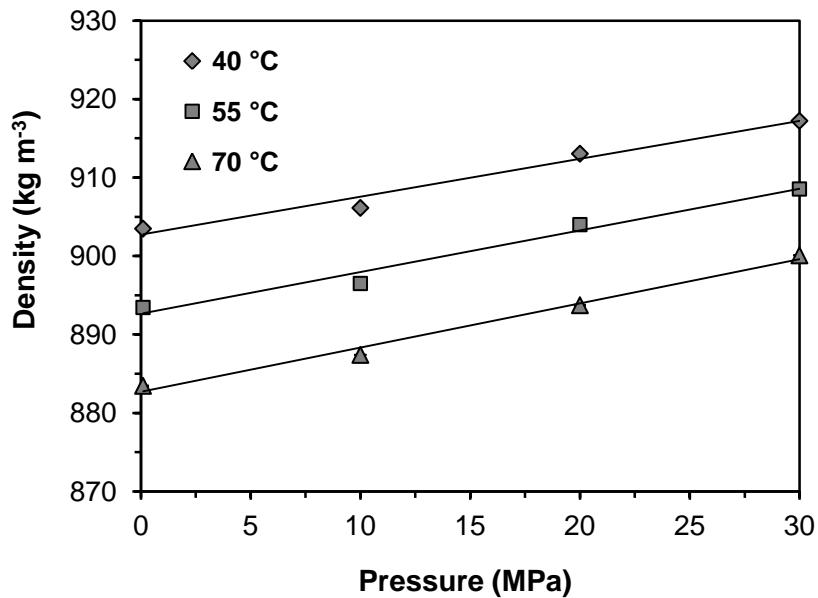


**Figure 4-7.** Density of pure canola oil at various temperatures and pressures.

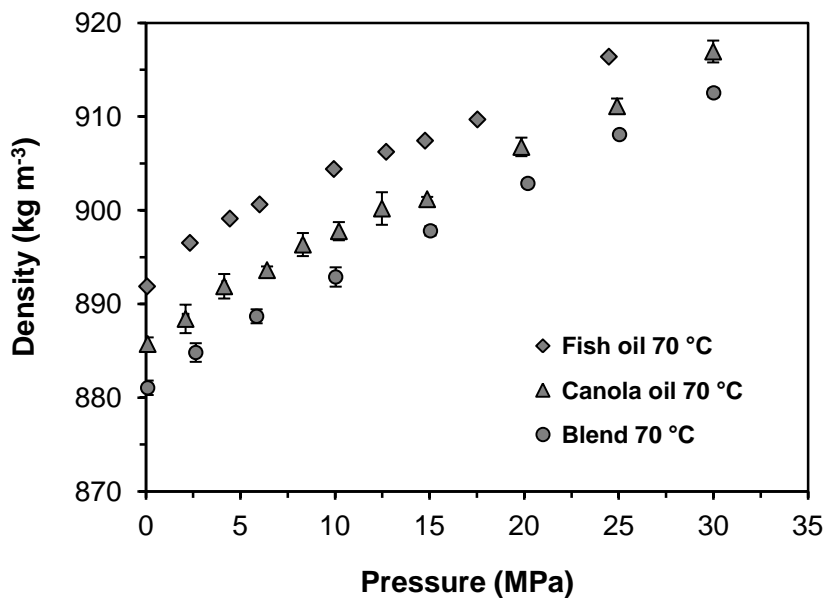


**Figure 4-8.** Density of canola oil and its blend with fully-hydrogenated canola oil (FHC) (30 wt.%) in equilibrium with high pressure CO<sub>2</sub> as a function of pressure determined in this study compared to literature data for CO<sub>2</sub>-saturated fish oil at 70 °C (Seifried and Temelli, 2009).

As shown in Figure 4-9, the density of canola oil at 40 °C increased with mass fraction of CO<sub>2</sub> up to about 0.2, where the pressure was about 10 MPa, and above that the mass fraction of CO<sub>2</sub> was almost constant but the density still increased indicating the effect of compression above 10 MPa on the density of the liquid lipid phase.

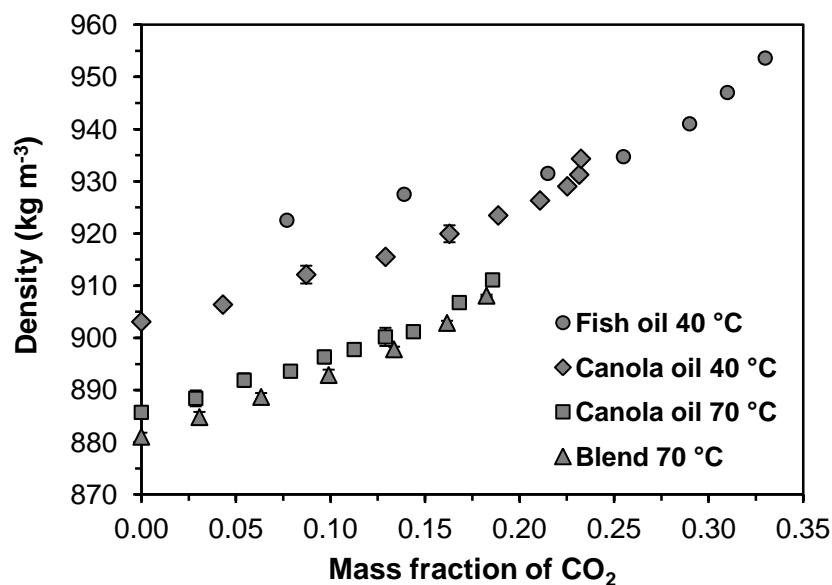


**Figure 4-9.** The density of canola oil at 40 and 70 °C and its blend with fully-hydrogenated canola oil (30 wt. %) at 70 °C in equilibrium with high pressure CO<sub>2</sub> versus the mass fraction of CO<sub>2</sub> in the liquid lipid phase in this study and the literature data for CO<sub>2</sub>-saturated fish oil at 40 °C (Seifried and Temelli, 2009).

However, for canola oil and the blend at 70 °C the density of CO<sub>2</sub>-expanded liquid lipid phase increased almost linearly up to CO<sub>2</sub> mass fraction of about 0.15, where the pressure was about 15 MPa, and above that the effect of compression started to show up because the density increased at a higher rate while the mass fraction of CO<sub>2</sub> increased more slowly. Therefore, it can be concluded that in the

first linear part of the curve, the density is mainly influenced by the solubility of CO<sub>2</sub> in the liquid lipid phase and in the second part the effect of compression on density is more pronounced. To further demonstrate the effect of the degree of unsaturation, the density of CO<sub>2</sub>-saturated fish oil obtained from the literature (Seifried and Temelli, 2009) was compared to that of canola oil at 40 °C (Fig. 4-9). For CO<sub>2</sub> mass fractions below 0.2, the density of highly unsaturated fish oil was higher. Even though the mass fraction of CO<sub>2</sub> in canola oil reached a plateau just above 0.2 that in fish oil continued to increase. Better understanding of the interactions at the molecular level between CO<sub>2</sub> and oils of different saturation levels resulting in such impact on density requires further research.

In order to correlate isothermal density of CO<sub>2</sub>-saturated canola oil and its blend with FHCO as a function of pressure, modified Tait equation (Eq. (4.21)) was used.

$$\rho_{mix}(T, P) = \frac{\rho(T, P_0)}{1 - C \ln(\frac{B(T) + P}{B(T) + P_0})} \quad (4.21)$$

where  $\rho_{mix}$  is the mixture density (kg m<sup>-3</sup>) at a given pressure and temperature, the subscript “0” refers to the low pressure, usually 0.1 MPa, and B and C are parameters derived from the fit and they are temperature dependent and independent, respectively. Modified Tait equation is widely used to fit liquid density data over wide pressure ranges (Dymond and Malhotra, 1988). The fitting parameters presented in Table 4-7 were obtained by minimizing AARD using the Solver program of Microsoft Excel. The AARD for all the conditions employed in

this study was less than about 0.1%, indicating this model can be used as a reliable tool for density determination of CO<sub>2</sub>-saturated canola oil and its blend with FHCO. As shown in Figure 4-6, the curves obtained with this model represented the experimental data very well.

**Table 4-7.** Modified Tait equation parameters (C=0.0446).<sup>a</sup>

Substance	T (°C)	B	AARD (%)	MaxRD (%) <sup>b</sup>
Canola oil	40	17	0.089	0.34
	55	20.1902	0.085	0.28
	70	27.8805	0.066	0.25
Blend <sup>c</sup>	70	26.25	0.104	0.28

<sup>a</sup> “C” is a temperature independent parameter derived from curve fitting to the experimental data.

<sup>b</sup> Refer to Table 4-3.

<sup>c</sup> Blend of canola oil and fully-hydrogenated canola oil (FHCO) (30 wt.%).

#### 4.4. Conclusions

The experimental data for the solubility of CO<sub>2</sub> in canola oil at 40 and 70 °C and its blend with FHCO (30 wt.%) at 70 °C in equilibrium with high pressure CO<sub>2</sub> were successfully described by Peng-Robinson and modified Soave-Redlich-Kwong equations of state using quadratic and Panagiotopoulos-Reid mixing rules. The use of quadratic mixing rules is recommended since less fitting parameters are needed. The relative volumetric expansion of canola oil in equilibrium with high pressure CO<sub>2</sub> at 40 °C increased with pressure up to 10 MPa and above that it leveled off, reaching a constant level. However, for canola oil and its blend at 70 °C, the volumetric expansion increased up to about 15 MPa and above that it still increased but more slowly without reaching a plateau within the range of

pressures studied. The density of CO<sub>2</sub>-saturated canola oil at 40 and 55 °C increased in a more pronounced manner up to 10 MPa because of the solubility of CO<sub>2</sub> in the liquid lipid phase and above that the density increased with a lower slope mainly due to the effect of compression. For canola oil and its blend, this pressure shifted to a higher level because of the lower solubility of CO<sub>2</sub> in the liquid lipid phase at high temperature. Comparison of the densities of canola oil, the blend, and the literature data for fish oil saturated with CO<sub>2</sub> at 70 °C revealed that the density increased with the degree of unsaturation at constant pressure and temperature. The experimental data for density were successfully correlated using the modified Tait equation. The findings of this study show that the physical properties of CO<sub>2</sub>-saturated or expanded lipids are profoundly dependent on temperature and pressure. These results contribute to our understanding that will lead to the development of novel processes for fats and oils such as extraction, reaction, and particle formation, which are mainly dependent on the mass transfer properties of starting materials.

#### **4.5. References**

AOCS Official and Recommended Practices. (2009). (6th ed.) AOCS Press, Champaign, IL, USA.

Calvignac, B., Rodier, E., Letourneau, J.J., dos Santos, P.M.A. and Fages, J. (2010). Cocoa butter saturated with supercritical carbon dioxide: Measurements and modelling of solubility, volumetric expansion, density and viscosity. *International Journal of Chemical Reactor Engineering*, **8**: A73.

Chang, C.M.J., Lee, M.S., Li, B.C. and Chen, P.Y. (2005). Vapour-liquid equilibria and densities of CO<sub>2</sub> with four unsaturated fatty acid esters at elevated pressures. *Fluid Phase Equilibria*, **233** (1): 56-65.

Dittmar, D., De Arévalo, A.M., Beckmann, C. and Eggers, R. (2005). Interfacial tension and density measurement of the system corn germ oil-carbon dioxide at low temperatures. *European Journal of Lipid Science and Technology*, **107** (1): 20-29.

Dymond, J.H. and Malhotra, R. (1988). The tait equation: 100 years on. *International Journal of Thermophysics*, **9** (6): 941-951.

Fernández-Ronco, M.P., Gracia, I., De Lucas, A. and Rodríguez, J.F. (2011). Measurement and modeling of the high-pressure phase equilibria of CO<sub>2</sub>-oleoresin capsicum. *Journal of Supercritical Fluids*, **57** (2): 112-119.

Jessop, P.G. and Subramaniam, B. (2007). Gas-expanded liquids. *Chemical Reviews*, **107** (6): 2666-2694.

Klein, T. and Schulz, S. (1989). Measurement and model prediction of vapour-liquid equilibria of mixtures of rapeseed oil and supercritical carbon dioxide. *Industrials and Engineering Chemistry Research*, **28** (7): 1073-1081.

Lemmon, E.W., McLinden, M.O. and Friend, D.G. (2010). Thermophysical properties of fluid systems. In *Nist chemistry webbook, nist standard reference database number 69*, P.J. Linstrom and W.G. Mallard, Eds. National Institute of Standards and Technology: Gaithersburg MD, p 2089.

Pfohl, O., Petkov, S. and Brunner, G. (2000). Pe 2000: A powerful tool to correlate phase equilibria. Munich, Herbert Utz Verlag GmbH.

Seifried, B. and Temelli, F. (2009). Density of marine lipids in equilibrium with carbon dioxide. *Journal of Supercritical Fluids*, **50** (2): 97-104.

Seifried, B. and Temelli, F. (2010). Unique properties of carbon dioxide-expanded lipids. *INFORM-International News on Fats, Oils and Related Materials*, **21** (1): 10-12+59.

Smith, R.L., Yamaguchi, T., Sato, T., Suzuki, H. and Arai, K. (1998). Volumetric behaviour of ethyl acetate, ethyl octanoate, ethyl laurate, ethyl linoleate, and fish oil ethyl esters in the presence of supercritical CO<sub>2</sub>. *Journal of Supercritical Fluids*, **13** (1-3): 29-36.

Staby, A. and Mollerup, J. (1993). Solubility of fish oil fatty acid ethyl esters in sub and supercritical carbon dioxide. *Journal of the American Oil Chemists' Society*, **70** (6): 583-588.

Subramaniam, B. (2010). Gas-expanded liquids for sustainable catalysis and novel materials: Recent advances. *Coordination Chemistry Reviews*, **254** (15-16): 1843-1853.

Tegetmeier, A., Dittmar, D., Fredenhagen, A. and Eggers, R. (2000). Density and volume of water and triglyceride mixtures in contact with carbon dioxide. *Chemical Engineering and Processing: Process Intensification*, **39** (5): 399-405.

Venter, M.J., Willems, P., Kareth, S., Weidner, E., Kuipers, N.J.M. and de Haan, A.B. (2007). Phase equilibria and physical properties of CO<sub>2</sub>-saturated cocoa butter mixtures at elevated pressures. *Journal of Supercritical Fluids*, **41** (2): 195-203.

Yu Z.R. (1992). Phase equilibria and enzymatic esterification of anhydrous milk fat in supercritical carbon dioxide. PhD dissertation, Cornell University, Ithaca, NY, USA, p 311.

## **5. Performance of two immobilized lipases for interesterification between canola oil and fully-hydrogenated canola oil under supercritical carbon dioxide<sup>1</sup>**

### **5.1. Introduction**

The functional, physicochemical and nutritional properties of triglycerides (TG) are determined by the nature and type of fatty acids in their structures. The most abundant TG in canola oil is triolein. As is also the case for other vegetable oils, canola oil is sometimes modified in order to enhance its physicochemical properties to meet the specifications for certain food applications. For example, it may be desirable to produce a solid fat, which can be achieved by partial hydrogenation of an unsaturated oil. However, the hardened fats produced in this manner contain *trans*-isomers, which are known to be undesirable from nutritional standpoint since they have been shown to be a major risk factor for cardiovascular disease (de Roos et al., 2002; Combe et al., 2007). Interesterification is an alternative approach for hardening oils by incorporating fully hydrogenated or stearin fractions, eliminating the formation of any *trans*-isomers. The most common type of interesterification for margarine and confectionary fat production is chemical interesterification, in which metal alkylate catalysts are used, leading to a fully random TG structure. Also, the catalysts used in this process are toxic and lead to darkening of the final products;

---

<sup>1</sup> A version of this chapter has been submitted to *LWT-Food Sci. Technol.* for consideration for publication. Jenab E., Temelli F., Curtis, J.M. and Zhao Y.Y. (2012). Performance of two immobilized lipases for interesterification between canola oil and fully-hydrogenated canola oil under supercritical carbon dioxide.

therefore, downstream processing is necessary to remove color compounds and catalysts. On the other hand, lipase-catalyzed interesterification can take place under milder conditions with fewer side reactions, leading to cleaner final products (Marangoni and Rousseau, 1995; Xu, 2003).

Supercritical fluids (SCF), especially supercritical carbon dioxide ( $\text{SCCO}_2$ ), are alternative reaction media for chemical and biocatalytic reactions. SCF technology is a rapidly growing alternative to some of the conventional methods of extraction, fractionation and reactions due to its numerous advantages (Section 2.1). As discussed in Section 2.3, supercritical fluids can be used as reaction media in lipase-catalyzed lipid reactions since the low viscosity and the high diffusivity of SCF enhance transport of substrates and products through the pores of enzyme support. This leads to easier access of substrates and removal of products to and from the active sites of the enzyme, resulting in higher reaction rates in SCF compared to those in organic solvent or solvent-free reaction systems. However, the solubility of vegetable oils in  $\text{SCCO}_2$  alone is such that high pressures and temperatures are required in order to conduct the reaction in a supercritical solution, making the process less feasible. Alternatively, solvent-free enzymatic reactions can be conducted by dissolving the  $\text{SCCO}_2$  in the liquid lipid phase and having a  $\text{CO}_2$ -expanded lipid (CX-lipid) phase to improve the mass transfer properties (Jessop and Subramaniam, 2007; Seifried and Temelli, 2010; Subramaniam, 2010).

Lipase-catalyzed reactions are desirable because of their selectivity towards fatty acid positions on the glycerol backbone, and consequently greater specificity

in reactions (Marangoni and Rousseau, 1995). However, the stability and activity of enzymes under SCCO<sub>2</sub> depends on many parameters including the type of enzyme, pressure and temperature of the reaction system, exposure time, depressurization rate, the number of pressurization/depressurization steps, and hydrophobicity and hydrophilicity of the enzyme support (Wimmer and Zarevucka, 2010). In high pressure batch stirred reactors, the exposure time to SCCO<sub>2</sub> and the number of pressurization/depressurization steps can have an important effect on enzyme efficiency (Hlavsova et al., 2008). However, such parameters have not been investigated for the interesterification between canola oil and fully-hydrogenated canola oil (FHCO).

The objectives of this study were: (a) to determine the performance of two immobilized lipases, Lipozyme TL IM and RM IM, under SCCO<sub>2</sub> for interesterification between canola oil and FHCO, (b) to assess the reusability of both enzymes for 4 × 7 h of interesterification using SCCO<sub>2</sub> at 65 °C and 17.5 MPa, (c) to investigate the effects of incubation of immobilized lipases under SCCO<sub>2</sub> (4, 8 and 12 h) and pressurization/depressurization cycles (4, 8 and 12 times) at 65 °C and 17.5 MPa on their efficiency of lipid interesterification and potential structural changes. In this study, all reactions and treatments involving SCCO<sub>2</sub> were performed at 65 °C and 17.5 MPa unless otherwise stated.

## **5.2. Materials and methods**

### **5.2.1. Materials**

Lipozyme RM IM, purchased from Sigma Aldrich (Oakville, ON, Canada) and Lipozyme TL IM, generously provided by Novozymes (Novozymes North America Inc., Franklinton, NC, USA) were used for the interesterification between canola oil and FHCO. Lipozyme RM IM is derived from lipases of *Mucor miehei* immobilized on Duolite ES 562 via adsorption, a macro-porous ion-exchange resin based on phenol-formaldehyde copolymer as a support matrix. The moisture content of Lipozyme RM IM was  $3.31 \pm 0.17\%$ , determined by using a gravimetric method based on drying in an oven at  $110^{\circ}\text{C}$  and 5 h. The average particle size of Lipozyme RM IM was  $585.7 \pm 169.5 \mu\text{m}$  ( $d_{10} = 370.9 \mu\text{m}$ ,  $d_{90} = 809.2 \mu\text{m}$ ) measured by a laser diffraction particle size analyzer (LS 13 320, Beckman Coulter, CA, USA). Lipozyme TL IM comes from lipases of *Thermomyces lanuginosus*, immobilized on a granulated silica carrier via ionic adsorption with a moisture content of  $4.66 \pm 0.48\%$  and average particle size of  $510 \pm 176.05 \mu\text{m}$  ( $d_{10} = 282.48 \mu\text{m}$ ,  $d_{90} = 746.5 \mu\text{m}$ ). These two enzymes were selected for this study because they are immobilized, *sn*-1,3 stereo-specific, in large scale production, and easily available from major enzyme manufacturers. FHCO was kindly provided by Richardson Oilseed Ltd. (Lethbridge, AB, Canada) and canola oil manufactured by the same company was purchased from a local market. The fatty acid composition of canola oil and FHCO has been reported previously in Section 4.2.1.

$\text{CO}_2$  (bone dry, Syphon UN 1013 Class 2.2) and  $\text{N}_2$  (extra dry, UN 1046 Class 2.2) were purchased from Praxair Canada Inc. (Mississauga, ON, Canada). All analytical grade solvents were from Fisher Scientific (Ottawa, ON, Canada) and GC and HPLC lipid standards and internal standards were purchased from Nu-Chek Prep Inc. (Elysian, MN, USA).

The prepared oil mixtures and the enzymes were kept in a desiccator at 4-5 °C to prevent further moisture absorption. The reaction products, blanketed with nitrogen, were kept at -20 °C prior to analysis.

### **5.2.2. Lipase-catalyzed interesterification**

The experimental apparatus (Phase equilibria unit, Sitec Sieber Engineering, Zurich, Switzerland) used for conducting the enzymatic reactions in equilibrium with  $\text{SCCO}_2$  has been illustrated in detail in Section 3.2.3.1. Immobilized lipase (10 wt.% of initial reaction mixture of canola oil and FHCO) was added to the previously blended 70:30 (w:w) mixture of canola oil and FHCO ( $\approx 2$  g), in a stainless steel cylindrical basket. Then, the basket containing the oil blend, enzyme, and a magnetic bar was placed into the 10 mL high pressure cell that had been previously heated to 65 °C. Then, the pressure of the cell was raised to the target pressure of 17.5 MPa by pumping  $\text{CO}_2$  using a syringe pump (Model 260D, Teledyne Isco, Lincoln, NE, USA) and monitored by a pressure transducer. The temperature of the cell, measured by a thermocouple located at the inner wall of the cell, was maintained at 65 °C and controlled by circulating hot water in the jacket surrounding the cell. The temperature of 65 °C was selected in order to

ensure a homogeneous liquid oil mixture in the reactor throughout the reaction, whereas the pressure of 17.5 MPa was selected as an intermediate level in the range of 10-30 MPa being used regularly for enzymatic reactions. At the end of the targeted reaction time, the reactor was depressurized carefully and the sample was filtered (Whatman filter paper no. 4) to remove the enzyme. Then, hot ( $\approx$ 65 °C) hexane was used to wash any oil residue from the enzyme.

In order to assess the reusability of the enzymes, residual hexane was removed by purging a gentle stream of nitrogen through the filtered enzyme and then the enzyme was placed inside the reactor again and the reaction protocol was repeated using the same amount of oil blend. The enzymes were reused 4 times for 7 h each at 17.5 MPa and 65 °C for the interesterification between canola oil and FHCO. The reactions at each condition were conducted at least in three replicates.

### **5.2.3. Activity of immobilized lipases exposed to SCCO<sub>2</sub> and pressurization/depressurization cycles**

In order to study how the exposure time to SCCO<sub>2</sub> affects the activity of immobilized lipases, both Lipozyme RM IM and TL IM were incubated in SCCO<sub>2</sub> at 17.5 MPa and 65 °C for 4, 8 and 12 h using the same high pressure cell described previously. Immobilized enzyme, about 0.4 g, was placed in a stainless steel basket for ease of removal at the end of a run prior to putting it in the reactor. Samples were charged into the cell, which was already heated to 65 °C. The cell was pressurized and maintained at 17.5 MPa and 65 °C for different

exposure times. To investigate the effect of the pressurization/depressurization steps on enzyme activity, both enzymes were exposed to 4, 8, and 12 pressurization/depressurization cycles. Each cycle lasted about 1 h and included a pressurization step at the rate of  $3.8 \pm 0.2$  MPa min<sup>-1</sup>, a holding time of 45 min in SCCO<sub>2</sub> at 17.5 MPa and 65 °C, and a depressurization step at the rate of  $1.5 \pm 0.1$  MPa min<sup>-1</sup>. Any change in the enzyme activity was investigated by performing the interesterification reaction between canola oil and FHCO (70:30, w:w) using SCCO<sub>2</sub> at 17.5 MPa and 65 °C for 2 h with untreated and SCCO<sub>2</sub>-treated immobilized lipases as described above.

#### **5.2.4. Analysis of reaction intermediates**

The gas chromatograph (GC, Varian 3400, Varian Inc., Walnut Creek, CA, USA) equipped with a flame ionization detector and an automatic ‘cool on column’ injector was used for the determination of free fatty acids (FFA), monoglycerides (MG), and diglycerides (DG). Reaction product samples were silylated prior to GC injection. About 10 mg of sample was weighed in a glass vial and 50 µL of 20 mg/mL dilaurin solution in chloroform was added as internal standard. The sample and internal standard were dissolved in 0.5 mL pyridine and then 100 µL of N, O-bis-(trimethylsilyl) trifluoracetamide (BSTFA) containing 1% trimethylchlorosilane (TMCS) solution was added as silylation agent. Then, the glass vials were placed in an oven at 70 °C for 20 min to complete the silylation process. Samples were diluted with 1 mL of chloroform and then 1 mL of silylated sample was transferred to a GC vial for injection. An aliquot (1 µL) of

each sample was injected onto a Restek MTX-Biodiesel TG column (15 m × 0.32 mm ID × 0.1 µm film thickness; Restek Corp., Bellefonte, PA, USA) with a retention gap (2 m × 0.53 mm ID). Hydrogen was used as carrier gas at a head pressure of 103.4 kPa. The injector temperature was programmed from 70 °C to 340 °C at 150 °C min<sup>-1</sup> and held for 25 min. The oven temperature was programmed with an initial hold at 50°C for 1 min, followed by an initial increase to 180 to 230 °C at 7 °C min<sup>-1</sup>, and a final increase from 230 to 380 °C at 30 °C min<sup>-1</sup>, held for 8.2 min. The detector temperature was set at 380 °C. For the quantification of reaction intermediates, peak area counts of FFA, MG and DG were divided by relative response factors of approximately 0.9, 0.9 and 1.1, respectively, determined by the injection of standards in a separate experiment.

### 5.2.5. Determination of degree of interesterification

The conversion rate of interesterification reaction between canola oil and FHCO was defined as the number of moles of 1,3-distearoyl-2-oleoyl-glycerol (SOS) and 2,3-dioleoyl-1-stearoyl-glycerol (SOO) and their isomers as major TG products of the reaction over the number of moles of initial substrates (5.1). The number of moles of initial substrates was calculated by considering the average molecular weight of the blend, 883.51 g/mol, using the fatty acid profile of canola oil and FHCO blend (70:30, w:w) previously determined by GC analysis in Section 3.2.1.

$$Degree\ of\ interesterification = \frac{[SOS]_{mol} + [SOO]_{mol}}{[initial\ substrates]_{mol}} \times 100 \quad (5.1)$$

TG profiles of the products were quantified by HPLC/APPI-MS using an Agilent 1200 liquid chromatograph (Agilent technologies, Palo Alto, CA, USA) coupled to a Q star Elite mass spectrometer (Applied Biosystems/MDS Sciex; Concord, ON, Canada) with a photospray<sup>TM</sup> photoionization source. Toluene as a dopant was delivered by an isocratic HPLC pump (Agilent Technologies, Palo Alto, CA, USA) at a flow rate of 20  $\mu\text{L min}^{-1}$ . Analyst QS 2.0 software was used for data acquisition and analysis. The sample solution (100  $\mu\text{L}$ ) in chloroform (0.25-0.5 mg/mL) was mixed with 100  $\mu\text{L}$  trinonadecanoic acid solution in chloroform (20  $\mu\text{g/mL}$ ) as internal standard, and then 10  $\mu\text{L}$  of the dilution was autoinjected into the HPLC system. TG were separated on an Ascentis C18 column (5 cm  $\times$  2.1 mm i.d., 3  $\mu\text{m}$ ) (Supelco, Bellefonte, PA, USA). A binary gradient system of acetonitrile and isopropanol was used at a flow rate of 0.2 mL  $\text{min}^{-1}$ . Gradient elution profile started with 70% acetonitrile and 30% isopropanol, changed to 10% acetonitrile and 90% isopropanol in 25 min, changed to 70% acetonitrile and 30% isopropanol in 0.1 min and then held for 10 min. In order to obtain calibration curves for triolein (OOO), tristearin (SSS), SOS, and SOO, standards at concentrations of 0.625, 1.25, 2.5, 5, 12.5, 25, 37.5, and 50  $\mu\text{g/mL}$  containing the internal standard at a concentration of 0.01  $\mu\text{g/mL}$  were injected onto the column.

## **5.2.6. Structural and morphological analysis of enzymes**

### **5.2.6.1. Fourier transform infrared spectroscopy (FTIR)**

Untreated and SCCO<sub>2</sub>-treated immobilized lipase samples (1-3 mg) were mixed thoroughly with about 350 mg of KBr (Fisher Scientific, Ottawa, ON, Canada). The mixture was transferred to a die with a barrel diameter of 13 mm, which was then placed in a pellet press and pressed for about 2 min. FTIR spectra were collected using a Nicolet 380 FTIR spectrometer (Thermo Electron Corporation, Madison, WI, USA) with deuterated triglycine sulfate and thermoelectricity cooled (DTGS-TEC) detector in the wavelength range of 600-2000 cm<sup>-1</sup>. CO<sub>2</sub> and water vapour were continuously purged out during the measurements with dry air. For each sample, 64 scans were performed with a resolution of 4 cm<sup>-1</sup> at room temperature using OMNIC software. Each spectrum was obtained based on an average of 3 cycles of 64 scans. A pure KBr pellet was used for background correction. For further signal processing and baseline corrections, MATLAB software (Version 7.10, MathWorks, Natick, MA, USA) was used.

### **5.2.6.2. Field emission scanning electron microscopy (FE-SEM)**

SCCO<sub>2</sub>-treated immobilized lipases with 12 pressurization/depressurization cycles and those reused for interesterification 4 times were selected for FE-SEM analysis. A JEOL 6301 FXV scanning electron microscope (Peabody, MA, USA) was used for this analysis. The enzyme grains were attached to the SEM stubs using silver paint, which was given enough time to dry at ambient conditions.

Then, the grains were sputter-coated with chromium in a xenon atmosphere using an Edward high-vacuum XE 200 Xenosput (Crawley, Sussex, England) prior to analysis.

#### **5.2.6.3. X-ray photoelectron spectroscopy (XPS)**

The carbon to nitrogen ratios of untreated and immobilized lipases exposed to  $\text{SCCO}_2$  for 12 h at 65 °C and 17.5 MPa were measured by XPS using an AXIS 165 spectrometer (Kratos Analytical, Manchester, UK) at the Alberta Centre for Surface Engineering and Science (ACSES), University of Alberta. The base pressure in the analytical chamber was lower than  $2 \times 10^{-8}$  Pa. A monochromatic Al K $\alpha$  source ( $h\nu = 1486.6$  eV) was used at a power of 210 W. A spot size of 400  $\times$  700  $\mu\text{m}$  was irradiated. The resolution of the instrument is 0.55 eV for the Ag 3d and 0.70 eV for Au 4f peaks. The survey scans were collected for binding energies spanning from 1100 eV to 0 with analyzer pass energy of 160 eV and a step of 0.35 eV. For the high-resolution spectra the pass energy was 20 eV with a step of 0.1 eV. Since the samples were charging, electron flood neutralization was applied to compensate for the photoelectrons leaving the surface.

#### **5.2.7. Statistical analysis**

Analysis of variance of results was carried out using General Linear Model Procedure of SAS Statistical Software, Version 9.2. Multiple comparisons of means, obtained from duplicate and triplicate experiments, were carried out by Duncan's test with  $\alpha$  value of 0.05.

### **5.3. Results and discussion**

#### **5.3.1. Performance and reusability of Lipozyme TL IM and RM IM**

The activities of two *sn*-1,3 stereo-specific immobilized lipases (Lipozyme TL IM and Lipozyme RM IM) in catalyzing the interesterification between canola oil and FHCO under  $\text{SCCO}_2$  conditions ( $65^\circ\text{C}$  and  $17.5 \text{ MPa}$ ) in a batch reactor were compared. As shown in Figure 5-1a, there were no significant differences ( $p > 0.05$ ) between the degrees of interesterification obtained using either immobilized lipase, over 7.5 h of reaction time. The degree of interesterification reached a plateau (27-28%) after about 2 h for both enzymes. Furthermore, there were no significant differences ( $p > 0.05$ ) between the total amounts of reaction intermediates (FFA, MG, and DG) produced during the reaction by either immobilized lipase (Fig. 5-1b) because both immobilized lipases had similar moisture contents. The total amount of reaction intermediates produced during the interesterification also reached a plateau (13-14 wt %) in about 2 h, demonstrating that side reactions such as hydrolysis occur at the same time as interesterification. During interesterification between canola oil and FHCO, the amount of reaction intermediates should be kept as low as possible because such hydrolysis products need to be removed by downstream processes prior to achieving the final base-stock for *trans*-free margarine production, thereby decreasing the yield of the overall process.

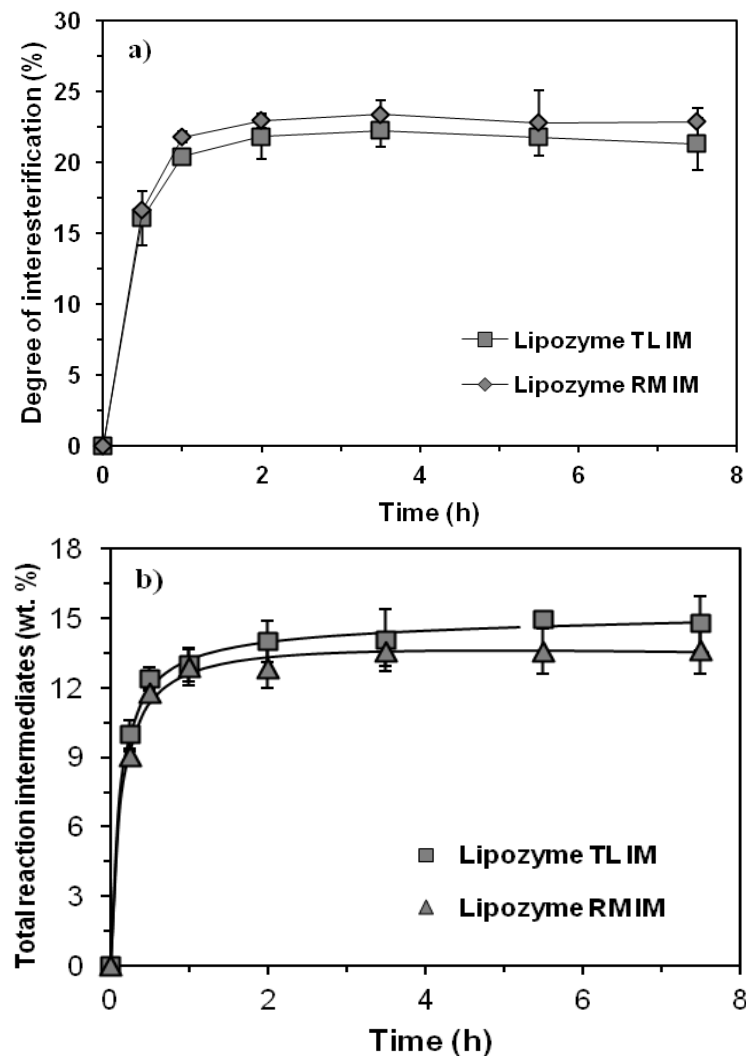


**Figure 5-1.** Performance of Lipozyme TL IM and RM IM for interesterification between canola oil and fully-hydrogenated canola oil (70:30 w/w) under  $\text{SCCO}_2$  at 65 °C and 17.5 MPa over 7.5 h: (a) Degree of interesterification and (b) total amount of produced intermediates during the reaction.

During the interesterification between canola oil and FHCO, triolein and tristearin were partially consumed as the main substrates of the reaction. At the same time, new TG components like SOO and SOS and their isomers, which have melting points between those of tristearin and triolein, were produced. For both

enzymes, the amounts of triolein and tristearin decreased to 4-6 and 1-2 mol %, respectively, equivalent to about 67 and 87% reduction from the starting amount. The amount of SOO and SOS, produced during the reaction, reached 19-20 and 6-8 mol %, respectively, after 2 h of reaction (Fig. 5-2).

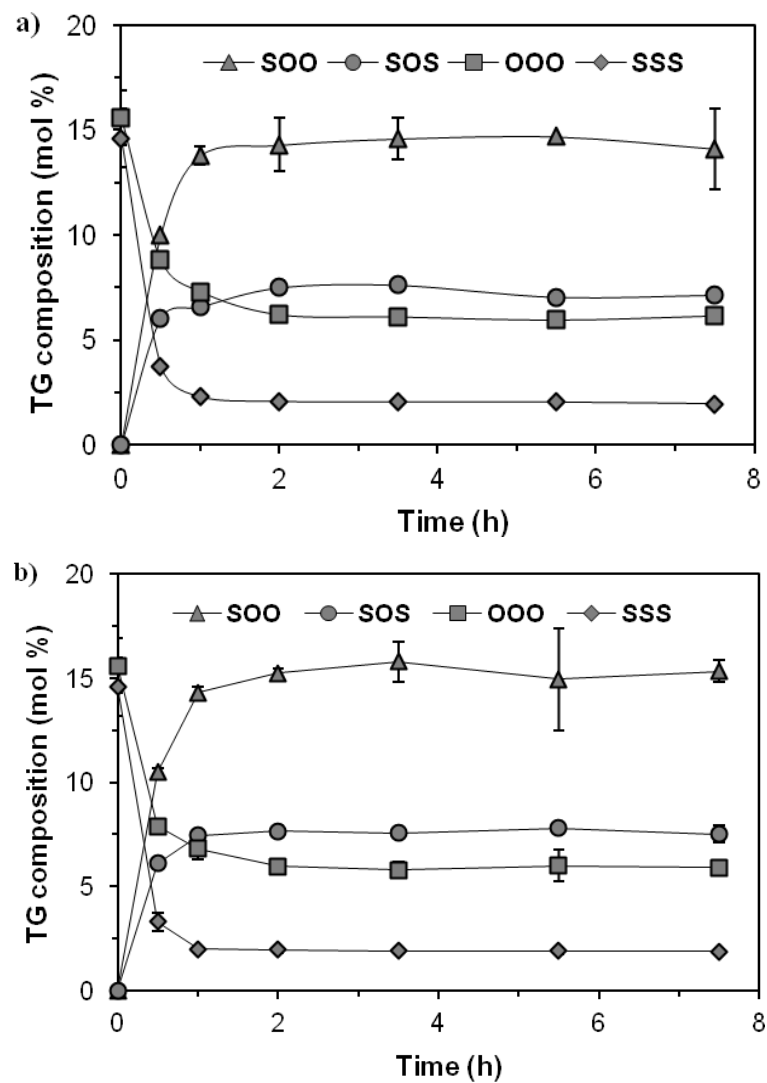


**Figure 5-2.** Triglyceride (TG) components of interesterified canola oil and fully-hydrogenated canola oil (70:30 w/w) under  $\text{SCCO}_2$  at  $65^\circ\text{C}$  and 17.5 MPa over 7.5 h of reaction: (a) Lipozyme TL IM and (b) Lipozyme RM IM.

The ability to reuse Lipozyme TL IM and RM IM under  $\text{SCCO}_2$  conditions was examined by using the same enzyme batch for 4 consecutive runs of 7 h each. It was found that the degrees of interesterification for both immobilized lipases were maintained at the same level ( $p > 0.05$ ). This can be seen in Table 5-1, which shows over the 4 times the same levels of TG reactants and interesterification products were obtained after each time the enzyme is reused.

**Table 5-1.** The effect of reusing Lipozyme TL IM and RM IM for interesterification between canola oil and fully-hydrogenated canola oil up to 4 times of 7 h each under  $\text{SCCO}_2$  at 65 °C and 17.5 MPa on triglycerides composition (mol.%) and degree of interesterification (%).

Type of enzyme	Reuse cycle			
	1	2	3	4
<i>Lipozyme TL IM</i>				
OOO	5.9 ± 0.36 <sup>a</sup>	6.35 ± 0.42 <sup>a</sup>	6.07 ± 0.51 <sup>a</sup>	5.97 ± 0.12 <sup>a</sup>
SSS	1.96 ± 0.01 <sup>b</sup>	2.03 ± 0.04 <sup>b</sup>	1.94 ± 0.04 <sup>b</sup>	1.98 ± 0.00 <sup>b</sup>
SOO	14.74 ± 1.63 <sup>c</sup>	14.25 ± 0.45 <sup>c</sup>	13.9 ± 1.75 <sup>c</sup>	14.38 ± 0.55 <sup>c</sup>
SOS	6.28 ± 0.34 <sup>d</sup>	6.29 ± 0.83 <sup>d</sup>	6.82 ± 0.33 <sup>d</sup>	6.70 ± 0.48 <sup>d</sup>
Degree of interesterification (%)	21.02 ± 1.29 <sup>e</sup>	20.54 ± 0.38 <sup>e</sup>	20.72 ± 1.43 <sup>e</sup>	21.08 ± 1.03 <sup>e</sup>
<i>Lipozyme RM IM</i>				
OOO	5.33 ± 0.44 <sup>a</sup>	6.02 ± 0.30 <sup>a</sup>	5.41 ± 0.32 <sup>a</sup>	5.53 ± 0.38 <sup>a</sup>
SSS	1.90 ± 0.07 <sup>b</sup>	1.93 ± 0.09 <sup>b</sup>	1.91 ± 0.21 <sup>b</sup>	1.96 ± 0.07 <sup>b</sup>
SOO	14.3 ± 1.32 <sup>c</sup>	14.7 ± 1.07 <sup>c</sup>	15.02 ± 0.03 <sup>c</sup>	14.42 ± 1.12 <sup>c</sup>
SOS	6.47 ± 0.16 <sup>d</sup>	6.47 ± 0.88 <sup>d</sup>	6.78 ± 1.60 <sup>d</sup>	7.22 ± 0.66 <sup>d</sup>
Degree of interesterification (%)	20.77 ± 1.48 <sup>e</sup>	21.17 ± 1.96 <sup>e</sup>	21.80 ± 1.63 <sup>e</sup>	21.64 ± 0.46 <sup>e</sup>

OOO, triolein; SSS, tristearin; SOO, 2,3-dioleoyl-1-stearoyl-glycerol; and SOS, 1,3-distearoyl-2-oleoyl-glycerol.

<sup>a-e</sup> Values with the same superscripts in each row for each enzyme type have no significant differences ( $p > 0.05$ ).

Interestingly, the amount of reaction intermediates such as FFA, MG, and DG (Table 5-2) and consequently the total amount of reaction intermediates

decreased significantly ( $p < 0.05$ ) after the first cycle and remained constant ( $p > 0.05$ ) during the three remaining reuse cycles for both enzymes (Fig. 5-3). This is due to the consumption of the free water content of the enzymes in the first cycle, leading to lower content of reaction intermediates in the following cycles without any significant changes ( $p > 0.05$ ) in the degrees of interesterification of the enzymes.

**Table 5-2.** The effect of reusing Lipozyme TL IM and RM IM for transesterification of canola oil and fully-hydrogenated canola oil up to 4 times of 7 h each under  $\text{SCCO}_2$  at  $65^\circ\text{C}$  and 17.5 MPa on reaction intermediates (or hydrolysis products) (wt.%).

Type of enzyme	Reuse cycle			
	1	2	3	4
<i>Lipozyme TL IM</i>				
FFA	$6.32 \pm 0.37^{\text{a}}$	$2.92 \pm 0.42^{\text{b}}$	$3.04 \pm 0.70^{\text{b}}$	$3.05 \pm 0.21^{\text{b}}$
MG	$0.56 \pm 0.06^{\text{b}}$	$0.25 \pm 0.07^{\text{c}}$	$0.18 \pm 0.08^{\text{c}}$	$0.21 \pm 0.04^{\text{c}}$
DG	$9.59 \pm 1.05^{\text{c}}$	$6.60 \pm 1.53^{\text{d}}$	$6.09 \pm 0.86^{\text{d}}$	$6.63 \pm 0.18^{\text{d}}$
<i>Lipozyme RM IM</i>				
FFA	$3.80 \pm 0.25^{\text{a}}$	$2.60 \pm 0.33^{\text{b}}$	$2.19 \pm 0.16^{\text{b}}$	$1.86 \pm 0.47^{\text{b}}$
MG	$0.33 \pm 0.03^{\text{b}}$	$0.17 \pm 0.06^{\text{c}}$	$0.10 \pm 0.05^{\text{c}}$	$0.11 \pm 0.05^{\text{c}}$
DG	$10.16 \pm 0.71^{\text{c}}$	$7.59 \pm 0.55^{\text{d}}$	$7.12 \pm 0.80^{\text{d}}$	$7.20 \pm 0.79^{\text{d}}$

FFA, free fatty acid; MG, monoglyceride; and DG, diglycerides.

<sup>a-d</sup> Values with the same superscripts in each row for each enzyme type have no significant differences ( $p > 0.05$ ).

These results are in agreement with those of Laudani et al. (2007) who studied the reusability of Lipozyme RM IM for the esterification of oleic acid and 1-octanol using  $\text{SCCO}_2$  at 10 MPa and  $50^\circ\text{C}$  in a bench-scale packed bed reactor. Using a 7 h synthesis followed by a 1 h washing step with pure  $\text{CO}_2$  at the same pressure and temperature, they observed that the level of conversion was maintained for over 50 runs (Laudani et al., 2007). The incorporation of a  $\text{CO}_2$

wash step after each run prohibited water, produced by the esterification reaction, from accumulating in the reactor and inhibiting enzyme activity.

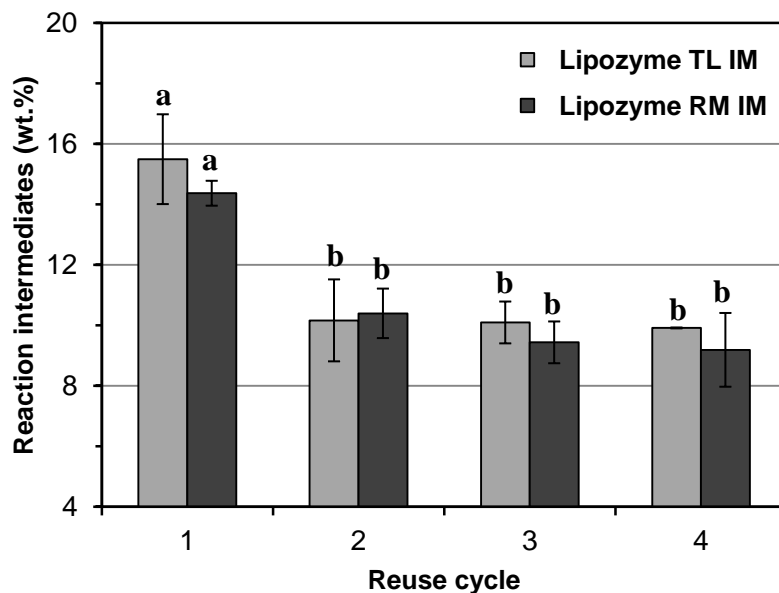


**Figure 5-3.** The effect of reusing of immobilized lipases for interesterification between canola oil and fully-hydrogenated canola oil (70:30 w/w) under  $\text{SCCO}_2$  at 65 °C and 17.5 MPa with each cycle of 7 h on the total amount of intermediates produced during the reaction. Bars with the same superscripts for each enzyme type have no significant difference ( $p > 0.05$ ).

In contrast, Rezaei and Temelli (2000) studied the stability of Lipozyme IM for the continuous hydrolysis of canola oil using  $\text{SCCO}_2$  at 38 MPa and 55°C. Over three consecutive runs of 8 h each, they observed a decline in TG consumption as well as FFA and MG production. This decrease in the conversion rate was probably due to the introduction of excess water for hydrolysis reaction and its accumulation in the reactor, leading to the decrease in enzyme efficiency.

FE-SEM was used to investigate any potential morphological changes in both immobilized lipases after the 4 cycles of reuse described above. Figure 5-4

gives the FE-SEM micrographs of Lipozyme RM IM and TL IM before and after treatment. Increasing the magnification from 50 to 30,000 times in these micrographs clearly showed that reusing both immobilized lipases leads to significant changes in the physical structure of enzyme beads of both immobilized lipases. It can be observed that for both immobilized lipases the surfaces became cracked, opening relatively substantial holes and fissures on the enzyme beads.

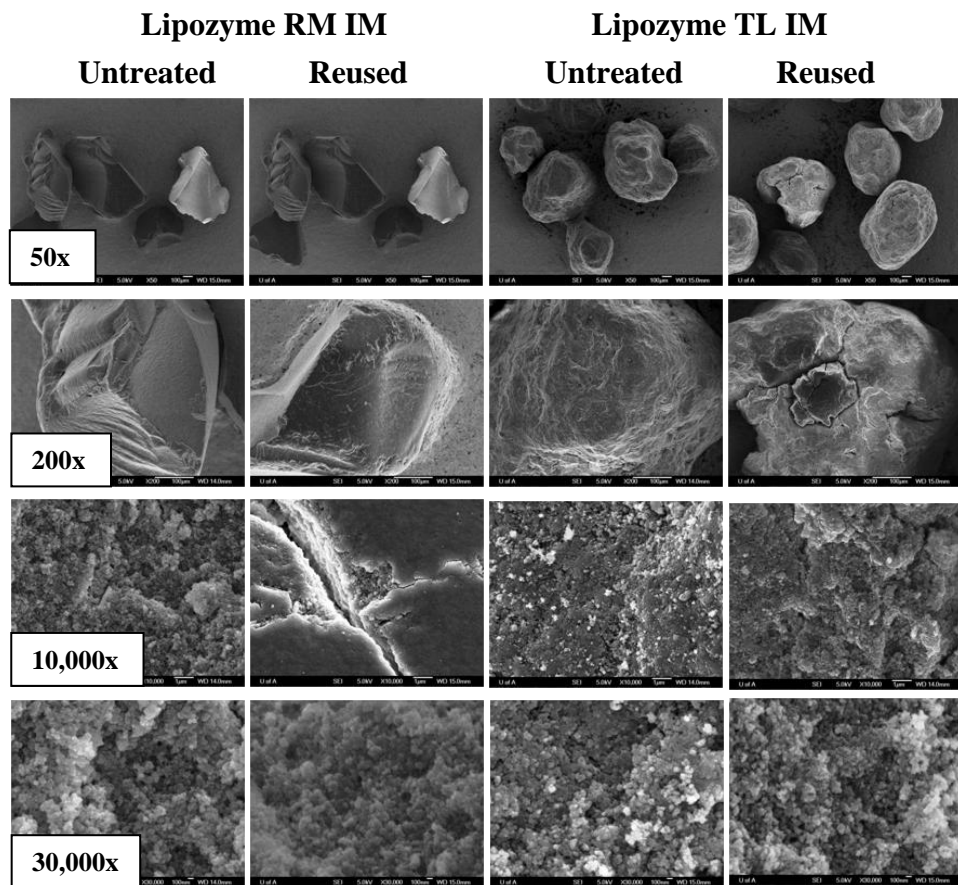


**Figure 5-4.** FE-SEM micrographs of immobilized lipases before and after reuse ( $4 \times 7$  h) for interesterification between canola oil and fully-hydrogenated canola oil under  $\text{SCCO}_2$  at  $65^\circ\text{C}$  and 17.5 MPa.

The mixing of the enzymes and the substrates inside the reactor using a magnetic bar and/or pressurization and depressurization of the high pressure reactor in each cycle of reaction could be the reason for such morphological changes. Whether any enzymes were released from the matrix into the lipid phase was not evaluated in this study. However, the activity of enzymes remained the same despite these morphological changes (Table 5-1).

### **5.3.2. Immobilized lipases under SCCO<sub>2</sub> conditions**

#### **5.3.2.1. Effect of exposure time and pressurization/depressurization on enzyme activity**

It is likely time of that the exposure to high pressure CO<sub>2</sub> may impact enzyme activity within the range of pressures and temperatures used for enzymatic lipid reactions in SCCO<sub>2</sub> media (Wimmer and Zarevucka, 2010). As well, in batch reactors where the enzyme is reused for several times, conformational changes may occur due to pressurization/depressurization cycles. Therefore, an understanding of the stability of enzymes exposed to SCCO<sub>2</sub> is important for any practical applications.

In order to evaluate the effect of exposure time of immobilized lipases to pure SCCO<sub>2</sub>, Lipozyme RM IM and Lipozyme TL IM were incubated under SCCO<sub>2</sub> for 4, 8, and 12 h. These lipase preparations, recovered from the high pressure reactor after applying a depressurization rate of  $1.5 \pm 0.1 \text{ MPa min}^{-1}$ , were used for the interesterification between canola oil and FHCO (70:30, w:w) using SCCO<sub>2</sub> at 17.5 MPa and 65°C for 2 h. For comparison, the same reaction

was also conducted using untreated enzymes. It is found that exposure of both immobilized lipases to  $\text{SCCO}_2$  for up to 12 h did not lead to any significant changes ( $p > 0.05$ ) in their activity compared to the untreated enzyme (Table 5-3). The TG composition of the reaction products obtained with treated enzymes was similar to that of the untreated enzymes for both lipases (Table 5-3).

**Table 5-3.** The effect of exposure time of Lipozyme TL IM and RM IM to  $\text{SCCO}_2$  at 65 °C and 17.5 MPa on triglyceride composition (mol%) and degree of interesterification between canola oil and fully-hydrogenated canola oil (70:30 w/w) under  $\text{SCCO}_2$  at the same conditions for 2 h. Interesterification with untreated enzymes at the same conditions is considered as control.

Type of enzyme	Exposure time (h)			
	Control	4	8	12
<i>Lipozyme TL IM</i>				
OOO	6.22 ± 0.04 <sup>a</sup>	5.85 ± 0.17 <sup>a</sup>	6.03 ± 0.14 <sup>a</sup>	5.72 ± 0.76 <sup>a</sup>
SSS	2.05 ± 0.10 <sup>b</sup>	1.86 ± 0.01 <sup>b</sup>	1.96 ± 0.00 <sup>b</sup>	2.02 ± 0.03 <sup>b</sup>
SOO	15.02 ± 0.63 <sup>c</sup>	14.11 ± 1.50 <sup>c</sup>	15.50 ± 0.38 <sup>c</sup>	14.73 ± 1.75 <sup>c</sup>
SOS	6.35 ± 0.19 <sup>d</sup>	5.89 ± 0.35 <sup>d</sup>	6.00 ± 0.40 <sup>d</sup>	6.16 ± 0.99 <sup>d</sup>
Degree of interesterification (%)	21.37 ± 0.82 <sup>e</sup>	20.00 ± 1.85 <sup>e</sup>	21.50 ± 0.02 <sup>e</sup>	20.89 ± 2.74 <sup>e</sup>
<i>Lipozyme RM IM</i>				
OOO	5.30 ± 0.10 <sup>a</sup>	5.41 ± 0.78 <sup>a</sup>	5.43 ± 0.99 <sup>a</sup>	5.13 ± 1.09 <sup>a</sup>
SSS	1.35 ± 0.13 <sup>b</sup>	1.33 ± 0.43 <sup>b</sup>	1.50 ± 0.35 <sup>b</sup>	1.44 ± 0.57 <sup>b</sup>
SOO	13.85 ± 0.22 <sup>c</sup>	14.02 ± 0.73 <sup>c</sup>	13.6 ± 1.45 <sup>c</sup>	14.36 ± 1.76 <sup>c</sup>
SOS	7.41 ± 0.31 <sup>d</sup>	8.01 ± 0.62 <sup>d</sup>	8.21 ± 0.16 <sup>d</sup>	7.62 ± 0.16 <sup>d</sup>
Degree of interesterification (%)	21.26 ± 0.53 <sup>e</sup>	21.16 ± 1.35 <sup>e</sup>	21.81 ± 1.28 <sup>e</sup>	21.98 ± 1.60 <sup>e</sup>

OOO, triolein; SSS, tristearin; SOO, 2, 3-dioleoyl-1-stearoyl-glycerol; and SOS, 1, 3-distearoyl-2-oleoyl-glycerol.

<sup>a-e</sup> Values with same superscripts in each row for each enzyme type have no significant difference ( $p > 0.05$ ).

Furthermore, there was no difference ( $p > 0.05$ ) between the total amounts and composition (FFA, MG, and DG) of the reaction intermediates for  $\text{SCCO}_2$  treated enzymes compared to those of untreated enzymes (Table 5-4).

Not only is the time of enzyme exposure to SCCO<sub>2</sub> conditions crucial for enzyme activity but also the number of pressurization/depressurization cycles when the enzymes are used for several consecutive reactions in batch and packed bed reactors. Therefore, both immobilized lipases were exposed to 12 pressurization/depressurization cycles with SCCO<sub>2</sub> to assess the effect on degree of interesterification. The results showed that pressurization/depressurization cycles did not have a significant ( $p > 0.05$ ) effect on degree of interesterification and the main TG composition (Table 5-5) of interesterified canola oil and FHCO compared to those obtained with untreated enzymes for both lipases.

**Table 5-4.** The effect of exposure time of Lipozyme TL IM and RM IM to SCCO<sub>2</sub> at 65 °C and 17.5 MPa on produced reaction intermediates (wt. %) of interesterified canola oil and fully-hydrogenated canola oil (70:30 w/w) under SCCO<sub>2</sub> at the same conditions for 2 h. Interesterification with untreated enzymes at the same conditions is considered as control.

Type of enzyme	Exposure time (h)			
	Control	4	8	12
<i>Lipozyme TL IM</i>				
FFA	4.38 ± 0.63 <sup>a</sup>	4.10 ± 0.33 <sup>a</sup>	4.58 ± 0.87 <sup>a</sup>	4.66 ± 0.03 <sup>a</sup>
MG	0.35 ± 0.02 <sup>b</sup>	0.31 ± 0.04 <sup>b</sup>	0.42 ± 0.05 <sup>b</sup>	0.34 ± 0.03 <sup>b</sup>
DG	7.84 ± 0.13 <sup>c</sup>	7.91 ± 0.05 <sup>c</sup>	7.58 ± 0.3 <sup>c</sup>	7.71 ± 0.73 <sup>c</sup>
Total	12.59 ± 0.52 <sup>d</sup>	12.35 ± 0.42 <sup>d</sup>	12.60 ± 1.22 <sup>d</sup>	12.73 ± 0.67 <sup>d</sup>
<i>Lipozyme RM IM</i>				
FFA	3.13 ± 0.12 <sup>a</sup>	2.97 ± 0.26 <sup>a</sup>	2.82 ± 0.21 <sup>a</sup>	3.17 ± 0.22 <sup>a</sup>
MG	0.30 ± 0.14 <sup>b</sup>	0.19 ± 0.04 <sup>b</sup>	0.13 ± 0.03 <sup>b</sup>	0.21 ± 0.00 <sup>b</sup>
DG	7.14 ± 0.57 <sup>c</sup>	6.74 ± 0.32 <sup>c</sup>	6.60 ± 0.05 <sup>c</sup>	6.29 ± 0.01 <sup>c</sup>
Total	10.42 ± 0.56 <sup>d</sup>	10.93 ± 0.63 <sup>d</sup>	10.58 ± 0.20 <sup>d</sup>	10.70 ± 0.21 <sup>d</sup>

FFA, free fatty acid; MG, monoglyceride; DG, diglyceride and TG, triglyceride.

<sup>a-d</sup> Values with the same superscripts in each row for each enzyme type have no significant differences ( $p > 0.05$ ).

Bauer et al. (2000) investigated the effects of treating a crude and purified preparation of esterase EP10 from *Burkholderia gladioli* with SCCO<sub>2</sub> at 35 and 75

°C at 15 MPa for 24 h on the enzymes activity and stability. They observed no significant change in the activity of purified esterase after treatment with SCCO<sub>2</sub> while that of crude esterase preparation decreased after incubation at 75 °C. A 20% increase in enzyme activity was observed for the crude esterase preparation after 30 pressurization/depressurization cycles of 1 h each with SCCO<sub>2</sub> at 15 MPa and 35 °C, while there was no change for the purified esterase.

**Table 5-5.** The effect of pressurization/depressurization cycles of Lipozyme TL IM and RM IM under SCCO<sub>2</sub> at 65 °C and 17.5 MPa on triglyceride composition (mol %) of interesterified canola oil and fully-hydrogenated canola oil (70:30 w:w) and degree of interesterification under SCCO<sub>2</sub> at the same conditions for 2 h. Interestesterification with untreated enzymes at the same conditions is considered as control.

Type of enzyme	Pressurization/depressurization cycles			
	Control	4	8	12
<i>Lipozyme TL IM</i>				
OOO	5.48 ± 0.04 <sup>a</sup>	5.05 ± 1.13 <sup>a</sup>	5.51 ± 0.87 <sup>a</sup>	5.63 ± 0.83 <sup>a</sup>
SSS	2.01 ± 0.10 <sup>b</sup>	1.98 ± 0.07 <sup>b</sup>	1.95 ± 0.11 <sup>b</sup>	2.03 ± 0.06 <sup>b</sup>
SOO	14.62 ± 0.63 <sup>c</sup>	15 ± 1.90 <sup>c</sup>	13.76 ± 0.93 <sup>c</sup>	14.85 ± 1.29 <sup>c</sup>
SOS	6.35 ± 0.19 <sup>d</sup>	6.78 ± 1.04 <sup>d</sup>	7.90 ± 0.31 <sup>d</sup>	7.26 ± 0.85 <sup>d</sup>
Degree of interesterification (%)	20.97 ± 0.82 <sup>e</sup>	21.78 ± 1.29 <sup>e</sup>	21.66 ± 1.24 <sup>e</sup>	22.11 ± 1.34 <sup>e</sup>
<i>Lipozyme RM IM</i>				
OOO	5.30 ± 0.1 <sup>a</sup>	5.00 ± 0.93 <sup>a</sup>	4.83 ± 1.13 <sup>a</sup>	4.72 ± 1.47 <sup>a</sup>
SSS	1.35 ± 0.13 <sup>b</sup>	1.51 ± 0.69 <sup>b</sup>	1.27 ± 0.41 <sup>b</sup>	1.51 ± 0.26 <sup>b</sup>
SOO	13.75 ± 0.22 <sup>c</sup>	14.32 ± 2.13 <sup>c</sup>	14.21 ± 0.02 <sup>c</sup>	13.45 ± 2.28 <sup>c</sup>
SOS	7.41 ± 0.31 <sup>d</sup>	8.23 ± 0.21 <sup>d</sup>	8.70 ± 0.91 <sup>d</sup>	8.52 ± 0.28 <sup>d</sup>
Degree of interesterification (%)	21.16 ± 0.53 <sup>e</sup>	22.55 ± 1.92 <sup>e</sup>	22.91 ± 0.89 <sup>e</sup>	21.97 ± 2.00 <sup>e</sup>

OOO, triolein; SSS, tristearin; SOO, 2, 3-dioleoyl-1-stearoyl-glycerol; and SOS, 1, 3-distearoyl-2-oleoyl-glycerol.

<sup>a-e</sup> Values with the same superscripts in each row for each enzyme type have no significant differences ( $p > 0.05$ ).

Giessauf and Gamse (2000) also showed that the treatment of crude porcine pancreatic lipase with high pressure CO<sub>2</sub> caused a time-dependent increase in enzyme activity. They reported 860% increase in activity compared to the untreated enzyme after exposing the enzyme to SCCO<sub>2</sub> for 24 h at 15 MPa and 75 °C. In addition, they showed that the enzyme activity increased by 191% compared to the untreated enzyme after 30 pressurization/depressurization cycles at 15 MPa and 35 °C (Giessauf and Gamse, 2000). The increase in activity might be due to extraction of impurities from the crude enzymes by CO<sub>2</sub> during the depressurization steps. Habulin and Knez (2001) reported that the activity of lipases from *Pseudomonas fluorescens*, *Rhizopus javanicus*, *Rhizopus niveus*, porcine pancreas and *Candida rugosa* did not change significantly after treating with CO<sub>2</sub> and propane at 30 MPa and 40 °C for 24 h compared to non-treated enzymes when they were used for esterification in a non-solvent system at 30 °C and atmospheric pressure.

Hlavsova et al. (2008) used Lipozyme®, lipase from *Mucor miehei* immobilized on macroporous resin, for the hydrolysis of blackcurrant oil using SCCO<sub>2</sub> at 40°C and 15 MPa in a continuous flow reactor. In a subsequent reaction, using the same enzyme for hydrolysis of *trans*-isomer of 2-(4-methoxybenzyl) cyclohexyl acetate, they obtained satisfactory reaction yields (40%) and excellent enantiomeric purity of the products (*E* = 472) compared to the untreated enzyme. Contrary to the above results and findings this study, Oliveira et al. (2006) observed a loss of about 14% for Lipozyme IM treated with high pressure CO<sub>2</sub> at 35°C and 7.1 MPa for 6 h.

In contrast to the degree of interesterification, the amount of hydrolysis products produced during the reaction including FFA, MG, and DG (Table 5-6) and their total amount (Fig. 5-5) decreased significantly compared to those obtained with untreated enzymes for both lipases after 12 pressurization/depressurization cycles. In fact, the total amount of reaction intermediates decreased by 50-60% after 12 pressurization/depressurization cycles compared to the control treatment using untreated enzymes.

**Table 5-6.** The effect of pressurization/depressurization cycles of Lipozyme TL IM and RM IM under  $\text{SCCO}_2$  at 65 °C and 17.5 MPa on reaction intermediates (wt. %) of interesterified canola oil and fully-hydrogenated canola oil (70:30 w/w) using  $\text{SCCO}_2$  at the same conditions for 2 h. Interesterification with untreated enzymes at the same conditions is considered as control.

Type of enzyme	Pressurization/depressurization cycles			
	Control	4	8	12
<i>Lipozyme TL IM</i>				
FFA	3.94 ± 0.63 <sup>a</sup>	3.61 ± 0.04 <sup>a</sup>	2.35 ± 0.16 <sup>b</sup>	1.82 ± 0.23 <sup>b</sup>
MG	0.35 ± 0.02 <sup>c</sup>	0.30 ± 0.01 <sup>c</sup>	0.09 ± 0.05 <sup>c</sup>	0.06 ± 0.01 <sup>c</sup>
DG	7.84 ± 0.13 <sup>d</sup>	6.43 ± 0.47 <sup>d</sup>	4.08 ± 0.30 <sup>e</sup>	2.91 ± 0.38 <sup>e</sup>
<i>Lipozyme RM IM</i>				
FFA	3.13 ± 0.12 <sup>a</sup>	2.55 ± 0.11 <sup>a</sup>	1.77 ± 0.32 <sup>b</sup>	1.43 ± 0.24 <sup>b</sup>
MG	0.30 ± 0.14 <sup>c</sup>	0.17 ± 0.04 <sup>c</sup>	0.11 ± 0.02 <sup>c</sup>	0.22 ± 0.16 <sup>c</sup>
DG	7.14 ± 0.57 <sup>d</sup>	5.88 ± 0.47 <sup>de</sup>	4.72 ± 0.17 <sup>ef</sup>	3.74 ± 1.05 <sup>fg</sup>

FFA, free fatty acid; MG, monoglyceride; and TG, triglyceride.

<sup>a-e</sup> Values with the same superscripts in each row for each enzyme type have no significant difference ( $p > 0.05$ ).

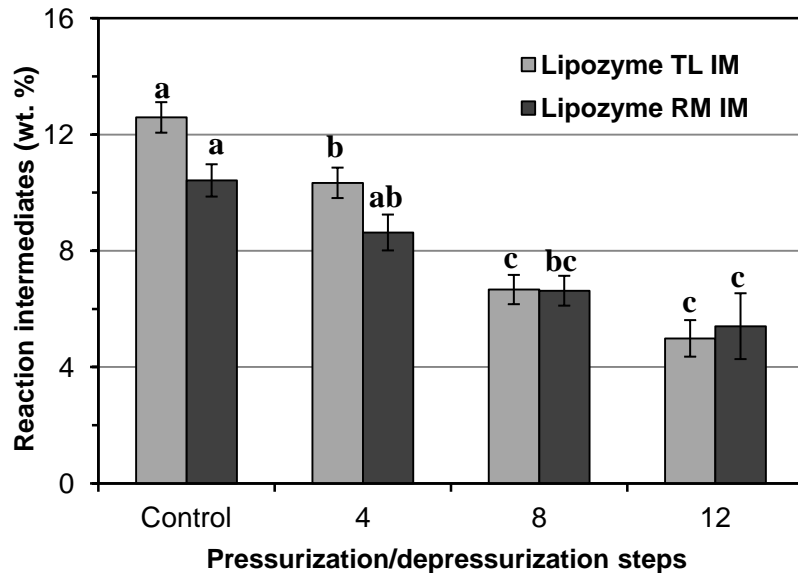


**Figure 5-5.** The effect of pressurization/depressurization cycles of Lipozyme TL IM and RM IM under  $\text{SCCO}_2$  at  $65^\circ\text{C}$  and 17.5 MPa on total amount of produced intermediates during interesterification of canola oil and fully-hydrogenated canola oil (70:30 w/w) under  $\text{SCCO}_2$  at the same conditions for 2 h. The interesterification with untreated enzymes is considered as control treatment. Bars with the same letter in each enzyme type have no significant difference ( $p > 0.05$ ).

Pressurization/depressurization cycles are somewhat equivalent to repeated extraction of free water of enzymes because  $\text{SCCO}_2$  may dissolve from 0.3 to 0.5% (w/w) water, depending on pressure and temperature (Wimmer and Zarevucka, 2010). Pressurization/depressurization has greater effect on water removal compared to long exposure to  $\text{SCCO}_2$  because the enzyme is exposed to fresh  $\text{CO}_2$  at the beginning of each pressurization step and thus water solubilization and mass transfer of free water of enzyme into the supercritical phase are enhanced. Then, upon depressurization, the  $\text{CO}_2$  phase and dissolved water in it are removed from the system.

As discussed in Section 2.3.3.2, enzymes need a certain amount of bound water to maintain their activity and this is an important factor in biocatalysis in

non-aqueous media. If the water content of CO<sub>2</sub> is too high or water is formed as a reaction product, the moisture level can increase to a value where the enzyme is inactivated. However, it is difficult to strip off the bound water of the enzymes with SCCO<sub>2</sub> at moderate pressures and temperatures. The optimum water content of the enzymes depends on many parameters such as the types of enzyme, support material, and reaction media, as well as water content of the reactants, and operating temperature and pressure. For instance, the presence of disulfide bonds in both Lipozyme TL IM and RM IM increases thermal stability. Kasche et al. (1988) showed that enzymes with S-S bridges were denatured by partial unfolding after incubation in humid high pressure CO<sub>2</sub>. This was probably caused by the escape of CO<sub>2</sub> dissolved in the bound water around the protein during the depressurization step; however, the extent of denaturation was negligible after incubation in dry SCCO<sub>2</sub>. In contrast, enzymes without S-S bridges were rapidly denatured when depressurized after incubation in both humid and dry SCCO<sub>2</sub>. Therefore, they concluded that enzyme catalyzed reactions in supercritical fluids should be preferably conducted using enzymes with S-S bridges.

### **5.3.2.2. Effect of exposure time and pressurization/depressurization on enzyme structure**

In this study, the conformational and morphological structures of SCCO<sub>2</sub>-treated and untreated immobilized lipases were investigated by FTIR and FE-SEM, respectively. Also, any potential interaction between high pressure CO<sub>2</sub> and immobilized lipases was assessed by XPS analysis.

In the FTIR analysis of the untreated and SCCO<sub>2</sub>-treated immobilized lipases (Figure 5-6a, c), the amide I band (between 1600 and 1700 cm<sup>-1</sup>) is mainly associated with carbonyl stretching of the peptide (Collins et al., 2008). This band consists of a group of overlapped signals, providing information about the secondary protein structure of the enzyme. Amide II band centered around 1547 cm<sup>-1</sup> results from N-H bending vibration and C-N stretching vibration (Collins et al., 2008). Amide III bands (between 1200 and 1400 cm<sup>-1</sup>) are due to the in-phase combination of the NH deformation vibration with CN, with a minor contribution from CO and CC stretching (Collins et al., 2008).

These polypeptide bands are complex and do not allow a direct correlation with the protein structure (Collins et al., 2011). Therefore, the spectral data between 1600 and 1700 cm<sup>-1</sup> were taken and plotted again in Figure 5-6b, d after baseline correction and normalization.

There was no significant difference between the untreated immobilized lipases and the ones exposed to 12 pressurization/depressurization cycles. According to these results, no substantial conformational changes in the secondary structure of the immobilized lipases were observed after enzyme treatment with SCCO<sub>2</sub>. Likewise, Bauer et al. (2000) did not observe any conformational changes in the purified preparation of esterase EP10 using fluorescence spectroscopy after treatment with SCCO<sub>2</sub> at 15 MPa/75°C/24 h and 30 pressurization/depressurization cycles at 15 MPa and 35°C. Similar behaviour was also reported by Giessauf and Gamse (2000) with no chemical modification of the reactive groups of porcine pancreatic lipase after determination of free

amino groups, free –SH groups and carbonyl content as well as no changes in the maximum emission of tryptophan fluorescence emission spectra.

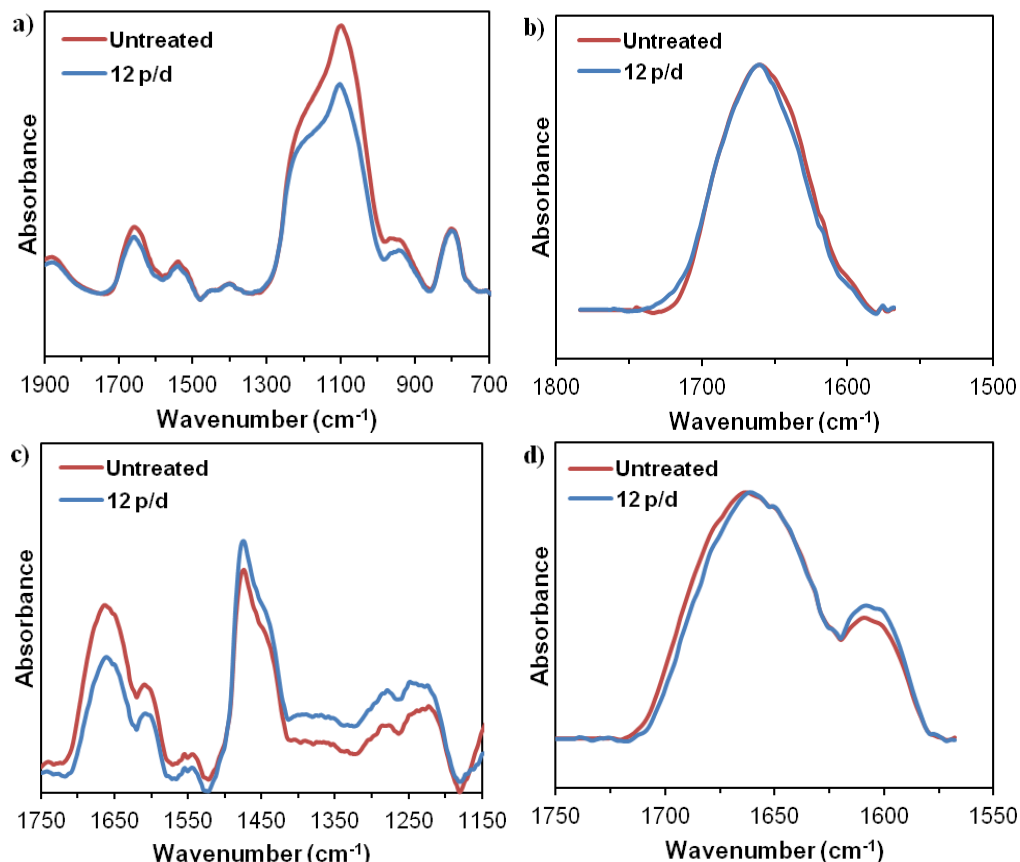


**Figure 5-6.** Infrared spectra of untreated and  $\text{SCCO}_2$ -treated Lipozyme RM IM and TL IM with 12 pressurization/depressurization cycles (12 p/d) at 17.5 MPa and 65°C in (a) and (c) and baseline corrected and normalized spectra in the region of amide I in (b) and (d): (a) and (b) represent Lipozyme TL IM; (c) and (d) represent Lipozyme RM IM.

The extreme condition of  $\text{SCCO}_2$  treatment (65°C, 17.5 MPa, and 12 pressurization/depressurization cycles) was chosen to observe any potential morphological changes compared to untreated immobilized lipases. The FE-SEM micrographs did not show any difference between treated and untreated

immobilized lipases (Fig. 5-7). These results confirm that the previously observed morphological changes in immobilized lipase, which was reused 4 times for interesterification (Fig. 5-4) were probably the result of mixing the substrates with enzyme inside the reactor with a magnetic stirrer and not due to pressurization/depressurization cycles.

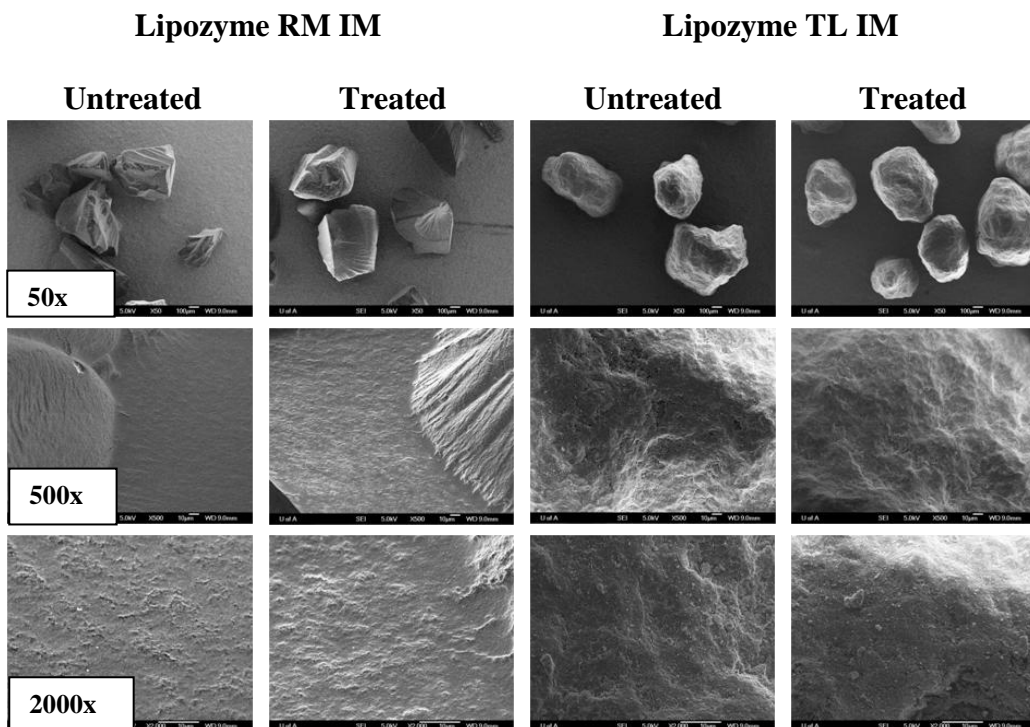


**Figure 5-7.** FE-SEM micrographs of immobilized lipases before and after 12 pressurization/depressurization cycles under  $\text{SCCO}_2$  at  $65^\circ\text{C}$  and 17.5 MPa.

It was shown that  $\text{CO}_2$  may form covalent complexes with the free amino groups on the surface of the enzyme (Kamat et al., 1995). These carbamates result in changes at lysine residues, and thus it could inhibit (or unpredictably affect) the enzyme. XPS results showed that the carbon to nitrogen ratios of untreated and

SCCO<sub>2</sub>-treated Lipozyme TL IM were 8.66 and 8.75, respectively, and those for Lipozyme RM IM were 6.42 and 7.03, respectively. These results suggest that there was no substantial change when both immobilized lipases were exposed to SCCO<sub>2</sub> at 65°C and 17.5 MPa for 12 h compared to untreated immobilized lipases; however, further research is needed to distinguish between potential interactions with the support material versus the enzyme.

#### **5.4. Conclusions**

The findings in this study demonstrate that both immobilized lipases studied, Lipozyme TL IM and RM IM, can be used to catalyze lipid interesterification in SCCO<sub>2</sub> media, without any loss of enzyme activity at typical conditions of temperature and pressure employed in many biotransformations. However, Lipozyme TL IM is more feasible than Lipozyme RM IM for interesterification of vegetable oils using SCCO<sub>2</sub> because of its much lower price and existing large scale production. During interesterification between canola oil and FHCO, the amount of reaction intermediates should be kept as low as possible because such hydrolysis products should be removed using downstream processes for producing base-stock for *trans*-free margarines, decreasing the overall yield of the interesterification process. Therefore, pre-treatment of immobilized lipases with SCCO<sub>2</sub> in order to reduce the amount of free water of enzymes could be beneficial to minimize the extent of hydrolysis and increase the overall yield of interesterification.

## 5.5. References

- Bauer, C., Steinberger, D.J., Schlauer, G., Gamse, T. and Marr, R. (2000). Activation and denaturation of hydrolases in dry and humid supercritical carbon dioxide (SC-CO<sub>2</sub>). *Journal of Supercritical Fluids*, **19** (1): 79-86.
- Collins, N.J., Leeke, G.A., Bridson, R.H., Hassan, F. and Grover, L.M. (2008). The influence of silica on pore diameter and distribution in PLA scaffolds produced using supercritical CO<sub>2</sub>. *Journal of Materials Science: Materials in Medicine*, **19** (4): 1497-1502.
- Collins, S.E., Lassalle, V. and Ferreira, M.L. (2011). FTIR-ATR characterization of free *Rhizomucor meihei* lipase (RML), Lipozyme RM IM and chitosan-immobilized RML. *Journal of Molecular Catalysis B: Enzymatic*, **72** (3-4): 220-228.
- Combe, N., Clouet, P., Chardigny, J.M., Lagarde, M. and Leger, C.L. (2007). *Trans* fatty acids, conjugated linoleic acids, and cardiovascular diseases. *European Journal of Lipid Science and Technology*, **109** (9): 945-953.
- de Roos, N.M., Schouten, E.G., Scheek, L.M., van Tol, A. and Katan, M.B. (2002). Replacement of dietary saturated fat with *trans* fat reduces serum paraoxonase activity in healthy men and women. *Metabolism-Clinical and Experimental*, **51** (12): 1534-1537.
- Giessauf, A. and Gamse, T. (2000). A simple process for increasing the specific activity of porcine pancreatic lipase by supercritical carbon dioxide treatment. *Journal of Molecular Catalysis B-Enzymatic*, **9** (1-3): 57-64.
- Habulin, M. and Knez, Z. (2001). Activity and stability of lipases from different sources in supercritical carbon dioxide and near-critical propane. *Journal of Chemical Technology and Biotechnology*, **76** (12): 1260-1266.
- Hlavsova, K., Wimmer, Z., Xanthakis, E., Bernasek, P., Sovova, H. and Zarevucka, M. (2008). Lipase activity enhancement by SC-CO<sub>2</sub> treatment. *Zeitschrift fur Naturforschung - Section B Journal of Chemical Sciences*, **63** (6): 779-784.
- Jessop, P.G. and Subramaniam, B. (2007). Gas-expanded liquids. *Chemical Reviews*, **107** (6): 2666-2694.
- Kamat, S.V., Beckman, E.J. and Russell, A.J. (1995). Enzyme activity in supercritical fluids. *Critical Reviews in Biotechnology*, **15** (1): 41-71.
- Kasche, V., Schlothauer, R. and Brunner, G. (1988). Enzyme denaturation in supercritical CO<sub>2</sub>: Stabilizing effect of s-s bonds during the depressurization step. *Biotechnology Letters*, **10** (8): 569-574.

Laudani, C.G., Habulin, M., Knez, Z., Della Porta, G. and Reverchon, E. (2007). Immobilized lipase-mediated long-chain fatty acid esterification in dense carbon dioxide: Bench-scale packed-bed reactor study. *Journal of Supercritical Fluids*, **41** (1): 74-81.

Marangoni, A.G. and Rousseau, D. (1995). Engineering triacylglycerols: The role of interesterification. *Trends in Food Science & Technology*, **6**: 329-335.

Oliveira, D., Fehrmann, A.C., Rubira, A.F., Kunita, M.H., Dariva, C. and Oliveira, J.V. (2006). Assessment of two immobilized lipases activity treated in compressed fluids. *Journal of Supercritical Fluids*, **38** (3): 373-382.

Rezaei, K. and Temelli, F. (2000). Lipase-catalyzed hydrolysis of canola oil in supercritical carbon dioxide. *Journal of the American Oil Chemists Society*, **77** (8): 903-909.

Seifried, B. and Temelli, F. (2010). Unique properties of carbon dioxide-expanded lipids. *INFORM - International News on Fats, Oils and Related Materials*, **21** (1): 10-12.

Subramaniam, B. (2010). Gas-expanded liquids for sustainable catalysis and novel materials: Recent advances. *Coordination Chemistry Reviews*, **254** (15-16): 1843-1853.

Wimmer, Z. and Zarevucka, M. (2010). A review on the effects of supercritical carbon dioxide on enzyme activity. *International Journal of Molecular Sciences*, **11** (1): 233-253.

Xu, X. (2003). Engineering of enzymatic reactions and reactors for lipid modification and synthesis. *European Journal of Lipid Science and Technology*, **105**: 289-304.

## **6. Lipase-catalyzed interesterification between canola oil and fully-hydrogenated canola oil in contact with supercritical carbon dioxide: optimization and physicochemical properties of products<sup>1</sup>**

### **6.1. Introduction**

Partial hydrogenation of vegetable oils for the production of base-stock for margarine and shortening leads to the formation of *trans*-fatty acids which are known to increase the risk of cardiovascular diseases. Therefore, considerable effort has been spent to find suitable alternative methods to produce *trans*-free base-stocks for various food applications. One alternative method is blending of a fully-hydrogenated oil rich in tristearin with a vegetable oil rich in triolein, followed by chemical or enzymatic interesterification (Gavriilidou and Boskou, 1991; List et al., 1995; Seriburi and Akoh, 1998; Ahmadi et al., 2008). In enzymatic interesterification, using regiospecific (1,3- or 2- specific) and fatty acid specific lipases as catalysts, the positioning of acyl groups on the glycerol back bone of triglycerides (TG) is controlled and a desired acyl group can be guided to a specific position. This results in products with predictable composition in contrast to chemical interesterification. Therefore, enzymatic interesterification with lipases of different properties is becoming more attractive

---

<sup>1</sup> A version of this chapter has been submitted to *Food Chem.* for consideration for publication. Jenab E., Temelli F. and Curtis, J.M. (2012). Lipase-catalyzed interesterification between canola oil and fully-hydrogenated canola oil in contact with supercritical carbon dioxide.

to convert some commodity oils such as soya bean oil, rape seed oil, lard, tallow, etc. to high value products and modified fats (Macrae, 1983; Miller et al., 1991; Liua et al., 1997; Xu, 2003).

Sustainable technologies have emerged in lipid processing because of strict environmental regulations related to the use of organic solvents as well as the increase in consumer demand for ‘natural’ products (Seifried and Temelli, 2010b). Supercritical CO<sub>2</sub> (SCCO<sub>2</sub>) as discussed in Section 2.1 can be an alternative to organic solvents. As well, SCCO<sub>2</sub> because of its numerous advantages can be used as reaction media in biocatalysis reactions (Section 2.3).

The solubility of triglycerides in SCCO<sub>2</sub> at moderate temperatures and pressures are relatively low, but it is still possible to benefit from the properties of SCCO<sub>2</sub> by dissolving it in the liquid lipid phase. As pressure is increased, CO<sub>2</sub> dissolves in the liquid lipid phase and lipids saturated with CO<sub>2</sub> under moderate pressure expand in volume and their physical properties like viscosity, density, and interfacial tension change substantially in a way to enhance mass transfer properties (Seifried and Temelli, 2009, 2010a; Seifried and Temelli, 2011).

Studying the effect of processing parameters on interesterification of CO<sub>2</sub>-expanded (CX) canola oil and fully-hydrogenated canola oil (FHCO) is important to find the optimal reaction conditions and for better understanding of interesterification under SCCO<sub>2</sub>. As well, the physicochemical properties of the final products should be investigated to assess whether their properties are suitable for product applications. Several studies have reported the enzymatic interesterification of oils under SCCO<sub>2</sub> for producing cocoa butter analog

(Shekarchizadeh et al., 2009) and structured lipids (Kim et al., 2004), and interesterification of vegetable oils by fatty acids (Yu et al., 1992; Liang et al., 1998). However, the literature lacks information on the enzymatic interesterification of canola oil and FHCO under  $\text{SCCO}_2$  and the physicochemical properties of the final products. Therefore, the objectives of this study were: (a) to determine the effects of enzyme load, pressure, and the ratio of initial reactants on the degree of interesterification under  $\text{SCCO}_2$ , (b) to determine the chemical composition of substrates and interesterified products, and (c) to assess the physical properties such as melting behaviour and solid fat content of the initial blends and products obtained at optimal reaction conditions.

## 6.2. Materials and methods

### 6.2.1. Materials

Lipozyme TL IM, with the specifications provided in Section 5.2.1, was used for the interesterification between canola oil and FHCO. Specifications and fatty acid composition of FHCO and canola oil were described in Section 4.2.1.

$\text{CO}_2$  (bone dry, Syphon UN 1013 Class 2.2) and  $\text{N}_2$  (extra dry, UN 1046 Class 2.2) were purchased from Praxair Canada Inc. (Mississauga, ON, Canada). All analytical grade solvents were from Fisher Scientific (Ottawa, ON, Canada) and GC and HPLC lipid standards and internal standards were purchased from Nu-Chek Prep Inc. (Elysian, MN, USA).

## 6.2.2. Process optimization

### 6.2.2.1. Experimental set up and reaction protocols

Lipase-catalyzed interesterification of CX canola oil and FHCO was conducted in batch mode using a Nova Swiss (Nova-Werke AG, Effretikon, Switzerland) high pressure, electrically heated, magnetically stirred 200 mL autoclave setup shown in Figure 6-1. Lipozyme TL IM (2, 6, and 10%, w/v of initial reactants) was loaded inside the vessel, which was heated to around 65 °C in order to have FHCO in the molten form. A total volume of 70 mL of substrates, consisting of canola oil and FHCO blend prepared at different ratios (10, 30, 50 wt.% FHCO) was added to the autoclave using a syringe.

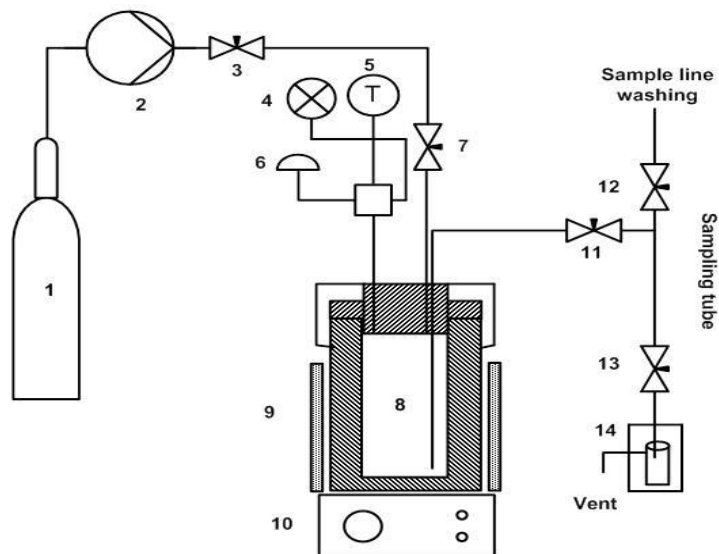


**Figure 6-1.** High pressure batch stirred reactor: 1, CO<sub>2</sub> cylinder; 2, Syringe pump; 3, 7, 11, 12, and 13, Shut-off valve; 4, Pressure gauge; 5, Temperature controller; 6, Rupture disk; 8, High pressure vessel; 9, Heating Jacket; 10, Stirrer; 14, Collector.

Once the autoclave was sealed, it was gently purged with CO<sub>2</sub> and then the autoclave was pressurized to 10, 17.5 and 25 MPa using a syringe pump (Model 260D, Teledyne Isco, Lincoln, NE, USA). After reaching stable temperature and pressure the magnetic stirrer was turned on. The sampling tube was filled with the reaction mixture ( $\leq 0.2$  mL) from the bottom of the vessel using a dip tube with a filter at the end after closing valves 12 and 13 and opening the valve 11. The sampling port made sample collection possible without significantly affecting the temperature and pressure inside the autoclave. During sample collection, the sampling tube was first washed by injecting hot hexane through the washing port to remove any residual material left and then dried by blowing air prior to taking the next sample. The samples were taken during 6-7.5 h of reactions.

In order to see the effect of CO<sub>2</sub> pressure, interesterification of canola oil and FHCO at optimal enzyme load and oil ratio was also conducted at atmospheric pressure using the same reactor under a blanket of N<sub>2</sub>. In this case, the samples were taken at different time intervals throughout the 8 h of reaction using a syringe through one outlet port of the reactor after stopping the stirrer for 1 min to let the immobilized enzymes settle at the bottom of the cell.

The prepared oil mixtures and the enzymes were kept in a desiccator at 4-5 °C to prevent further moisture absorption. The reaction products, blanketed with nitrogen, were kept at -20 °C prior to analysis.

### 6.2.2.2. Determination of degree of interesterification

The degree of interesterification between canola oil and FHCO was defined as the number of moles of 1,3-distearoyl-2-oleoyl-glycerol (SOS), 2,3-dioleoyl-1-stearoyl-glycerol (SOO), 1-linoleoyl-2-oleoyl-3-stearoyl-glycerol (LOS) and their isomers as major TG products of the reaction over the number of moles of initial substrates (Eq. (6.1)). The number of moles of initial substrates was calculated by considering the average molecular weight of the blends using the fatty acid profiles of canola oil and FHCO blend determined previously by GC analysis (Table 4-1).

$$\text{Degree of interesterification (\%)} = \frac{[\text{SOS}]_{\text{mol}} + [\text{SOO}]_{\text{mol}} + [\text{LOS}]_{\text{mol}}}{[\text{initial substrates}]_{\text{mol}}} \times 100 \quad (6.1)$$

Specific TG components (SOS, SOO, LOS) of the products were quantified by HPLC/APPI-MS using an Agilent 1200 liquid chromatograph (Agilent Technologies, Palo Alto, CA, USA) coupled to a Q star Elite mass spectrometer (Applied Biosystems/MDS Sciex; Concord, ON, Canada) with a photospray<sup>TM</sup> photoionization source. Toluene as a dopant was delivered by an isocratic HPLC pump (Agilent Technologies, Palo Alto, CA, USA) at a flow rate of 20  $\mu\text{L min}^{-1}$ . Analyst QS 2.0 software was used for data acquisition and analysis. Sample solution (100  $\mu\text{L}$ ) in chloroform (0.25-0.5 mg/mL) was mixed with 100  $\mu\text{L}$  trinonadecanoic acid solution in chloroform (20  $\mu\text{g/mL}$ ) as internal standard, and then 10  $\mu\text{L}$  of the mixture was autoinjected into the HPLC system. TG were separated using an Ascentis C18 column (15 cm  $\times$  2.1 mm, 3  $\mu\text{m}$ ) (Supelco, Bellefonte, PA,

USA). A binary gradient system of acetonitrile and isopropanol was used at a flowrate of  $0.2 \text{ mL min}^{-1}$ . Gradient elution profile started with 80% acetonitrile and 20% isopropanol, changed to 10% acetonitrile and 90% isopropanol in 27 min, then to 80% acetonitrile and 20% isopropanol in 4 min and held for 7 min. In order to obtain the calibration curves for triolein (OOO), tristearin (SSS), SOS, and SOO, standards at concentrations of 0.625, 1.25, 2.5, 5, 12.5, 25, 37.5, and 50  $\mu\text{g/mL}$  containing the internal standard at a concentration of 0.01  $\mu\text{g/mL}$  were injected into the column.

The reactions at each condition were conducted at least in three replicates.

### **6.2.3. Characterization of the products**

#### **6.2.3.1. Reaction protocol**

To determine the physicochemical properties of the final products obtained at optimal conditions, interesterification was conducted in the same high pressure batch stirred reactor described previously (Fig. 6-1). At the end of the 2 h reaction, the reactor was depressurized and opened and the interesterified product was collected after settlement of immobilized enzymes for further analysis. The batch of Lipozyme TL IM used in this reaction was previously dried with  $\text{SCCO}_2$  at  $65^\circ\text{C}/20 \text{ MPa}$  for 5 h at a flow rate of  $1.5 \text{ L min}^{-1}$  (measured at ambient conditions) in order to reduce its moisture content and consequently the amount of reaction intermediates (specifically hydrolysis products) in the final products. This treatment was necessary based on the results of our previous study presented in Section 5.3.2.1, which demonstrated that the formation of hydrolysis products

can be reduced by decreasing the amount of water present in the original enzyme. For this purpose, a laboratory scale supercritical fluid extraction system (Newport Scientific, Inc., Jessup, MD) was used. Around 40 g of Lipozyme TL IM was loaded in a stainless steel basket, which was placed in a 300 mL extraction cell. The details of the extraction system and its operation can be found elsewhere (Dunford and Temelli, 1995). The reactions at each condition were conducted at least in two replicates.

#### **6.2.3.2. Purification of the reaction products**

In order to determine the physicochemical properties of the interesterified products to assess their potential in final product formulations, the amount of reaction intermediates should be minimized. The extraction of free fatty acids from fatty materials using solvents has a long history and it has been shown that, in principle, this process is feasible using short-chain alcohols as solvent, especially ethanol (Rodrigues et al., 2007). Ethanol has low toxicity and high selectivity for free fatty acids and can be recovered easily in the process (Rodrigues et al., 2007). Therefore, the reaction products were purified by washing 7 times with ethanol, containing around 7% water at 50 °C with solvent-to-oil ratio of 1.2-1.3 using a separatory funnel (Rousseau and Marangoni, 1998; Rodrigues et al., 2007). Residual traces of ethanol were removed by using a rotary. The amounts of reaction intermediates in the purified samples were analyzed to check the efficiency of the purification procedure.

### **6.2.3.3. Determination of the reaction intermediates**

The amounts of reaction intermediates, including free fatty acids (FFA), monoglycerides (MG), and diglycerides (DG) in the initial blends and reaction products before and after purification were quantified by injection of silylated samples into an automatic ‘cool on column’ injection gas chromatograph equipped with flame ionization detector. The details of this method were described in Section 5.2.4.

### **6.2.3.4. Determination of the triglyceride composition**

TG profiles of the initial blends and enzymatically interesterified samples were analyzed using a reversed-phase high-performance liquid chromatograph (RP-HPLC) (Varian ProStar, Varian Inc., Walnut Creek, CA, USA) equipped with an evapourative light scattering detector (ELSD) (2000 ES, Alltech Associates Inc., Deerfield, IL, USA) operated at 50 °C with a nitrogen flow rate of 2 L/min. Aliquots of sample solutions (10 µL) in chloroform (1-2 mg/mL), containing 0.1 mg/mL triarachidin as internal standard were injected onto Varian Microsorb-MV-100-5 C18 column (250×4.6 mm). A binary gradient system of acetonitrile and dichloromethane was used at a flow rate of 1 mL/min. Gradient elution started with 65% acetonitrile and 35% dichloromethane and held for 25 min, changed to 20% acetonitrile/80% dichloromethane in 1 min and held for 2 min, programmed to 65% acetonitrile/35% dichloromethane in 1 min and held for 6 min. Triglycerides were identified by comparison of the retention data with

authentic standards, including relative retention time calculated using triolein as reference.

#### **6.2.3.5. Melting characteristics**

Differential scanning calorimetry (DSC) (Q100, TA Instruments, New Castle, DE, USA) was used to determine the melting and crystallization behaviours of initial blends and interesterified products. A sample (5-7 mg) was hermetically sealed in an aluminum pan, with an empty pan serving as a reference. Analysis was performed according to the AOCS official method Cj 1-94 (AOCS, 2009). Briefly, the sample was initially heated rapidly from room temperature to 80 °C and held for 10 min to erase the crystal memory; cooled to -60 °C at 10 °C/min and held for 30 min; then heated to 80 °C at 5 °C/min to determine the crystallization and melting profiles.

#### **6.2.3.6. Solid fat content**

The solid fat contents (SFC) of canola oil and FHCO blend before and after interesterification in equilibrium with high pressure CO<sub>2</sub> were measured at temperatures between 10 and 60 °C. For this purpose, the minispec mq20 NMR analyzer (Bruker, Milton, ON, Canada) was used according to the AOCS official method Cd 16b-93 (AOCS, 2009). Briefly, the test sample was melted at 100 °C and stored for 15 min at 100 °C, at least 5 min at 60 °C, then 60 ± 2 min at 0 °C, and then for 30-35 min at each chosen measuring temperature between 10 and 60 °C.

## **6.3. Results and discussion**

### **6.3.1. Effect of reaction parameters on degree of interesterification**

The interesterification reaction between canola oil and FHCO in the presence of an immobilized lipase was optimized with respect to various reaction parameters like enzyme concentration, pressure, and substrate blend ratio with the objective of maximizing degree of interesterification.

The effect of Lipozyme TL IM addition at 2, 6, and 10% (w/v of initial substrates) level on the degree of interesterification between canola oil and FHCO (70:30, w/w) was studied at 65 °C and 17.5 MPa. As shown in Figure 6-2, the degree of interesterification reached its equilibrium level of about 25-26% in about 1 h for enzyme loads of 6 and 10%, but it required more than 4 h when the enzyme load was 2%. Based on these results, enzyme load of 6% was selected for the next set of reactions, to assess the effects of pressure and substrate ratio on the degree of interesterification. Sun et al. (2012) studied the effect of enzyme loading of Lipozyme TL IM on the formation of octanoic acid esters during the alcoholysis of coconut oil with fusel alcohols. They found that the optimum enzyme load was 5-15% (w/w of initial substrates) and a further increase in the enzyme amount caused a decrease in the amount of octanoic acid esters produced. Such a reduction in conversion was due to the higher viscosity of the reaction medium with the addition of higher amounts of enzyme, resulting in less effective transfer of the substrates to the active sites of the enzyme (Yadav and Trivedi, 2003).

As demonstrated in our previous studies (Chapters 3 and 4), the quantity of CO<sub>2</sub> solubilized in the liquid lipid phase and consequently the mixture viscosity are a strong function of pressure. An 80-90% drop in viscosity was obtained by increasing the pressure from atmospheric pressure up to 10 MPa. Therefore, the pressure of CO<sub>2</sub> can influence the mass transfer properties of substrates in such a reaction mixture and thus the reaction rate.

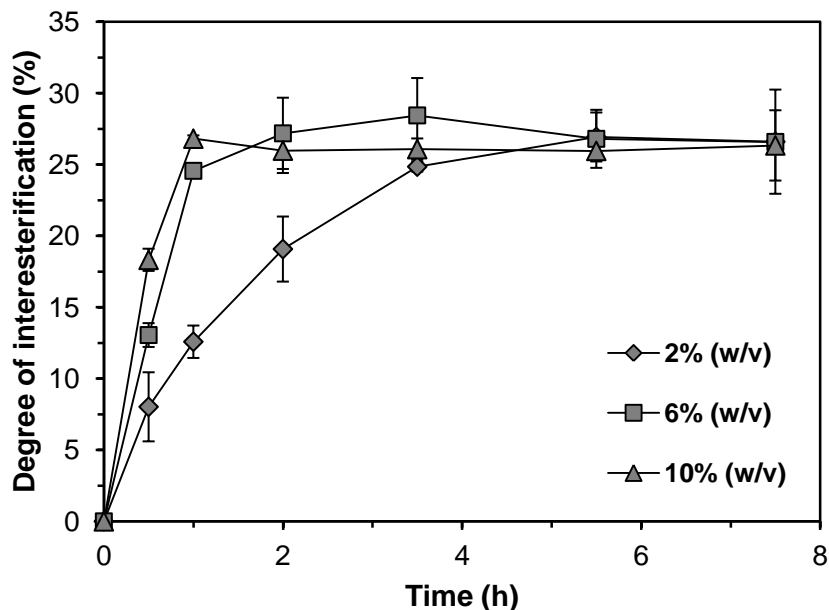


**Figure 6-2.** Effect of Lipozyme TL IM load (w/v of initial substrates) on the degree of interesterification between canola oil and fully-hydrogenated canola oil (FHCO) (70:30, w/w) in contact with SCCO<sub>2</sub> at 65 °C and 17.5 MPa over 7.5 h.

In an effort to assess the effect of pressure, the lipase-catalyzed interesterification of CX-canola oil and FHCO (70:30, w/w) at 65 °C and enzyme load of 6% (w/v of initial substrates) was conducted at 10, 17.5 and 25 MPa. The results shown in Figure 6-3 reveal that the degree of interesterification of the

reaction at equilibrium state decreases with an increase in pressure. This is probably due to the effect of pressure on the density of CX-lipids and the solubility of the reactants and products in the  $\text{SCCO}_2$  phase.

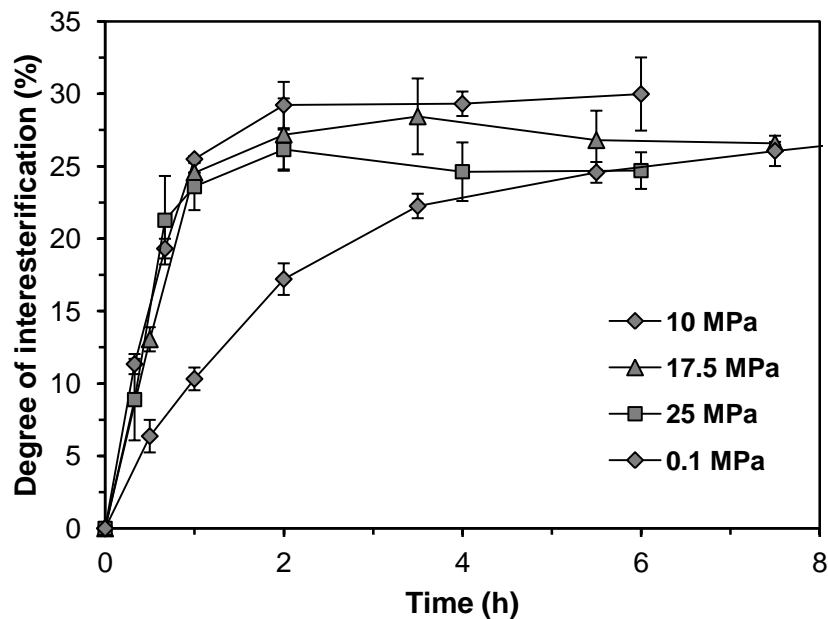


**Figure 6-3.** Effect of pressure on the degree of interesterification of lipase-catalyzed interesterification between canola oil and fully-hydrogenated canola oil (FHCO) (70:30, w/w) with Lipozyme TL IM at 6% (w/v) of initial substrates in contact with  $\text{SCCO}_2$  at 65 °C over 7.5 h.

The density of CX-lipids increases with pressure at constant temperature, causing a negative effect on mass transfer properties as discussed in Section 4.3.3. The solubility of TG in  $\text{SCCO}_2$ , especially triolein, increases with pressure, leading to a decrease in triolein concentration in the liquid lipid phase. As well, the solubility of  $\text{CO}_2$  in the liquid lipid phase increases with pressure, leading to dilution of substrates in the liquid phase. In addition, the phase behaviour of the reaction mixture is also influenced by pressure, resulting in changes in the

distribution of components between the liquid phase and the supercritical phase, which in turn impacts the degree of interesterification. It is interesting to note that the reaction conducted at atmospheric pressure still did not reach the equilibrium degree of interesterification after 6-7 h as opposed to 1-2 h at higher pressures, demonstrating the importance of the effect of CO<sub>2</sub> solubilization in the liquid lipid phase at higher pressures and consequently its positive influence on degree of interesterification. Laudani et al. (2007) investigated the effect of pressure on lipase-catalyzed synthesis of *n*-octyl oleate in SCCO<sub>2</sub> by varying the pressure between 8 and 30 MPa at 50 °C. They found that the reaction yield increased with pressure from 8 to 10 MPa and decreased with a further increase in pressure. Miller et al. (1991) also reported that the reaction rate of interesterification between trilaurin and myristic acid, catalyzed by lipase from *R. miehei* in SCCO<sub>2</sub> increased as pressure was increased from 8.3 to 11 MPa.

The effect of different ratios of canola oil and FHCO blends on degree of interesterification was studied at levels of 10, 30 and 50% (w/w) FHCO. Fats with high levels of trisaturated TG like FHCO are used widely in interesterification reactions to modify the physicochemical properties of an oil with a high level of triunsaturated TG (Ahmadi et al., 2008; Costales-Rodriguez et al., 2009). Triolein and dioleoyl-linoleoyl glycerol as the main TG in canola oil and tristearin as the main TG in FHCO are the main reactants from the initial substrates of the reaction under investigation. As observed in Figure 6-4, an increase in the amount of FHCO in the initial blend from 10 to 30% increased the degree of interesterification substantially but the change in conversion rate was marginal

with a further increase in FHCO from 30 to 50%. However, this does not mean that the final interesterified products have the same physicochemical properties because the specific TG components present dictate the final product properties. Therefore, the physicochemical properties of the products obtained using different blend ratios were evaluated in more detail.

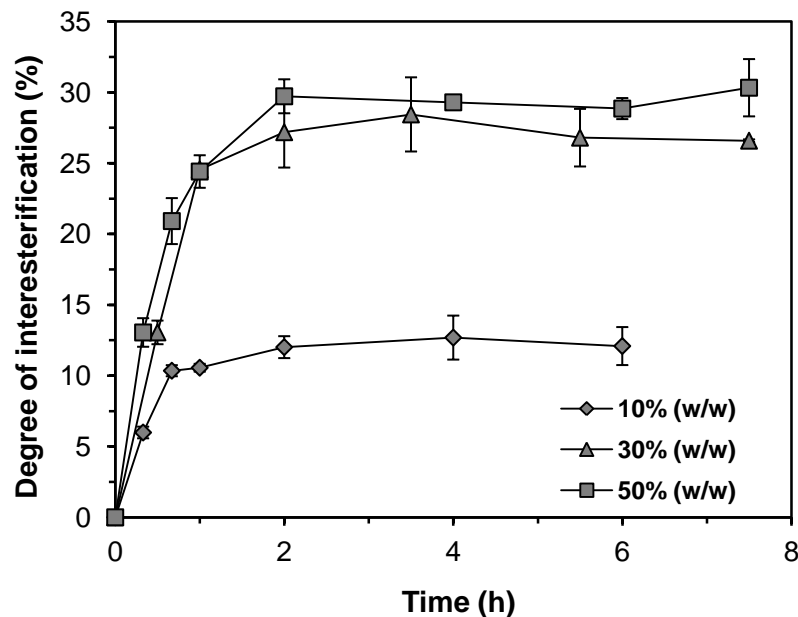


**Figure 6-4.** Effect of fully-hydrogenated canola oil (FHCO) ratio (% , w/w) in the blend of canola oil and FHCO on lipase-catalyzed interesterification in contact with  $\text{SCCO}_2$  at  $65^\circ\text{C}$  and 10 MPa over 7.5 h.

### 6.3.2. Physicochemical properties of the products

#### 6.3.2.1. Chemical composition of the products

The fatty acid composition of canola oil and FHCO as the initial substrates of interesterification was reported in Table 4-1, where canola oil had around 57%

oleic acid and the FHCO had around 90% stearic acid as their major fatty acids. The TG profiles of canola oil and FHCO are presented in Table 6-1. The major TG components of canola oil are OOO (49%) and LOO (30%) and those of FHCO are SSS (91%) and SSP (7%).

One issue in the enzymatically-Interesterified products is the presence of the reaction intermediates like FFA, MG and DG, which have impact on the quality of the final products. The amounts of these compounds are highly dependent on the amount of water present in the system.

**Table 6-1.** Triglyceride composition (% peak area) of canola oil and fully-hydrogenated canola oil (FHCO).<sup>a</sup>

Triglycerides <sup>b</sup>	Canola oil	FHCO
LnLO	2.8±0.1	-
LLO	4.5±0.1	-
LnOO	7.9±0.2	-
LOO	29.8±0.05	-
LOP	2.1±0.01	-
OOO	48.9±0.5	-
POO	2.8±0.05	-
PPP	0.4±0.01	
SOO	0.8±0.02	-
SSP	-	7.4±0.02
SSS	-	91.4±0.01
SSC20	-	1.2±0.03

<sup>a</sup> Mean±standard deviation based on at least two determinations.

<sup>b</sup> Ln, linolenic acid; L, linoleic acid; O, oleic acid; P, palmitic acid; S, stearic acid; SSC20, distearoyl-arachidic acid.

One way to decrease the amount of these undesirable compounds is the treatment of the enzyme in order to reduce its free moisture content. The moisture content of Lipozyme TL IM used in this study is around 5% (wt.%) (as determined in Section 5.2.1) and based on the information provided by the

manufacturer the essential moisture content for this enzyme to maintain its activity is 2-3% (wt.%). Therefore, to minimize the formation of hydrolysis products, the excess water of the enzyme was first extracted by  $\text{SCCO}_2$  and then the reactions were conducted using  $\text{SCCO}_2$ -treated enzyme at  $65\text{ }^\circ\text{C}/10\text{ MPa}$  for 2 h. The moisture content of Lipozyme TL IM was  $2.73\pm0.23\%$  (wt.%) after  $\text{SCCO}_2$  treatment. The amounts of FFA and DG formed during interesterification between canola oil and FHCO using the blend ratio of 70:30 (w:w, respectively) in equilibrium with  $\text{SCCO}_2$  using the untreated Lipozyme TL IM were  $3.94\pm0.63\%$  and  $7.84\pm0.13\%$ , respectively, after 2 h (Table 5-6). These amounts reduced to  $1.93\pm0.14\%$  and  $4.58\pm0.19\%$  for FFA and DG, respectively, where the  $\text{SCCO}_2$ -dried Lipozyme TL IM was used. However, these reduced amounts are still not sufficient to match the specifications of base-stocks used for margarine production and the samples required further purification because the oil used in margarines and shortenings should be of the highest quality, be as bland as possible, and freshly deodorized (Shulka, 2005). Therefore, reaction products were purified with ethanol to further reduce their FFA and DG contents.

Table 6-2 shows the amount of reaction intermediates in the non-interesterified initial blends (NIB), enzymatically interesterified product (EIP), and purified enzymatically interesterified product (PEIP). The total amount of reaction intermediates reduced to  $4.22\pm0.91\%$ ,  $5.24\pm0.23\%$  and  $4.52\pm0.38\%$  in the purified enzymatically interesterified products obtained using 10, 20, and 50% FHCO in the initial blend, respectively.

**Table 6-2.** Amounts of reaction intermediates (wt.%) of non-interesterified initial blends (NIB) of canola oil and fully-hydrogenated canola oil (FHCO) and enzymatically interesterified productss (EIP) and purified enzymatically interesterified products (PEIP) in contact with  $\text{SCCO}_2$  at 65 °C and 10 MPa after 2 h using  $\text{SCCO}_2$ -dried enzymes.<sup>a</sup>

Blend ratio	Reaction intermediates <sup>b</sup>	Treatments		
		NIB	EIP	PEIP
10% FHCO	FFA	0.68±0.00	3.38±0.47	0.46±0.09
	DG	3.03±0.64	8.20±0.88	3.78±0.82
	Total	3.71±0.64	11.58±1.35	4.22±0.91
30% FHCO	FFA	1.24±0.08	3.17±0.14	0.67±0.08
	DG	3.51±0.51	8.09±0.19	4.57±0.15
	Total	4.75±0.59	11.26±0.32	5.24±0.23
50% FHCO	FFA	1.63±0.03	3.63±0.17	0.57±0.11
	DG	4.31±0.58	10.20±0.46	3.95±0.27
	Total	6.11±0.69	14.04±0.64	4.52±0.38

<sup>a</sup> Mean±standard deviation based on at least two replications.

<sup>b</sup> FFA, free fatty acids and DG, diglycerides.

The TG composition of the interesterified products has a direct effect on their physical properties like melting and crystallization behaviours, solid fat content and rheological behaviour (Silva et al., 2009). TG composition of the NIB and PEIP obtained using  $\text{SCCO}_2$ -dried enzyme at 65 °C and 10 MPa for 2 h is presented in Table 6-3.

As expected, interesterification induced changes in the TG composition of the initial blends. The major TG components in the initial blends with low melting point (LOO and OOO) and high melting point (SSS) decreased after the reaction while new TG components such as LOS, SOO, and SOS having intermediate melting points between those of OOO and SSS were formed.

**Table 6-3.** Triglyceride composition (% peak area) of non-interesterified initial blends (NIB) of canola oil and fully-hydrogenated canola oil (FHCO) and purified enzymatically interesterified products (PEIP) obtained at 65 °C and 10 MPa after 2 h using  $\text{SCCO}_2$ -dried enzyme.<sup>a</sup>

Triglycerides <sup>b</sup>	10% FHCO		30% FHCO		50% FHCO	
	NIB	PEIP	NIB	PEIP	NIB	PEIP
LnLO	2.48±0.04	2.26±0.01	1.90±0.01	0.79±0.00	1.18±0.00	-
LLO	4.00±0.04	3.30±0.02	2.97±0.06	1.18±0.00	2.05±0.01	-
LnOO	6.88±0.15	6.84±0.00	4.99±0.09	2.38±0.02	3.21±0.04	-
LOO	27.01±0.16	24.50±0.25	19.43±0.08	10.87±0.05	12.77±0.11	2.32±0.26
LOP	1.90±0.01	-	1.66±0.06	-	1.10±0.05	-
(LOP+LLS+SOLn)	-	4.22±0.01	-	6.46±0.02	-	3.67±0.04
OOO	45.33±0.03	33.45±0.01	34.14±0.24	13.48±0.06	23.84±0.06	3.14±0.41
LOS	-	5.56±0.01	-	13.83±0.08	-	10.04±0.23
POO	2.63±0.01	2.41±0.15	2.39±0.06	2.26±0.05	1.78±0.02	0.95±0.06
PPP	-	-	-	-	-	-
PLS/SLnS	-	-	-	1.00±0.02	-	1.78±0.06
SOO	0.61±0.02	10.09±0.01	0.53±0.02	28.83±0.08	-	21.94±0.62
SSL	-	0.49±0.01	-	2.25±0.05	-	5.42±0.2
SOP	-	-	-	2.22±0.03	-	2.97±0.1
SOS	-	0.71±0.02	-	12.30±0.04	-	34.16±0.83
SSP	0.39±0.03	-	2.42±0.04	0.63±0.01	2.74±0.02	2.07±0.07
SSS	8.56±0.31	-	28.76±0.24	1.56±0.02	43.63±0.71	11.78±1.06
SSC20	-	-	0.52±0.05	-	0.61±0.03	-

<sup>a</sup> Mean±standard deviation based on at least two replications.

<sup>b</sup> Ln, linolenic acid; L, linoleic acid; O, oleic acid; P, palmitic acid; S, stearic acid; SSC20, distearoyl-arachidic acid.

These results are in good agreement with the findings of other studies (Seriburi and Akoh, 1998; Ahmadi et al., 2008). For example, Seriburi and Akoh (1998) studied the interesterification of triolein and tristearin at different molar ratios as the total amount of new TG (SOS+SOO) formed increased to 70% after enzymatic interesterification of triolein and tristearin at equimolar concentrations for 24 h at 55 °C.

### **6.3.2.2. Melting and crystallization behaviour**

DSC provides information about the amount of energy exchanged for melting and crystallization of fats and oils. Fat melting is an endothermic process in which energy is absorbed, whereas crystallization is an exothermic process in which energy is released (Ribeiro et al., 2009a). Depending on the TG composition and the method employed for DSC analysis, fats and oils exhibit complicated thermal behaviour.

Three peaks were observed in the melting profile of FHCO (Fig. 6-5) at temperatures of 48.96 °C ( $\Delta H=9.49 \text{ J/g}$ ), 60.35 °C ( $\Delta H=110.78 \text{ J/g}$ ) and 65.81 °C ( $\Delta H=2.86 \text{ J/g}$ ). These peaks correspond to the  $\alpha$ -to- $\beta'$ ,  $\beta'$ -to- $\beta$  and  $\beta$ -to-liquid transitions (Seriburi and Akoh, 1998; Ahmadi et al., 2008).

In the melting profile of canola oil (Fig. 6-5a), it was not possible to obtain sharp and resolved peaks because of the presence of different TG components. However, for triolein, which is the main TG component of canola oil, Seriburi and Akoh (1998) observed two peaks at -15.2 °C and -2.4 °C corresponding to  $\beta_3'$  and  $\beta_1'$ , respectively.

The DSC of initial blends and the interesterified products showed that the peak associated with the FHCO portion of the initial blends completely disappeared in the interesterified products (Fig. 6-5a). After interesterification, new peaks appeared in between the peaks related to canola oil and FHCO. These new peaks corresponded to the new TG components formed during the reaction like dioleoyl-stearoyl, stearoyl-oleoyl-linoleoyl, distearoyl-oleoyl glycerol and their isomers.

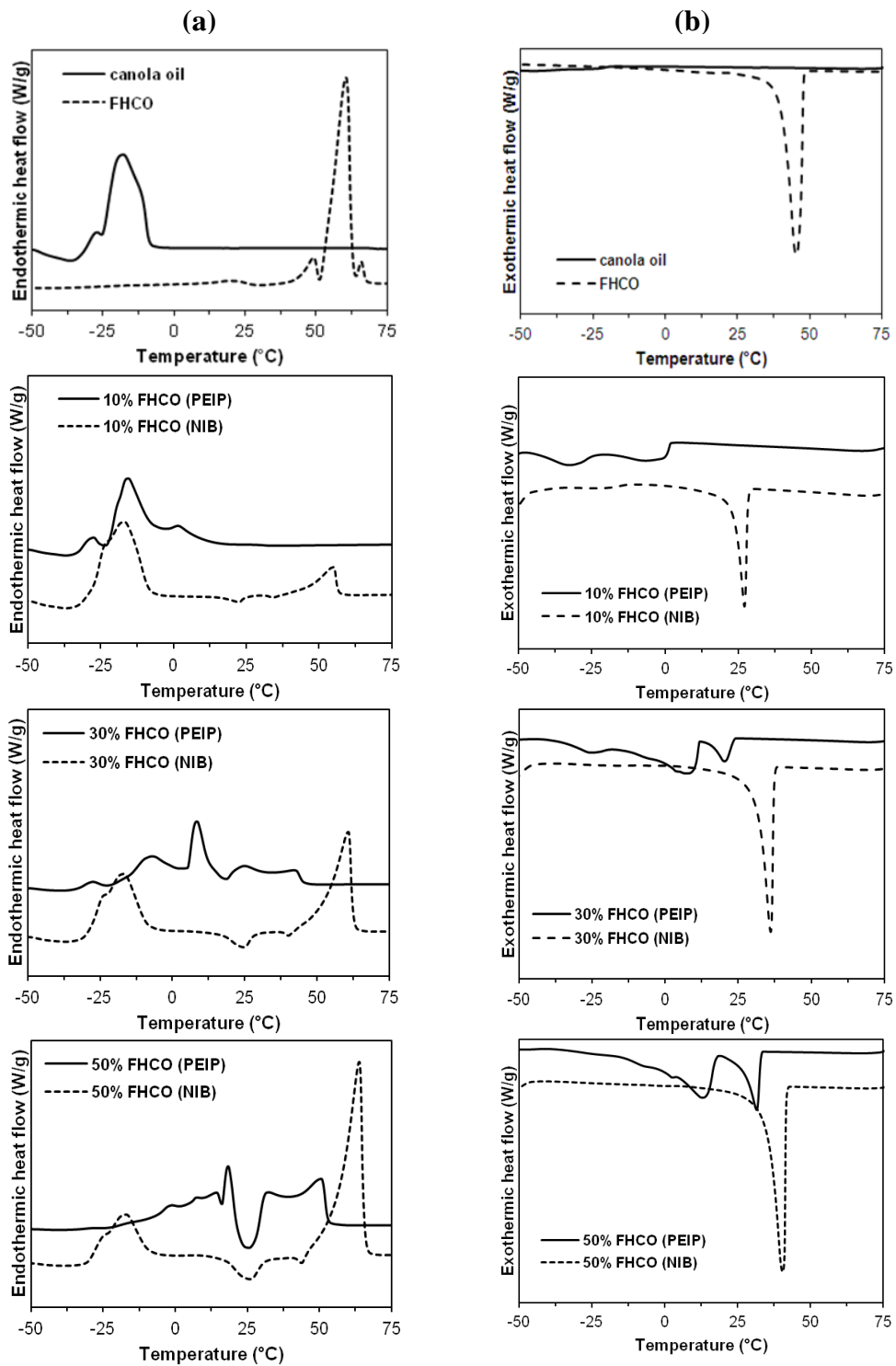


**Figure 6-5.** DSC of canola oil, fully hydrogenated canola oil (FHCO), their non-interesterified initial blends (NIB) and purified enzymatically interesterified products (PEIP) in contact with  $\text{SCCO}_2$  at 65 °C and 10 MPa after 2 h using  $\text{SCCO}_2$ -dried enzyme: (a) melting profile and (b) crystallization profile.

The newly formed peaks in the products were much broader than the peaks in the initial blends due to the formation of various TG components after interesterification. As the ratio of FHCO in the initial blend increased, the peaks for the lower melting polymorphs shifted towards higher melting ranges (Fig. 6-5a). The sharpest peak at the high melting region in the blend with 10% FHCO shifted from 54.98 °C ( $\Delta H=13.66$  J/g) to 63.74 °C ( $\Delta H=82.88$  J/g) in the blend with 50% FHCO.

In the crystallization thermographs of initial blends, a single peak can be seen (Fig. 6-5b), which is related to FHCO, containing mainly high melting tristearin. The peak crystallization temperatures, referring to the temperature at which the biggest proportion of lipid species crystallizes with maximum thermal effect, were 27.15, 36.20, 40.51, and 45.22 °C in the initial blends with 10, 30, and 50% FHCO and pure FHCO, respectively.

These data showed that the peak crystallization temperature increased with an increase in the proportion of hard fat blended with canola oil. Also, the crystallization enthalpy increased from 10.64 J/g in the initial blend with 10% FHCO to 59.10 J/g in the blend with 50% FHCO and 138.8 J/g in FHCO. These results confirmed the results of Humphrey et al. (2003), which showed that an increase in the number of molecules with simultaneous crystallization leads to a larger energy release by the system. Enzymatic interesterification resulted in the appearance of other peaks in the crystallization thermograms (Fig. 6-5b), which is characteristic of the increase in the middle-melting-point TG (SSO, SOO, and LOS) content due to the exchange of acyl groups between TG. The onset

crystallization temperatures decreased from 28.27 °C in 10% FHCO to 1.81 °C, from 37.27 °C in 30% FHCO to 23.50 °C and from 41.64 °C in 50% FHCO to 33.01 °C after enzymatic interesterification. These results are in good agreement with those of Ribeiro et al. (2009b) who studied the effect of chemical interesterification between canola oil and fully-hydrogenated cotton seed oil blend on crystallization behaviour.

### **6.3.2.3. Solid fat content**

SFC is the percentage of lipids present in a product in solid form at various temperatures and the values are important to evaluate the suitability of fat and oil mixtures for use in margarine or shortening formulations. The amount of SFC at specific temperatures is related to the rheological behaviour of the formulation at the time of packaging, storing and consuming. For instance, the SFC at 35 °C reflects the melting behaviour in the mouth; therefore, the SFC of the blends used for margarines should be as low as possible to avoid any sandy or coarse texture in the mouth (Costales-Rodriguez et al., 2009). The SFC of NIB and PEIP is displayed in Figure 6-6 as a function of temperature.

SFC increased substantially with an increase in the amount of FHCO in the initial blends because of the increase in the amount of high melting tristearin (Fig. 6-6). In the initial blends, a noticeable reduction in the amount of solid started at temperatures above 40 °C. However, enzymatic interesterification considerably decreased the solid fat content of interesterified products compared to the initial

blends at different temperatures studied except for 50% FHCO in which the SFC at 10 °C was almost the same before and after interesterification.

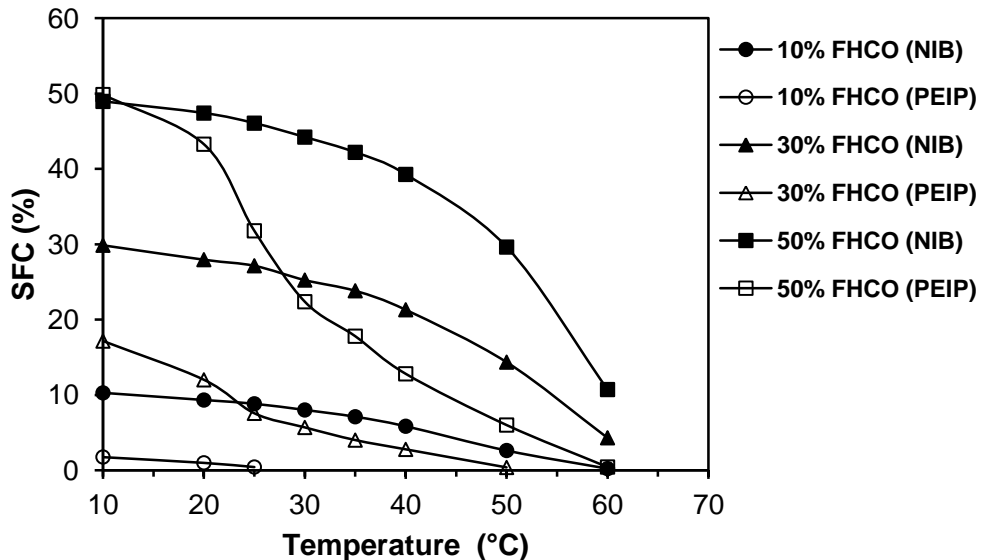


**Figure 6-6.** SFC evolution of non-interesterified initial blends (NIB) of canola oil and fully-hydrogenated canola oil (FHCO) and purified enzymatically interesterified products (PEIP) of canola oil and FHCO in contact with  $\text{SCCO}_2$  at 65 °C and 10 MPa after 2 h using  $\text{SCCO}_2$ -treated enzyme.

The presence of high melting tristearin in the initial blends resulted in higher SFC of the samples at different temperatures while in enzymatically interesterified products high melting tristearin was converted to low and medium melting point TG, causing a remarkable decrease in the SFC. The lowest SFC belonged to the enzymatically interesterified product of 10% FHCO blend in which the SFC was less than 0.5%, or the product was in liquid form, at 25 °C. The results of this study showing that the SFC of enzymatically interesterified products were lower than those of the initial blends at all studied temperatures was in good agreement with the results of other studies (Petrauskaitė et al., 1998;

Rodriguez et al., 2001; Silva et al., 2009), except for Ahmadi et al. (2008) who indicated that the chemically and enzymatically interesterified samples of high-oleic sunflower oil and FHCO had higher SFC compared to their initial blends at temperatures between 0 and 40 °C.

#### **6.4. Conclusions**

This study was devoted to exploring the feasibility of producing base-stock for zero-*trans* margarines by enzymatic catalysis in equilibrium with SCCO<sub>2</sub>. The commercial lipase, Lipozyme TL IM, was very efficient in catalysing the interesterification of canola oil and FHCO under SCCO<sub>2</sub>. The optimal reaction conditions to obtain the maximum degree of interesterification were 65 °C, 10 MPa and 2 h of reaction time at an enzyme concentration of 6% (w/v) of initial substrates. It was also demonstrated that the TG composition, melting and crystallization behaviour, and SFC of initial blends of canola oil and FHCO were considerably modified after enzymatic interesterification.

#### **6.5. References**

- Ahmadi, L., Wright, A.J. and Marangoni, A.G. (2008). Chemical and enzymatic interesterification of tristearin/triolein-rich blends: Chemical composition, solid fat content and thermal properties. *European Journal of Lipid Science and Technology*, **110** (11): 1014-1024.
- AOCS Official and Recommended Practices. (2009). (6th ed.) AOCS Press, Champaign, IL, USA.
- Costales-Rodriguez, R., Gibon, V., Verhe, R. and De Greyt, W. (2009). Chemical and enzymatic interesterification of a blend of palm stearin: Soybean oil for low *trans*-margarine formulation. *Journal of the American Oil Chemists' Society*, **86** (7): 681-697.

Dunford, N.T. and Temelli, F. (1995). Extraction of phospholipids from canola with supercritical carbon dioxide and ethanol. *Journal of the American Oil Chemists' Society*, **72** (9): 1009-1015.

Gavriilidou, V. and Boskou, D. (1991). Chemical interesterification of olive oil-tristearin blends for margaines. *International Journal of Food Science and Technology*, **26** (5): 451-456.

Humphrey, K.L., Moquin, P.H.L. and Narine, S.S. (2003). Phase behaviour of a binary lipid shortening system: From molecules to rheology. *Journal of the American Oil Chemists' Society*, **80** (12): 1175-1182.

Kim, I.H., Ko, S.N., Lee, S.M., Chung, S.H., Kim, H., Lee, K.T. and Ha, T.Y. (2004). Production of structured lipids by lipase-catalyzed acidolysis in supercritical carbon dioxide: Effect on acyl migration. *Journal of the American Oil Chemists' Society*, **81** (6): 537-541.

Laudani, C.G., Habulin, M., Knez, Z., Della Porta, G. and Reverchon, E. (2007). Immobilized lipase-mediated long-chain fatty acid esterification in dense carbon dioxide: Bench-scale packed-bed reactor study. *Journal of Supercritical Fluids*, **41** (1): 74-81.

Liang, M.T., Chen, C.H. and Liang, R.C. (1998). Interesterification of edible palm oil by stearic acid in supercritical carbon dioxide. *Journal of Supercritical Fluids*, **13** (1-3): 211-216.

List, G.R., Mounts, T.L., Orthoefer, F. and Neff, W.E. (1995). Margarine and shortening oils by interesterification of liquid and trisaturated triglycerides. *Journal of the American Oil Chemists' Society*, **72** (3): 379-382.

Liu, K.J., Cheng, H.M., Chang, R.C. and Shaw, J.F. (1997). Synthesis of cocoa butter equivalent by lipase-catalyzed interesterification in supercritical carbon dioxide. *Journal of the American Oil Chemists' Society*, **74** (11): 1477-1482.

Macrae, A.R. (1983). Lipase-catalyzed interesterification of oils and fats. *Journal of the American Oil Chemists' Society*, **60** (2): 243A-246A.

Miller, D.A., Blanch, H.W. and Prausnitz, J.M. (1991). Enzyme-catalyzed interesterification of triglycerides in supercritical carbon dioxide. *Industrial and Engineering Chemistry Research*, **30** (5): 939-946.

Petrauskaitė, V., De Greyt, W., Kellens, M. and Huyghebaert, A. (1998). Physical and chemical properties of *trans*-free fats produced by chemical interesterification of vegetable oil blends. *Journal of the American Oil Chemists' Society*, **75** (4): 489-493.

Ribeiro, A.P.B., Basso, R.C., Grimaldi, R., Gioielli, L.A., dos Santos, A.O., Cardoso, L.P. and Goncalves, L.A.G. (2009a). Influence of chemical

interesterification on thermal behaviour, microstructure, polymorphism and crystallization properties of canola oil and fully hydrogenated cottonseed oil blends. *Food Research International*, **42** (8): 1153-1162.

Ribeiro, A.P.B., Basso, R.C., Grimaldi, R., Gioielli, L.A. and Goncalves, L.A.G. (2009b). Effect of chemical interesterification on physicochemical properties and industrial applications of canola oil and fully hydrogenated cottonseed oil blends. *Journal of Food Lipids*, **16** (3): 362-381.

Rodrigues, C.E.C., Gonçalves, C.B., Batista, E. and Meirelles, J.A. (2007). Deacidification of vegetable oils by solvent extraction. *Recent Patents on Engineering*, **1**: 95-102.

Rodriguez, A., Castro, E., Salinas, M.C., Lopez, R. and Miranda, M. (2001). Interesterification of tallow and sunflower oil. *Journal of the American Oil Chemists' Society*, **78** (4): 431-436.

Rousseau, D. and Marangoni, A.G. (1998). The effects of interesterification on physical and sensory attributes of butterfat and butterfat-canola oil spreads. *Food Research International*, **31** (5): 381-388.

Seifried, B. and Temelli, F. (2009). Density of marine lipids in equilibrium with carbon dioxide. *Journal of Supercritical Fluids*, **50** (2): 97-104.

Seifried, B. and Temelli, F. (2010a). Interfacial tension of marine lipids in contact with high pressure carbon dioxide. *Journal of Supercritical Fluids*, **52** (2): 203-214.

Seifried, B. and Temelli, F. (2010b). Unique properties of carbon dioxide-expanded lipids. *INFORM-International News on Fats, Oils and Related Materials*, **21** (1): 10-12.

Seifried, B. and Temelli, F. (2011). Viscosity and rheological behaviour of carbon dioxide-expanded fish oil triglycerides: Measurement and modeling. *Journal of Supercritical Fluids*, **59**: 27-35.

Seriburi, V. and Akoh, C.C. (1998). Enzymatic interesterification of triolein and tristearin: Chemical structure and differential scanning calorimetric analysis of the products. *Journal of the American Oil Chemists' Society*, **75** (6): 711-716.

Shekarchizadeh, H., Kadivar, M., Ghaziaskar, H.S. and Rezayat, M. (2009). Optimization of enzymatic synthesis of cocoa butter analog from camel hump fat in supercritical carbon dioxide by response surface method (RSM). *Journal of Supercritical Fluids*, **49** (2): 209-215.

Shukla, V.K.S. (2005). Margarine and baking fats (Chapter 27). In *Healthful lipids*, C.C. Akoh and O.M. Lai, Eds., AOCS Press, Champaign, IL, USA.

Silva, R.C., Cotting, L.N., Poltronieri, T.P., Balcao, V.M., de Almeida, D.B., Goncalves, L.A.G., Grimaldi, R. and Gioielli, L.A. (2009). The effects of enzymatic interesterification on the physical-chemical properties of blends of lard and soybean oil. *LWT-Food Science and Technology*, **42** (7): 1275-1282.

Sun, J., Yu, B., Curran, P. and Liu, S.-Q. (2012). Lipase-catalysed transesterification of coconut oil with fusel alcohols in a solvent-free system. *Food Chemistry*, **134** (1): 89-94.

Xu, X. (2003). Engineering of enzymatic reactions and reactors for lipid modification and synthesis. *European Journal of Lipid Science and Technology*, **105**: 289-304.

Yadav, G.D. and Trivedi, A.H. (2003). Kinetic modeling of immobilized-lipase catalyzed transesterification of n-octanol with vinyl acetate in non-aqueous media. *Enzyme and Microbial Technology*, **32** (7): 783-789.

Yu, Z.R., Rizvi, S.S.H. and Zollweg, J.A. (1992). Enzymatic esterification of fatty-acid mixtures from milk-fat and anhydrous milk-fat with canola oil in supercritical carbon-dioxide. *Biotechnology Progress*, **8** (6): 508-513.

## **7. Polymorphism, microstructure and rheological properties of enzymatically interesterified canola oil and fully-hydrogenated canola oil under supercritical carbon dioxide<sup>1</sup>**

### **7.1. Introduction**

Partial hydrogenation and interesterification are two processes used to produce margarine fats. However, the more commonly used process of partial hydrogenation has one major disadvantage, namely the formation of *trans* fatty acids during the process (Puri, 1978). *Trans*-isomers are known to be undesirable from a nutritional standpoint, having been shown to be a major risk factor for cardiovascular disease (Tardy et al., 2011). Therefore, interesterification of liquid oil with fully-hydrogenated fats has received great interest as an alternative process for the production of *trans*-free margarine fats (List et al., 1995). Interesterification, which is the exchange of fatty acids on glycerol backbones, can be performed either chemically or enzymatically. Compared to chemical interesterification, enzymatic interesterification can take place under milder conditions with fewer side reactions, leading to cleaner final products. In chemical interesterification, which is completely random shuffling of fatty acids on glycerol backbones, it is hard to achieve partial interesterification because the reaction happens very fast (Marangoni and Rousseau, 1995).

---

<sup>1</sup> A version of this chapter has been submitted to *J. Am. Oil Chem. Soc.* for consideration for publication. Jenab E. and Temelli F. (2012). Polymorphism, microstructure, and rheological properties of enzymatically interesterified canola oil and fully-hydrogenated canola oil under supercritical carbon dioxide.

Solvent-free reactions like enzymatic reactions can be conducted using CO<sub>2</sub>-expanded (CX) lipids under supercritical CO<sub>2</sub> (SCCO<sub>2</sub>). A mixture of lipid reactants in contact with SCCO<sub>2</sub> expands as CO<sub>2</sub> dissolves in the liquid lipid phase, causing viscosity to decrease and reaction rate to increase by improving mass transfer properties (Seifried and Temelli, 2010). In previous chapters, the physical properties of canola oil and its blend with fully-hydrogenated canola oil (FHCO) in equilibrium with SCCO<sub>2</sub> (Chapters 3 and 4), optimization of lipase-catalyzed interesterification between canola oil and FHCO under SCCO<sub>2</sub> and some physicochemical properties of the interesterified products (Chapters 5 and 6) were investigated.

Both enzymatic and chemical interesterification change the distribution of acyl groups on the glycerol backbone, which has an effect on polymorphism, microstructure, and rheological properties. These parameters are important for better understanding of the relationships between the composition, processing parameters and functional properties of the final products (Ahmadi et al., 2008, 2009). However, such information is not available for interesterified products obtained under supercritical conditions. Therefore, the objective of this study was to compare the polymorphism, microstructure, and rheological properties of the initial blends of canola oil and FHCO with those of interesterified products obtained under SCCO<sub>2</sub>. The interesterification between canola oil and FHCO under SCCO<sub>2</sub> was conducted at 10 MPa and 65 °C for 2 h using 6% of Lipozyme TL IM based on the results of Chapter 6.

## **7.2. Materials and methods**

### **7.2.1. Materials**

Lipozyme TL IM, with the specifications provided Section 5.2.1, was used for the interesterification between canola oil and FHCO. The same specifications and fatty acid composition of FHCO and canola oil used in this study were described in Section 4.2.1. CO<sub>2</sub> and N<sub>2</sub> with similar specifications as described in Section 6.2.1 were also used in this study.

### **7.2.2. Enzymatic interesterification under SCCO<sub>2</sub>**

Lipase-catalyzed interesterification of CO<sub>2</sub>-expanded canola oil and FHCO blend was conducted in batch mode in a Nova Swiss (Nova-Werke AG, Effretikon, Switzerland) high pressure, electrically heated, magnetically stirred 200 mL autoclave setup. The details of the experimental setup can be found in Section 6.2.3.1. Lipozyme TL IM was dried with SCCO<sub>2</sub> at 65 °C/20 MPa for 5 h prior to the reaction as reported previously in Section 6.2.3.1 in order to reduce its moisture content and consequently the amount of reaction intermediates formed due to the hydrolysis side reaction in the final products. The prepared oil mixtures and enzymes were kept in a desiccator at 4-5 °C to prevent further moisture absorption. Lipozyme TL IM dried with SCCO<sub>2</sub> was loaded inside the high pressure vessel at a level of 6% (w/v) of initial substrates and then the temperature was increased to around 65 °C. A total volume of 70 mL of initial reactants, consisting of canola oil and FHCO blend prepared at different ratios (10, 30, 50 wt.% FHCO) was added to the autoclave using a syringe. Once the autoclave was

sealed, the reaction mixture was first purged with CO<sub>2</sub> and then pressurized to 10 MPa using a syringe pump (Model 260D, Teledyne Isco, Lincoln, NE, USA). The magnetic stirrer was turned on to mix the autoclave contents once the system reached stable temperature and pressure. After 2 h of reaction, the magnetic stirrer was stopped, the system was depressurized and the interesterified product was removed after the settlement of immobilized enzyme beads for further analysis. The reaction products, blanketed with nitrogen, were kept at -20 °C until analysis. The reactions at each condition were conducted at least in two replicates.

#### **7.2.3. Purification of the reaction products**

In order to remove free fatty acids (FFA), monoglycerides (MG) and diglycerides (DG) formed as reaction intermediates from the final reaction products, the samples obtained after 2 h of interesterification reaction were purified using the procedure described in Section 6.2.3.2.

#### **7.2.4. X-ray diffraction analysis**

About 150 µL of melted sample was poured into the hollow section of the copper X-ray slide. The copper slides were transferred into the Linkam stage where they were initially heated rapidly from room temperature to 80 °C and held for 10 min to erase the crystal memory; cooled to 24 °C at 1 °C/min and held for 12 h before X-ray diffraction (XRD) analysis. A Rigaku Ultima IV XRD unit (Rigaku America, Woodlands, TX, USA) equipped with a scintillation detector with an Fe filter was used. The cobalt tube was set to 38 kV and 38 mA with

wavelength K average of 1.790260. The samples were run from 2 to 35 degrees on continuous scan at  $2\theta$   $\text{min}^{-1}$  with a step size of 0.02. The XRD unit was equipped with a medium/low temperature stage with the ability to control the temperature within  $\pm 0.5$  °C. This stage enabled the analysis to be conducted at the tempering temperature. Data interpretation was done using MDI Jade 9.1 software (Livermore, CA, USA).

### **7.2.5. Polarized light microscopy**

The microstructure of the initial blends of canola oil and FHCO and the interesterified products was observed using polarized light microscopy (PLM). A drop of melted sample was placed at the centre of preheated slides and then a slide cover was gently placed over the fat droplet to spread it on the slide and remove any air bubbles. The slide was transferred into a programmable hot/cold stage (Linkam LTS 350, Linkam Scientific Instruments, Tadworth, Surrey, UK) and the sample was initially heated rapidly from room temperature to 80 °C and held for 10 min to erase the crystal memory; cooled to 24 °C at 1 °C/min and then held for 12 h. The slide as it was inside the Linkam stage was placed on the microscope stage. A high-resolution polarized light microscope (DMRX, Leica Microsystems, Wetzlar, GmbH, Germany) equipped with a digital camera (C4724-95-12NRB, Hamamatsu corporation, Bridgewater, NJ, USA) was used. The microscope assembly was controlled by Openlab 3.0.8 software (Improvision, Coventry, UK).

### **7.2.6. Rheological properties**

Rheological characterization of the samples was carried out by a rheometer (UDS 200, Paar Physica, Graz, Austria), equipped with parallel plate geometry. To avoid slippage, sandpaper (coarse number of 60) was attached to the upper plate (25 mm diameter). The lower plate had a rough surface. The temperature of the sample was maintained at 24 °C using the Peltier plate base. Molten samples were poured inside a metal mold with a diameter of 25 mm and thickness of 3 mm, which was placed at the centre of the lower plate of the rheometer. After a conditioning period of 2 h, the metal mold was removed and the test was started on the formed disk of sample at the desired temperature. Storage ( $G'$ ) and loss ( $G''$ ) moduli as a function of strain were determined using amplitude sweep at constant frequency of 1 Hz within the range of 0.005 to 5% strain. Then, the curves obtained were used to identify the linear viscoelastic (LVE) range and to determine  $G'$  and  $G''$  within this range. The maximum gap between the plates was such that the upper plate would just contact the sample surface. The analyses were conducted at least in two replicates.

## **7.3. Results and discussion**

It was previously established that conducting interesterification between canola oil and FHCO under  $\text{SCCO}_2$  increased the reaction rate and equilibrium was reached in less than 2 h at 10 MPa and 65 °C compared to 6 h at atmospheric pressure and the same temperature. It is also important to investigate the polymorphism, microstructure and rheological properties of the interesterified

products obtained under optimal conditions compared to the non-interesterified blends. This information would lead to better understanding of the process and the quality of the products targeting base-stock for margarine or pastry shortenings.

### **7.3.1. Polymorphism of the initial blends and the interesterified products**

Phase behaviour of a fat product has a direct influence on its functional properties. Therefore, an understanding and knowledge of the polymorphism of a fat product is essential whether it is a pure triglyceride (TG), margarine or pastry shortening (Timms, 1984). Differences in phase behaviour caused by differences in the polymorphism among different fat blends can be measured by XRD in which a change in the peak shape or position is indicative of a change in polymorphic behaviour (Humphrey et al., 2003). Fats and pure TG occur in any one of the three basic polymorphic forms designated as  $\alpha$ ,  $\beta'$ , and  $\beta$ , which are related to the characteristic packing of hydrocarbon chains of the triglycerides, where  $\alpha$  is the least stable and the lowest melting point form and  $\beta$  is the most stable and highest melting point form. Transformations from  $\alpha$  to  $\beta'$  and then to  $\beta$  take place in that order and are irreversible.

Figure 7-1a shows the XRD spectra for the initial blends of canola oil and FHCO and the interesterified products after storing them for 12 h at 24 °C. Polymorphic transformation can be clearly seen from the short spacing peaks (wide-angle X-ray scattering reflection). Different peaks with different “d” values, which represent centroid distances, are present in each sample and these

peaks can be associated quantitatively with possible polymorphic forms that have been defined for lipids.

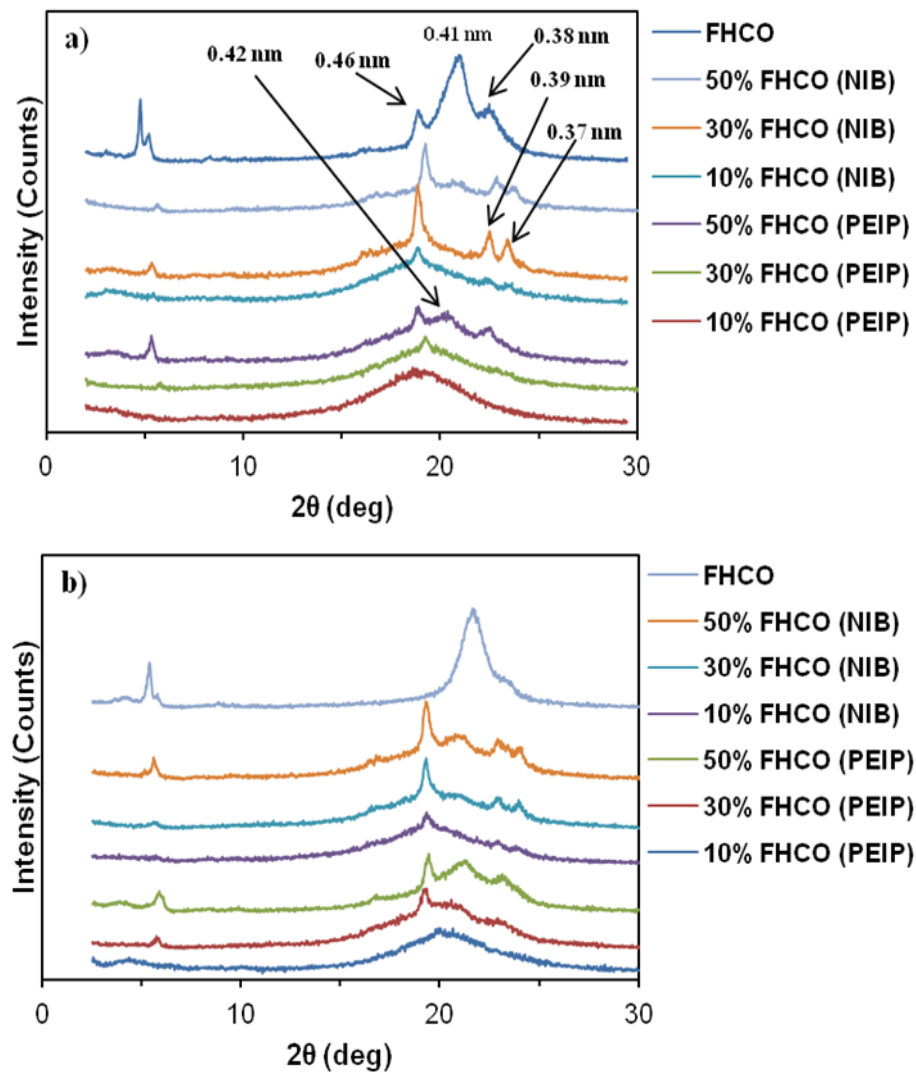


**Figure 7-1.** X-ray diffraction patterns for non-interesterified initial blends (NIB) and purified enzymatically interesterified products (PEIP) of canola oil and fully-hydrogenated canola oil (FHCO) crystallized for 12 h at (a) 24 °C and (b) 5 °C.

For instance, tristearin in  $\beta$  form shows three short spacing peaks at 0.46, 0.39, and 0.37 nm, whereas  $\alpha$  form shows one short spacing peak at 0.415 nm and

in  $\beta'$  form shows two peaks at 0.42 and 0.38 nm (Garti et al., 1982; Oh et al., 2002). FHCO, containing tristearin as the predominant TG (Table 6-1), showed three peaks with  $d$  values of 0.46, 0.41, and 0.38 nm, representing  $\beta$ ,  $\alpha$ , and  $\beta'$  forms, respectively. However, the dominant polymorphic form in FHCO was the  $\alpha$  form. In the non-interesterified initial blends (NIB) of canola oil and FHCO containing 10, 30, and 50 wt.% FHCO, three short spacing peaks at 0.46, 0.39, and 0.37 nm, representing  $\beta$  polymorphic forms were observed.

Blending of FHCO with canola oil caused a transition from  $\alpha$  to  $\beta$  form which is more stable (Fig 7-1a). The findings of this study are in agreement with those of other researchers (Rodriguez et al., 2001; Humphrey et al., 2003; Zhang et al., 2004; Wright et al., 2005; Ahmadi et al., 2008), who showed that adding liquid oil to a saturated fat results in the formation of thermodynamically stable polymorphic forms. Lipase-catalyzed interesterification between canola oil and FHCO under  $\text{SCCO}_2$  at 65 °C and 10 MPa for 2 h changed the polymorphic forms present in the initial blends (Fig. 7-1a). No peaks were observed in the purified enzymatically interesterified product (PEIP) obtained from the blend containing 10 wt.% FHCO. This sample was actually in the liquid state at 24 °C as was confirmed with differential scanning calorimetry (DSC) previously in Section 6.3.2.2.

The diffractogram obtained at 24 °C showed low intensity peaks, which is typical of amorphous materials. The PEIP sample for 30 wt.% FHCO showed just one short spacing peak at 0.46 nm representing the  $\beta$  polymorph (Fig. 7-1a). But for the PEIP sample of 50 wt.% FHCO, three short spacing peaks were observed

at 0.42 and 0.38 representing the  $\beta'$  form and 0.46 representing  $\beta$  form. Table 7-1 shows the details of the polyphormic forms of NIB and PEIP samples.

**Table 7-1.** Polymorphic forms of non-interesterified blends (NIB) and purified enzymatically interesterified products (PEIP) of canola oil and fully-hydrogenated canola oil (FHCO) crystallized at 24 °C and 5 °C for 12 h.

Blends	Temperature (°C)			
	24		5	
	NIB	PEIP	NIB	PEIP
FHCO	0.46 ( $\beta$ ), 0.41 ( $\alpha$ ), 0.38 ( $\beta'$ )	-	0.41 ( $\alpha$ ), 0.38 ( $\beta'$ )	-
50% FHCO	0.46 ( $\beta$ ), 0.42 ( $\beta'$ ), 0.41 ( $\alpha$ ), 0.39 ( $\beta$ ), 0.37 ( $\beta$ )	0.46 ( $\beta$ ), 0.42 ( $\beta'$ ), 0.38 ( $\beta'$ )	0.46 ( $\beta$ ), 0.42 ( $\beta'$ ), 0.39 ( $\beta$ ), 0.37 ( $\beta$ )	0.46 ( $\beta$ ), 0.42 ( $\beta'$ ), 0.38 ( $\beta'$ )
30% FHCO	0.46 ( $\beta$ ), 0.39 ( $\beta$ ), 0.37 ( $\beta$ )	0.46 ( $\beta$ )	0.46 ( $\beta$ ), 0.42 ( $\beta'$ ), 0.39 ( $\beta$ ), 0.37 ( $\beta$ )	0.46 ( $\beta$ ), 0.42 ( $\beta'$ ), 0.38 ( $\beta'$ )
10% FHCO	0.46 ( $\beta$ ), 0.39 ( $\beta$ ), 0.37 ( $\beta$ )	-	0.46 ( $\beta$ ), 0.39 ( $\beta$ ), 0.37 ( $\beta$ )	-

The formation of  $\beta'$  polymorph after enzymatic interesterification is because of the formation of mixed TG (Table 6-3). The interesterified products of canola oil and FHCO contain mainly SOO, LOS, and SOS; TG with a heterogeneous fatty acid distribution on their glycerol backbone compared to the initial blends, which mainly contain OOO, LOO, and SSS (Table 6-1). The mixed TG have a greater tendency to be in the  $\beta'$  form (Siew et al., 2007; Ahmadi et al., 2008; Lee et al., 2008). The results of this study are in agreement with those of other studies

reporting polymorphism changes for interesterified products, regardless of whether it is obtained enzymatically or chemically (Rousseau et al., 1996, 1998; Ahmadi et al., 2008).

It should also be taken into consideration that the formation of different polymorphic forms is highly dependent on the rate of cooling and storage time; for example, pure tristearin can be in  $\alpha$ ,  $\beta'$ , or  $\beta$  forms depending on how the induction of polymorphic forms is performed (Sato and Kuroda, 1987; Kellens et al., 1990). Therefore, the XRD spectra of NIB and PEIP samples of canola oil and FHCO were also studied at 5 °C. As shown in Figure 7-1b, the intensity of short spacing peaks in some samples stored at 5 °C increased compared to the ones stored at 24 °C. Most notable changes can be observed in FHCO and PEIP samples of 30 and 50 wt.% FHCO blends (Fig. 7-1b and Table 7-1). No short spacing peak was observed for the  $\beta$  polymorph at 0.46 nm in FHCO stored at 5 °C. Also, PEIP samples of 30 and 50 wt.% FHCO blends, stored at 5 °C showed more intense short spacing peaks for  $\beta'$  polymorphs at 0.42 and 0.38 nm.

The  $\beta'$  form is the most suitable crystal polymorphic form in margarines, spreads, and shortenings because it is associated with smooth texture in the product as opposed to the  $\beta$  form resulting in a brittle fat with a sandy and coarse texture. However,  $\beta$  polymorphs are desirable in chocolate products (Rousseau et al., 1998).

### **7.3.2. Microstructure of initial blends and interesterified products**

Enzymatic interesterification between canola oil and FHCO changes crystal morphology because of changing distribution of acyl groups on the glycerol backbone as well as polymorphism, which must be confirmed by XRD measurements as discussed above. On the other hand, PLM is the most commonly used technique for the visualization of fat microstructural network. However, it should be taken into consideration that PLM is a subjective method and highly dependent on the preparation of slides as well as the part of the slide being observed through the microscope.

Regardless, PLM method has been applied with the intent of explaining textural differences between fat blends and to show morphological alterations in crystal growth (Gioielli et al., 2003). Figure 7-2 shows the effects of blending of canola oil and FHCO at different ratios and enzymatic interesterification on crystal morphology at 24 °C after 12 h of crystallization. PLM of FHCO showed asymmetrical spherulitic particles and fine crystals, forming dense aggregates.

In NIB samples of canola oil and FHCO, increasing the amount of FHCO in the blend caused formation of more densely packed aggregates of crystals, but no substantial changes were observed in the morphology of crystals. As well, NIB samples with 30 and 50% FHCO showed larger, loose and highly asymmetrical particles. The grainy and sandy texture of non-interesterified blends of canola oil and FHCO is related to the presence of these large spherulites and spherulitic aggregates due to the presence of a high amount of tristearin in the blends. Deman

et al. (1989) and Rousseau et al. (1996) showed similar microstructures for fats having significant amounts of tristearin.

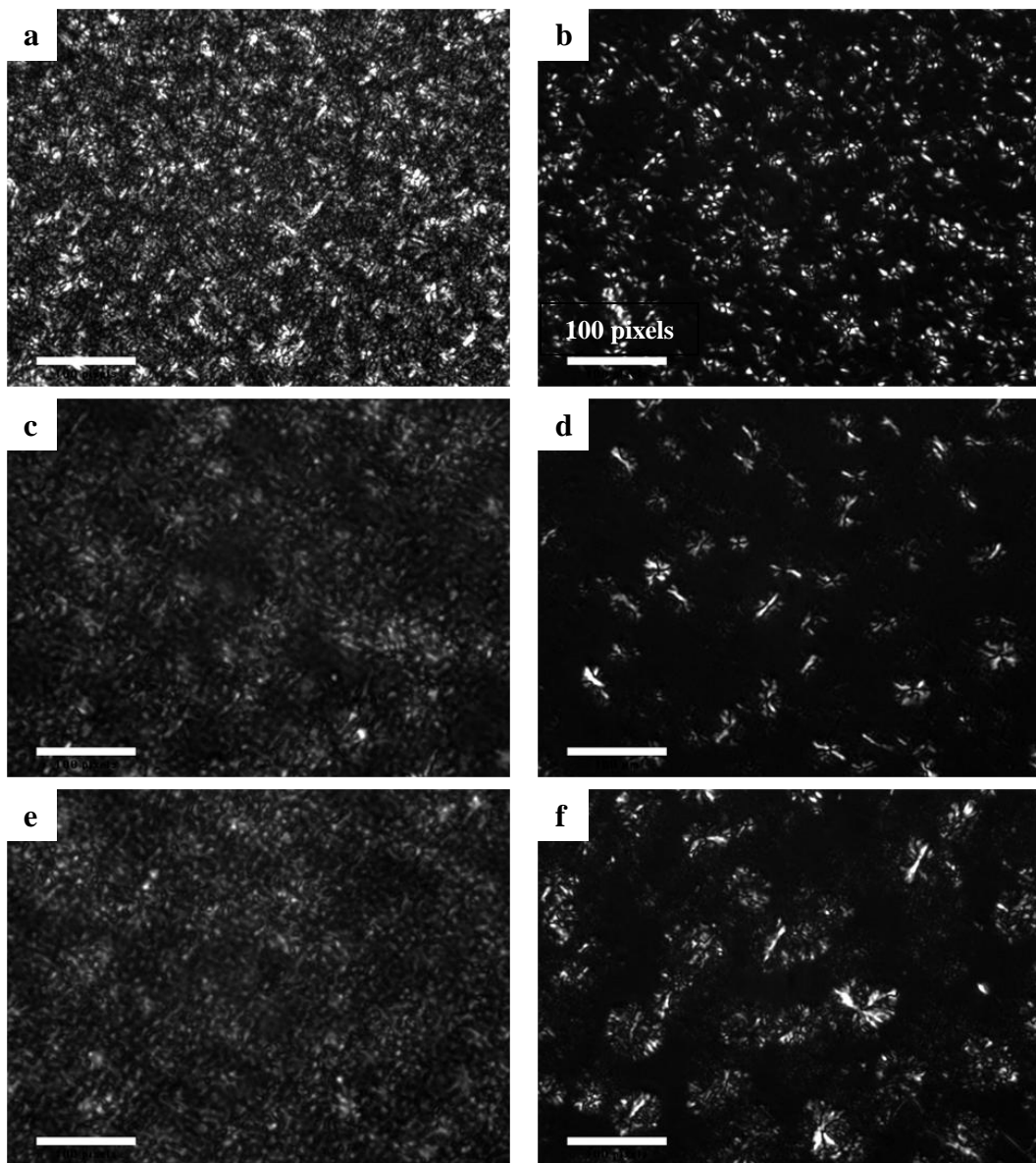


**Figure 7-2.** Crystal morphology of non-interesterified initial blends (NIB) and purified enzymatically interesterified products (PEIP) of canola oil and fully-hydrogenated canola oil (FHCO) crystallized at 24 °C for 12 h: (a) FHCO; (b) 10% FHCO (NIB); (c) 30% FHCO (NIB); (d) 30% FHCO (PEIP); (e) 50% FHCO (NIB); and (f) 50% FHCO (PEIP).

After enzymatic interesterification, complete modification of the crystal morphology was apparent in the products. The PEIP samples contained less crystal particles compared to non-interesterified blends. This is due to the reduction in the amount of tristearin after enzymatic interesterification. The amount of tristearin in the blends with 10%, 30%, and 50% FHCO reduced from around 9, 29, and 44% to around 0, 2, and 12% after enzymatic interesterification under  $\text{SCCO}_2$  for 2 h, respectively (Table 6-3). After enzymatic interesterification, spherulites also became more symmetrical, and a distinct high-density core surrounded by a lower-density halo region became evident (Fig. 7-2d, g). These results are in good agreement with those of Rousseau et al. (1998) who investigated the crystal morphology of lard and canola oil blends and their interesterified products. The formation of different crystal structures after enzymatic interesterification was caused by alterations in TG composition, modifying the relative strength of bonds among crystal elements in an aggregate and among aggregates (Shi et al., 2005). Furthermore, changes in the solid fat content inherent to the interesterification process also affect crystal network. By decreasing the solid fat content after enzymatic interesterification (Fig. 6-6), a larger area and a greater mobility for crystal formations would be available.

Finally, microstructural changes in the blends of canola oil and FHCO due to enzymatic interesterification are because of the modifications in morphology and density of the crystalline network resulting in changes in textural and functional properties of the final interesterified products.

### **7.3.3. Rheological properties of initial blends and interesterified products**

In order to determine the limits of linear viscoelastic behaviour of NIB and PEIP samples, a strain sweep was conducted by varying the amplitude of input signal at a constant frequency and the critical strain value was identified. The amplitude sweep dependence of the storage modulus ( $G'$ ) (solid-like or elastic behaviour) and loss modulus ( $G''$ ) (liquid-like or viscous behaviour) of NIB and PEIP of canola oil and FHCO is presented in Figure 7-3. The  $G'$  and  $G''$  of viscoelastic materials measure the stored energy, representing the elastic portion, and the energy dissipated as heat, representing the viscous portion, respectively.  $G'$  of all blends were higher than  $G''$  over the whole strain levels in the linear viscoelastic (LVE) range and both  $G'$  and  $G''$  of all samples decreased after the LVE range boundary. The LVE range boundary shifted to lower lower strain values for the PEIP samples compared to the NIB samples. It is important to establish the LVE range because the rheological properties are stress or strain independent in this range. Therefore,  $G'$  and  $G''$  of NIB and PEIP samples were determined in the LVE range after finding the amplitude sweep dependence of  $G'$  and  $G''$  (Steffe, 1996).

As shown in Figure 7-4, the storage or elastic modulus of the NIB sample with 50% FHCO was higher than that of the NIB sample with 30% FHCO considering the LVE range at 25 °C. The NIB sample with 10% FHCO at 25 °C behaved like a Newtonian fluid. Enzymatic interesterification between canola oil and FHCO under  $\text{SCCO}_2$  after 2 h reduced the solid-like behaviour of the initial blends by decreasing  $G'$ .

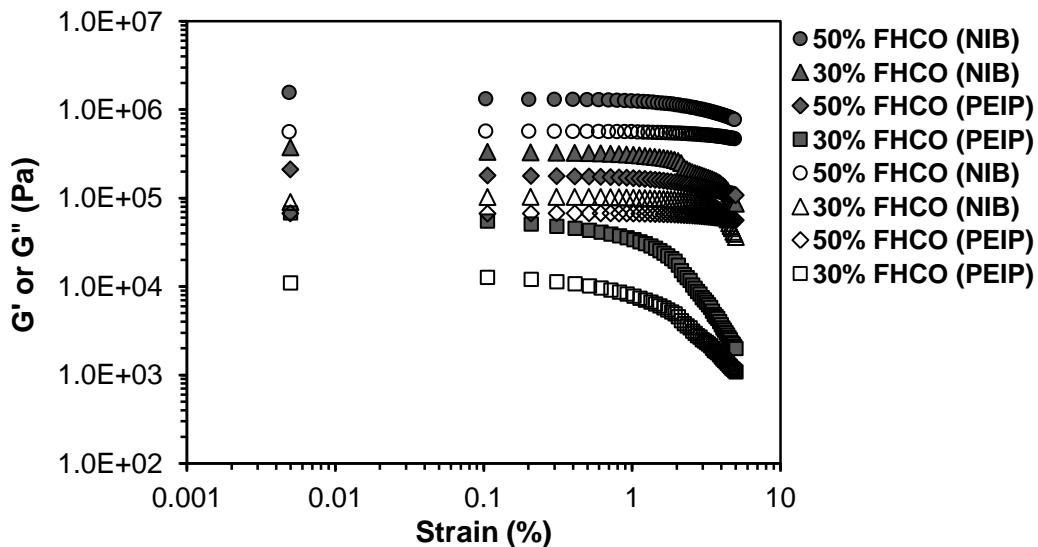


**Figure 7-3.** Storage ( $G'$ ) and loss ( $G''$ ) moduli as a function of strain for non-interesterified initial blends (NIB) and purified enzymatically interesterified products (PEIP) of canola oil and fully-hydrogenated canola oil (FHCO) crystallized at  $25^{\circ}\text{C}$  for 2 h. Solid and empty markers represent  $G'$  and  $G''$ , respectively.

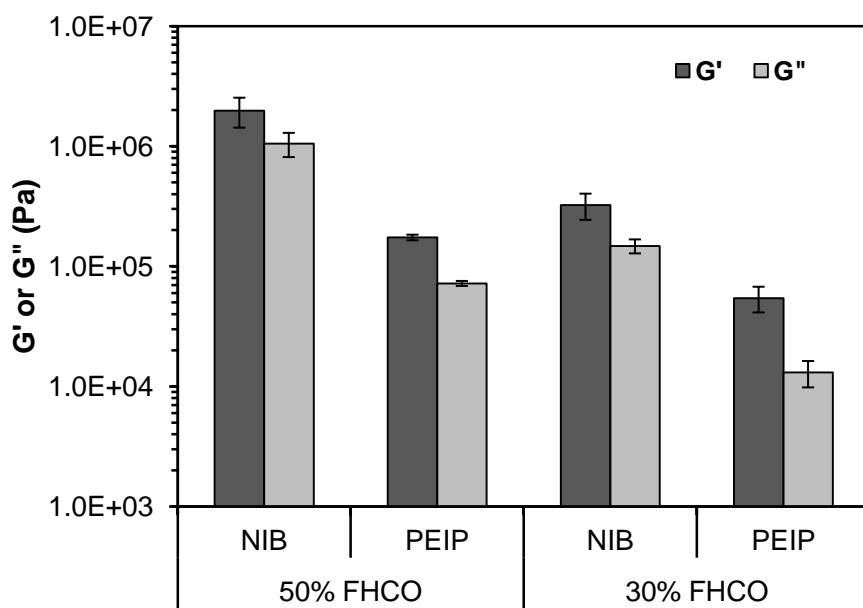


**Figure 7-4.** Storage ( $G'$ ) and loss ( $G''$ ) moduli determined in the linear viscoelastic (LVE) range of non-interesterified initial blends (NIB) and purified enzymatically interesterified products (PEIP) of canola oil and fully-hydrogenated canola oil (FHCO) crystallized at  $24^{\circ}\text{C}$  for 2 h.

The lower G' of the NIB sample with 30% FHCO compared to the blend with 50% FHCO and of the PEIP samples compared to the NIB samples can be related to the TG composition, the solid fat content, polymorphic form and morphology of the samples as well as the actual structure of the three-dimensional network formed by fat crystals, and the interaction between solid and liquid triglycerides (Kawanari et al., 1981; Deman, 1983; Juriaanse and Heertje, 1988; Marangoni and Rousseau, 1998).

As shown previously in Figure 6-6, the SFC of NIB samples containing 50 and 30% FHCO at 25 °C decreased from 46 and 27% to 32 and 7.6%, respectively, after enzymatic interesterification under  $\text{SCCO}_2$  at 10 MPa and 65 °C for 2 h. Marangoni and Rousseau (1998) showed that there was a power law relationship between G' and the SFC of non-interesterified and enzymatically interesterified blends of lard–canola oil and palm oil–soybean oil. In addition, the microstructure of a fat depends directly on the type of fatty acids and consequently the type of TG present in the fat crystal network (Ahmadi et al., 2009). Ahmadi et al. (2009) showed that there was a positive correlation between the elastic modulus and the amount of stearic acid as a saturated fatty acid with a high melting point fatty acid. They also found a strong correlation between G' and TG composition, including a strong positive correlation between G' and tristearin and a strong negative correlation between G' and triolein.

#### **7.4. Conclusions**

Lipase-catalyzed interesterification resulted in a change in the polymorphism and microstructural and rheological properties due to the formation of new mixed TG as the rearrangement of fatty acids within or between TG. More desirable crystal polymorph ( $\beta'$  form) was found in the interesterified fats. It was demonstrated that similar characteristics of the products can be obtained using enzymatic interesterification under  $\text{SCCO}_2$  employing a much shorter reaction time compared to enzymatic interesterification products obtained under atmospheric pressure reported in the literature.

#### **7.5. References**

- Ahmadi, L., Wright, A.J. and Marangoni, A.G. (2008). Chemical and enzymatic interesterification of tristearin/triolein-rich blends: Microstructure and polymorphism. *European Journal of Lipid Science and Technology*, **110** (11): 1025-1034.
- Ahmadi, L., Wright, A.J. and Marangoni, A.G. (2009). Structural and mechanical behaviour of tristearin/triolein-rich mixtures and the modification achieved by interesterification. *Food Biophysics*, **4** (2): 64-76.
- DeMan, J.M. (1983). Consistency of fats - a review. *Journal of the American Oil Chemists' Society*, **60** (1): 82-87.
- DeMan, L., DeMan, J.M. and Blackman, B. (1989). Polymorphic behaviour of some fully hydrogenated oils and their mixtures with liquid oil. *Journal of the American Oil Chemists Society*, **66** (12): 1777-1780.
- Garti, N., Wellner, E. and Sarig, S. (1982). Crystal-structure modifications of tristearin by food emulsifiers. *Journal of the American Oil Chemists' Society*, **59** (4): 181-185.
- Gioielli, L.A., Simoes, I.S. and Rodrigues, J.N. (2003). Crystal morphology and interactions of binary and ternary mixtures of hydrogenated fats. *Journal of Food Engineering*, **57** (4): 347-355.

Humphrey, K.L., Moquin, P.H.L. and Narine, S.S. (2003). Phase behaviour of a binary lipid shortening system: From molecules to rheology. *Journal of the American Oil Chemists' Society*, **80** (12): 1175-1182.

Juriaanse, A.C. and Heertje, I. (1988). Microstructure of shortenings, margarine and butter - a review. *Food Microstructure*, **7** (2): 181-188.

Kawanari, M., Hamann, D.D., Swartzel, K.R. and Hansen, A.P. (1981). Rheological and texture studies of butter. *Journal of Texture Studies*, **12** (4): 483-505.

Kellens, M., Meeussen, W. and Reynaers, H. (1990). Crystallization and phase-transition studies of tripalmitin. *Chemistry and Physics of Lipids*, **55** (2): 163-178.

Lee, J.H., Akoh, C.C. and Lee, K.T. (2008). Physical properties of *trans*-free bakery shortening produced by lipase-catalyzed interesterification. *Journal of the American Oil Chemists' Society*, **85** (1): 1-11.

List, G.R., Mounts, T.L., Orthofer, F. and Neff, W.E. (1995). Margarine and shortening oils by interesterification of liquid and trisaturated triglycerides. *Journal of the American Oil Chemists' Society*, **72** (3): 379-382.

Marangoni, A.G. and Rousseau, D. (1995). Engineering triacylglycerols: The role of interesterification. *Trends in Food Science & Technology*, **6**: 329-335.

Marangoni, A.G. and Rousseau, D. (1998). The influence of chemical interesterification on the physicochemical properties of complex fat systems. 3. Rheology and fractality of the crystal network. *Journal of the American Oil Chemists' Society*, **75** (11): 1633-1636.

Oh, J.H., McCurdy, A.R., Clark, S. and Swanson, B.G. (2002). Characterization and thermal stability of polymorphic forms of synthesized tristearin. *Journal of Food Science*, **67** (8): 2911-2917.

Puri, P.S. (1978). Correlations for *trans*-isomer formation during partial hydrogenation of oils and fats. *Journal of the American Oil Chemists' Society*, **55** (12): 865-869.

Rodrigues, C.E.C., Gonçalves, C.B., Batista, E. and Meirelles, J.A. (2007). Deacidification of vegetable oils by solvent extraction. *Recent Patents on Engineering*, **1**: 95-102.

Rousseau, D., Hill, A.R. and Marangoni, A.G. (1996). Restructuring butterfat through blending and chemical interesterification .2. Microstructure and polymorphism. *Journal of the American Oil Chemists' Society*, **73** (8): 973-981.

Rousseau, D., Marangoni, A.G. and Jeffrey, K.R. (1998). The influence of chemical interesterification on the physicochemical properties of complex fat

systems. 2. Morphology and polymorphism. *Journal of the American Oil Chemists' Society*, **75** (12): 1833-1839.

Sato, K. and Kuroda, T. (1987). Kinetics of melt crystallization and transformation of tripalmitin polymorphs. *Journal of the American Oil Chemists' Society*, **64** (1): 124-127.

Seifried, B. and Temelli, F. (2010). Unique properties of carbon dioxide-expanded lipids. *INFORM-International News on Fats, Oils and Related Materials*, **21** (1): 10-12.

Shi, Y.P., Liang, B.M. and Hartel, R.W. (2005). Crystal morphology, microstructure, and textural properties of model lipid systems. *Journal of the American Oil Chemists' Society*, **82** (6): 399-408.

Siew, W.L., Cheah, K.Y. and Tang, W.L. (2007). Physical properties of lipase-catalyzed interesterification of palm stearin with canola oil blends. *European Journal of Lipid Science and Technology*, **109** (2): 97-106.

Steffe, J.F. (1996). Rheological methods in food process engineering. East Lansing, MI, USA, Freeman Press.

Tardy, A.L., Morio, B., Chardigny, J.M. and Malpuech-Brugere, C. (2011). Ruminant and industrial sources of *trans*-fat and cardiovascular and diabetic diseases. *Nutrition Research Reviews*, **24** (1): 111-117.

Timms, R.E. (1984). Phase-behaviour of fats and their mixtures. *Progress in Lipid Research*, **23** (1): 1-38.

Wright, A.J., Batte, H.D. and Marangoni, A.G. (2005). Effects of canola oil dilution on anhydrous milk fat crystallization and fractionation behaviour. *Journal of Dairy Science*, **88** (6): 1955-1965.

Zhang, H., Smith, P. and Adler-Nissen, J. (2004). Effects of degree of enzymatic interesterification on the physical properties of margarine fats: Solid fat content, crystallization behaviour, crystal morphology, and crystal network. *Journal of Agricultural and Food Chemistry*, **52** (14): 4423-4431.

## **8. Concluding remarks**

### **8.1. Summary and conclusions**

Partial hydrogenation of vegetable oils is an important process in the edible oil industry because of its wide spread application in food manufacturing such as the production of bakery products, margarine, shortening, confectionary, and frying fats (Beers et al., 2008). One of the shortcomings of partial hydrogenation is the geometric isomerization of *cis*-double bonds, which leads to the formation of *trans* fatty acids (TFA) that impacts the physical and chemical properties of the hardened fat. However, numerous clinical trials and observational studies conducted over the past two decades consistently provide strong evidence that the consumption of TFA produced during the hydrogenation process adversely affects cardiovascular health (Micha and Mozaffarian, 2009; Mozaffarian et al., 2009). On the other hand, naturally occurring TFA present in other products like conjugated linoleic acid (CLA) in milk have been associated with health benefits. Therefore, a distinction needs to be made between these types of TFA.

Enzymatic interesterification could be a feasible way of producing low-*trans* plastic fat with advantages of mild conditions, minimal side products and region specificity, which can avoid the formation of TFA effectively (Marangoni and Rousseau, 1995; Xu, 2003). The interesterification reactions between a high melting fat and liquid oil lead to the exchange of fatty acids within and between triglycerides (TG), resulting in the formation of new altered TG molecules, and

thus can produce semisolid fats with desirable tenderness, texture, and mouthfeel characteristics, and extended shelf life (Xu, 2000).

Canola oil, having a low amount of saturated fatty acids (around 7%), high amount of oleic acid (around 60%), and containing  $\omega$ -6 and  $\omega$ -3 in a nutritionally-preferred ratio of 2:1 is one of the commonly-used vegetable oils for cooking purposes (Ratnayake and Daun, 2004). Therefore, canola oil as liquid oil and fully-hydrogenated canola oil (FHCO) as a high melting fat are potential initial substrates for enzymatic interesterification to produce base-stock for margarine and pastry shortenings.

Supercritical fluid technology may offer the potential to overcome the disadvantage of long reaction times associated with conventional enzymatic reactions. Carbon dioxide ( $\text{CO}_2$ ) with its moderate critical point ( $T_c=31.1\text{ }^\circ\text{C}$ ,  $P_c=7.4\text{ MPa}$ ) could be a suitable reaction medium for lipase-catalyzed interesterification between canola oil and FHCO. During enzymatic reactions carried out in supercritical  $\text{CO}_2$  ( $\text{SCCO}_2$ ) media,  $\text{CO}_2$  can expand the liquid reactant mixture, especially lipid-type substances and form  $\text{CO}_2$ -expanded (CX) lipid, due to pressure increase and dissolution of  $\text{CO}_2$ , causing viscosity reduction, and improvement of the mass transfer properties of reactants and products.

Therefore, with an overall goal of developing a process for producing base-stock for margarines and pastry shortening using lipase-catalyzed interesterification between canola oil and FHCO under  $\text{SCCO}_2$  conditions, this thesis research was presented in two major parts. In the first part (Chapters 3 and 4) some physicochemical properties of canola oil and its blend with FHCO in

equilibrium with high pressure CO<sub>2</sub> such as viscosity, CO<sub>2</sub> solubility in the liquid lipid phase, and density were studied to generate fundamental data to enhance our understanding of this complex system. Then, the second part (Chapters 5, 6 and 7) focused on process optimization and characterization of the reaction products.

In Chapter 3, the viscosity of canola oil at 40, 50, 65, and 75 °C and its blend with FHCO (30 wt.%) at 65 °C in equilibrium with high pressure CO<sub>2</sub> was measured at pressures of up to 12.4 MPa using a rotational rheometer equipped with a high pressure cell. The solubility of CO<sub>2</sub> in canola oil at 40 and 65 °C and its blend with FHCO at 65 °C was also determined at pressures of up to 20 MPa using a high pressure view cell. The viscosity of canola oil at 40, 50, 65, and 75 °C and its blend with FHCO at 65 °C decreased exponentially to 87.2, 84.7, 74.8, 66.2, and 74.2% of its value at atmospheric pressure, respectively, with a pressure increase up to 12.4 MPa. The viscosity of the samples decreased with an increase in temperature, but the effect of temperature was diminished above 10 MPa. The viscosities of CX-canola oil and its blend with FHCO at 65 °C were similar up to 12.4 MPa. The samples exhibited shear-thickening behaviour as the flow behaviour index reached almost 1.2 at elevated pressures. The mass fraction of CO<sub>2</sub> in canola oil at 40 and 65 °C and its blend with FHCO at 65 °C reached 24 and 21% at 20 MPa, respectively. The Grunberg and Nissan model was used to correlate the viscosity of CX-lipid samples.

In Chapter 4, the experimental data of CO<sub>2</sub> solubility in canola oil at 40 and 70 °C and its blend with FHCO (30 wt.%) at 70 °C at pressures of up to 25 MPa were correlated using Peng-Robinson and modified Soave-Redlich-Kwong

equations of state with quadratic and Panagiotopoulos-Reid mixing rules. The relative volumetric expansion of canola oil at 40 °C/20 MPa and at 70 °C/25 MPa and its blend with FHCO (30 wt.%) at 70 °C/25 MPa in equilibrium with CO<sub>2</sub> was 41, 46, and 43%, respectively. The relative volumetric expansion of canola oil in equilibrium with high pressure CO<sub>2</sub> at 40 °C increased with pressure up to 10 MPa and above that pressure it leveled off. However, for canola oil and its blend at 70 °C, the volumetric expansion increased up to about 15 MPa and above that pressure it still increased but more slowly without reaching a plateau within the range of pressures studied. The densities of canola oil at 40, 55, and 70 °C and its blend with FHCO at 70 °C in equilibrium with CO<sub>2</sub> were measured up to 30 MPa and the density increased by 4.7, 4.3, 3.5, and 3.6% of its value at atmospheric pressure, respectively. The density of CO<sub>2</sub>-saturated canola oil at 40 and 55 °C increased in a more pronounced manner up to 10 MPa because of the solubility of CO<sub>2</sub> in the liquid lipid phase and above that the density increased at a slower rate mainly due to the effect of compression. The density of CX-lipids increased with pressure and decreased with temperature.

The findings in Chapters 3 and 4 emphasized the importance of the physicochemical properties of CO<sub>2</sub>-saturated lipids for designing high pressure processes and especially here for better understanding of the enzymatic interesterification between canola oil and FHCO using SCCO<sub>2</sub>, since these properties influence the reaction rates due to changes in mass transfer properties.

Although a mixture of lipid reactants in contact with high pressure CO<sub>2</sub> expands as CO<sub>2</sub> dissolves in the liquid lipid phase, causing viscosity to decrease

and reaction rate to increase, performance and stability of enzymes may be affected negatively. Therefore, in Chapter 5, the performance and reusability of two commercially available immobilized lipases, Lipozyme RM IM and TL IM, for the interesterification between canola oil and FHCO under  $\text{SCCO}_2$  were studied using a high pressure batch stirred reactor at 65 °C and 17.5 MPa. The influence of exposure time (4, 8, and 12 h) and pressurization/depressurization steps (4, 8, and 12 times) on enzyme activity were studied. There was no significant difference ( $p > 0.05$ ) in the performance of the two enzymes over reaction time, reaching equilibrium conversion rate of about 23% after 2 h. Although FE-SEM images illustrated some morphological changes on the surface of the enzyme beads after 4 x 7 h of reuse, similar conversion rates were achieved at all reuse cycles. Treatment of both immobilized lipases in  $\text{SCCO}_2$  at 65 °C/17.5 MPa did not lead to any significant changes ( $p > 0.05$ ) in conversion rate compared to untreated enzymes. However, the amount of produced reaction intermediates including free fatty acids (FFA), monoglycerides (MG) and diglycerides (DG) decreased by 50-60 wt.% in interesterified canola oil and FHCO using  $\text{SCCO}_2$ -treated enzymes with 12 pressurization/depressurization cycles compared to untreated enzymes mainly due to the removal of water from the enzymes. FTIR and FE-SEM results showed no significant changes in conformational and morphological structure of enzymes after 12 pressurization/depressurization cycles. Also, exposing the enzymes to  $\text{SCCO}_2$  did not lead to any interaction with  $\text{CO}_2$  based on XPS results. Lipozyme TL IM because of its much lower price, more convenient access, and large scale

production is more feasible than Lipozyme RM IM for interesterification of vegetable oils using  $\text{SCCO}_2$ . Therefore, additional studies were performed using Lipozyme TL IM.

The reactions using CX-lipids are strongly influenced by various process parameters. In Chapter 6, CX-canola oil and FHCO were interesterified using Lipozyme TL IM in a high pressure stirred batch reactor. The effects of enzyme load, pressure, substrate ratio and reaction time on conversion rate defined as the formation of mixed TG from trisaturated and triunsaturated TG were investigated. The optimal enzyme load, pressure, substrate ratio and time for the conversion rate to reach the highest level of 27% at equilibrium were 6% (w/v) of initial substrates, 10 MPa, 30% (w/w) FHCO blend and 2 h, respectively. The physicochemical properties of initial blends and interesterified products at different FHCO ratios at optimal reaction conditions were determined by evaluating their TG composition, thermal behaviour and solid fat content (SFC). As expected, the amounts of trisaturated and triunsaturated TG decreased and the amounts of mixed TG increased after interesterification. The formation of mixed TG components resulted in a lower melting point and a broader melting transition for interesterified products.

In an effort to further characterize the products, blends of canola oil and FHCO with 10, 30, and 50% (wt.%) FHCO were interesterified enzymatically using Lipozyme TL IM (6% of initial substrates, w/v) under  $\text{SCCO}_2$  at 10 MPa and 65 °C for 2 h (Chapter 7). Changes in polymorphic behaviour and crystal morphology of non-interesterified blends (NIB) and enzymatically interesterified

products (EIP) were studied using X-ray diffraction spectroscopy (XRD) and polarized light microscopy (PLM). As well, the effects of blending canola oil and FHCO and enzymatic interesterification on rheological behaviour were investigated. XRD analysis showed the predominance of  $\alpha$  form in FHCO; however, blending of FHCO with canola oil induced the formation of  $\beta$  form after crystallizing the samples at 24 °C and 5 °C for 12 h. Enzymatic interesterification changed the polymorphic behaviour with the appearance of  $\beta'$  form. Enzymatic interesterification also dramatically changed crystal morphology. The EIP samples contained less crystal particles compared to NIB, but the crystals were more symmetrical. The elastic modulus (solid-like behaviour) ( $G'$ ) was lower in NIB with 30% (wt.%) FHCO compared to the one with 50% (wt.%) FHCO. Also, enzymatic interesterification had a strong effect on  $G'$  of the samples as it decreased after interesterification.

## 8.2. Recommendations for future work

Although the reaction under  $\text{SCCO}_2$  has been conducted in a high pressure batch reactor in this thesis research, the findings could be used to develop the interesterification reactions using continuous packed bed reactors. Attempts were made to conduct the reaction in a continuous reactor, but some challenges encountered with the existing system forced us to discontinue this effort. Due to the high melting point of the initial blends and interesterified products, feeding the initial substrates to the packed bed reactor and collecting the sample after expansion through the micrometering valve were challenging due to solidification

of the fat and plugging of the high pressure tubing. It was also a big challenge to control the flow rate of CO<sub>2</sub>, which is an important parameter in continuous reactions under SCCO<sub>2</sub> conditions, again due to solidifying of the interesterified products in the tube after the micrometering valve. It is recommended to modify the existing unit to be able to heat all the tubing to avoid such plugging problems. Further study is necessary to optimize the associated reaction parameters in continuous reactors under SCCO<sub>2</sub>. Employing continuous packed bed reactors would ease reuse of the immobilized enzymes without any additional treatment to separate the enzyme from substrates or products, leading to cost reduction. Even though stability of the immobilized enzymes was demonstrated over 4×7 h reuse cycles in this research, further research on longer term stability in a continuous reactor mode would be invaluable for potential scale up of this process.

Two other parameters that influence the physicochemical properties of final products are the type of vegetable oil used as initial substrate and the conversion rate. Therefore, further studies using other vegetable oils are worthwhile to assess its influence on the physicochemical properties of the final products. In this thesis research, the physicochemical properties were determined for final products corresponding to equilibrium conversion rate. Since the composition of reaction products changes as a function of time, it would be valuable to investigate the physical properties of the reactions products obtained at different times.

Margarine is a water-in-fat emulsion composed of 80-84% fat and the rest being aqueous solution. These products should have suitable spreadability, hardness, crystal network and emulsion stability against phase separation in the

final product. The base-stock produced in this research or its mixture with other vegetable oils has great potential for use in the final margarine products. It is recommended to use the base-stock for the production of margarines employing the standard protocols of the margarine industry followed by evaluation of the properties of the final products. As well, over ten different types of margarines are produced in the industry, including regular, whipped, soft tub, liquid, diet, spread, *trans*- free fatty acids, restaurant and bakery types. Thus, the base-stocks produced under different conditions having different properties could be suitable for specific types of margarine, which require further assessment.

Both immobilized lipases (Lipozyme TL IM and RM IM) used in this research were *sn*-1,3 specific as claimed by the manufacturer. However, such specificity of the enzymes is determined under conventional conditions and not under SCCO<sub>2</sub>. Therefore, it is worthwhile to investigate whether the enzymes exhibit the same behaviour under SCCO<sub>2</sub> environment. As well, determination of the fatty acid composition at *sn*-2 position of the TG components in the final interesterified products is important from the nutritional perspective.

It is also valuable to investigate whether the enzyme molecules have been released from the support matrix of the immobilized lipases to the liquid lipid phase using protein assays.

### **8.3. Potential significance**

This thesis presents fundamental data as well as applied research in the area of enzymatic interesterification under SCCO<sub>2</sub>. The findings for the fundamental

data such as viscosity, density, volumetric expansion, and the solubility of CO<sub>2</sub> in the liquid lipid phase are critical not only for the interesterification reaction investigated but also for other process and applications development involving similar lipid mixtures. These fundamental data as well as optimized reaction conditions are essential for process and equipment design. As well, the information on physicochemical properties of final reaction products will aid in the formulation of more healthy fat and oil products and address a critical industrial demand in terms of formulation options for margarines, spreads, and shortenings.

There have been major recent developments in the use of immobilized lipases for interesterification reactions at commercial scale because the use of metal catalysts for hydrogenation and thus the formation of *trans* fatty acids is eliminated. Conducting enzymatic reactions under SCCO<sub>2</sub> is a novel technology offering great potential as an alternative to conventional methods using organic solvents and solvent-free reactions. The findings of this thesis research demonstrate the major advantages offered by the supercritical technology for interesterification reactions. Substantial reduction in reaction time down to 1-2 h together with the reduction in the viscosity of the lipid mixture offers significant energy and cost savings. In addition, the potential for integration of the unit operations of extraction of canola oil with SCCO<sub>2</sub> with reaction in a second step should not be overlooked. This thesis research focusing on the interesterification operation is an important contribution towards developing integrated fats and oils processing using SCCO<sub>2</sub>.

#### **8.4. References**

- Beers, A., Ariaansz, R. and Okonek, D. (2008). *Trans* fatty acids. In *Trans isomer control in hydrogenation of edible oils*, A.J. Dijkstra, R.J. Hamilton and W. Hamm, Eds. Blackwell Publishing Ltd: Oxford, pp 147-180.
- Marangoni, A.G. and Rousseau, D. (1995). Engineering triacylglycerols: The role of interesterification. *Trends in Food Science & Technology*, **6**: 329-335.
- Micha, R. and Mozaffarian, D. (2009). *Trans* fatty acids: Effects on metabolic syndrome, heart disease and diabetes. *Nature Reviews Endocrinology*, **5** (6): 335-344.
- Mozaffarian, D., Aro, A. and Willett, W.C. (2009). Health effects of *trans*-fatty acids: Experimental and observational evidence. *European Journal of Clinical Nutrition*, **63**: S5-S21.
- Ratnayake, W.M.N. and Daun, J.K. (2004). Chemical composition of canola and rapeseed oils. In *Rapeseed and canola oil: Production, processing, properties and uses*, F.D. Gunstone, Ed. CRC Press: Boca Raton, FL, USA, pp 37-79.
- Xu, X. (2000). Production of specific-structured triacylglycerols by lipase-catalyzed reactions: A review. *European Journal of Lipid Science and Technology*, **102** (4): 287-303.
- Xu, X. (2003). Engineering of enzymatic reactions and reactors for lipid modification and synthesis. *European Journal of Lipid Science and Technology*, **105**: 289-304.